Functional analyses of sphingolipid biosynthesis in an apicomplexan parasite

ALQAISI, AMJED,QAYS,IBRAHIM

Functional analyses of sphingolipid biosynthesis in an apicomplexan parasite

Amjed Qays Ibrahim Alqaisi

Doctor of Philosophy

September 2017

Durham University

Department of Biosciences

Supervisor

Paul W. Denny

Abstract

The phylum Apicomplexa includes many protozoan parasites that cause serious human and animal disease, for example *Plasmodium*, *Eimeria* and *Toxoplasma*. Treatments against these parasites are limited and novel solutions are urgently required. Recently, research has focused on parasite specific features of lipid biosynthesis as drug targets. In particular the biosynthesis of sphingolipids, which have essential roles in many processes, has been highlighted as a potential target.

Using the model apicomplexan *Toxoplasma gondii* we are studying the role of parasite and host sphingolipid biosynthesis in invasion and proliferation. Serine palmitoyltransferase (SPT) catalyzes the first step in sphingolipid biosynthesis, and our results demonstrated that the expression of host cell SPT is unaffected by *Toxoplasma* infection. In mammals the primary complex sphingolipid is sphingomyelin (SM), again our data demonstrated that the SM synthases (1 and 2) are not influenced by infection. Together these data indicated that parasite manipulation of host sphingolipid biosynthesis does not occur, supporting the hypothesis that *Toxoplasma* is dependant on *de novo* sphingolipid biosynthesis. To characterise this pathway, we showed that the *Toxoplasma Tg*SPT1 and 2 are, like other eukaryotes, localised and active in the endoplasmic reticulum. However, uniquely, they have a prokaryotic origin. Metabolic labelling showed that several distinct complex sphingolipids are synthesized independently by the parasite. The fungal inositol phosphorylceramide (IPC) synthase inhibitor aureobasidin A (AbA) has been reported to target *Toxoplasma* IPC synthesis. However, our results demonstrated that whilst AbA, and an orthologue, are active against the parasite, their effect on *Toxoplasma de novo* sphingolipid biosynthesis is negligible. In addition, by using *Leishmania major* as a model we have analysed the global effect of compounds recognised as IPC synthase inhibitors in this kinetoplastid protozoan parasite. The results showed that ceramide levels increased in treated parasites, perhaps leading to parasite death via secondary signalling dysfunction. These data confirmed that the sphingolipid biosynthetic pathway is targeted by these anti-leishmanial compounds.

Finally, the anti-leishmanial drug miltefosine showed reduced activity against a transgenic strain of *L. major* lacking sphingolipid biosynthesis ΔLCB2 compared to wild type. This suggested the sphingolipid synthesis has a role in sensitivity to the drug, metabolomic analyses supported this.

Taken together, the present findings further characterised the *T. gondii* sphingolipid biosynthetic pathway and indicated the potential to target this in drug discovery efforts. In addition, metabolomic and lipidomic approaches confirmed that clemastine targets *L. major* IPCS.

Dedication

You are near if I don't see you.

You are with me, even if you are far away.

You are in my heart, in my thoughts, in my life always.

To my beloved ***father***

Acknowledgment

I express my appreciation and acknowledgement to the Almighty God for giving me the power and enabling me to finish this work through His strength.

I would like to express my great gratitude to my supervisor, Paul W. Denny for his time, advice, patient, support, enthusiastic encouragement and guidance during the research preparation and patiently read and commented on this thesis.

Also, many deep thanks to Dr. Ehmke Pohl, for his support and for his advice about some problems which I have during my PhD work. Also, a big thank to Dr. Omar Harb (University of Pennsylvania, Biology department), for his assistance, and encourage within my PhD study

I would like to express my sincere appreciation to the financial support from The Iraqi Ministry of Higher Education and Scientific Research – Baghdad University, which made this research possible.

Many deep thanks to Professor Dr. Michael Barrett/Glasgow University/Institute of Infection, Immunity and Inflammation for his help, advise and comments in metabolomic work and results analysis.

I must deeply acknowledge Ian Edwards, and for everyone in lab 229 particularly Alison J. Mbekani, Elizabeth Pinneh, Emily Cardew and Marrika Beecroft for the time spent in discussion which created a friendly social friendship. Joanne Robson, the technician in Department of Biosciences/Microscopy and Bioimaging Facility for her help to get the microscopy images.

I would like to extend my thanks to my master supervisor Fawzia Al-Shanawi for her encouragement, and support, and to Dr. Harith Al-Warid for his assistance, Akil Harfash, Jaafar Jotheri, Omar Salih, Aslan Jalal, Sinan Azzawi, Ahmed Obaid and all my friends here in UK for their help and support.

To save the best for last, I must give special thanks to my mother for her support, and her encouragement that gave me the ability to achieve my goals. Words cannot

describe how lucky I am to have my mother, and all my brothers in my life. They have selflessly given more to me than I ever could have asked for. I love you, and look forward to our lifelong journey. Also, a big thanks to my mother and father in law for their support and help, and to my Aunts.

A huge thank to my wife for supporting me during these years of PhD study. I cannot imagine being able to reach this time writing these words without here and my children being with me at Durham supporting and allowing me to dedicate four years of my life to this research.

Also, a huge thanks to my brother in law (Affan) and his wife for their help and support.

Amjed

Table of Contents

1.1 Phylum Apicomplexa.....1

1.2 Apicomplexa classification.....1

1.3 An Introduction to *Toxoplasma gondii*.....2

1.4 Ultrastructure.....5

1.4.1 Apical complex.....6

1.4.2 The conoid.....7

1.4.3 The micronemes.....7

1.4.4 The rhoptries.....8

1.4.5 Dense granules.....8

1.4.6 Polar rings.....9

1.4.7 Pre-conoidal rings.....9

1.4.8 Microtubules.....9

1.5 Host-parasite interaction.....10

1.6 The Life Cycle of *Toxoplasma gondii*.....12

1.7 Diagnosis and treatment of *Toxoplasma gondii* infection.....15

1.8 Sphingolipids.....17

1.9 Sphingolipids in *Toxoplasma gondii*.....22

1.10 Kinetoplastids.....25

1.11 Leishmaniasis.....25

1.11.1 Life cycle.....28

1.11.2 Diagnosis.....30

1.11.3 Treatment.....30

1.11.4 Anti-leishmanial drug targets.....32

1.11.5 Leishmania spp. sphingolipid biosynthetic pathway.....32

1.12 Aim of the study.....33

2.1 Materials.....34

2.2 Transformation protocol.....37

2.2.1 Preparation of Luria broth (LB) broth and LB agar.....37

2.2.1.1 LB broth.....37

2.2.1.2 LB Agar.....37

2.2.2 Transformation to the competent cells 37
2.3 Gel Electrophoresis 38
2.4 Cell culture 38
2.5 RNA Extraction from CHO cells 38
2.6 Preparation cDNA from RNA 39
2.7 Metabolic labelling of *Toxoplasma gondii*, vero cells 41
2.8 Metabolic labelling of Yeast 42
2.9 Yeast susceptibility assay 43
2.10 Study the effect of AbA and Cmpd20 on *Toxoplasma gondii* proliferation 43
2.11 *Toxoplasma gondii* serine palmitoyltransferase 2 (*Tg*SPT2) expression and purification 44
2.11.1 Bacterial pellet lysis 45
2.11.2 Immobilised Metal Affinity Chromatography (IMAC) 46
2.11.3 Analyses of Protein 46
2.11.3.1 Resolving solutions 46
2.11.3.2 Stacking solutions 46
2.11.3.3 Staining solution 46
2.11.3.4 De-Staining solution 46
2.11.3.5 Running Buffer 10X 46
2.11.4 *Tg*SPT2 Activity Assay 47
2.11.5 *Tg*SPT2 secondary structure prediction 47
2.12 *Tg*SPT2 localisation 47
2.12.1 Construction of the plasmid pG1*Tg*SPT2_YFP 48
2.12.1.1 *Tg*SPT2 LIC primers 48
2.12.1.2.A T4 processing protocol: 48
2.12.1.2.B Insert (*Tg*SPT2) 50
2.12.1.2.C Annealing 51
2.12.1.2.D pG27 *Tg*SPT2_YFP mapping 52
2.12.3 Infusion cloning 52
2.12.3.A Preparation of linearized vector (pG1) 52
2.12.3.B PCR primer design and PCR 53
2.12.3.C Infusion cloning reaction 53

2.12.3.D pG1*Tg*SPT2YFP sequence 54
2.12.4 Electroporation 54
2.12.4.1 HFF and *Toxoplasma gondii* cell culture 54
2.12.4.2 Nucleofection reactions 55
2.12.4.3 DNA 55
2.12.5 Fixing cells 56
2.12.6 Staining 56
2.13 *Tg*SPT2 knockout (KO) 56
2.13.1 KO Plasmid (pTub5CatSagF1F2) construction and mapping 56
2.13.2 Deletion of *Tg*SPT1 and 2 by homologous recombination 58
2.14 Metabolomics analyses 59
2.14.1 Effect of clemastine and benzazepine (CMPD35) on *Leishmania major* FV1 metabolome 60
2.14.1.1 Half time to cell death assay 60
2.14.1.2 Cell extraction for metabolomics 60
2.14.2 Screening the efficacy of miltefosine against *Leishmania major* FV1 (WT) and *Leishmania major* ΔLCB2 (MT) 61
2.15 Lipidomic analyses 63
2.15.1 The effect of clemastine and benzazepane (CMPD35) on the lipid profile of *Leishmania major* FV1 63
2.15.2 Lipid extraction from *Leishmania major* FV1 (WT) (Bligh and Dyer 1959) 64
2.16 Bioinformatic tools 65
2.16.1 BLAST 65
2.16.2 ClustalW Omega 65
2.16.3 Phobius tool 65
2.16.4 Hydrophobicity profile 65
3.1 Bioinformatic analyses of the *T. gondii* serine palmitoyltransferase 66
3.2 Gene information 67
3.2.1 *Tg*SPT1 67
3.2.2 *Tg*SPT2 68
3.3 Gene Expression 69
3.4 Gene origin 70

4.1 Introduction 78

4.2 *Toxoplasma gondii* serine palmitoyltransferase 2 (*Tg*SPT2) expression and purification 78

4.3 *Tg*SPT2 activity assay 79

4.4 The sub-cellular localization of *Tg*SPT2 80

4.4.1 *Tg*SPT2 co-localization with the Golgi marker GRASP_RFP 81

4.4.2 *Tg*SPT2 co-localization with the ER marker GFP_HDEL 82

4.5 *Tg*SPT2 knockout (KO) 83

4.5.1 KO Plasmid (pTub5CatSagF1F2) construction and mapping 83

4.5.2 *Tg*SPT1 and 2 knockouts 85

5.1 Introduction to Aureobasidin A and its derivative compound 20 (Cmpd20) 87

5.2 The response of host (CHO) sphingolipid biosynthesis pathway to *T. gondii* infection 88

5-3 The effect of known anti-fungal sphingolipid biosynthesis inhibitors aureobasidin A (AbA) and an analogue (Cmpd 20) on *Toxoplasma* proliferation in acute and chronic infection 89

5.3.1 The effect of compounds on *T. gondii* proliferation in acute infection 89

5.3.2 The compounds effects on *T. gondii* proliferation in chronic infection 96

6.1 Introduction 98

6.2 Effect of clemastine and benzazepine (CMPD35) on the Leishmania major FV1 metabolome 100

6.2.1 Results of half-time to cell death assay 100

6.3 Metabolomic analyses of clemastine and benzazepine (CMPD35) treated *Leishmania major* 103

6.3.1 SL metabolite flux in *Leishmania major* promastigotes treated with clemastine 104

6.3.2 SL metabolite flux in *Leishmania major* promastigotes treated with benzazepine (CMPD35) 105

6.4 Lipidomic analyses 109

7.1 Introduction 111

7.2 Establishing the efficacy of miltefosine against wild type and ΔLCB2 mutant *Leishmania major* 112

7.3 The effects of miltefosine on the *Leishmania major* wild type and ΔLCB2 metabolomes 112

8.1 General Discussion 114
8.2 Future work 117
References 118
Research publication 151

List of Figures

Figure (1-1) Congenital toxoplasmosis..... 3
Figure (1-2) *T. gondii* cell structure 6
Figure (1-3) Apical complex 10
Figure (1-4) The Life Cycle of *Toxoplasma gondii* 14
Figure (1-5) Sphingolipid biosynthesis pathways of mammalian and fungal cells... 21
Figure (1-6) showing the sources for sphingolipid for *Toxoplasma gondii*..... 24
Figure (1-7) Depiction of the *Leishmania spp.* life cycle 29
Figure (2-1) pOPIN3C plasmid map (generated by SnapGene)..... 45
Figure (2-2) pG27 LIC-YFP-DHFR (generated by SnapGene)..... 49
Figure (2-3) pG1 plasmid (generated by SnapGene)..... 52
Figure (2-4) The KO plasmid pTub5CatSag1F1F2 map..... 58
Figure (2-5) preparation of serial compound dilutions..... 62
Figure(3-1) *Tg*SPT1 model showing the exon and intron areas from (ToxoDB.org)..... 67
Figure (3-2) *Tg*SPT2 model showing the exon and intron areas from (ToxoDB.org)..... 68
Figure (3-3) Alignment sequence of TGGT1_290980 and TGME49_290980 (*Tg*SPT1); and TGGT1_290970 and TGME49_290970 (*Tg*SPT2)..... 68
Figure (3-4) Gene expression profiles for *Tg*SPT1 and *Tg*SPT2 in *T. gondii* life cycle stages..... 69
Figure (3-5) ClustalW for SPT alignment in eukaryotic (human and yeast) and bacterial SPT sequences..... 71
Figure (3-6) Phylogenetic tree produced from a genetic distance matrix showing the relationship between the eukaryotic catalytic subunit of serine palmitoyltransferase (LCB2) and the prokaryotic and apicomplexan orthologues (SPT)..... 74
Figure (3-7) Sequence alignment of the predicted serine palmitoyltransferases from 4 members of the Apicomplexa (*Toxoplasma gondii* – *Tg*SPT1 and 2; *Eimeria tenella* – *Et*SPT; *Plasmodium falciparum* – *Pf*SPT; and *P. vivax* – *Pv*SPT) and the characterised enzyme from the prokaryote *Sphingomonas paucimobilis* (*Sp*SPT)..... 75
Figure (3-8) Transmembrane prediction for A. *Tg*SPT1 and B. *Tg*SPT2 by using Phobius tool..... 77
Figure (3-9) the hydrophobicity of Kyte and Doolittle parameter to predict the hydrophobicity/hydrophilicity of A. *Tg*SPT1 and B. *Tg*SPT2..... 77
Figure (4-1) SDS-PAGE showed that the molecular weight of the purified protein was 60 kDa..... 79

Figure (4-2) Mass spectrometry of lipids extracted froman *in vitro* reaction of the *Tg*SPT2 Δ158 fusion with serine and palmitoyl CoA as substrates and PLP as co-factor…… 80
Figure (4-3) Subcellular localisation of *Tg*SPT2 and GRASP imaged using the Zeiss LSM 880 microscope with Airyscan with appropriate filters…….. 81
Figure (4-4) DeltaVision OMX imaged 125 nm optical slice of *T. gondii* within a parasitophorous vacuole (PV) of a HFF infected cell…….. 82
Figure (4-5) *Tg*SPT1 and *Tg*SPT2 knockout by using homologous recombinant-ion…….. 83
Figure (4-6) Gel electrophoresis of restriction enzyme digests…….. 84
Figure (4-7) PCR screen for *Tg*SPT1 and 2 deletions. *T. gondii* ΔKu80-HX and *T. gondii* SPTKO-ΔKu80-HX…… 86
Figure (5-1) Chemical structure of AbA (A) and its analogue Compound 20 (B). generated by using ChemDraw software…….. 87
Figure (5-2) RT-PCR shows expression of host sphingolipid biosynthetic enzymes are largely unaffected by *Toxoplasma* infection. β-tubulin used as housekeeping gene control (HKG)…….. 89
Figure (5-3) ED_{50} of AbA (A) and Cmpd20 (B) µg mL^{-1} against the RH-HX-KOYFP2-DHFR *T. gondii* tachyzoites in HFF cells…….. 90
Figure (5-4) ED_{50} of AbA (A) and Cmpd20 (B) µg mL^{-1} wash out 2 h post compound, and AbA (C) and Cmpd20 (D) washout 8 h post compound…….. 91
Figure (5-5) Figure (5-5) ED_{50} of AbA (A) and Cmpd20 (B) µg mL^{-1} 2 h exposure to isolated RH-HX-KOYFP2-DHFR *T. gondii* tachyzoites…….. 92
Figure (5-6) Yeast dependent on the expression of the *Toxoplasma* AUR1p orthologue *Tg*SLS (YPH499-HIS-GAL-AUR1 pRS426 *Tg*SLS) are resistant to Aureobasidin A (AbA) and Compound 20 (Cmpd 20) at 5 and 10 µg mL^{-1}…….. 93
Figure (5-7) Vero cells (Host), isolated *T. gondii* tachyzoites (*T.gondii*) and *Saccharomyces cerevisiae* (Yeast), labeled for 1 h with NBD-C6-ceramide and complex sphingolipids then fractionated by HPTLC…….. 95
Figure (5-8) Isolated *Toxoplasma* tachyzoites treated with Aureobasidin A (AbA) and Compound 20 (Cmpd 20) at 10 µg mL^{-1} for 1 (A), 4 (B) and 7 (C) hours before labelling with NBD-C6-ceramide for 1 h…… 96
Figure (5-9) ED_{50} of Aureobasidin A (A, AbA) or Compound 20 (B, Cmpd20) µg mL^{-1} against the *T. gondii* Pru bradyzoites in Human Foreskin Fibroblast (HFF) cells…… 97
Figure (6-1) Sphingolipid biosynthesis pathway in *L. major* …….. 104
Figure (6-2) Metabolites that are changed in sphingolipid biosynthesis pathway when *L. major* are treated with clemastine (Cle)…… 107
Figure (6-3) Metabolites that are changed in sphingolipid biosynthesis pathway when *L. major* are treated with benzazepine (CMPD35)…….. 108

Figure (6-4) Lipidomics analyses of *Leishmania major* promastigotes treated with vehicle (DMSO; A), or 5 µM clemastine (B) for 72 hours……. 110
Figure (7-1) Chemical structure of miltefosine…… 111
Figure (7-2) Efficacy of miltefosine against wild type and ΔLCB2 *Leishmania major.* log (miltefosine; µM) vs % parasite proliferation…… 112
Figure (7-3) Fold change in abundance of all sphingolipids detected in LC-MS analyses of wild type and ΔLCB2 *Leishmania major* treated or un-treated with 10 µM or 30 µM of miltefosine…… 113

List of Tables

Table (2-1) Materials and their source 34
Table (3-1) Active site and PLP binding residues within mammalian SPT2 (human and yeast) and *T. gondii* SPT1 and 2. Comparing with the bacterial model (*Sp*SPT)…… 73
Table (6-1) Clemastine treated *Leishmania major*…….. 101
Table (6-2) CMPD35 treated *Leishmania major*…… 102
Table (6-3) 42-hour clemastine and CMPD35 treatment of *Leishmania major*…. 102
Table (6-4) Metabolites that are changed when *Leishmania major* are treated with clemastine (Cle) or benzazepine (CMPD35). 106

List of Abbreviation

a.a.	Amino acid
AbA	Aureobasidin A
AIDS	Acquired immune deficiency syndrome
AMA	Apical membrane antigen
Apr	Apical polar ring
APS	Ammonium per sulphate
aSMase	Acid Sphingomyelin synthase
C-1-P	Ceramide-1-phosphate
CATI	Canadian AIDS international exchange
CDC	Centres for disease control and prevention
CERT	Ceramide transfer proteins
CHO	Chinese hamster ovary cells
CL	Cutaneous leishmaniasis
Cle	Clemastine
CMW	Chloroform:Methanol:Water
DAPI	Diamino-2-phenylindale dihydrochloride
DCL	Diffuse Cutaneous leishmaniasis
DMEM	Dulbecco's modified eagle medium
ELISA	Enzyme linked immunosorbent assay
EPC	Ethanolamine phosphorylceramide
ER	Endoplasmic reticulum
ESI	Electron spray assay
FV1	Friedlin virulent
GAPs	Gliding associated proteins

GC-MS	Gas chromatography mass spectrometry
GOI	Gene of interest
GPI	Glycosylphospgatidyl inositol
GRAs	Dense Granule proteins
GSLs	Glycosphingolipids
HFF	Human foreskin fibroblast
HSAN-1	Hereditary sensory and autonomic neuropathy type I
IFAT	Immunofluorescence antibody test
IFN-γ	Interferon gamma
IMC	Inner membrane complex
IPC	Inositol phosphorylceramide
IPCs	Inositol phosphorylceramide synthase
KDS	ketodihydrosphingosine
LB	Lauria broth
LCB	Long chain base
LC-MS	Liquid chromatography mass spectrometry
MCL	Mucocutaneous leishmaniasis
MICs	Microneme proteins
MS	Mass spectrometry
MT	Mutant type
MβCD	Methyl-β-cytodextrin
NPI	Neglected parasitic infection
nSMase	Neutral Sphingomyelin synthase
PCR	Polymerase chain reaction
PKDL	Post-kalazar dermal leishmaniasis

PLP	Pyridoxal phosphate
PM	Plasma membrane
PPM	Parasite plasma membrane
PV	Parasitophorous vacuole
PVM	Parasitophorous vacuole membrane
QC	Quality control
Rab	Intercepting Golgi-derived vesicles
RNG2	Ring protein 2
RONs	Rhoptry neck proteins
S-1-P	Sphingosine-1-phosphate
SAGs	Surface antigen proteins
SB^v	Pentavalent antomonials
SLs	Sphingolipids
SM	Sphingomyelin
SMS	Sphingomyelin synthase
SPT	Serine palmitoyltransferase
SRS	Surface antigen 1 related sequence proteins
T2DM	Type II diabetes mellitus
UPLC	Ultraperformance liquid chromatography
VL	Visceral leishmaniasis
WT	Wild type
YFP	Yellow fluorescent protein
YPD	Yeast extract agar

Chapter One:
Introduction and Literature Review

1.1 Phylum Apicomplexa

The protozoan phylum apicomplexa encompasses many unicellular and obligate intracellular parasites (Black and Boothroyd, 2000; Blader and Saeij, 2010; Graindorge *et al*., 2016) that are considered a principal source of serious disease in humans and cattle (Wasmuth *et al.,* 2009; Hammoudi *et al*. 2015; Coffey *et al*., 2016; Francia *et al*., 2016). All of the approximately 5000 species are parasitic (Hu *et al*. 2006; Meissner, 2013) and able to proliferate within different host cells, for instance lymphocytes, red blood cells, macrophages, muscle tissues, liver cells, intestinal epithelial tissues and neuronal cells (Frénal and Soldati, 2009; Ramakrishnan *et al*., 2015). For example, infection with *Plasmodium* species, the causative agent of malaria, leads to roughly 216 million cases in all over the world, and 445.000 death cases, 90% of them in Africa (Alonso and Noor, 2017)

Another important apicomplexan parasite is *Toxoplasma gondii* which causes toxoplasmosis or cat litter disease. This parasite infects up to one-third of the human population (Flegr, 2013; Sumpf *et al.,* 2017), and is classified by the Center for Disease Control and Prevention (CDC) as causing a Neglected Parasitic Infection. Together with other coccidian apicomplexans (e.g. *Eimeria* - coccidiosis) *T. gondii* also leads to a global agricultural loss of >$3 billion per annum (Dalloul and Lillehoj, 2006). These parasites are characterized by having an apical complex and many organelles like micronemes and rhoptries which play an essential role in the attachment to the host cells, invasion (Isaza and Alzate, 2016) and parasitophorous vacuole formation (Wasmuth *et al*., 2009).

1.2 Apicomplexa classification

This phylum is classified into five major pedigrees according to the phenotypic characteristics: Gregarinasina, Piroplasmorida, Haemosporoida, *Cryptosporidium* and Coccidia (Isaza and Alzate, 2016):

1. Gregarinasina is a subclass includes parasites that infect invertebrate animals (Meissner *et al.*, 2013) particularly annelids (Chambouvet *et al.,* 2016) and insects (Isaza and Alzate, 2016). However, Chambouvet *et al.* (2016) found that *Nematopsis tenporariae,* a gregarian parasite belonging to this subclass, infected

a vertebrate host (frog) by microscopic examination and molecular biology data (ribosomal DNA sequencing) of liver cells from the tadpoles of three different frog species (*Rana temporaria*, *Rana dalmatina* and *Hyla arborea*).

2. Piroplasmorida consists of many tick-borne apicomplexan parasites. For example: *Babesia spp.* and *Theileria spp.* that infect mammals and birds (Lack *et al*, 2012) and cause babesiosis and theileriosis respectively (Isaza and Alzate, 2016).
3. Haemosporoida is an order that includes many important parasites, for instance *Plasmodium spp.* the causative agent of malaria, the king of the diseases.
4. *Cryptosporidium* spp. are parasites that cause severe diarrhea in children, *Cryptosporidium* is ranked the second cause of diarrhea in children less than 2 years after rotavirus in many part of the developing world (Checkley *et al.*, 2015). They also cause serious, life-threatening, diseases in immune-deficient and organ transplant patients (Hunter and Nicholas, 2002; Vinayak *et al.,* 2015).
5. Coccidia is a subclass that includes many parasites that cause a serious disease in humans and economically important animals (Clark and Black, 2012; Meissner, 2013). For instance, *Neospora,* which causes abortion in cattle (Okamoto and Kee;ing, 2014), and *Toxoplasma gondii,* a serious risk in immune-deficient patients, especially those with AIDS (Black ad Boothroyd, 2000).

1.3 An Introduction to *Toxoplasma gondii*

Toxoplasma is an important apicomplexan parasite which causes toxoplasmosis, commonly known as a cat litter disease (Palencia *et al.,* 2017). This genus has only one species *T. gondii* which can infect any nucleated mammalian cells (Frénal and Soldati, 2009; Blader and Saeij, 2010; Sher *et al.,* 2016).

T. gondii was first discovered by scientists at the beginning of the 20th century (Nicolle and Manceaux, 1908, 1909; Splendore, 1908 in Dubey, 2009). The genus name is derived from the Greek word toxon, meaning “bow” and referring to the crescent shape of the organism” (Black and Boothroyd, 2000). *T. gondii* is used as a model apicomplexan parasite for many reasons: availability of many genetic tools (Gubbels *et al.,* 2004), ease of laboratory propagation (Kim and Weiss, 2004) due to their ability

to invade any type of cell (Sher *et al.,* 2016), and it is easy to manipulate its genome (Wang *et al.,* 2016).

T. gondii is an obligate intracellular parasite that has a huge impact on both human and animal health. In humans, it causes serious damage to the unborn child (congenital toxoplasmosis) (Montoya and Liesenfeld, 2004; Palencia *et al.,* 2017) and toxoplasmosis, particularly in immunocompromised patients. In animals, it is the important cause of abortion in livestock, and can cause serious economic losses to sheep and goat breeders (Coffey *et al.,* 2016).

In congenital toxoplasmosis acute infection leads, depending on the pregnancy period, either to abortion or intellectual retardation (Black and Boothroyd, 2000) for instance hydrocephalus, intracranial calcification and chorioretinitis in the fetus (Holland, 2003 ; Palencia *et al.,* 2017) (figure 1-1).

Figure (1-1) Congenital toxoplasmosis (www.pathobio.sdu.edu.cn)

T. gondii is composed of three clonal lineages of differing virulence and epidemiology, Type I, II and III (Blader and Saeij, 2010). Type I strains is characterised by its ability to grow rapidly in tissue culture, and mostly found in ocular toxoplasmosis cases and acute toxoplasmosis, also it found that this strain is highly virulent against mice (Grigg *et al.,* 2001). On the other hand, Type II and Type III are less virulent in mice and form cysts *in vitro* (Weiss *et al.,* 2009).

T. gondii have four infective stages in their life cycles (Weiss and Kim, 2007) and require intermediate (non-feline) and final (feline) hosts to complete their life cycle

(Black and Boothroyd, 2000; Blader and Saeij, 2010). The intermediate hosts like humans have two stages. Tachyzoites represent the rapidly multiplying stage (Montoya and Liesenfield, 2004; Katris *et al.,* 2014). responsible for acute toxoplasmosis. The tachyzoite stage is also used for *in vitro* studies because it is the most amenable to experimental work (Weiss and Kim, 2007). The other stage in the intermediate host is the slow growing bradyzoite form responsible for chronic toxoplasmosis. This stage is converted to tissue cysts to avoid the host immune system and establish the toxoplasmosis chronic infection (Weiss and Kim, 2000).

It is worth mentioning that there is a difference in protein expression in both *T. gondii* tachyzoite and bradyzoite stages, for instance the tachyzoite expresses the following surface antigens proteins (SAGs) and surface antigen 1 related sequence proteins (SRS): SAG1, SAG2, SAG3, SRS1, SRS2 and SRS3. On the other hand, bradyzoite express the following proteins: SAG2C, SAG2X, SRS9 and SAG4 (Mineo *et al.,* 1993). The final, feline, hosts also maintain merozoite and sporozoite stages (Weiss and Kim, 2007).

T. gondii can cause deleterious effects on the host cell as exemplified in tissue damage due to the invasion of the parasite, then parasite proliferation which leads to lysis and invasion of new host cells (Hu *et al.,* 2006). *T. gondii* can infect many organs in the body including the brain, spinal cord, eyes, heart, lungs, skin, liver, and gastrointestinal tract (CATI, 1997; Del Grande *et al.,* 2017), however the infection is mostly asymptomatic in healthy persons because the immune system plays an essential role in reducing the parasite's spread (Black and Boothroyd, 2000) by producing interferon gamma (IFN-γ). This is fundamental in innate resistance to *T. gondii,* allowing it to remain dormant as bradyzoites in tissue cysts for the life time of the host (Sher *et al.,* 2016). These tissue cysts reside in muscle cells and brain, and it has been suggested that there is a relationship between *T. gondii* chronic infection and neurological disorders such as schizophrenia and epilepsy (Fekadu *et al.*, 2010; Kamerkar and Davis, 2012). Recent studies showing high level of anti *T. gondii* IgG antibodies in schizophrenia patients when compared to healthy controls (Yolken *et al.,* 2009; Pedersen *et al.*, 2012; Del Grande *et al.,* 2017). However, the parasite can cause a fatal disease in individuals suffering from immune deficiencies such as AIDS (CATI, 1997; Black and Boothroyd, 2000; Hu *et al.,* 2006; William *et al.,* 2012; Palencia

et al., 2017), as *T. gondii* can avoid the immune system (Black and Boothroyd, 2000) and bradyzoites within tissue cysts can convert to rapidly dividing tachyzoites (Sher *et al.,* 2016).

There are several routes of infection in humans, including eating uncooked infected meat and by ingestion of cat faeces from contaminated soil or domestic litter. To avoid infection of vulnerable people (e.g. during pregnancy or HIV+) it is recommended to cook the meat well, wear gloves when working in the garden, wash all fruits and vegetables thoroughly before eating, wash hands carefully after handling raw meat, fruit, vegetables and soil, and avoid touching cat faeces (Peters *et al.,* 2015; Del Grande *et al.,* 2017).

1.4 Ultrastructure

All *T. gondii* stages are characterized by crescent shape 2-7 µm long (Weiss and Kim, 2007) (Figure 1-2); structural features include:

1. A unique anterior cytoskeleton structure called the apical complex (figure 1-2A ; 1-3) from which the phylum name is derived (Pfluger *et al.,* 2005; Hu *et al.,* 2006). This complex is composed of conoid (figure 1-2B), apical rings (figure 1-2C), micronemes (figure 1-2D), rhoptries (figure 1-3E), dense granules (figure 1-2F) (Morrissette and Sibley, 2002) and subpellicular microtubules (figure 1-2G) (Weiss and Kim, 2007; Graindorge *et al.,* 2016).
2. Organelles derived from endosymbiotic processes, the mitochondria (figure 1-2H) and apicoplast (figure 1-2I) (van Dooren and Stripen, 2013; Sheiner *et al.,* 2013; Ngano *et al.,* 2014). The apicoplast is indispensable for apicomplexan parasite growth and survival because of its role in the synthesis of many important metabolites for instance: heme, fatty acids, isoprenoid and iron sulphur synthesis (Fichera and Ross, 1997).
3. Eukaryotic organelles like a nucleus (figure 1-2J) located close to the cell center, the nuclear envelope (figure 1-2K) associated with endoplasmic reticulum (ER) (figure 1-2L), and 3-5 Golgi cisternae (Ngo *et al.,* 2000; Weiss and Kim, 2007; Sheiner *et al.,* 2013). ER is the organelle where the parasite's proteins are synthesized, then trafficked to the anterior end of the organelle and continue

their journey to the Golgi apparatus and the specialized organelles (Joiner and Roos, 2002). Golgi apparatus is involved in rhoptry biogenesis and also forms the inner membrane complex (IMC) (figure 1-2M), a unique structure in *T. gondii* (Hu *et al*., 2002).

Figure (1-2) *T. gondii* cell structure (adopted and modified from Baum *et al.,* 2006) A: apical complex, B: conoid, C: apical rings, D: micronemes, E: rhoptries, F: dense granules, G: subpellicular microtubules, H: mitochondria, I: apicoplast, J: nucleus, K: nuclear membrane, L: endoplasmic reticulum, M: inner membrane complex.

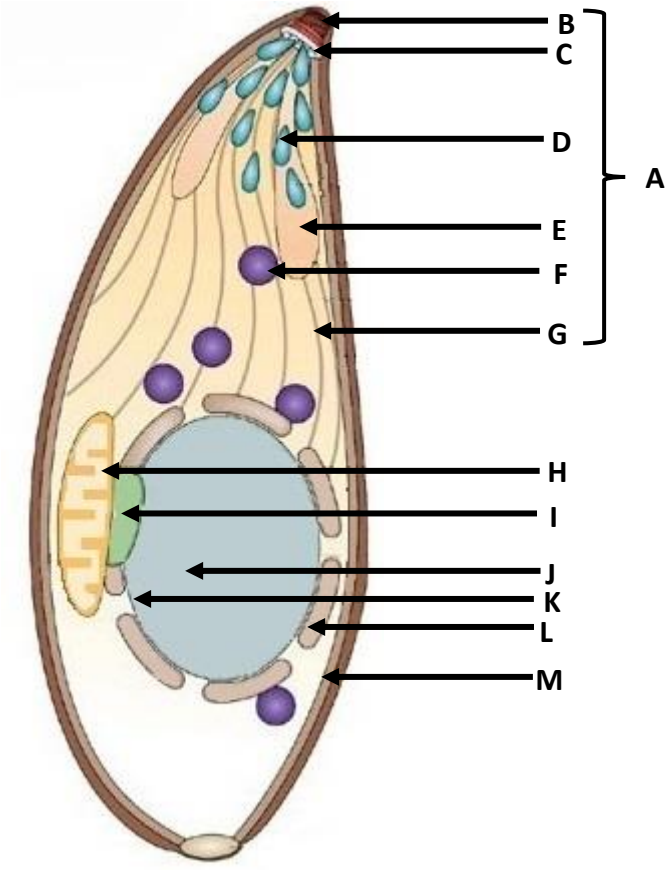

1.4.1 Apical complex

Phylum apicomplexa, including *T. gondii* is characterized by having a unique apical complex (Hu *et al.,* 2006; Shanmugasundram *et al.,* 2012) located at the anterior end of the parasite (Morissette and Sibley, 2002; Healsip *et al.,* 2009). This complex plays a substantial role in the parasite's cell division and host cell invasion processes (Shen and Sibley, 2012 ; Kemp *et al.,* 2013 ; Katris *et al.,* 2014) because it contains secretory

organelles such as rhoptries, micronemes and dense granules (Blader and Saeij, 2009). At the anterior tip of this complex is the conoid (Figure 1-3 A).

1.4.2 The conoid

The conoid is defined as a tube-like structure, consisting of 14 tubulin filaments arranged tightly together as a counter clockwise spiral (Morissette and Sibley, 2002; Hu *et al.,* 2002). It is approximately 280 nm long with a diameter of 380 nm (Hu *et al.,* 2002). The conoid has more than 170 proteins (Hu *et al.,* 2006). Two of them, lysine methyltransferase and ring protein 2 (RNG2), have demonstrated a role in the parasite's motility (Healsip *et al.,* 2011 ; Katris *et al.,* 2014). The conoid is immotile and retracted in an intracellular tachyzoite, but extruded and motile in an extracellular parasite where it helps the host cell invasion process (Del Carmen *et al.,* 2009) (Figure 1-3 B). High Ca^{+2} concentration is thought to be necessary for conoid extrusion due to the Ca^{+2} role in activation of microneme secretion which are play an important role in conoid extrusion (Del Carmen *et al.,* 2009). Furthermore, Carey *et al.* (2004) used an inhibitor to block conoid extrusion and found that the parasites lost their ability to invade the host cell. However, this inhibitor did not effect motility and microneme secretion (Weiss and Kim, 2007).

Unlike other apicomplexan parasites *Plasmodium* spp. lack this structure, possibly it is not needed as this parasite infects red blood cells easily (Mondragon and Frixione, 1996). In contrast, *T. gondii* must penetrate rigorous barriers such as the intestinal epithelium cells, and conoid is essential for this.

1.4.3 The micronemes

Micronemes are secretory organelle located at the apical tip near the conoid (Carruthers and Sibley, 1997; Sher *et al*., 2016). The word microneme is derived from the Greek word "small thread", and their number range between 50 and 100 (Weiss and Kim, 2007). These structures secrete many microneme proteins (MICs) (Ngo *et al.,* 2000) that are indispensable for the invasion process (Blackman and Carrunthers, 2013; Coffey *et al.,* 2016). For example, apical membrane antigen 1 (AMA1) orients the parasite to the host cell and is involved in invasion (Mital *et al.,* 2005;

Krishnamurthy *et al.,* 2016) and the formation of the moving junction between the parasite and the host (Graindorge *et al.,* 2016). Furthermore, micronemes secrete proteins like MIC2, an adhesin regarded an important for motility, and MIC8 which is important for rhoptry secretion (Brossier and Sibley, 2005; Giovannini *et al.,* 2011).

1.4.4 The rhoptries

Rhoptries are club-shaped secretory organelles located at the anterior end of the parasite (Coffey *et al.,* 2016; Graindorge *et al.,* 2016). Each parasite has 8-16 rhoptries (Porchet-Hernnere *et al.,* 1983 ; Black and Boothroyd, 2000). They secrete rhoptry proteins (ROPs) (Ngo *et al.,* 2000) such as ROP16 and ROP18 which both help the parasite during the invasion process and are associated with lipids to form parasitophorous vacuole membrane (PVM) that segregates the parasite from the host cell (Coffey *et al.,* 2016; Sher *et al.,* 2016). parasitophorous vacuole (PV) is a unique compartment found in apicomplexan infection where the parasite can salvage the nutrients from the host for their advantage, and it facilitates fast egress and dissemination from the host cell (Ngo *et al.,* 2000; Frénal and Soldati, 2009; Katris *et al.,* 2014). Suss-Toby *et al.* (1996) and Blader and Saeij *et al.* (2010) proposed that the PVM lipids are derived only from the host plasma membrane, and there is no evidence that there are taken from host intracellular organelles such as the ER, Golgi apparatus and lysosome. Importantly, the PV protects the parasite from the external environment and gives it the ability to survive and replicate (Sibley *et al.,* 1985; Sher *et al.,* 2016).

1.4.5 Dense granules

These are generally defined as secretory organelles that releases their proteins (GRAs such as GRA16 and GRA24) (Ngo *et al.,* 2000) (Graindorge *et al.,* 2016) after PV formation (Montoya and Liesenfield, 2004). These proteins are transferred through the PVM to the host cell cytoplasm and nucleus (Bougdour *et al.,* 2014) where they cause a manipulation of host cell pathways, remodeling them for the benefit of the pathogen (Bougdour *et al.,* 2014).

1.4.6 Polar rings

These are located beneath the conoid (Figure 1-3 C), and serve as the origin of twenty-two subpellicular microtubules (Figure 1-3 D). (Hu *et al.,* 2006) that work as the microtubular organizing center and are responsible for the parasite's shape and stability (Black and Boothroyd, 2000; Katris *et al.,* 2014; Wakeman *et al.,* 2014; Francia *et al.,* 2016).

1.4.7 Pre-conoidal rings

This structure surrounds the conoid at the anterior end (Figure 1-3 E). From these rings two intraconoidal apical microtubules (Figure 1-3 F) emanate and pass via the conoid's center to end within the body of the cell (Black and Boothroyd, 2000).

1.4.8 Microtubules

T. gondii has many microtubules indispensable for parasite survival and propagation. For instance, twenty-two subpellicular microtubules (Figure 1-3 D). which are responsible for parasite's shape and polarity, emanate from apical polar ring (APR). In addition, two intra-conoidal microtubules (Figure 1-3 F) begin in the APR and penetrate the conoid ending within the body of the cell. These function as an underpinning structure for the secretion of proteins from dense granules, micronemes and rhoptries during invasion (Carruthers and Sibley, 1997; Hu *et al.,* 2006; Healsip *et al.,* 2009).

Figure (1-3) Apical complex (adopted and modified from Liu *et al.,* 2013)

A: apical complex, B: conoid, C: polar rings, D: subpellicular microtubules, E: pre-conoida ring, F: intra conoidal microtubules.

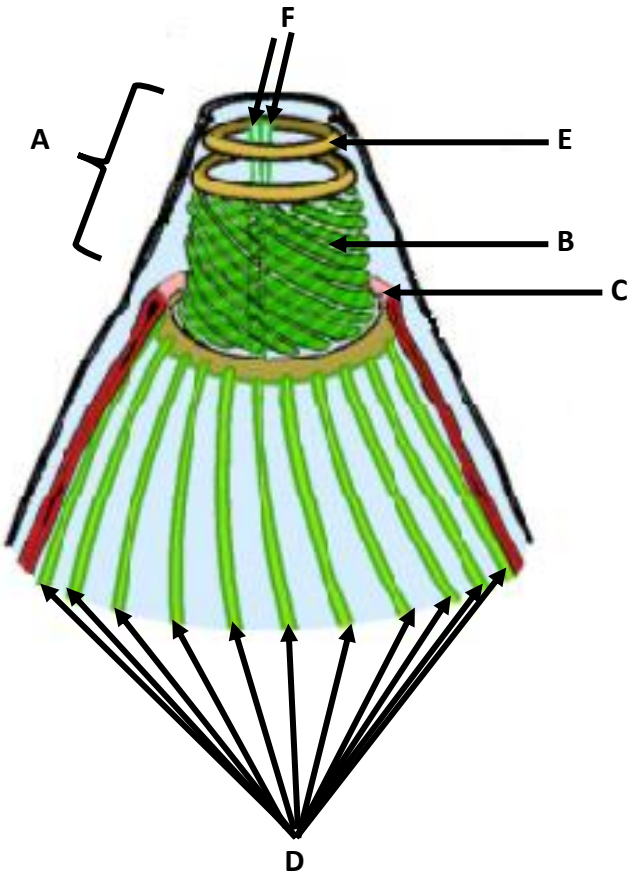

1.5 Host-parasite interaction

T. gondii is regarded as one of the most successful intracellular parasites (including viruses, bacteria and fungi) (Roy and Mocarski, 2007) because it can invade any nucleated host cell (Graindorge *et al.,* 2016).

To overcome the negative charge of both parasite and host cell membranes *T. gondii* requires receptor-ligand interactions. The parasite plasma membrane consists of from the set of surface antigen proteins (SAGs) predominantly SAG1 (Manger *et al.,* 1998) which linked by glycosylphosphatidylinositol (GPI) to the membrane, these mediate attachments to the host cell (Black and Boothroyd, 2000).

Several studies demonstrated that the host cell pathways manipulated by the parasite after invasion by using cDNA microarray (a large gene-scale gene expression

analysis). These experiments indicated that the expression of more than 1000 host genes involved in fundamental processes (including inflammation, apoptosis, metabolism, growth and differentiation) was manipulated (Blader *et al.*, 2001; Chaussabel *et al.,* 2003). Blader *et al.*, 2001 stated that these changes belong to one of three specific classes: (1) 'Pro host' when the host expresses genes required for host defense; (2) 'Pro parasite' when the host expresses genes required for parasite growth; and finally (3) 'Bystander' which means that the expressed genes influence both host defense and parasite growth.

As mentioned above, a recent study has shown that after invasion the *T. gondii* manipulates host expression in the nucleus using the dense granule proteins GRA16 and GRA24 (Coffey *et al.,* 2016). These and other parasite factors manipulate host cell gene expression to create an advantageous environment for survival (Bougdour *et al.,* 2014), for example by avoiding lysosomal degradation and establishing a safe PV.

T. gondii lytic cycle comprises five stages: the attachment, invasion, PV formation, proliferation and egress to infect neighbouring host cell (Black and Boothroyd, 2000). To facilitate these processes *T. gondii* has a unique molecular machinery called the glideosome composed of myosin A and gliding associated proteins (GAPs). The glideosome is located in the space between the inner membrane complex (IMC) and the parasite plasma membrane (PPM) (Soldati*,* 2008). IMC is a unique structure in *T. gondii* (Frénal and Soldati-Favre, 2009) composed from flattened vesicles located between subpellicular microtubules and PPM (Cavalier and Smith, 1991; Graindorge *et al.,* 2016), due to the presence of this structure *T. gondii* and the other apicomplexans belong to the class, Alveolata (Cintra and Souza, 1985; Frénal and Soldati, 2009). In *T. gondii,* the glideosome consists of two myosin A heavy and light chains in addition two glideosome associated proteins (GAPs) GAP45 and GAP50, all of these anchor the glideosome to IMC (Daher and Soldati-Favre, 2009). The glideosome function is to translocate the microneme proteins (adhesins) from the anterior end to the posterior end of the parasite and to allow it to drive into the host cell (Graindorge *et al.,* 2016). In addition, the adhesins play another role, in association with proteins such as *Tg*AMA1 (Mital *et al.,* 2005), in the formation of a complex (Besteiro *et al.,* 2011) with a group of proteins secreted from an elongated

section of the rhoptries called the rhoptry neck contains rhoptry neck proteins (RONs) (Blader and Saeij, 2010). This complex establishes a tight zone, called the moving junction, by which the parasite can enter the host cell (Shen and Sibley, 2012; Katries *et al.,* 2014; Graindorge *et al.,* 2016; Krishnamurthy *et al.,* 2016). *T. gondii* can then start their journey through the host cell (Frénal and Soldati, 2009).

Bioinformatic analyses of the parasite genome gave clues on how the parasite survives within the host cell by the having the ability to salvage small molecules such as glucose, arginine, tryptophan, iron and purine nucleosides. These molecules cannot be synthesized by *T. gondii de novo* pathways but can diffuse through the PVM to reach the parasite (Fox *et al.,* 2004).

Li *et al.,* 2013 found that the parasite salvages some lipid molecules from the host. Certain lipids were absent in the extracellular parasite but present in intracellular *T. gondii,* indicating that the parasite salvaged these from the host.

1.6 The Life Cycle of *Toxoplasma gondii*

T. gondii needs final and intermediate hosts to complete its life cycle (Black and Boothroyd, 2000; Frénal and Sldati, 2009) (figure 1-4). The final, or definitive hosts for this parasite are domestic cats and other members of the family Felidae. The intermediate hosts are pigs, sheep, birds and rodents. The life cycle begins when cats shed unsporulated oocysts (figure 1-4-1) in their faeces which then take from 1-5 days to sporulate in the environment and become infectious. The intermediate hosts (e.g. birds and rodents in nature; pigs and sheep in agriculture) become infected by ingesting soil, water or plant materials contaminated with oocysts (which represent the infective stage) (Del Grande *et al.,* 2017), after ingestion the oocysts (figure 1-4-2) transform into the fast dividing tachyzoite stage (Sump *et al.,* 2017), invade the host lamina propria and gut epithelium (Frencia *et al.,* 2016), then replicate asexually inside the host cell through a unique replication process in *T. gondii* called endodyogeny (Gubbels *et al.,* 2008). In this process, the mother cell is divided by internal budding into two daughter cells (Nishi *et al.,* 2008), the parasites then egress from the host cell to infect new cells (Sher *et al.,* 2017). These tachyzoites proliferate in many locations, such as neural and muscle tissue, eyes, and the placenta (Many

and Koren, 2006). Tachyzoites can develop into tissue cyst bradyzoites (figure 1-4-3) to protect themselves from the human immune system, these cysts may remain throughout the life of the host (Black and Bothroyd, 2000; CDC, 2013). If ingested, for example in contaminated meat, the host stomach digests the wall of tissue cyst releasing the bradyzoite which is then convert to tachyzoites which can then infect most cells (Blader and Saeij, 2010). Definitive hosts, such as domestic cats, become infected either by eating intermediate hosts that contain tissue cysts (figure 1-4-4), or by ingestion of the sporulated oocysts shed by other Felidae (CDC, 2013; Del Grande *et al.,* 2017) (figure 1-4-5).

Humans, who are end point intermediate hosts (Sher *et al.,* 2016), can be infected by (CDC, 2013):

1. Eating the uncooked meat containing tissue cysts (figure 1-4-6).
2. Ingestion of foods and water contaminated with cat faeces or via contaminated environmental samples (such as fecal-contaminated soil or cat litter boxes) (figure 1-4-7).
3. By blood transfusion or organ transplantation (figure 1-4-8).
4. Transplacentally from mother to fetus (figure 1-4-9).

Figure (1-4) The Life Cycle of *Toxoplasma gondii* (adopted from Woodhall *et al.*, 2014)

1. Oocysts. 2. Oocysts transform into tachyzoites. 3. Tachyzoite localized in muscle tissue or neural develop into tissue cyst bradyzoites. 4. Cats may also infected by eating intermediate hosts that contain tissue cysts. 5. Animals can become infected by ingesting oocysts. Humans can become infected by many ways: 6. By eating raw meat that contains tissue cysts. 7. Eating food or drinking water contaminated with cat feces. 8. By blood transfusion or organ transplantation. 9. From mother to fetus by via the placenta. Diagnosis is usually through serology but *T. gondii* 10. Can be directly detected in tissue cysts or 11, Its DNA can be detected in amniotic fluid using molecular techniques such PCR

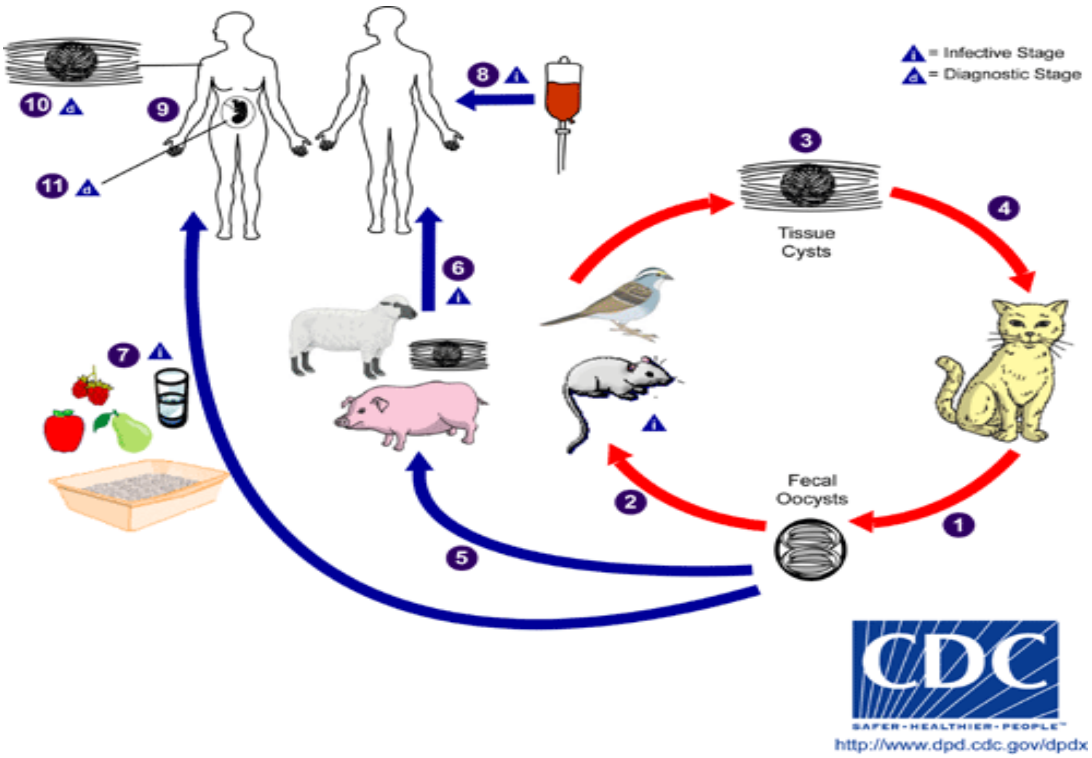

1.7 Diagnosis and treatment of *Toxoplasma gondii* infection

Laboratory diagnosis for infection by *T. gondii* relies on the detection of specific anti-*Toxoplasma* immunoglobulins from blood (IgM for recent and IgG for historic infections) or PCR from urine samples (Many and Koren, 2006; Calderaro *et al*., 2009). Although it is possible to detect, it is very difficult to treat.

When *T. gondii* infects the host, the first response it mediated by macrophages, lymphocytes and dendritic cells (Filisetti and Candolfi, 2004). IFN-γ production triggers the anti-parasitic activity of macrophages and natural killer cells, including the production of reactive oxygen intermediates such as nitric oxide (Lang *et al*., 2007). This immune response usually controls the parasite but does not clear the infection, however in some circumstances, especially in immunocompromised patients and congenitally infected children, infection can cause severe disease. Therefore, the need to use drugs to control the infection by *T. gondii* is clear (Barbosa *et al*., 2012).

The treatment of apicomplexan parasite infection depends upon chemotherapies which target several pathways important in metabolism, for instance folate metabolism, hemoglobin digestion and fatty acid biosynthesis (Muller and Hemphil, 2011). There are several drugs that are used for the treatment of *Toxoplasma* infection, such as sulfonamides and pyrimethamine which both inhibit folate metabolism, and spiramycin whose mode of action is unknown (Karimi, 2011; Palencia *et al.,* 2017).

Furthermore, numerous drugs which are used for *T. gondii* treatment usually depend on mode of infection, for instance: spiramycin in case of acute toxoplasmosis in pregnant women; a combination of pyrimethamine, sulfadiazine and leucovorin in case of infection after 12-18 weeks of gestation; pyrimethamine, sulfadiazine, leucovorin and corticosteroid in case of congenital toxoplasmosis infection in the infant. Finally, acquired immune deficiency syndrome (AIDS) patients who are infected by acute toxoplasmosis can be treated by the following drugs: pyrimethamine and sulfadiazine plus leucovorin or clindamycin; trimethoprim; leucovorin plus one of the following: clarithromycin, atovaquone, azithromycin or dapsone (Montoya and Liesenfeld, 2004).

However, these drugs can cause many side effects such as nausea, vomiting, fatigue, dizziness, dry mouth, headache, itching, muscle aches and pains (Bihari, 2008). These range from acute, thus requiring medical attention, to mild and of little concern. Principally they can also lead to treatment non-compliance (Bihari, 2008). For example, spiramycin causes gastrointestinal symptoms, sulfonamides are associated with neonatal jaundice and pyrimethamine is an antagonist of folic acid and so it is generally not recommended for use during pregnancy (Many and Koren, 2006). These drugs are effective against the tachyzoite in acute disease, but do no effect the encysted bradyzoite stage (Palencia *et al.,* 2017). In addition, combination therapy with pyrimethamine and sulfadiazine is associated with multiple toxicity problems such as the suppression of bone marrow function and congenital malformations in the early stages of pregnancy (Barbosa *et al*., 2012). Such major side-effects, coupled with a lack of efficacy, are regarded as the main causes of failure in the process of drug development (Tatonetti *et al*., 2009; Coppens, 2013).

Therefore there is need to look for the alternative treatments focusing on parasite specific, essential metabolic pathways that are not found in their host. To disrupt these parasite pathways, specific small molecule inhibitors of drug targets (enzymes, receptors, ion channels etc) need to be identified (Gashaw *et al*., 2012). In order to meet the challenges of new therapy discovery*,* recent work has focused on the lipid species and biosynthetic enzymes found in *T. gondii,* and other apicomplexan parasites, but not in their mammalian hosts (Denny *et al.,* 2006; Mina *et al.,* 2009). These pathways are now regarded as appropriate drug targets in efforts to find alternative *T. gondii* treatments with less side effects than current therapies (Sonda and Hehl, 2006; Denny *et al.,* 2006).

1.8 Sphingolipids

Lipids are important structural components of cell membranes regulating the permeability between the extracellular and intracellular compartments (Ohanian and Ohanian, 2001; Pralhada Rao *et al*., 2013). There are two major classes of lipids, glycerolipids and sphingolipids (SLs), and both play an important role in numerous cell processes, including signal transduction (Ohanian and Ohanian, 2001; Pratt *et al*.,2013).

SLs were first discovered by Thudichum in 1876, and are regarded as an essential class of lipids that are ubiquitous constituents of eukaryotic membranes (Bartke and Hannun, 2009). SLs play a major role in regulating many important processes, such as apoptosis, angiogenesis, genetic diseases and chemotherapy resistance (Ogretmen and Hannun*,* 2004; Merill, 2002; Heung, 2006; Pratt *et al.,* 2013). The basic structural characteristic of SLs is a sphingoid backbone, which can be distinguished amongst mammalian and yeast and plant cells. In mammals sphingosine is the most common sphingoid base, whilst phytosphingosine is more common in yeast and plants (Ohanian and Ohanian, 2001). There are many enzymes and metabolites involved in mammalian SL biosynthesis, changes in enzyme activity and metabolite levels as result of alterations in gene expression can lead to severe diseases such as Alzheimer's disease (Haldar *et al*., 2002).

The initial steps of *de novo* SL synthesis lead to the formation of ceramide (Michael and Echten-Deckert, 1997; Bartke and Hannun, 2009).This occurs on the cytosolic surface of the ER (Bartke and Hannun, 2009 ; Romano *et al.,* 2013) and begins with the condensation of serine and palmitoyl coenzyme A to form 3-keto-dihydrosphingosine (KDS), a reaction catalyzed by the enzyme serine palmitoyltransferase (SPT) (Denny *et al.,* 2006 ; Bartke and Hannun, 2009 ; Beattie *et al.,* 2013 ; Genin *et al.,* 2016). Three kinds of SPT-related genes have been identified in eukaryotes, SPTLC1 (LCB1), SPTLC2 (LCB2) and SPTLC3 (Hanada *et al.,* 2003; Ikushiro and Hayashi, 2011; Genin *et al.,* 2016) (figure 1-5). The active site of SPT is centered on a lysine (Merrill, 2002). The core eukaryotic SPT is a heterodimer, containing LCB1 and LCB2 (Buede *et al*., 1991, Nagiec *et al*., 1994). In mammals, an additional subunit SPTLC3 has been identified (Hornemann *et al.,* 2006). Mutation in

human LCB1 and LCB2 (Han *et al*., 2009) leads to hereditary sensory and autonomic neuropathy type I (HSAN1) (Beattie *et al.,* 2013).

KDS is subsequently reduced to dihydrosphingosine, then acylated and desaturated to form ceramide in mammals whereas, in yeast and plants, dihydrosphingosine is hydroxylated to form phytosphingosine before acylation to create phytoceramide (Heung *et al.,* 2006). In mammalian systems, the ceramide formed is incorporated into complex SLs such as sphingomyelin (SM) and glycosphingolipids (GSLs) in the Golgi apparatus, whilst in fungal and plant cells phytoceramide is used to form inositol-containing complex SLs, inositolphosphoryl ceramide (IPC) and its mannosylated derivatives. Many fungi also use phytoceramide to produce glucosylceramide (Figure 1-5).

Sphingosine and ceramide perform key roles in this pathway, for instance as substrates to produce sphingosine-1-phosphate (S-1-P) and ceramide-1-phosphate (C1P). Ceramide and sphingosine works as tumor-suppressor lipids by modulating cellular processes like apoptosis, growth arrest and differentiation. Meanwhile C1P and S1P acts as tumor-promoting lipids participated in cell proliferation, migration, inflammation and blood vessel development (Hanada, 2005, Pralhada Rao *et al*., 2013). High levels of pro-growth SLs like S1P lead to an increase in the proliferation of cancer cells which results in the avoidance of therapy-induced apoptosis (Gottesman, 2002). Low levels of cellular ceramide induce the same effect (Pralhada Rao *et al*., 2013).

Two metabolic pathways result in ceramide formation, the first one is the *de novo* anabolic route oulined above which consists of a series of enzymatic reactions which produce ceramide from the simple components (Delgado *et al.,* 2006). The second is a catabolic pathway, the hydrolysis of complex SLs particularly SM and glycosphingolipids (GSLs) (Delgado *et al*., 2006). Ceramide accumulation induces cellular apoptosis and is associated with many diseases such as Type II Diabetes Mellitus (T2DM) (Chavez *et al*., 2003), Alzheimer's disease (Beattie *et al*., 2013, Lindholm *et al*., 2006) and hepatocellular carcinoma (Pralhada Rao *et al*., 2013).

SL biosynthesis appears to be largely conserved in the parasitic protozoa. However, whilst some parasites such as *P. falciparum* produce SM like mammalian cells others,

for example the kinetoplastid *Leishmania* species, produce fungal/plant-like IPC (Mina *et al.,* 2009), the following key SLs are produced from this pathway:

1. SM is an abundant ingredient of animal plasma membranes where it forms 5-15% of total lipids (Tafesse *et al.*, 2007). SM production is catalyzed by SM synthase (SMS). There are two orthologues of this enzyme in mammals SMS1 and SMS2: SMS1 located at the Golgi apparatus and SMS2 at the plasma membrane (Huitema *et al*., 2004, Tafesse *et al*., 2007). SM is found in a high concentration in the outer leaflet of the plasma membrane where, by its affinity to sterols, it helps establish a solid barrier to the extracellular environment and forms specialized microdomains in the plasma membrane (PM) called lipid rafts (Denny *et al*., 2006). These rafts play essential roles in signal transduction and the polarized trafficking of lipid modified proteins (Simons, and Ikonen, 1997; Pratt *et al.,* 2013). These sterol and sphingolipid rich lipid rafts are found in parasites such as *Entamoeba histolytica, Giradia lamblia, Leishmania* spp*., Trypanosoma* spp. and *T. gondii.* The lipid rafts play fundamental roles in invasion by regulating the adhesion to host, perturbing host cell rafts leading to the dysregulation of membrane function and easing the establishment of infection, and eluding the host immune response (Goldston *et al*., 2012). In order to show the roles of lipid rafts in adhesion, *Giardia lamblia* and *Entamoeba histolytica* were treated with a cyclic compound chelating cholesterol, methl-β-cyclodextrin (MβCD), were unable to adhere to the host cells (Humen *et al*., 2011, Welter *et al*., 2011). Moreover, Goldston *et al.,* 2012 showed that *T. cruzi* treated with MβCD were inhibited in invasion, suggesting a role for lipid rafts in this process. Additionally, lipid rafts work as a reservoir for lipid signaling molecules including ceramide, sphingosine and S-1-P which are responsible for many pivotal intracellular processes such as apoptosis, cell proliferation and differentiation (Ogretmen and Hannun, 2004, Spiegel and Milstien, 2003).
2. IPC synthesis is catalyzed by inositol phosphorylceramide synthase (IPCS) through the transfer of a phosphorylinositol head group from phosphatidylinositol to ceramide (Denny *et al*., 2006) (figure 1-5). IPCS (and IPC) is absent in mammalian cells and so it is regarded as one of the most attractive drug targets for certain fungal and protozoan pathogens. Indeed, modulation of

the production of SLs is regarded as one of the primary new strategies in therapeutic treatment of infectious and non-infectious diseases (Wedsworth, 2013), thus most of the future studies in this field will be focused on the enzymes that play important roles in sphingolipid biosynthesis, such as SPT and IPCS (Denny *et al.,* 2006; Mina *et al.,* 2009). There are small numbers of specific inhibitors for SPT all of which are natural products, for example lipoxamycin, viridiofungin A, sphingofungins and myriocin (Wedsworth, 2013). Similarly there are a few specific, natural compound, inhibitors of the fungal IPCS, such as cyclic depsipeptide aureobasidin A (AbA) which was isolated from the fungus *Aureobasidium pullulans* R106 (Ikai *et al.* 1991 ; Takesako *et al.* 1993).

All eukaryotic cells thus far studied (animal, plant, protozoa and fungi) synthesize SLs *de novo*. In addition, even though non-eukaryotes do not generally synthesize these lipids, many bacterial and viral pathogens depend on the host SLs to promote virulence (Casadevall and Pirofski, 2003; Heung *et al.,* 2006). Some studies have reported that the eukaryotic parasites, such as *T. gondii,* also salvage lipids from the host, including cholesterol and phospholipids (Coppens *et al.,* 2000; Charron *et al.,* 2002). However, *T. gondii* also depends on *de novo* lipid synthesis, for instance of phosphatidyl choline (PC) particularly when host PC is limited (Charron *et al.,* 2002). This study demonstrated that host PC is not essential for parasite growth and survival and indicated the importance *de novo* synthesis in parasitism (Pratt *et al.,* 2013 ; Alqaisi *et al.,* 2017).

The recent studies have focused on the SL biosynthetic pathway because the final products, and the synthetic enzymes, are different in mammals, fungi, plants and protozoan parasites (Denny *et al.,* 2006; Suzuki *et al.,* 2008; Romano *et al.,* 2013).

Figure (1-5) Sphingolipid biosynthesis pathways of mammalian and fungal cells (adopted and modified from Hanada, 2004).

SPT: serine palmitoyltransferase; IPCS: inositol phosphorylceramide synthase

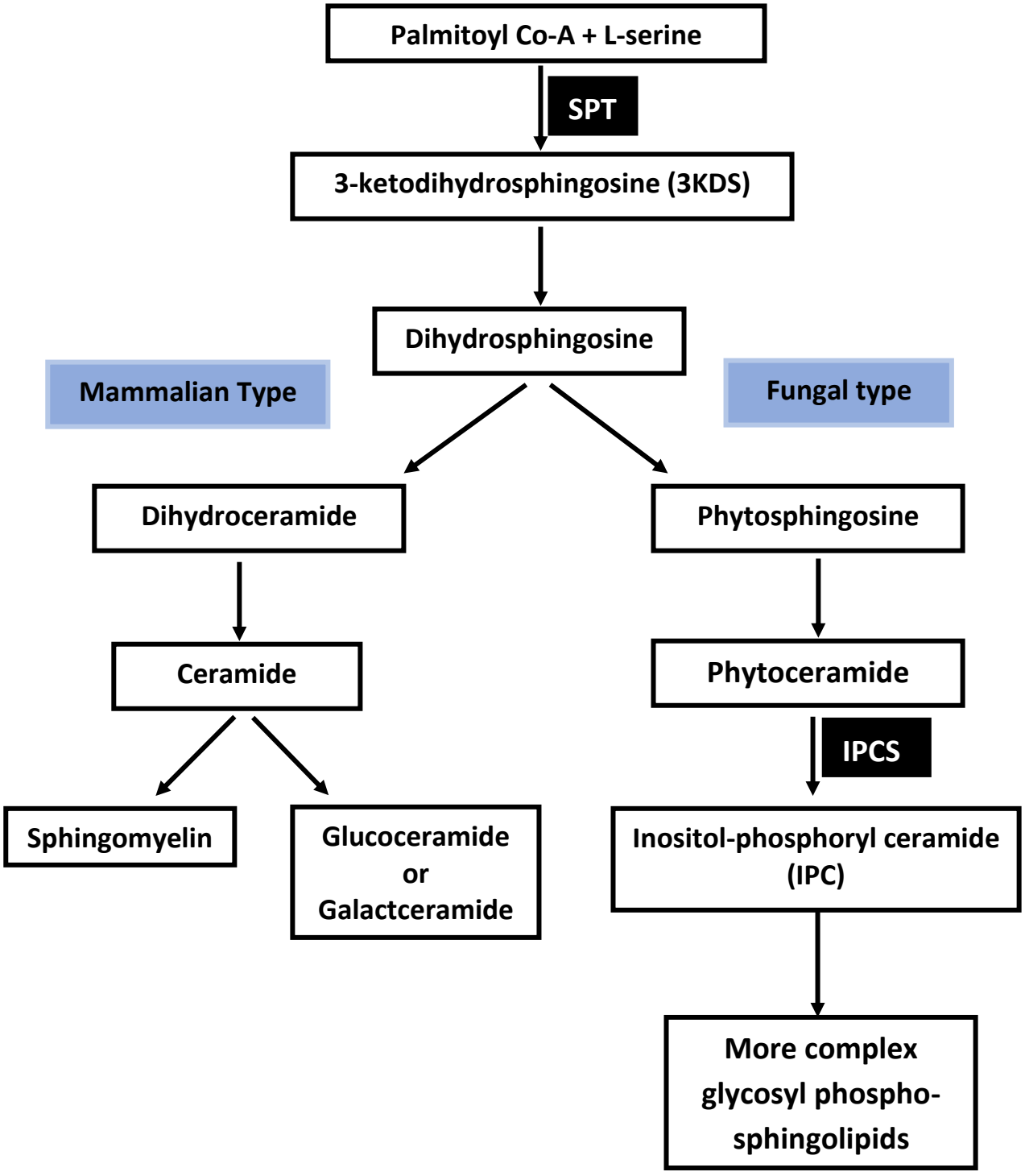

1.9 Sphingolipids in *Toxoplasma gondii*

The negative impact of protozoan pathogens on human health and prosperity is enormous, for example malaria which is caused by the apicomplexan *Plasmodium* spp., is responsible for approximately 214 million cases and more than 439.000 deaths each year. Trypanosomatid parasites, which include *Trypanosoma cruzi*, *Trypanosoma brucei* and *Leishmania spp,* infect 20-30 million people worldwide, causing various diseases ranging from disfiguring skin lesions to lethal systemic disease. Other protozoan parasites like *Giardia spp*. and *Entameoba histolytica* can also cause severe human disease (Zhang *et al.,* 2009). There are currently no vaccines available for any of these diseases and there is a lack of effective drugs for many of them. Many of the available therapies are characterized by low efficacy, high toxicity and wide spread resistance (Simmaro *et al.,* 2004; Croft and Coombs, 2003). Therefore, recent work has focused on identifying parasite-specific essential pathways and developing the novel inhibitors that target them (Zhang *et al.,* 2009).

The structure and function of sphingolipids in parasitic protozoa differ when compared with mammals, fungi and plants. Some protozoa, such as the trypanosomatid *Leishmania spp*., synthesize large amounts of unglycosylated IPC, whereas the related parasite *Trypanosoma brucei* synthesizes SM in addition to IPC (Zhang *et al.,* 2009). The apicomplexan parasite *Plasmodium* spp. synthesizes SM and GSL like their mammalian host, whilst its relative *T. gondii* also synthesizes non-mammalian IPC. IPC, and the biosynthetic enzyme IPCS, are essential for fungi (Mandala *et al*., 1998), plants and trypanosomatid species (Sonda *et al.,* 2005; Pratt *et al.,* 2013). *T. gondii* also contains other SL, including high levels of ethanolamine phosphorylceramide (EPC) but lower levels of SM compared with the mammalian cell host (Welti *et al.*, 2007). In fact, *T. gondii* have more than 20 species of SL consisting of either saturated or unsaturated fatty acids (Lige *et al*., 2011). Despite the ability of *T. gondii* to support *de novo* synthesis the parasite also scavenges SLs from the host cell via the host Golgi or the endocytic system (Bisanz *et al*., 2006; Pratt *et al.,* 2013; Romano *et al.,* 2013).

The many sources of SL for *T. gondii* are listed below:

1. When added exogenously, ceramide is directed towards the host cell Golgi apparatus, where it can be incorporated into SM or GSL and salvaged by the infecting *T. gondii* (Pratt *et al.,* 2013; Romano *et al.,* 2013) (Figure 1-6 A).
2. In the host cell ceramide produced by *de novo* synthesis in the endoplasmic reticulum is transported to Golgi apparatus and converted to SM or GSL which then can be salvaged by *T. gondii* through intercepting Golgi-derived vesicles (Rab14, Rab30 and Rab34) (Romano *et al.*, 2013). When *T. gondii* invades a mammalian it forms its own-membraneous compartment, the PV. Notably the PV is located near the host Golgi and here the parasite can hijack Golgi-derived vesicles and scavenge SL (Romano *et al.,* 2013). These vesicles and soluble transporters in the cytosol, such as ceramide transfer protein (CERT) play important roles in the trafficking of SL (Bartke and Hannun, 2009) (figure 1-6 B).
3. Neutral sphingomyelinase (nSMase), which is in the host plasma membrane (figure 1-6 C) catalyses the hydrolysis of SM, converting it to ceramide which can be scavenged by *T. gondii.*
4. Acid sphoingomyelinase (aSMase) performs a similar role to the neutral sphingomyelinase but is located in the endolysosome (figure 1-6 D).
5. *T. gondii de novo* synthesis, like all eukaryotes, begins with condensation of serine and palmitoyl CoA, catalyzed by serine palmitoyl transferase (SPT), to form 3-ketodihydroshingosine (KDS) which is then converted to ceramide which is subsequently converted to either SM or IPC (Azzouz *et al.,* 2002; Pratt *et al.,* 2013) (figure 1-6 E).

Figure (1-6) showing the sources for sphingolipid for *Toxoplasma gondii* (modified from Romano *et al.,* 2013). PM: plasma membrane; SM: sphingomyeline; SPT: serine palmitoyl transferase; CerS: ceramide synthase; Des: desaturate; ER: endoplasmic reticulum; nSMase: neutral sphingomyelinase; aSMase: acid sphingomelinase; CER: ceramide transport proteins; PV: parasitophorous vacuole; IPC: inositol phosphorylceramide; IPCs: inositol phosphorylceramide synthase.

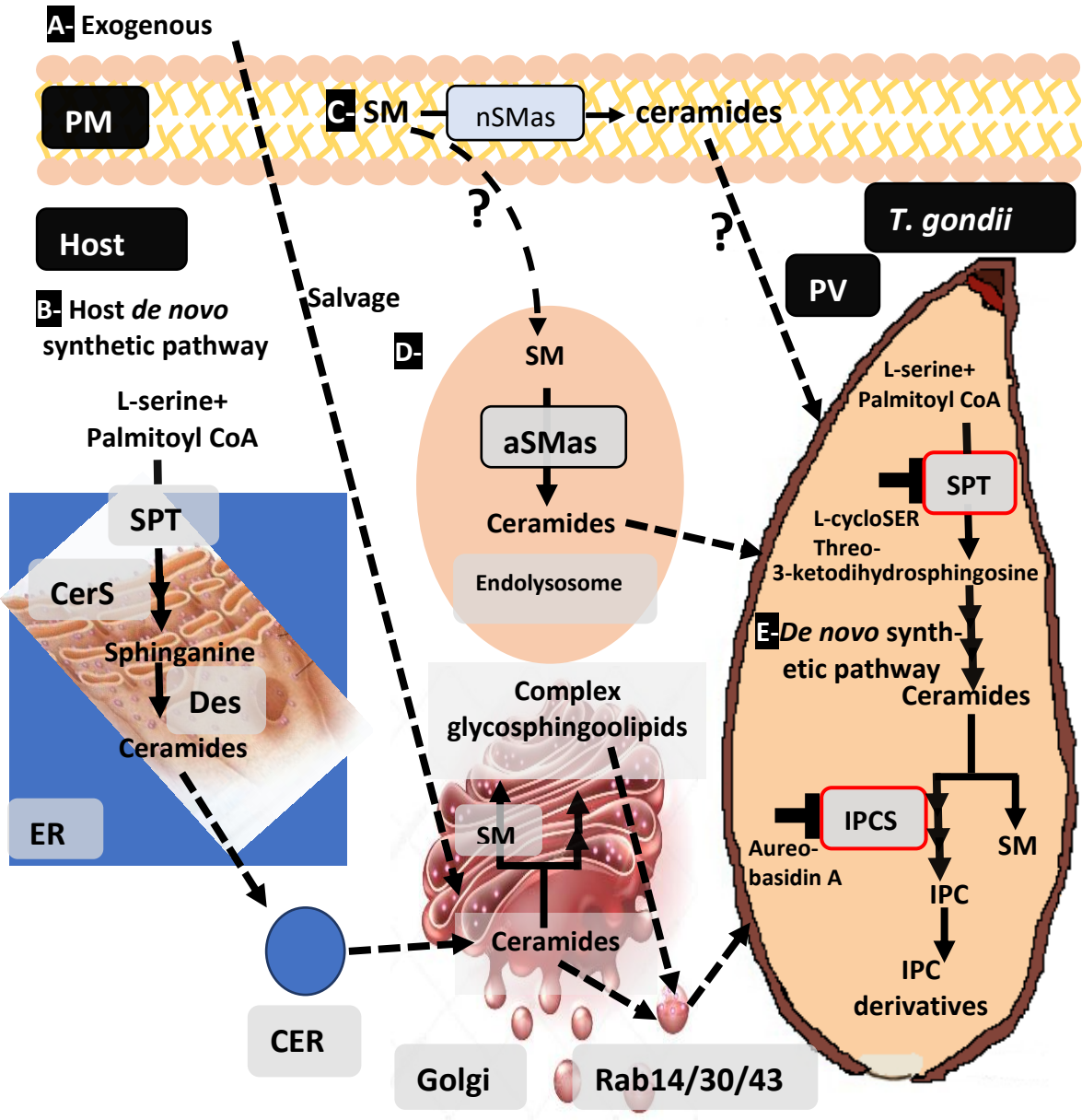

1.10 Kinetoplastids

Kinetoplastids are flagellated parasites characterised by having a structure called kinetoplast which contains DNA, this group includes *Trypanosoma brucei* which causes African sleeping sickness, *Trypanosoma cruzi* the causative agent of Chagas disease, and *Leishmania spp.* which cause leishmaniasis (Burri and Brun, 2003). All the members have a singular flagellum that originates from a basal body near the kinetoplast (region containing the mitochondrial genome) and extends to the outside of the cell (Landfear and Sanchez, 2015). Approximately 500 million persons in tropical and sub-tropical areas are at risk of infection with these parasites, 20 million are estimated to be infected and at least 100.000 deaths result each year (Stuart *et al.,* 2008; Pana *et al.,* 2015). In this study, *Leishmania major* was used as a model to show the global role of SL biosynthesis pathway in the parasite by exploiting the in-house availability of IPCS inhibitors.

1.11 Leishmaniasis

Leishmaniasis is a widespread disease caused by *Leishmania spp. and* transmitted by the sandfly vector. It is estimated that more than 150 million individuals in 98 countries are infected (Alvar *et al.,* 2012; Hurrell *et al.,* 2016), and that 350 million life at risk of infection (Leifso *et al.,* 2007; Bolt *et al.,* 2016; Hurrell *et al.,* 2016). Leishmaniasis has the highest burden of morbidity of all protozoan infections after malaria (Field *et al.,* 2010; Savoia, 2015). This disease is endemic in regions such as Latin America, South East Asia, East Africa and the Mediterranean (Pace, 2014). Distribution is exacerbated in countries suffering from conflict and poor health systems (Beyrer *et al.,* 2007; Kerridge *et al.,* 2012). In addition, it has been demonstrated that *Leishmania*/HIV co-infection in problem in the Mediterranean region and beyond (Monge-Maillo *et al.,* 2014).

Against this backdrop, the World Health Organisiation (WHO) is focusing on leishmaniasis and on the development of the new tools to find effective drugs or vaccines (Desjeux, 2004).

Leishmaniasis is categorized depending on its geographical distribution into two types:

1. Old World leishmaniasis, including the areas of Southern Europe, Mediterranean, Middle East, Asia and Africa (Ready, 2000; McGwire and Satoskar, 2013). In this type, the parasite is transmitted to human by sandflies of the genus *Phlebotomus* (Mansueto *et al.*, 2014; Vermelho *et al.,* 2017).
2. New World leishmaniasis including Latin American (Ready, 2000; McGwire and Satoskar, 2013). In this type, the parasite is transmitted to human by sandflies of the genus *Lutzomiya* (Mansueto *et al.*, 2014; Vermelho *et al.,* 2017).

Leishmania have more than 53 species (Cotton, 2017), 20 of them are infective to humans (Naula *et al.*, 2005; Mansueto *et al.,* 2014; Cotton, 2017). *Leishmania spp.* cause four main diseases depending on the localization of infected macroophages in mammalian tissue, these diseases are: cutaneous (CL), visceral (VL), mucocutaneous (MCL) (Naula *et al.,* 2005) and diffuse cutaneous leishmaniasis (DCL) (Akhoundi *et al.,* 2016). An estimated two million new cases of leishmaniasis occur per year; 500.000 VL and 1.500.000 CL (Mansueto *et al*., 2014; Hurrell *et al*., 2016). The manifestation of these diseases ranges from superficial infection to fatal visceral disease of humans and other animals such as the dogs (Handman and Bullen, 2002), which are a domestic reservoir host for *Leishmania spp.* and play an essential role in the transmission cycle between humans and sandflies (Gramiccia and Gradoni, 2005; Chávez-Fumagalli *et al.,* 2015).

Leishmania spp. can avoid the host immune system using many strategies such as manipulating numerous pathways related to cell signaling and phagocytosis, and modifying the production of cytokines and chemokines in the infected macrophage (Mougneau *et al.,* 2011; Gupta *et al.,* 2013). *Leishmania spp.* can also terminate the apoptotic process of the macrophage. These strategies help the parasite to avoid the immune system and proliferate (Guttierrez-Kobeh *et al.,* 2013).

The most important species that cause CL and MCL are: *L. tropica* which causes CL or dry oriental sore (Hotez, 2008; Handman and Bullen, 2002) and is widely distributed in Asia, Africa and the Middle East (Joshi *et al*.,2008) - particularly Iraq, Iran, Afghanistan, Syria, Morocco, Palestine, Saudi Arabia and Yemen (Postigo, 2010); *L. major,* which has a rodent reservoir (*Rhombomys, Psammomys* and *Arvicanthis*; Handman and Bullen, 2002) and causes a CL or rural, wet oriental sore (Handman and Bullen, 2002 ; Hotez, 2008), it is widely distributed in Iraq, Iran, Afghanistan,

Egypt, Libya, Jordan, Morocco, Palestine, Saudi Arabia, Tunisia, Yemen and Pakistan (Postigo, 2010); *L. braziliensis,* also infects sloths and dogs (Handman and Bullen, 2002), causes CL or MCL in Latin America, particularly Brazil (Carneiro *et al.,* 2016); *L. aethiopica,* also infects the Rock Hyrax, causes CL or DCL primarily in East Africa (Handman and Bullen, 2002). *L. mexicana* which also infects forest rodents, causes CL or DCL (Hotez, 2010), and is found in US, particularly along the border with Mexico (Hotez, 2008).

CL is mostly found in 10 countries: Columbia, Peru, Brazil, Costa Rica, Iran, Syria, Ethiopia, Algeria, Afghanistan and North Sudan (Alvar *et al.,* 2012; Akhoundi *et al.,* 2016). The disease is characterized by a localized lesion at the site of insect bite (Hurrell *et al.,* 2016; Cotton, 2017), particularly on the exposed areas of the body such as the face, forearms and lower legs (Naula *et al.,* 2005; McGwire and Satoskar, 2013). The manifestation starts with a tiny erythema developing into a papule then a nodule, after 2 weeks to 6 months a lesion develops (Reinthinger *et al.,* 2007) with a diameter ranging between few millimeters to several centimeters (Ashford, 2000). MCL is primarily caused by *L. braziliensis,* the symptoms can appear after many years following the initial bite and are characterised by metastatic lesions manifest on the nasal or buccal mucosa, these then develop to destroy parts of face because of the erosion of cartilage (Ashford, 2000; Naula *et al.,* 2005; McGwire and Satoskar, 2013). The distribution of DCL is limited to Latin America (Venezuela and Republic of Dominican) and East Africa (Ethiopia and Kenya). The lesions in this case spread all over the body (Ashford, 2000).

The most important *Leishmania spp.* that cause VL are *L. donovani,* particularly in the Old World, and *L. infantum* in the Mediterranean region and Brazil, where is known by its synonym *L. infantum chagasi* (McGwire and Satoskar, 2013; Messaoud *et al.,* 2017). VL is seen in humans, dogs and savannah rodents (Handman and Bullen, 2002) and is known as kala azar in India, with post kala azar dermal leishmaniasis (PKDL) a major complication. VL is widely distributed but more than 90% of all cases occur in six countries: India, Bangladesh, Sudan, South Sudan, Brazil and Ethiopia (Alvar *et al.,* 2012; Akhoundi *et al.,* 2016). McGregor, 1998 reported that more than 10% of the population died in an outbreak in Southern Sudan because of this infection. VL is characterized by an ulcerated lesion at the site of insect bite (Ashford, 2000) from

where the parasites spread from the skin to other organs, particularly the spleen and liver (Cotton, 2017). This is accompanied by systemic signs appearing after weeks, sometimes years, such as splenomegaly, hepatomegaly and anemia which ultimately lead to the organ failure (Desjeux, 2001; Rice *et al.,* 2016) and death if left untreated (Ashford, 2000 ; Desjeux, 2004 ; Hurrell *et al.,* 2016). In some cases VL symptoms are like those of autoimmune disease which can lead to misdiagnosis and inappropriate treatment, therefore caution is required in diagnosis (Xynos *et al.,* 2009; Sotirakou and Wozniak, 2011).

PKDL is characterised by skin mottling two years after the complete cure of VL (Ashford, 2000).

Furthermore, *Leishmania spp.* are also classified according to the location of development in sandfly gut: *Leishmania leishmania* and *Leishmania viannia* (Foulet *et al.,* 2007; Pace, 2014).

1.11.1 Life cycle

Leishmania spp. are heteroxenous parasites which means they require two hosts to complete the life cycle (Dantas-Torres *et al.,* 2010; Solano-Gallego *et al.,* 2012; Akhoundi *et al.,* 2016): a vertebrate host (including humans) and an invertebrate vector, the sandfly (Handman and Bullen, 2002). *Leishmania spp.* has two life cycle stages, the intracellular amastigote stage in vertebrate host macrophages, and the extracellular promastigote stage in sandfly vector (Leifso *et al.,* 2007; Singh and Singh, 2012; Hurrell *et al.,* 2016). Life cycle starts when the vertebrate hosts are infected by *Leishmania spp.* via the bite of infected female sandfly (Akhoundi *et al.,* 2016). Inside the vertebrate host, the inoculated metacyclic promastigotes (the infective stage) are phagocytosed by macrophages which form a phagosome, this fuses with lysosome to form a phagolysosome where the promastigote differentiates into the amastigote (the pathogenic stage) (Handman and Bullen, 2002; Sereno *et al.,* 2007) (figure 1-7). In CL the infected macrophages are derived from inflammatory monocytes, whilst in VL the parasites infect Kupffer cells, the macrophage cells in both the spleen and bone marrow (Kaye and Scott, 2011; Ribeiro-Gomes *et al*., 2012). The CL symptoms takes 2 weeks to 3 months to be shown (Goto and Lindoso, 2010), whilst it takes 1-12 months in ML (Fletcher *et al.*, 2015). The amastigote is characterised by its round shape (diameter 5 µm) and the ability to survive and

multiply within phagolysosomes (Ashford, 2000; Cotton, 2017). Amastigotes have kinetoplasts like promastigotes, but only immature flagella, they multiply by longitudinal binary fission until the host cell bursts and the parasites infect another cell (Ashford, 2000). Subsequently, a sandfly can ingest this stage via a blood meal when they feed on the blood from infected person, then inside the insect gut it transforms into the promastigote stage which is characterised by an elongated body and a well developed flagellum emanating from the kinetoplast (Ashford, 2000). This stage needs 8-20 days to transform to infective metacyclic promastigotes (Gossage *et al.,* 2003; Desjeux, 2004). In some cases, *Leishmania spp.* can be transmitted from human to human without the insect vector, such as by organ transplantation, sexual contact and blood transfusion (Ansari *et al* 2013; Monge-Maillo and López-Vélez, 2013). Leishmaniasis can also spread from an endemic to non-endemic area by many ways, such as urbanization, natural catastrophe, tourism and armed combat (Reithinger *et al.,* 2007; Soreno *et al.,* 2007).

Figure (1-7) Depiction of the *Leishmania spp.* life cycle (adopted and modified from Stuart *et al.,* 2008)

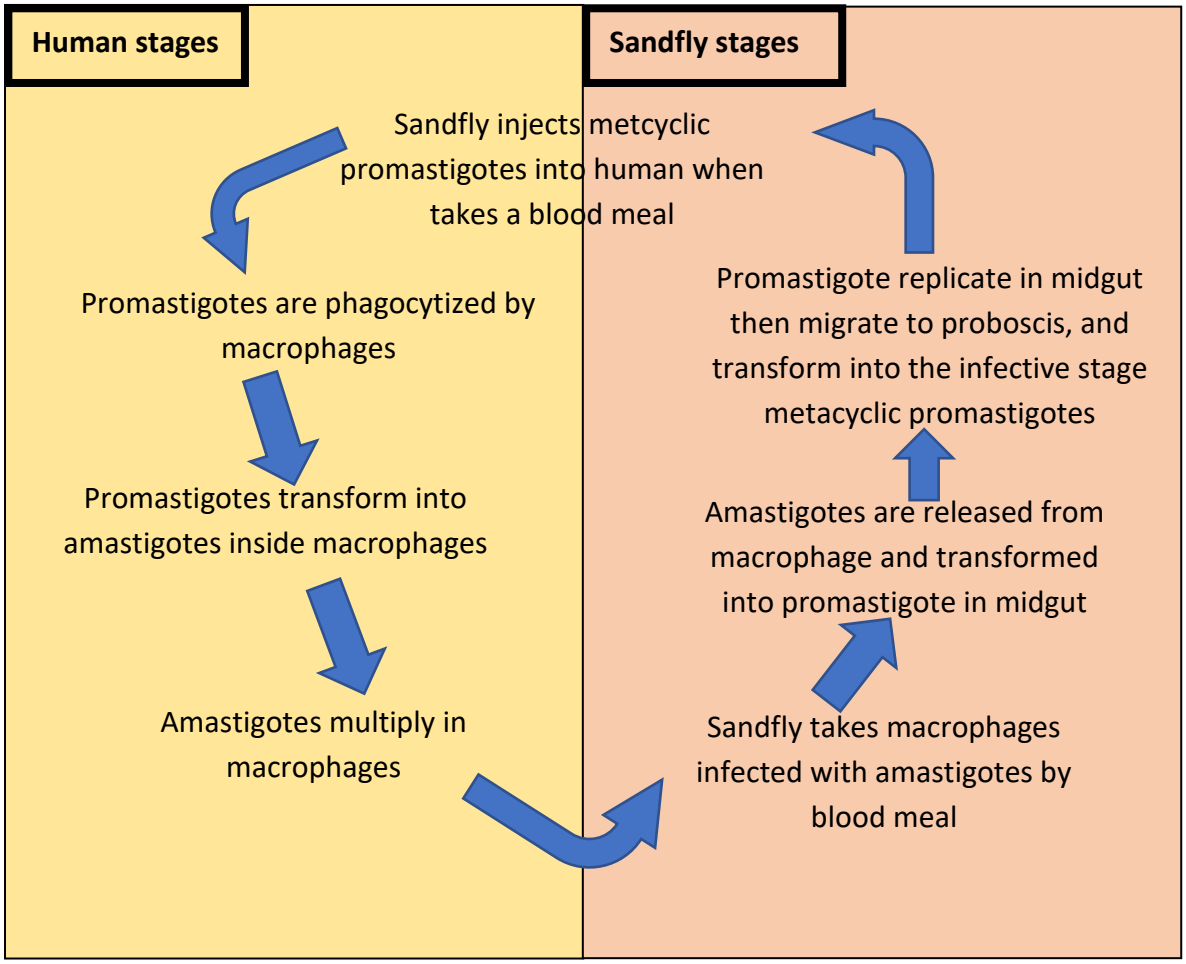

1.11.2 Diagnosis

Depending on its location and the infecting species, leishmaniais is diagnosed by one of these methods:

1. In CL a skin biopsy to examined microscopically for amastigotes (Reed, 1996; Desjeux, 2004; Stuart *et al.,* 2008).
2. In VL amastigotes are looked for microscopically in a blood smear or aspirates from bone marrow or spleen (Ashford, 2000).
3. In VL serological tests are also used such as Enzyme Linked Immunosorbent Assay (ELISA), the ImmunoFluorescence Antibody Test (IFAT) and direct agglutination (Desjeux, 2004).

1.11.3 Treatment

A limited range of drugs is available for use against *Leishmania spp.* infections (Bolt *et al.,* 2016). The historic, first line drugs are the pentavalent antimonials (Sb^{v}), Pentostam (sodium stibogluconate) and Glucantime (meglumine antimoniate) (Tuon *et al.,* 2008; Kedzierski *et al.,* 2009; Chadbourne *et al.,* 2011; Chávez-Fumagalli *et al.,* 2015). These drugs have an unclear mode of action, exhibit many side effects exemplified by renal failure and cardiotoxicity (Chappuise *et al.,* 2007; McGwire and Satoskar, 2013; Chávez-Fumagalli *et al.,* 2015), and require parenteral administration (Demicheli *et al.,* 2004). In addition, because they have been in use for more than 70 years, ago, the parasite is showing resistance against pentavalent antimonials (Croft and Coombs, 2003; Chappuise *et al.,* 2007; Bolt *et al.,* 2016).

Paromomycin is an aminoglycoside antibiotic that is active against both bacteria and *Leishmania spp.* (Singh and Singh, 2012). Its mechanism of action against bacteria is the inhibition of protein synthesis by binding to 16s rRNA, it is unclear in *Leishmania spp.* Paromomycin has many side effects such as nephrotoxicity and effects on the vestibular system, particularly related to the inner ear leading to vestibular instability. This drug also requires parenteral administration (Ben Salah *et al.,* 2013). Amphotericin B (Fungizone) is very active against *Leishmania spp.* and has become a first line drug in a liposomal formulation (AmBisome) (Meyerhoff, 1999; Goldstone *et al.,* 2012; McGwire and Satoskar, 2013; Chávez-Fumagalli *et al.,* 2015).

Amphotericin B was first established as an anti-fungal (Marcondes *et al.,* 2011). Fungi contain ergosterol as their primary sterol and the mechanism of action of amphotericin B is binding to this sterol that is also a plasma membrane component in *Leishmania spp.* (Barratt and Legrand, 2005 ; Chávez-Fumagalli *et al.,* 2015 ; Vermelho *et al.,* 2017). This leads to cell death because of increased cell permeability and the leaking of intracellular contents (Seifert, 2011; Castillo *et al.,* 2010; Goldstone *et al.,* 2012; Vermelho *et al.,* 2017). AmBisome is used for VL treatment in the endemic areas such as Bihar, India where resistance to antimonials compounds is a problem (Saravoltaz *et al.,* 2006). However, its high cost is a limiting factor (Sundar *et al.,* 2001; Desjeux, 2004; Chávez-Fumagalli *et al.,* 2015). Amphotericin B requires parenteral administration and exhibits side-effects such as nephrotoxicity, liver damage, hemolysis and cardiac alterations, although these are reduced in the liposomal formulation AmBisome (Annaloro *et al.,* 2009; Singh and Singh, 2012).

Pentamidine is a second line drug (Singh and Singh, 2012), and its mode of action has been proposed as binding with macromolecules such as DNA, RNA, lipids and proteins. Pentamidine has many side effects including cardiotoxicity such as heart failure, hypotension, in addition to hypoglycemia, leukopenia, anemia and nephrotoxicity. In addition, it requires parenteral administration (Hellier *et al.,* 2000).

Miltefosine was developed as an anti-cancer drug (Dorlo *et al.,* 2012; Rice *et al.,* 2016) and is the first oral drug for leishmaniasis. It is now used for CL and VL (Croft and Coombs, 2003; Soto *et al.,* 2009; Bolt *et al.,* 2016), particularly from 2002 in India (George *et al.,* 2006). Its mode of action has been proposed to be the manipulation of *Leishmania spp.* intracellular Ca^{+2} homeostasis (Serrano-Martin, 2009; Benaim *et al.,* 2013). Ca^{+2} plays important roles in parasite invasion and differentiation (Moreno and Docampo, 2003; Benaim *et al.,* 2013), so disruption of Ca^{+2} homeostasis can be anti-parasitic. Its adverse effects are nausea and vomiting, and because it is teratogenic it is not recommended for the treatment of pregnant women (Naula *et al.,* 2005; Sundar *et al.,* 2006; Dorlo *et al.,* 2012; Singh and Singh, 2012).

In addition to the drugs above, other types of treatment are used for leishmaniasis such as: cryotherapy used to treat CL caused by *L. tropica, L. aethiopica* and *L. infantum,* with liquid nitrogen once to up to five times for 3-7 days (Negera *et al.,* 2012); and heat therapy which is recommended for HIV patients with CL who do not

respond to the classical treatments, the lesion is heated to 50˚C for 30 seconds up to 3 times per day (Reithinger *et al.,* 2005; Bumb *et al.,* 2013).

1.11.4 Anti-leishmanial drug targets

No active vaccines are available against *Leishmania spp.* (Chadbourne *et al.,* 2011; Bolt *et al.,* 2016) in addition, as described above, drug treatments are limited with many problems. Therefore, there is now a need to design effective drugs with less adverse side-effects (Vyas and Gupta, 2006). However, the development of new drugs takes between 10 and 20 years and costs up to $1 billion (Bleicher *et al.,* 2003; Hughes *et al.,* 2011). Therefore new, well validated drug targets are essential. The properties of such targets are: i. It is fundamental for parasite growth and survival; ii. It is preferably unique to the parasite; iii. If both host and the parasite have the same pathway, a drug should be selective (Fairlamb, 2003; Frearson *et al.,* 2007). Also it is important to develop more than one drug for each pathogen to obviate the resistance when it emerges (Stuart *et al.,* 2008).

Thus, the recent studies have focused on the fundamental metabolic pathways in *Leishmania spp.,* and particularly on the enzymes that catalyze reactions in these pathways that may be new drug targets (Denny *et al.,* 2006; Singh and Singh, 2012; Pratt *et al.,* 2013; Vermelho *et al.,* 2017).

1.11.5 Leishmania spp. sphingolipid biosynthetic pathway

The primary complex SL in *Leishmania spp* is IPC, which is estimated as comprising 5-10% of total membrane lipids (Zhang *et al.,* 2005). As discussed above, IPC synthase (IPCS) is a non-mammalian enzyme that catalyzes the transfer of phosphorylinositol from phosphatidylinositol to the 1-OH group of ceramides or phytoceramide to form IPC (Lester and Dickson, 1992; Hsu *et al.,* 2007; Mandlik *et al.,* 2012). IPCS is an essential enzyme in *Saccharomyces cerevisiae,* where it is known as AUR1p (Nagiec *et al.,* 1997; Hsu *et al.,* 2007) and is an attractive target for anti-fungal drugs such as aureobasidin A (Nagiec *et al.,* 1997; Zhong *et al.,* 2000; Wuts *et al.,* 2015). Zhang *et al.,* (2003) showed that both *Leishmania spp.* stages (amastigote and promastigote)

have a high IPC levels and IPCS is an attractive drug target in this protozoan parasite (Denny *et al.* (2006).

1.12 Aim of the study

It has been shown that the salvage of SLs from the host is non-essential for *Toxoplasma gondii* proliferation and pathogenesis, indicating the importance of *de novo* SL synthesis in this protozoan pathogen (Pratt *et al.,* 2013). It is well known that the enzymes that mediate protozoan SL biosynthesis represent key drug targets (Denny *et al*., 2006; Young *et al.,* 2012) and the currently poorly characterized pathway in *Toxoplasma* has also been proposed as a target for chemotherapeutic intervention (Sonda *et al.,* 2005; Pratt *et al.,* 2013). Using bioinformatics and biochemical approaches the pivotal, but divergent, enzymes in *Toxoplasma* biosynthesis have been identified in the Denny laboratory. This project aims to functionally characterize key identified enzymes in the biosynthetic pathway and investigate the possibility of targeting the pathways therapeutically. In addition, using *Leishmania major* and the availability of in house identified inhibitors, the global role of SLs in a model protozoan was investigated using metabolomic and lipidomic approaches.

Chapter Two:
Materials and Methods

2.1 Materials

The materials used in this study were described in table (2.1):

Table 2.1 The materials and their source:

Materials	Source
96 well assay plate, black plate	Costar
96 well assay plate, cell culture cluster, flat bottom with low evaporation lid	Costar
Acid glass beads	SIGMA
Agar Granulated broth	Melford
Alamar blue	Invitrogen
Aureobasidin A and analogue Cmpd20	AureoGen
Chloroform	Fisher
Chloroform Chromasolv	SIGMA
DAPI Fluoromount	Southern Biotech
Dream Taq DNA Polymerase	Thermo Scientific
Dulbecco's Modified Eagle Medium DMEM	Gibco® by Life Technologies
EDTA	SIGMA
Efficiency® DH5α competent cells	Invitrogen
Ethanol	Fisher
F-12+Glutamax™ nutrient Mixture (Ham)	Gibco® by Life Technologies
Fetal calf serum	Labtech

FluoroBrite™ DMEM Media	Gibco® by Life Technologies
ImPromII Reverse Transcriptase System	Promega
In-Fusion® HD Cloning Kit	Takara
KCl	BDH
LB broth granulated	MELFORD
L-Serine	SIGMA
L-Glutamine	SIGMA
Membrane filters 5 µM and 3 µM	Millipore
Methanol	Fisher
Methanol LC-MS ultra chromasolv UPLC-MS	FLUKA
Midiprep kit	QIAGEN
Miniprep kit	QIAGEN
NaCl	MELFORD
NBD-C_6-Ceramide complexed to Bovine Serum Albumin (BSA)	Life Technologies
PBS tablets	Invitrogen
PBS tablets	Gibco
Penicillin/Streptomycin-Glutamine solution	Hyclone
Platinum® Taq DNA Polymerase High Fidelity	Life Technologies
Palmitoyl Co-A	SIGMA
Power broth	Molecular Dimension

Restriction enzymes: NotI, XhoI, HindIII, SacII, PacI and EcorI	Thermo Scientific
RNeasy Mini Kit	QIAGEN
Schneider's Insect Medium	SIGMA
Schneider's medium	SIGMA
SDS	SIGMA
SYBR®Green Jump Start™	SIGMA-ALDRICH
T4 DNA Polymerase LIC qualified	Novagen
Terreffic broth	SIGMA
Tris	SIGMA
Trypsin-EDTA 10X 5%	Gibco® by Life Technologies

Vero cells, RHΔHX *Toxoplasma gondii* and the plasmid *Tg*CATtsag1KO were supplied by Dominique Soldati, University of Geneva. Δku80-HXG *T. gondii* (Huynh and Carruthers, 2009) were supplied by Vern Curruthers, University of Michigan. RH-HX-KO-YFP2-DHFR *T. gondii* were supplied by Boris Streipen, University of Georgia. The plasmids pG27 LIC-YFP-DHFR and pG1 mycGFPPfmyoAtailTy were supplied by Markus Meissner, University of Glasgow. P30 GFP_HDEL (Pfluger *et al.,* 2005) and P30 GRASP_RFP (Catherine and Linstedt, 2016) were supplied by Kristin Hager, University of Notre Dame. Mouse anti-TY monoclonal antibody was supplied by Keith Gull, University of Oxford. Human Foreskin Fibroblast (HFF) cells were supplied by ATCC (UK). Chinese Hamster Ovary (CHO) cells were supplied by the Riken Cell Bank (Japan).

2.2 Transformation protocol

2.2.1 Preparation of Luria broth (LB) broth and LB agar

2.2.1.1 LB broth

This broth was prepared by adding 25 g of LB broth in 1L distilled water

2.2.1.2 LB Agar

This agar was prepared by adding 25g of LB broth, 15 g of agar-agar in 1L distilled water.

2.2.2 Transformation to the competent cells

Aliquots of the chemically competent cells E. coli DH5α were thawed on ice, once thawed 50 µl of the cells were transferred to an Eppendorf tube, then 1-5 µl of the diluted plasmid DNA (100 pg – 100 ng) were added, and mixed well by swirling the tube, then incubated on ice for 30 minutes (mins). Heat shock was performed in a water bath at 42°C for 30 seconds (sec), then cells are put on ice again for 2 mins. 250 µl of LB broth or pre-warmed S.O.C. media without antibiotics was added to the cells, then incubated for 1 hr in a shaking incubator at 37 °C.

About 100-200 µl of cells were plated on the LB agar with antibiotic (Ampicillin 100 mg/ml), and left for several minutes to dry, then incubated at 37 °C for 16-20 hours.

2.2.3 Isolation of Plasmid

A single colony from an LB agar plate was taken, and inoculated into a 5 mL LB broth with appropriate antibiotics (Ampicillin 100 mg/ml), and mixed together in a shaker incubator at 37°C overnight. The plasmid DNA was prepared using a miniprep kit (QIAGEN) according to manufacturer's protocol. The plasmid DNA concentration was measured by nanodrop (ThermoFisher).

2.3 Gel Electrophoresis

Agarose gel 0.8% (V/V) was prepared by dissolved 8.0g of agarose in 1000 ml 1X TAE buffer (SIGMA). DNA samples were mixed with 6X DNA loading dye (1:5, QIAGEN), then loaded on the agarose gel then, using BioRad 3000 power pack, run at 100 volts for 45 mins.

2.4 Cell culture

Dulbecco's Modified Eagle Medium (DMEM) was used for cell culture, and was prepared by adding heat-inactivated Fetal Calf Serum 10% and penicillin/streptomycin 1%. Vero and HFF cells, and RHΔHX, RH-HX-KO-YFP2-DHFR and Δku80-HXG *T.* gondii were maintained in DMEM media at 37°C and 5% CO_2 CHO cells were maintained in F-12+Glutamax™ nutrient mixture (Ham), 10% Fetal Calf Serum and 1% penicillin/streptomycin, at 37°C and 5% CO_2.

2.5 RNA Extraction from CHO cells

Two T25 flasks of CHO cells maintained in DMEM media were prepared and one infected with $5x10^6$ parasites. After 72 hours CHO cells were detached from the T25 flasks by adding Trypsin/EDTA and the RNA extracted using the RNeasy kit according to the QIAGEN protocol. The concentration of RNA was measured by a Nanodrop 2000 Spectrophotometer (Thermo Scientific).

2.6 Preparation cDNA from RNA

The ImPromII Reverse Transcriptase System protocol provided by Promega was followed to synthesize cDNA from RNA samples:

1. The experimental RNA was thawed on ice.
2. The reaction sample was made for each of infected and uninfected CHO cells in cooling condition as follows:

	Infected CHO Samples		**Uninfected CHO Samples**	
	Experimental	**Negative**	**Experimental**	**Negative**
RNA (up to 1 µg)	X µl	-	X µl	-
Random primers	1 µl	1 µl	1 µl	1 µl
Nuclease-free water	X µl	4 µl	X µl	4 µl
Final volume	**5 µl.**	**5 µl.**	**5 µl.**	**5 µl.**

The positive control was prepared as following:

3. 1.2 Kb Kanamycin Positive Control RNA (1 µg) 2 µl
4. Oligo (dT) Primer (0.5 µg/reaction) 1 µl
5. Nuclease free-water 2 µl
6. The tubes were placed into a preheated 70°C heat block for 5 mins then immediately chilled in ice-water at least 5 mins. before centrifugation for 10 seconds.
7. Reverse transcriptase reaction mix was prepared as follows:

Nuclease free water	5.7 µl
ImPromII 5x Reaction Buffer	4.0 µl
$MgCl_2$	2.8 µl
dNTP mix	1.0 µl
Recombinant RNasin	0.5 µl
ImPomII Reverse transctiptase	1.5 µl
Final volume	**15 µl**

8. 15 µl was added to 5 µl of each reaction sample and mixed together to make a final volume 20 µl.
9. Using an Eppendorff Thermocyler the following protocol was followed:

a. Anneal: 25°C for 5 mins

b. Extend: 42°C for 1 hr.

c. Inactivate Reverse Transcriptase: 70°C for 15 mins.

10. Then for PCR amplification the following primers used were:

Cgβ-tubuline forward primer:	5′TAAAACGACGGCCAG*TG*AGC3′
Cgβ-tubuline reverse primer:	5′TCTCC*TG*GCGAG*TG*C*TG*C3′
CgLCB2 Forward primer:	5′CAGACAACTT*TG*TTTTCGG3′
CgLCB2 Reverse primer:	5′GGG*TG*GCAT*TG*TAGGGC3′
CgSMS1Forward primer:	5′GCTCTTAGACA*TG*ATCGAGAC3′
CgSMS1Reverse primer:	5′CCAACTA*TG*CAGAAAAATCTT3′
CgSMS2Forward primer:	5′AGCTTATCCAACGGGCTACG3′
CgSMS2Reverse Primer:	5′GAGTCTCCGT*TG*AGCTTCGG3′

For conventional PCR and the following steps were followed.

Preparation master mix of PCR was as follows:

10X Dream Taq Buffer	5 µl
dNTP mix 2mM	5 µl
Forward primer	1 µl
Reverse Primer	1 µl
cDNA	1 µl
Dream Taq DNA Polymerase	0.5 µl
Nuclease Free water	36.5 µl
Total volume	**50 µl**

For LCB2, SMS1 and SMS2 primers and β-tubulin primers, 35 cycles of amplification in an Eppendorf thermocycler following the program:

Process	Time	Temperature
Initial denaturation	95°C	3 mins.
Denaturation	95°C	30 sec.
Annealing	55°C	30 sec.
Extension	72°C	1 min.
Final extension	72°C	15 mins.

11. After PCR amplification, all the samples were separated on a 0.8% agarose gel in tris-acetate buffer.
12. For Real Time PCR the SYBR®Green Jump Start™ Taq ReadyMixä (SIGMA ALDRICH; Catalog number: S4438) was utilised following the manufacturer's protocol and the Real Time Thermal cycler Rotor-Gene™ 3000 (Corbett Research).

2.7 Metabolic labelling of *Toxoplasma gondii*, vero cells

T. gondii RHΔHX tachyzoite infected vero cells were disrupted by passing through a narrow-gauge needle (23G) and the milieu filtered through 3 µm polycarbonate filters to remove contaminating host material (Weiss and Kim, 2007). *T. gondii* were isolated by centrifugation at 1430g for 15 minutes at room temperature, and then resuspended in DMEM without serum and counted using a Neubauer haemocytometer. 10^7 parasites were resuspended in 1ml of serum-free DMEM, washed twice, then incubated with 990 µl free serum medium and 10 µl of Aureobasidin A AbA (1 mg/ml) or its analogue Compound 20 (Cmpd20) (1 mg/ml) for 1, 4 and 7 hours. After washing 2 times with serum-free DMEM, 10 µl of 0.5 mM fluorescent NBD-C_6-ceramide complexed to Bovine Serum Albumin (BSA) was added and the samples incubated at 37°C for 1 hour. *T. gondii* tachyzoites were then pelleted by centrifugation and washed twice with DMEM, membrane lipids were then extracted by bi-phasic separation, 200 µl of

Chloroform : Methanol : Water (10:10:3 v/v/v) was added to the dry pellet and the samples were incubated overnight before the addition of 50 µl of water and the separation of the organic phase containing the extracted lipids. The organic solvent phase was concentrated in Rotavapor Eppendorf concentrator 5301 at 30 °C for 20 minutes and the dried pellets resuspended in 20 ul for C:M:W 10:10:3. Thin Layer Chromatography fractionation was then carried out using high performance (HP) TLC silica plates with a solvent phase of Chloroform : Methanol : 0.25% KCl (55:45:10 v/v/v) for 30 – 45 minutes. The plate was scanned by using the Fuji®FLA 3000 and analysed by AIDA Image FLA software. Vero cells were scraped from tissue culture flasks and washed twice with dH_2O, then resuspended at 10^6/ml, and resuspended in 990 µl serum-free media and 10 µl of Aureobasidin A AbA (1 mg/ml) or its analogue Cmpd20 (1 mg/ml), and incubated for 1, 4 and 7 hours at 37 °C and 5% CO_2, then washed 2 times with serum-free DMEM. To monitor sphingolipid biosynthesis in vero cells, 10 µl of 0.5 mM fluorescent NBD-C_6-Ceramide complexed to BSA was added and the samples then incubated at 37°C and 5% CO_2 for 1 hour. Cells were then pelleted by centrifugation and prepared and analysed as above.

2.8 Metabolic labelling of Yeast

YPH499 yeast cells were used in this experiment. A colony from an YPD agar plate was inoculated into YPD broth and grown in a shaking incubator at 30°C overnight. The cells were harvested by centrifugation at 1000g for 5 mins at 4°C, and resuspended in 990 µl YPD at a concentration of 2.5 OD 600nm. The cells were incubated for 1 hour at 30 °C, then 10 µl of Aureobasidin A AbA (1 mg/ml) or its analogue Cmpd20 (1 mg/ml) was added, and the cell further incubated for 1, 4 and 7 hours at 30 °C. 10 µl of 0.5 mM fluorescent NBD-C_6-Ceramide complexed to BSA was added then the cells were harvested again by centrifugation, washed twice with PBS, resuspended in 0.4 ml Chloroform: Methanol (1:1 v\v) and homogenized using acid washed glass beads 0.6 ml. Following centrifugation, the solvent phase was prepared and analysed as above.

2.9 Yeast susceptibility assay

YPH499-HIS-GAL-AUR1 complemented with *TgSLS* or AUR1 (Denny *et al.,* 2006; Pratt *et al.,* 2013) were assayed for susceptibility to Aureobasidin A (AbA) and Cmpd20. The transgenic yeast strains were maintained on SGR -HIS -URA agar (0.17% Bacto yeast nitrogen base, 0.5% ammonium sulphate, 4% galactose, 2% raffinose, containing the appropriate nutritional supplements) at 30°C. To analyse susceptibility to AbA and Cmpd20 plates containing 5 and 10 µg/ml of the compounds were prepared and 10 µl of an aqueous suspension of one yeast colony spotted onto the surface before incubation at 30 ◦C.

2.10 Study the effect of AbA and Cmpd20 on *Toxoplasma gondii* proliferation

This experiment was designed to determine the 50% effective dose (ED_{50}) of fungal inositolphosphoryl ceramide (IPC) inhibitors Aureobasidin A (AbA) and its analogue Cmpd20 on *Toxoplasma gondii* proliferation using a 96-well plate growth assay (Gubbels *et al.,* 2002). In order to reduce the media fluorescent background, DMEM media without phenol red (Life technologies) was used in this experiment, 1% glutamine, 1% of sodium pyruvate, 1% penicillin/ streptomycin and 10% FCS were added to the media.

The protocol as following:

Day1: The primary cell line human foreskin fibroblasts (HFF) cells were seeded in black 96 black well plates, clear bottom with lid (Costar), concentration $1x10^5$ cell/ml in 100 µl DMEM media without phenol red. Cell incubated at 37°C and 5% CO_2 for 24 hours.

Day2: The media was removed, and the cells were washed with PBS, then *T. gondii* RH-HX-KO-YFP2-DHFR (Gubbels *et al.,* 2002) tachyzoites at 6250 parasite/well in 50 µl were added.

Day3: The compounds (AbA and Cmpd20, in DMSO) in concentrations starting from 10 µg/ml and Equilibriate DMSO concentration were added in each well. Wells were washed at 1,4 or 7 hours with media if required.

The plate was read every 24 hours for 7 days by using Synergy H4 Hybrid Reader (BioTek) excitation 510 and emission 540.

To measure the effect of the 2 compounds on *T. gondii* invasion the parasite cells were treated at the same range of concentration for 1,4 and 7 hours before infecting the HFF cells and proceeding as above.

2.11 *Toxoplasma gondii* serine palmitoyltransferase 2 (*Tg*SPT2) expression and purification

The open reading frame of *Tg*SPT2, lacking the first 158 amino acids, was codon optimised for *E. coli,* synthesized and cloned into the expression vector pOPIN3C by GenScript (figure 2-1). Rossetta II *E. coli* were transformed as above, with the plasmid pOPIN_HIS_SUMO_C3_*Tg*SPT2. and selected on LB agar plates containing 50µg/ml ampicillin and 17 µg/ml chloramphenicol. The plates were incubated at 37°C overnight and a single colony added to 20 ml starter culture Power Broth (PB) media: prepared by adding PB broth 52g to 8 ml glycerol 50%, then the final volume 1 liter was prepared by adding high purify water, then autoclaved at 121°C for 15 mins. After autoclaving, ampicillin to 50 µg/ml, chloramphenicol to 17 µg/ml and 1% w/v glucose were added to this media. The cells were incubated at 37°C and 175 rpm overnight. After overnight incubation, 10 ml of starter culture was transferred into 500 ml Terrific Broth (TB) media culture: prepared by adding 30g TB broth to 10 ml glycerol 50%, then the volume filled up to 1 litre, the media autoclaved at 121°C for 15 mins, then ampicillin to 50 µg/ml and chloramphenicol to 17 µg/ml were added to this media. The culture was incubated at 37°C and 140 rpm until the optical density (O.D.) reached to OD_{600} = 0.5, the growth was followed up by measuring 1 ml each hour, when the growth reached to this point the temperature was shifted down to 25°C and incubation continued for 22-24 hours, 140 rpm. The growth was then transferred to the centrifuge tube (500 ml), spun at 4000g at 4°C for 30 mins, the supernatant was discarded, and the pellets were weighed and stored in sterile 50 ml falcon tubes at -80°C until use.

Figure (2-1) pOPIN3C plasmid map (generated by SnapGene) (Berrow *et al.*, 2007)

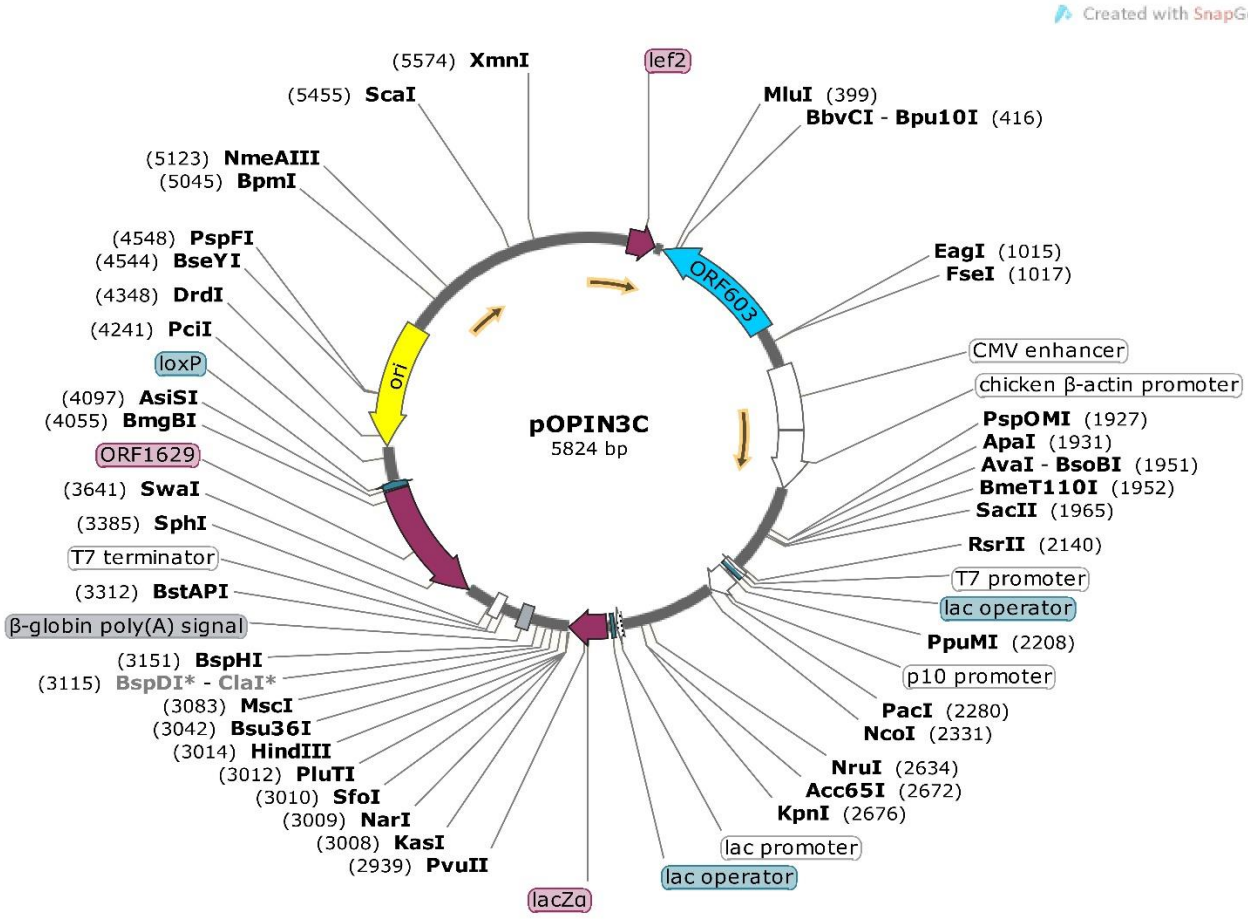

2.11.1 Bacterial pellet lysis

The pellets were thawed on ice, 2 ml of lysis buffer (50 mM Tris Base, 500 mM NaCl, 20 mM imidazole, 0.2% Tween 20 (v/v) at pH 7.5) was used to suspend the pellet by adding 2ml per 1 g pellet. 1 tablet of mini EDTA-free protease inhibitor was added per 15 ml, 50 mg/ml deoxyribonuclease (DNase) and 50 mg/ml ribonuclease (RNase) were added. The solution was mixed by vortex until the pellet was fully suspended. The suspension was sonicated with 2 pulses for 5 mins (30 seconds sonication and 30 seconds on ice). The mixture was centrifugated at 42000g for 30 mins at 4°C in order to remove cell debris and insoluble fractions. The supernatant was then passed through a 0.22 µm filter to remove any debris.

2.11.2 Immobilised Metal Affinity Chromatography (IMAC)

By using an AKTA Explorer Fast Protein Liquid Chromatography (FPLC), a HIS Trap FF 5 ml column (GE Helathcare) was first washed with water, then equilibrated with wash buffer (50 mM Tris Base, 500 mM NaCl, 20 mM imidazole, 25 μM PLP, 5% glycerol (v/v) and pH 7.6. The supernatant from cell lysis was loaded onto the column via injection of the sample. An AKTA program was run to incrementally add elution buffer (50mM Tris Base, 500mM NaCl, 1M imidazole, 25μM PLP, 5% glycerol (V/V), pH 7.6) to the IMAC column at a gradient of 0-100%. 5ml protein containing fractions were collected and put together in one Vivaspin 20 (Generon) Falcon tube, centrifuged for 15 mins, and the protein concentration measured by Nanodrop (Thermo Scientific).

2.11.3 Analyses of Protein

The resultant protein was analysed by using Sodium Dodecyl Sulphate Polyacrylamide Gel Electrophoresis (SDS-PAGE) at 180V, 400 mA for 1 hour., the solution and buffers used in this gel are as follows:

2.11.3.1 Resolving solutions

This solution was prepared as following: 30% acrylamide, resolving Buffer [187 g Tris Base (1.5 M), pH 8.8 with HCL; 4g SDS (0.4%), dH2O to 1L], ammonium persulphate (APS) 10%, dH_2O, TEMED.

2.11.3.2 Stacking solutions

This solution was prepared as following: 30% acrylamide, stacking Buffer [60.5 g Tris Base; 4.0 g SDS (0.4%); dH_2O to 1L], APS 10%, dH2O, TEMED.

2.11.3.3 Staining solution

This solution was prepared as following: methanol 50%, Glacial acetic acid 10%, Coomassie R25 0.25%.

2.11.3.4 De-Staining solution

This solution was prepared as following: methanol 30%, Glacial Acetic Acid 10%, dH_2O.

2.11.3.5 Running Buffer 10X

This solution was prepared as following: Glycine [144g], SDS [10 g], Tris [30 g].

2.11.4 *Tg*SPT2 Activity Assay

*Tg*SPT2 activity assay was determined by production of 3-ketodihydrosphingosine (KDS) by purified *Tg*SPT2 from the substrates L-serine and palmitoyl CoA. By using a 3KDa MWCO slide-A-Lyzer dialysis cassette, 5.65 mg/ml of purified HIS tagged *Tg*PT2 was dialysed against activity assay buffer (50 mM 4-(2-hydroxyethyl)-1-piperazineethanesulfonic acid (HEPES), 150 mM KCL,0.2 mM EDTA, 5% glycerol and 25 µM PLP) (Mina *et al.,* 2017)**.** After dialysis, 1 ml activity assay solution was prepared in a glass vial by mixing 20 µM dialysed *Tg*SPT2, 20 mM L-serine and 1.6 mM of palmitoyl Co-A. The solution was incubated for 75 mins at 37°C. After incubation, 1 ml of 2:1 $CHCl_3$:CH_3OH (v/v) was added to the activity assay solution, vortexed and centrifuged at 10000g for 5 mins to separate aqueous and organic layers. The organic layer was extracted and evaporated by using the vacuum centrifuge at 5000g and 60°C. The residues were resuspended by adding 150 µl MeOH and KDS formation analysed using ultra-performance liquid chromatography (UPLC) electron spray ionisation (ESI) MS (Mina *et al.,* 2017).

2.11.5 *Tg*SPT2 secondary structure prediction

Easy Sequencing in PostScript (ESPript 3.0) (Gouet and Courcelle, 2003). In this study, *Toxoplasma gondii* was used as a model for the Apicomplexa. *Toxoplasma gondii* serine palmitoyltransferase (*Tg*SPT), *Eimeria tennela* SPT, *Plasmodium falciparum* SPT, *Plasmodium vivax* SPT and *Cryptosporidium muris* SPT are similar to well-studied bacterial SPT from *Sphingomonas paucimobilis* (PDB: 2W8T) were analysed by using ClustalW Omega programme (Sievers and Higgins, 2014).

2.12 *Tg*SPT2 localisation

The plasmid construct pG1*Tg*SPT2_YFP was used for the detection of *Tg*SPT2 co-localised with markers for the Golgi apparatus (Golgi Reassembly Stacking Protein [GRASP] tagged with Red Fluorescent Protein [RFP] (Pfluger *et al.,* 2005)) and endoplasmic reticulum (ER retention signal HDEL tagged with Green Fluorescent Protein [GFP] (Boevink *et al.,* 1999). The following steps describe the process:

2.12.1 Construction of the plasmid pG1*Tg*SPT2_YFP

*Tg*SPT2 was cloned into pG27 using Ligation Independent Cloning (LIC) to tag the C-terminal with Yellow Fluorescent Protein (YFP) and form pG27*Tg*SPT2_YFP. *Tg*SPT2_YFP was then subcloned, using the Infusion system, into pG1 which is designed for transient transfection 24-72 hr and expression under the control of the high level Tub8 promotor.

2.12.1.1 *Tg*SPT2 LIC primers

The plasmid pG27 LIC-YFP-DHFR was used for YFP tagging *Tg*SPT2 (Figure 2-2). The primer set to amplify *Tg*SPT2 from a GenScript synthesized plasmid were designed for LIC cloning as following:

The forward primer was engineered to contain a GC (bold) upstream of the ATG (underlined) start codon.

Coding strand primer (Forward) [*Tg*SPT2 forward]	TACTTCCAATCCAATTTAAT**GC**ATGTT CGGAAGCGTCTTTGT C
Non-coding strand primer (Reverse) [*Tg*SPT2 Reverse]	TCCTCCACTTCCAATTTTAGCCAGCGTTAT AGGTCCGTCTTCC

2.12.1.2.A T4 processing protocol:

2.12.1.2.A.1: PacI digest LIC vector (pG27-YFP-DHFR) :

Plasmid pG27 LIC-YFP-DHFR Figure (2-2) was cut using the PacI restriction enzyme (5 units of enzyme/µg at 37°C overnight), then the Qiagen PCR purification kit was used to remove the enzyme and buffer. Complete linearization was confirmed by running on a 0.8% agarose gel.

Figure (2-2) pG27 LIC-YFP-DHFR (generated by SnapGene)(provided by Markus Meissner, Glasgow University)

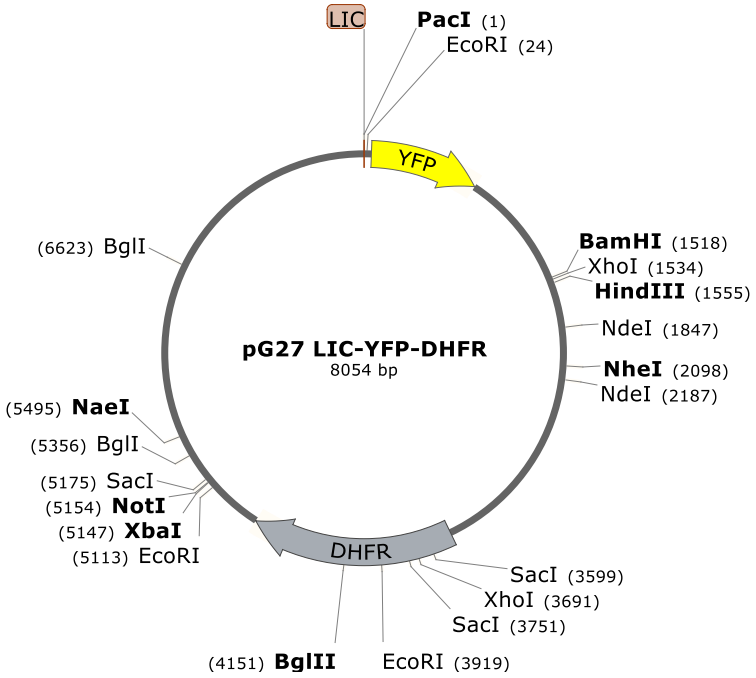

YFP: yellow fluorescent protein

DHFR: Dihydrofolate reductase

2.12.1.2.A.2: T4 reaction:

The reaction was prepared by following Novagen manual (T4 DNA Polymerase LIC qualified):

Approximately 1.2-1.8 µg linear DNA was used, and 60 µl reaction was prepared as follows: 6 µl of 10x buffer, 3 µl of 100 mM DTT, 2.4 µl of 100 mM dGTP, 6.0 µl of template DNA (200-300 ng/µl), 1.5 µl of T4 DNA Polymerase, and 41.1 µl of dH2O.

The reaction was mixed on ice, then using a 3Prime Techne PCR machine as following: the reaction incubated for 30 mins at 22°C, then shifted to 75°C for 20 mins, and the temperature reduced to 4°C. the resultant was stored at -20°C until needed.

2.12.1.2.B Insert (*Tg*SPT2)

The plasmid pU57 containing *Tg*SPT2_TGGT1 open reading frame (ORF) provided by GeneScript was transformed into DH5α *E. coli* (as above) and transformants selected on LB agar with 50 µg/ml ampicillin. A single colony was inoculated into 5ml LB broth with 50 µg/ml ampicillin and incubated at 37°C overnight. Plasmid DNA was isolated using the Qiagen Miniprep Kit and concentration measured by Nanodrop.

2.12.1.2.B.1 PCR using LIC primers (2.12.1.1)

*Tg*SPT2_TGGT1 was from the plasmid above following the Invitrogen Platinum Taq DNA Polymerase High Fidelity protocol in a ^{3}Prime TECHNE PCR machine as following

1. *Tg*SPT2 template < 500 ng.
2. 0.2 µM forward and reverse primers.
3. 50 µl PCR reaction prepared as follows:

Components	***Tg*SPT2 PCR reaction (µl)**
- dH_2O	38.8
- 10x high fidelity buffer	5.0
- 10 mM dNTP mix	1.0
- 50 mM MgSO4	2.0
- Platinum Taq DNA High Fidelty Polymerase	0.2
- 10 µM forward primer	1.0
- 10 µM reverse primer	1.0
- Template DNA	1.0
Final Volume	**50.0**

4. PCR thermocycler

Step		Temperature (°C)	Time
Initial temperature		94	30s-2min
Denature	25-35	94	15s
Anneal	PCR	~ 55	30s
Extension	Cycles	68	1 min/Kb
Hold		4	

5. Analyse 10 µl of reaction mix by agarose gel electrophoresis.
6. The mixture was cleaned using a Qiagen Gel Extraction Kit, then DNA concentration measured by Nanodrop.

2.12.1.2.B.2: T4 reaction

By following the protocol provided by Markus Meissner (personal communication) the following steps were done:

A. 20 µl reaction was prepared as follows:
   i. 2.0 µl 10x buffer
   ii. 1.0 µl 100 mM DTT
   iii. 0.8 µl 100 mM dCTP
   iv. 5.0 µl template DNA (200-300 ng/ µl)
   v. 0.5 µl T4 DNA Polymerase
   vi. 10.7 µl dH_2O

A. The reaction mixed gently on ice, and then incubated in the PCR machine as follows:
   i. Incubated for 30 mins at 22°C.
   ii. Shift to 75 °C for 20 mins.
   iii. Temperature reduced to 4°C.

2.12.1.2.C Annealing

1. 0.1 µl of treated vector and 0.2 µl treated insert were mixed on ice.
2. The reaction was incubated at room temperature for 10 minutes.

3. 1 µl of 25 mM EDTA was added, and the reaction incubated for 5 minutes at room temperature.
4. The temperature was reduced to 4°C.
5. 1 µl was used to transform DH5α E coli as above.

2.12.1.2.D pG27 *Tg*SPT2_YFP mapping

Following isolation of plasmid from transformants as above, restriction mapping was done using EcoR1 to confirm identity.

2.12.3 Infusion cloning

*Tg*SPT2_ YFP was subcloned, using Infusion, from pG27 *Tg*SPT2_YFP into the plasmid pG1 (Figure 2-3) to allow transient expression in *T. gondii.* expression. The Clontech InFusion HD Cloning guidance was followed:

2.12.3.A Preparation of linearized vector (pG1)

The restriction enzymes (EcoRI and PacI) were used to cut pG1 plasmid, removing the GFP and TY tags and linearizing the plasmid. All digestion product separated on an agarose gel 0.8% as above. The DNA fragment was using the Qiagen gel extraction kit following the manufacturer's instructions.

Figure (2-3) pG1 plasmid (generated by SnapGene)

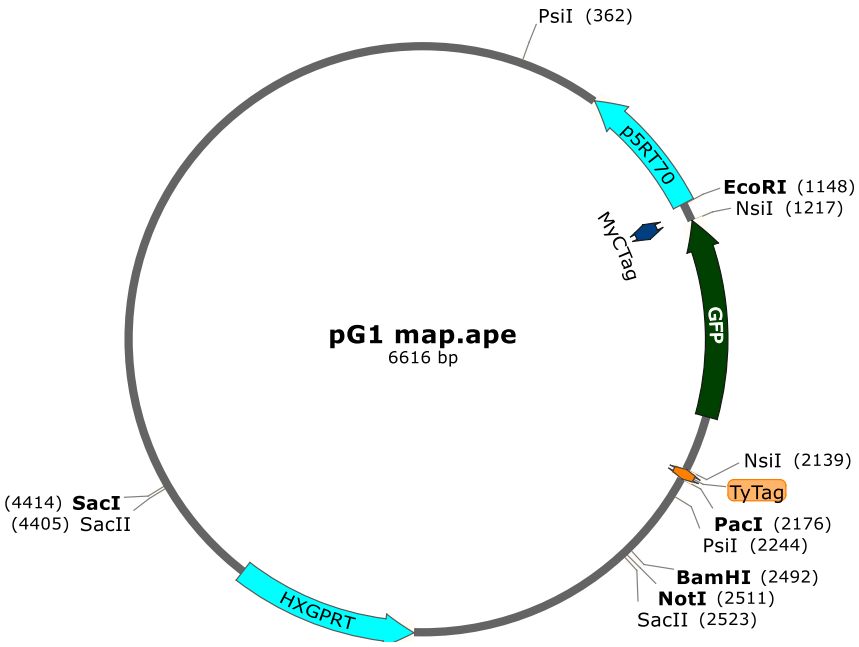

2.12.3.B PCR primer design and PCR

InFusion primers must be designed in a way to use gene specific primers (*Tg*SPT2YFP) containing extensions ends (15-18 bp) homologous to the ends of linearized vector (pG1). The following primers were used in this study:

FORWARD 5'CATTTTTTCTTGAATTCAAATGTTCGGAAGCGTCTTTG'3

REVERSE 5'GTGAGCACAACGGTGATTAATTAATTTACTTGTACAGCTCGTC'3

Hi Fidelity PCR amplification for cloning was used in this study, CloneAmp HIFI PCR Mix following the manufacturer's (Takara: Clontech) instructions:

1. Prepare the Master Mix as following:

CloneAMP HiFi PCR Premix	12.5 µl
10 µM forward primer	5.0 µl
10 µM reverse primer	5.0 µl
pG27 *Tg*SPT2_YFP	2.0 µl
dH_2O	0.5 µl

2. PCR machine programmed as following:

Step		**Temperature (°C)**	**Time**
Initial temperature		94	30s-2min
Denature	25-35 PCR	98	15s
Anneal	Cycles	~ 55	30s
Extension		72	1 min/Kb
Hold		4	

3. The product was run, as before, on a 0.8% agarose gel to check the amplification of the fragment (*Tg*SPT2_YFP).

2.12.3.C Infusion cloning reaction

1. Infusion cloning reaction was prepared as following:

5x In-Fusion HD enzyme	2 µl
Linearized vector (50-200 ng)	2 µl
Purified PCR fragment (*Tg*SPT2_YFP)	4 µl

dH_2O	2 µl
Final volume	**10 µl**

2. The reaction was mixed well and incubated for 15 minutes at 50°C, then placed on ice.
3. 2.5 µl of reaction was transformed into to 50 µl Stella *E. coli* cells (from kit) as directed.
4. An individual colony was inoculated into 5 ml LB broth containing 50 µg/ml ampicillin and incubated at 37°C overnight.
5. Plasmid DNA was isolated by using Qiagen Miniprep Kit.
6. Plasmid DNA was digested by using the restriction enzyme EcoRI to verify the new construct pG1*Tg*SPT2_YFP.

2.12.3.D pG1*Tg*SPT2YFP sequence

Following primers were used to sequence the constructed plasmid pG1*Tg*SPT2_YFP:

FWSPT21 TGT TCT AAC CAC GCA CCC TG

RVSPT21 TGC CTC GGT TGT CCA ATC ATG TAG

FWSPT22 GGC ATC AAG GTG AAC TTC AAG

RVSPT22 CCG GTT AAC ACA ATT CTT GCC C

FWYFP1 GCG GAC AAG AAA TAC GAA GTC

RVYFP1 ACT TCT TCA AGT CCG CCA TGC C

2.12.4 Electroporation

4D-Nucleofector™ X Unit (Lonza) was used to transfect *T. gondii* RHΔHX with pG1*Tg*SPT2_YFP and Plasmids for expression of GRASP_RFP and GFP_HDEL were used to label the Golgi and ER respectively.

The AMAXA transfection protocol provided by Lonza was as follows:

2.12.4.1 HFF and *Toxoplasma gondii* cell culture

1. Fresh HFF cells were trypsinized from a T25 flask, and transferred to 24 well plate with 13 mm coverslips, and the wells filled with 1 ml DMEM

containing 10 % FCS serum, and 1% penicillin/streptomycin. The plates were incubated at 37°C and 5% CO_2 incubator until use, 3-5 days .

2. *Toxoplasma gondii* tachyzoite infected HFF cells were scraped from a flask and parasites released by passage through a 23G needle. Parasites were then separated from the host material using 3 µm Millipore polycarbonate filters, harvested by centrifugation at 1430g for 15 minutes, and resuspended by adding the desired volume of DMEM media.

2.12.4.2 Nucleofection reactions

Two reactions below were used in this experiment in order to know the *Tg*SPT2 subcellular-localization by using the co transfection with P30 CRASP_RFP (Golgi marker) and GFP_HDEL (ER marker) by following the AMAXA transfection protocol provided by LONZA:

1. pG1*Tg*SPT2_YFP (25 µg) + P30 GRASP_RFP (10 µg)
2. pG1*Tg*SPT2_YFP (25 µg) + P30 GFP_HDEL (10 µg)

2.12.4.3 DNA

1. Purified plasmid DNA was resuspended in 100 µl TE buffer.
2. 11 µl of 3M sodium acetate (NaOAc) (pH5.2) was added.
3. DNA was precipitated by adding 250 µl 100% ethanol and incubating at -20°C for 20 minutes.
4. DNA was pelleted by centrifugation at 9500g, 4°C for 30 minutes.
5. The supernatant was discarded and the pellet washed in 500 µl 70% ethanol before pelleting as in 4 and air-dried by leaving the lid off in biosafety cabinet for 20-30 minutes.
6. 10^7 parasites per reaction was pelleted by centrifugation and resuspended in 100 µl of P3 buffer (Nucleofector solution). This was then added to the dried DNA samples and transferred to an AMAXA cuvette.
7. Nucleofector programme (FI-158, which is the specific program for *Toxoplasma gondii* transfection) was used.
8. 300 µl pre-warmed DMEM media containing 10% FCS and 1% penicillin/streptomycin was added to the cuvette post transfection. 10 µl or 20 µl of this was transferred to 4 wells of a 24 well plate seeded with

HFF cells as described, and the cells then incubated for 48 or 24 hours respectively.

2.12.5 Fixing cells

1. The cells were washed with 500 µl volumes of PBS at room temperature.
2. 300 µl of 4% paraformaldehyde (PFA) in PBS was added to each well, and incubated at room temperature for 15 minutes.
3. The wells were washed with 500 µl PBS (3x5 minutes).

2.12.6 Staining

1. The cells were permeabilized with 0.4% (v/v) triton X-100 in PBS for 10 minutes.
2. Washed with PBS 3x for 5 minutes.
3. After PBS washing (3x for 5 minutes), the cells were mounted using 4',6-Diamino-2-phenylindole dihydrochloride (DAPI) Fluoromount (Southern BioTech) to stain the nuclei. The edges were sealed with 2-layers of nail polish.
4. Zeiss Apotome microscope was used to examine the protein localisation by using the filters (DAPI, Green, Rhodamine, and Yellow) and the 63X oil objective lens.
5. For high resolution imaging, the Zeiss LSM 880 microscope with Airyscan was used with appropriate filters (Red, Yellow and Blue), and the 63X oil objective lens.

2.13 *Tg*SPT2 knockout (KO)

2.13.1 KO Plasmid (pTub5CatSagF1F2) construction and mapping

The plasmid that used in this study was **pTub5CatSag1F1F2** (figure 2-4) (personal communication with Hosam Shams-Eldin and Philip Stahl/University of Marburg), a construct designed to knockout the 2 tandem copies of *T. gondii* SPT was made and supplied. This vector was transformed into the competent DH5α *E. coli* as described above.

To map the vector, single digestions with restriction enzymes NotI and XhoI and double digestions with restriction enzymes NotI + XhoI and NotI + HindIII were performed. The protocol used in both single and double digestion was:

For single digestion:

Plasmid DNA 1 µg/µl	0.5 µl
Nuclease free water	15.5 µl
Restriction enzyme 10x Buffer	2 µl
Restriction enzyme	2 µl
Total volume	20 µl

For double digestion:

Plasmid DNA 1 µg/µl	0.5 µl
Nuclease free water	13.5 µl
Restriction enzyme 10x Buffer	2 µl
Restriction enzyme 1	2 µl
Restriction enzyme 2	2 µl
Total volume	20 µl

Figure (2-4) The KO plasmid pTub5CatSag1F1F2 map

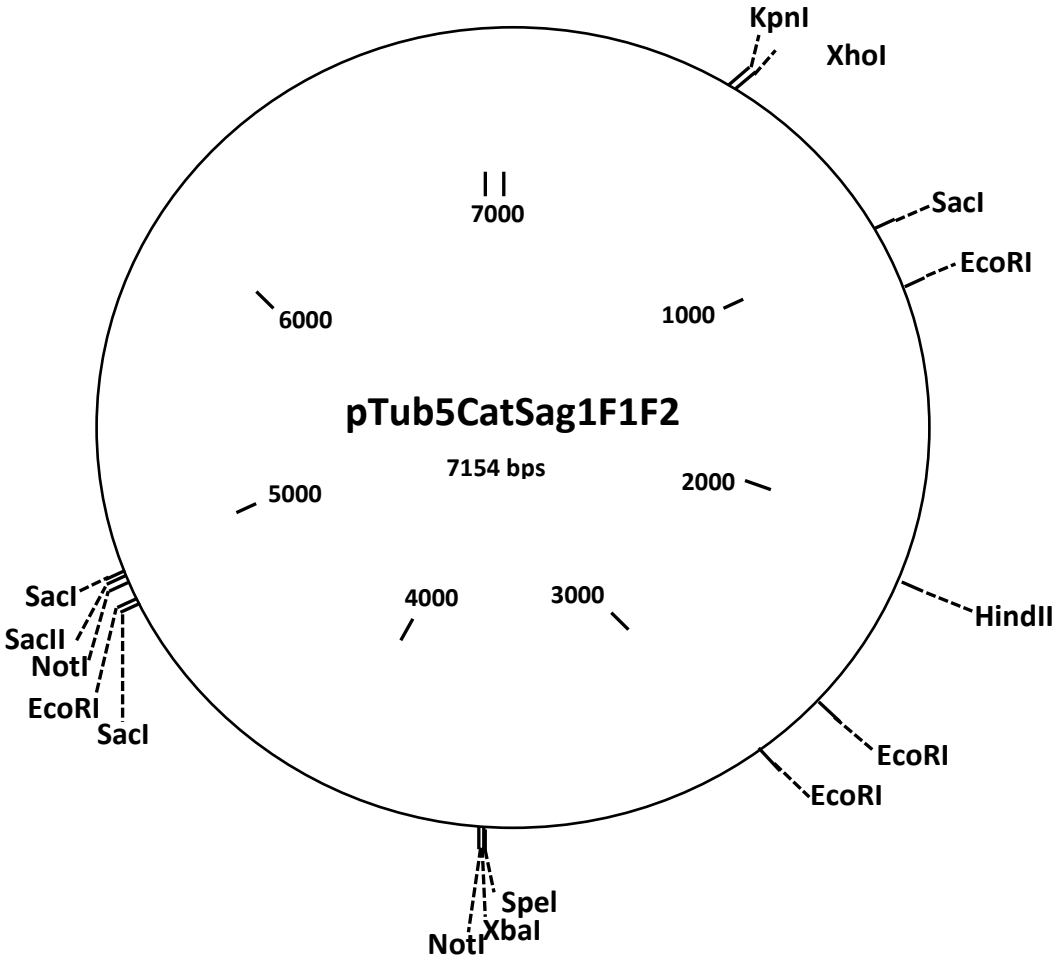

2.13.2 Deletion of *Tg*SPT1 and 2 by homologous recombination

25 µg of pTub5CatSag1F1F2 was linearized by digestion with XhoI as above. Following ethanol precipitation this was transfected into *T. gondii* Δku80-HXG in the same manner as described for transient expression constructs. However, 20 µM of chloramphenicol was added to the transfected cultures and resistant parasites selected after 3 rounds of egress. A mock transfection (no DNA) was used as a control.

DNA extracted for RHKu80 (control), or RHdeltaKu80_SPTKO (expt)

1. 1 × T75 culture plates infected HFFs, > 85% lysed
2. Cells scratched, homogenised through a syringe
3. Suspension was filtered through 3µm filters

4. gDNA extracted using QIAamp DNA Mini Kit

The primers below were designed to amplify the flank regions (XhoI and SacI) and CAT marker

P1 (TgSPT 5' Flank A XhoI): CCCCTCGAGCCCTCCACACGCTGAATTTCG

P4 (TgSPT 3' Flank B SacI): CCCGAGCTCTTGATCGCAACTTTCTGTGCAGTA

P5 (CAT F): CCACCGTTGATATATCCC

P6 (CAT R): GTAATTCATTAAGCATTCTGC

Then 25 µl PCR reaction volume of each sample was prepared, and PCR machine programmed as follows:

Step	Temperature (°C)	Time
Denature	90	30s
Anneal	64	30s
Extension	72	9 s
Final extension	72	10 min

2.14 Metabolomics analyses

Leishmania major was used as model to study the global effect of inhibiting Inositol Phosphorylceramide Synthase (IPCS). IPCS is a non-mammalian enzyme found in sphingolipid biosynthesis pathway in this parasite. It is a potential drug target in *Leishmania* spp. and other protozoa, including apicomplexan parasites such as *T. gondii*.

Two compounds, clemastine and a benzazepine (CMPD35), already identified as an IPCS inhibitors were used against the *L. major* Friedlin Virulent (FV1) strain (wild type [WT]) to study the effect of these compounds and IPCS inhibition on the metabolome of the parasite.

Also, we studied the metabolomic effects of miltefosine (the only oral therapy for treatment of leishmaniasis; Croft and Engel, 2006) on *L. major* FV1 (WT) and a mutant strain (MT) *L. major* ΔLCB2 (Denny *et al.,* 2006), which lacks the ability to synthesize sphingolipid.

2.14.1 Effect of clemastine and benzazepine (CMPD35) on *Leishmania major* FV1 metabolome

2.14.1.1 Half time to cell death assay

The stocks for both compounds (10 mM) were prepared in Dimethylsulfoxide (DMSO). Assays were prepared in sterile 24 well-plates. In each well the compounds were diluted to 2x the desired concentrations of 10μM and 5 μM (triplicates) for clemastine, and 80 μM and 40 μM (triplicates) for the benzazepine, in 500 μl of Schneider's media supplemented with 10% heat-inactivated FCS, and 1% penicillin/streptomycin. Then 500 μl of *L. major* FV1 promastigotes at a concentration $1x10^7$/ml were added to each well, to give a final volume of 1 ml/well. The plate was incubated at 26°C and morphology and numbers of parasite were examined at 20, 24 and 42 hours.

2.14.1.2 Cell extraction for metabolomics

From previous experimentation (2.13.1.1), the best time for metabolomic analyses was after 42 hours with 10 μM of clemastine and 40 μM of the benzazepine, CMPD35. At this time point the WT parasite morphology changed from an elongated to a round shape but maintained viability. Promastigote *L. major* FV1 ($5x10^7$ cells at $5x10^6$/ml) were seeded into T25 tissue culture flasks containing Schneider's medium supplemented with 10% heat-inactivated FCS, and 1% penicillin/streptomycin, in triplicate for each sample. Each compound was added to the required concentration and an equivalent volume of DMSO was added to control flasks as following:

Groups	Addition
Leishmania major FV1 + Clemastine (10 mM)	10 ml + 10 μl + 30 μl DMSO
Leishmania major FV1 + CMPD35 (10 mM)	10 ml + 40 μl
Leishmania major FV1 + DMSO (100%)	10 ml + 40 μl

After incubation at 26°C for 42 hours, the promastigotes were counted in all flasks and $5x10^7$ cells were prepared from each sample for metabolomic extraction, following the protocol below provided by Mike Barrett (Glasgow) (personal communication):

1. $5x10^7$ cells per each sample (3 replicates) were harvested in logarithmic phase by centrifugation at 1430g for 15 minutes.
2. The temperature was quenched rapidly using a dry ice/ethanol bath and mixing vigorously to avoid the freezing and cell lysis.
3. The samples were kept on ice, then centrifuged at 1250g for 10 minutes at 4°C.
4. The supernatant was discarded and 1 ml left in which to resuspend the cells.
5. The cells were transferred to an Eppendorf tube, and centrifuged at 2260g for 10 minutes at 4°C, all the medium was then removed.
6. The cells were washed, and resuspended with 1 ml PBS at 4°C. Centrifuged at 2260g for 10 minutes at 4°C and all PBS removed.
7. The pellet resuspended by adding 200 µl extraction solvent (Chloroform:Methanol:Water (CMW) 1:3:1 v/v/v) at 4°C and mixing well.
8. 200 µl CMW sample was prepared as a blank.
9. The samples left on a shaker incubator at max speed in the cold room (4°C) for 1 hour.
10. Samples were centrifuged at 18890g for 10 minutes at 4°C.
11. 180 µl was taken from the supernatant and placed into screw-top vial, 20 µl was taken from each sample and mixed together in a one vial tube to used it as a quality control (QC).
12. Argon was added to each sample before storing at -80°C until analyses by liquid chromatography-mass spectrometry (LCMS).
13. The samples analysed by Erin Manson at the Glasgow Polyomics Research Centre.
14. The metabolomic data was evaluated using IDEOM in an Excel template (Creek *et al.,* 2012).

2.14.2 Screening the efficacy of miltefosine against *Leishmania major* FV1 (WT) and *Leishmania major* ΔLCB2 (MT)

L. major FV1 and *L. major* **Δ**LCB2 were inoculated into fresh Schneider's medium supplemented with 10% FCS and 1% penicillin/streptomycin at $1x10^6$ parasites/ml in a 96 well plate (50 µl each well). Serial dilutions of miltefosine at

100 µM, 50 µM, 25 µM, 12.5 µM, 6.25 µM and 3.125 µM, prepared from a miltefosine stock solution in ethanol (10 mM), were made as following. The compounds were prepared at 2x concentration in triplicate, ethanol alone was added to the negative control by prepare 200 µM in 700 µl ethanol, then add 350 µl from this tube and added to the next tube already have 350 µl media, mixed well to get 100 µM, same to prepare the other concentrations (figure 2-5).

Then 50 µl of desired concentration was added to each well, containing 50 µl of parasites, to give a final volume of 100 µl. The plates were incubated at 26°C for different periods of time (figure 2-5).

Figure (2-5) preparation of serial compound dilutions

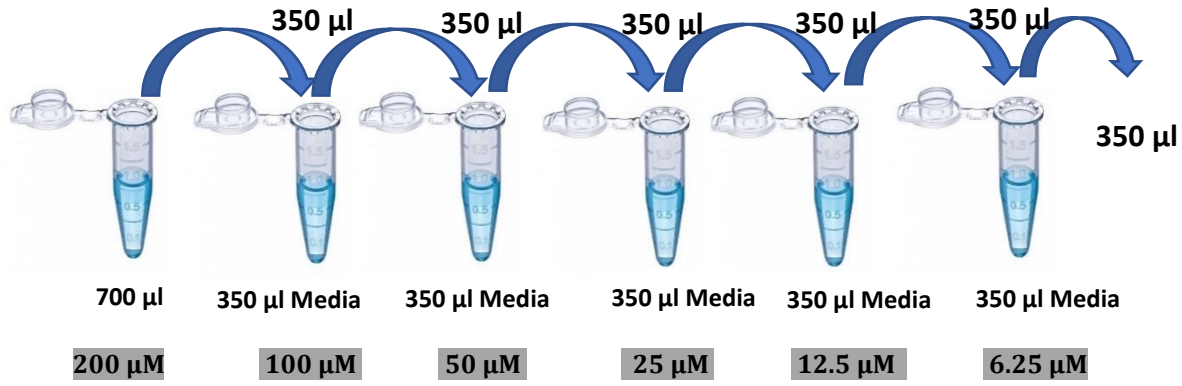

After 48 hrs incubation, Alamar Blue was used for detection of cell viability, (it allows measurement of reduction-oxidation (redox) reactions). 10 µl of Alamar Blue was added to each well and incubated for 4 hrs at 26°C, cell viability was monitored by changing color from blue (oxidation state) to pink (reduction state) (Rampersad, 2012). In addition, fluorescence changes were measured using FLx800 Fluorescent Reader (BioTek) plate reader (Excitation 540/35, Emission 600/40). The data was analysed by using Excel. The effective Dose for 50% cytotoxicity (ED_{50}) was calculated using Prism 7 software (GraphPad).

2.14.3 The effects of miltefosine on the *Leishmania major* FV1 (WT) and *Leishmania major* ΔLCB2 (MT) metabolome*

This experiment was designed to determine the mechanism of action of the drug miltefosine through analyses of changes to the parasite (WT and MT) metabolome. 1X ED_{50} (WT) and 3X ED_{50} (WT) concentrations against WT and MT *L. major* were used for 72 hours as follows:

*Collaboration with Emily Armitage and Mike Barrett

L. major FV1 and *L. major* ΔLCB2 promastigotes were inoculated in Schneider's medium supplemented with 10% FCS without penicillin/streptomycin. All samples were grown and harvested in the logarithmic phase and counted. $5x10^7$ cells was prepared for each sample. The samples were divided into 6 groups, each group had 6 replicates as following:

6 replicates with 1 x ED_{50} (10 μM) concentration of drug (WT)

6 replicates with 3 x ED_{50} (30 μM) concentration of drug (WT)

6 replicates with 1 x ED_{50} (10 μM) concentration of drug (MT)

6 replicates with 3 x ED_{50} (30 μM) concentration of drug (MT)

6 replicates with DMSO control (WT)

6 replicates with DMSO control (MT)

The samples were incubated with miltefosine or DMSO for 5 hours at 26°C, then the parasites counted and $5x10^7$ parasites collected. The work flow is given below:

1. The samples were centrifuged at 1500g for 10 minutes at 4°C.
2. The supernatant was discarded, and 2 ml PBS was added to each sample, and mixed well.
3. The sample was transferred to cryovials tube, centrifuged for 15 mins at 1500g at 4°C.
4. The supernatant was discarded and 200 μl ice cold 100% methanol added, and samples stored at -80°C until use.
5. All the samples were analyzed by GlaxoSmithKline Espaňa (GSK).

2.15 Lipidomic analyses

This experiment was designed with collaboration with Terry Smith (University of St. Andrews), to analyze the effect of clemastine and the benzazepane (CMPD35) on the lipid profile of *Leishmania major* FV1.

2.15.1 The effect of clemastine and benzazepane (CMPD35) on the lipid profile of *Leishmania major* FV1

L. major FV1 promastigotes were inoculated into Schneider's medium supplemented with 10% FCS with 1% penicillin/streptomycin. $5x10^7$ cells per

sample were divided into three T25 flasks each with 10 ml of media, clemastine or CMPD35 were added at concentrations of 10 µM and 40 µM, DMSO was added as a control:

a. *L. major* FV1 + 40 µl DMSO (control)
b. *L. major* FV1 + 40 µM CMPD35 DMSO
c. *L. major* FV1 + 10 µM clemastine + 30 µl DMSO
d. *L. major* FV1 + 5 µM clemastine + 35 µl DMSO
e. *L. major* FV1 + 1 µM clemastine + 39 µl DMSO
f. *L. major* FV1 + 0.5 µM clemastine + 40 µl DMSO
g. *L. major* FV1 + 0.1 µM clemastine + 40 µl DMSO

All flasks were incubated at 26°C for 42 hours.

2.15.2 Lipid extraction from *Leishmania major* FV1 (WT) (Bligh and Dyer 1959)

1. *Leishmania major* FV1 promastigotes were counted to prepare 10^8 cells in logarithmic phase for each sample. Cells were harvested by centrifugation at 800g for 10 minutes.
2. The pellet was then resuspended in 1 ml PBS, and divided into four 250 µl samples in glass tubes.
3. 930 µl of 1:2 Chloroform:Methanol (v/v) was added and the samples vortexed vigorously for 15 minutes.
4. 312.5 µl of chloroform was added, then vortexed for 5 minutess.
5. 312.5 µl of dH_2O was added, then vortexed for 5 minutes.
6. After Centrifugation at 1000g, room temperature for 15 minutes 2 layers were apparent. The top, which is aqueous layer, and bottom one which is the organic or lipid layer.
7. The organic or lipid layer was transferred to a new glass vial using a glass Pasteur pipette.
8. This layer was dried under N_2, and stored at 4°c until use.
9. The samples were sent to Terry Smith (University of St Andrews) for analysis of the lipid profile by using electron spray-mass spectrometry (ES-MS) and gas chromatography-mass spectrometry (GC-MS).

2.16 Bioinformatic tools

2.16.1 BLAST

Using the two candidate *Tg*SPT protein sequences previously identified in toxoDB.org (Mina et al, 2017) a BLAST search was performed against the National Center for Biotechnology Information (NCBI) database using default settings (Mount, 2007).

2.16.2 ClustalW Omega

Identified sequences were aligned using ClustalW Omega with output format (Sievers and Higgins, 2014).

2.16.3 Phobius tool

The transmembrane domains of *Tg*SPT1 and *Tg*SPT2 were predicted using Phobius. The parameters were set with long graphics (Käll and Sonnhammer 2004).

2.16.4 Hydrophobicity profile

The hydrophobicity/hydrophilicity of *Tg*SPT1 and *Tg*SPT2 using Hphob. (Kyte and Doolittle 1982).

Chapter Three: Bioinformatic analyses of the T. gondii serine palmitoyltransferase

3.1 Bioinformatic analyses of the *T. gondii* serine palmitoyltransferase

Bioinformatics is an intradisciplinary scientific field includes molecular biology, biochemistry and genetics with computer science to study the protein functions and properties (Luscombe *et al.,* 2001; Bai *et al.,* 2012). Bioinformatic analyses is dependent on three types of data:

A. DNA or protein sequence. For DNA this includes the detection of coding and non-coding regions, i.e determination of the number of exons and introns. For protein sequence, this includes the identification of conserved sequence motifs and functional prediction (Luscombe *et al.,* 2001).
B. Macromolecular structure. Showing the protein properties such as secondary or tertiary protein structure, protein-protein interactions, biochemical data, phylogenetic analysis and metabolic pathways (Luscombe *et al.* 2001).
C. Functional genomic experiments results including gene expression (Luscombe *et al.,* 2001).

All the information above is available in EupathDB (http://eupathdb.org/eupathdb/), a group of databases for many organisms including *AmoebaDB*, *CryptoDB*, *FungiDB*, *MicrosporidiaDB*, *PiroplasmaDB, PlasmoDB, TrichDB, TriTrypDB, OrthoMCL* and finally *ToxoDB* (Madrid-Aliste *et al*., 2009; Weiss *et al*., 2009). ToxoDB is specified to provide genetic information and functional data bases for the *T. gondii* genome which consists of 14 chromosomes, and is about 63 Mb (Khan *et al.,* 2005 ; Gajria *et al.,* 2007). ToxoDB also provides a gateway to the annotation and genome sequence and function of the *T. gondii* strains GT1 and RH (Type I), ME49 (Type II) and VEG (Type III). ToxoDB is used in this study to analyses an important enzyme catalysing the first step in the *de novo T. gondii* sphingolipid biosynthesis pathway, serine palmitoyltransferase (SPT). *T. gondii* have two closely related encoded SPTs, *Tg*SPT1 and *Tg*SPT2.

In this chapter, we will use bioinformatic tools and ToxoDB to predict the gene function, origin of the gene (bacterial or eukaryotic), transmembrane domains, expression levels and hydrophobicity/hydrophilicity for *Tg*SPT1 and *Tg*SPT2 (http://www.toxodb.org).

3.2 Gene information

Serine palmitoyltransferase (SPT; E.C. 2.3.1.50) belongs to the pyridoxal phosphate α-oxoamine synthase family (Hanada, 2003 ; Hornemann *et al.,* 2009). This family includes enzymes which catalyse the condensation of a particular amino acid (a.a.) with an acyl-CoA thioester substrate (Eliot and Kirsch, 2004; Yard *et al*., 2007).

SPT is catalyses the first step in the sphingolipid biosynthesis pathway, the condensation of L-serine with palmitoyl Co-A to produce 3-ketodihydrosphingosine (3-KDS) (Lowther *et al.,* 2012; Beattie *et al.,* 2013). From ToxoDB, two potential *T. gondii* SPTs, *Tg*SPT1 and *Tg*SPT2 (68% identical), were identified previously (Mina *et al.,* 2017).

3.2.1 *Tg*SPT1

The gene ID within ToxoDB is TGGT1_290980, this gene is located on the chromosome IX, spanning the area between nucleotide 3,815,226 and 3,817,238. The gene is predicted to have 2 exons, exon 1 3,815,226 to 3,816,330 and exon 2 3,816,588 to 3,817,238, and 1 intron, 3,816,331 to 3,816,587 (figure 3-1). The predicted encoded protein is 571 a.a. with a molecular weight 63.6 KDa.

Figure (3-1) *Tg*SPT1 model showing the exon and intron areas from (ToxoDB.org)

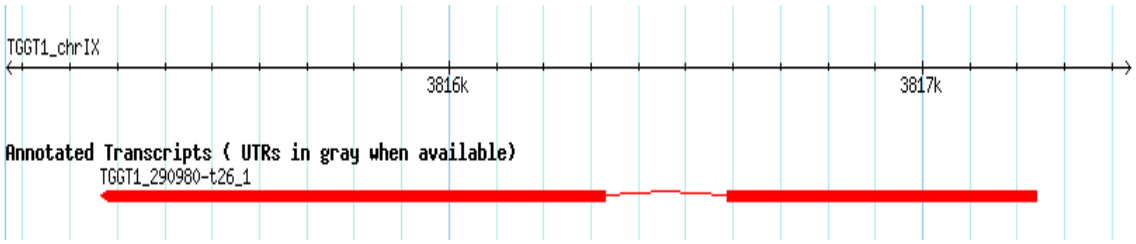

In ToxoDB most of data for gene expression are from the Type II ME49 strain. Using the Blast protein tool (Mount, 2007), *Tg*SPT1 from ME49 (TGME49_290980) was shown to have 100% identity with the predicted protein from GT1 (TGGT1_290980) therefore the expression data from type II *T. gondii* (TGME49_290980) was analysed here and below with confidence that it relates to other strains (figure 3-3).

3.2.2 *Tg*SPT2

The gene ID within the ToxoDB is TGGT1_290970, this gene is located on Chromosome IX, nucleotide 3,811,046 to 3,812,950. The gene is predicted to have have 2 exons, the first from 3,811,046 to 3,812,128 and, the other from 3,812,300 to 3,812,950, and 1 intron, 3,812,129 to 3,812,299 (figure 3-2). The predicted encoded protein is 577 a.a with a molecular weight of 64.7 KDa.

Figure (3-2) *Tg*SPT2 model showing the exon and intron areas from (ToxoDB.org)

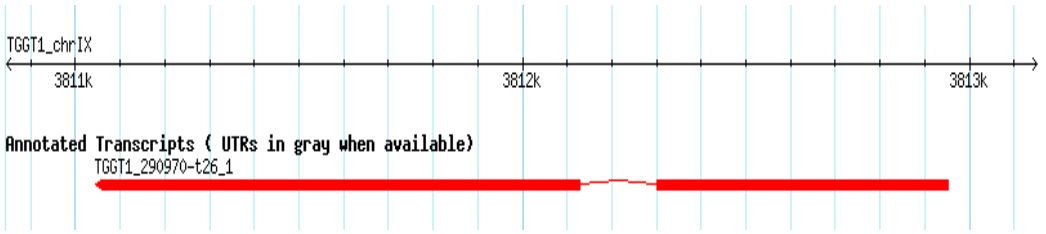

Like *Tg*SPT1, using Blast the predicted protein sequence from type I GT1 *T. gondii* was shown to be 100% identical to that in type II ME49 (TgME49_290970) (figure 3-3).

Figure (3-3) Alignment sequence of TGGT1_290980 and TGME49_290980 (*Tg*SPT1); and TGGT1_290970 and TGME49_290970 (*Tg*SPT2). Each is 100% identical to its counterpart in the other strains.

```
TGGT1_290970        -MFGSVFVLDSDPMGFIGNRNVEWTTNLDFFYCAFFSASLLGVLLAFFTDDVSSGSLRWS        59
TGME49_290970       -MFGSVFVLDSDPMGFIGNRNVEWTTNLDFFYCAFFSASLLGVLLAFFTDDVSSGSLRWS        59
TGGT1_290980        MASGATYFTRGTGSPFL-GAGVEWASNIDLFLCAFLSASVLGILLAFFNDEVSWGSLRWS        59
TGME49_290980       MASGATYFTRGTGSPFL-GAGVEWASNIDLFLCAFLSASVLGILLAFFNDEVSWGSLRWS        59
                       *:.:.  .    *: . .***::*:*:* ***:***:**:*****.*:** ******
TGGT1_290970        WIVMELLPVPRLSNHVAVKDVEGALITAAKQASGKSQVFAKIVTAAHEGTLKVLLAQWCT        119
TGME49_290970       WIVMELLPVPRLSNHVAVKDVEGALITAAKQASGKSQVFAKIVTAAHEGTLKVLLAQWCT        119
TGGT1_290980        WIATQLLPITPCSSHAVYKDVETALAKAARNKAGSKRALEEFLAALQDGTVMVLLSKWSA        119
TGME49_290980       WIATQLLPITPCSSHAVYKDVETALAKAARNKAGSKRALEEFLAALQDGTVMVLLSKWSA        119
                    **. :***:   *.*.. **** ** .**:: :*..:.: ::::* ::**: ***::*.:
TGGT1_290970        KLHLRCWFCWHTLKLRYTAESRRQLLYQVNKVLLRLENRKGEKEVQSYLDIKRYMQTNNL        179
TGME49_290970       KLHLRCWFCWHTLKLRYTAESRRQLLYQVNKVLLRLENRKGEKEVQSYLDIKRYMQTNNL        179
TGGT1_290980        RGFERLAFYWQALKIKYTAQSRRQFFYQMQKVQLKLEIKPGETEMQSYNDAKRYMKSRDL        179
TGME49_290980       RGFERLAFYWQALKIKYTAQSRRQFFYQMQKVQLKLEIKPGETEMQSYNDAKRYMKSRDL        179
                    : . *  * *::**::***:****::**::** *:** : **.*:*** * ****::.:*
TGGT1_290970        WYFAFRISDVKSQYITCEGKRAYHMSSYSYLDFMREPLVQEAALAAGRMWSTGNHGARML        239
TGME49_290970       WYFAFRISDVKSQYITCEGKRAYHMSSYSYLDFMREPLVQEAALAAGRMWSTGNHGARML        239
TGGT1_290980        WPFAYEVSNVKDTQVICEGVRAYPMSSYSYLDFVREPLVQEAALAAGRTWSTGNHGARML        239
TGME49_290980       WPFAYEVSNVKDTQVICEGVRAYPMSSYSYLDFVREPLVQEAALAAGRTWSTGNHGARML        239
                    * **:.:*:**.  : *** *** *********:************** ***********
TGGT1_290970        GGNPTVIRELEQIIGRFFGREDALLCATGFLAAMSSICAVAKKGDLIIGDNRLHTSLRVG        299
TGME49_290970       GGNPTVIRELEQIIGRFFGREDALLCATGFLAAMSSICAVAKKGDLIIGDNRLHTSLRVG        299
TGGT1_290980        GGNMRILRDLEKMVGRFFGREDSLLCATGFLATMSSICAVAKEGDLIVGDNRLHASLRSG        299
TGME49_290980       GGNMRILRDLEKMVGRFFGREDSLLCATGFLATMSSICAVAKEGDLIVGDNRLHASLRSG        299
                    ***  ::*:**:::********:*********:*********:****:******:*** *
TGGT1_290970        MKLSGAKEVLFRHNNWQHLTQILGSMRRKYIDCWIVIESVYSMDGDIADLPTVRRLADQY        359
TGME49_290970       MKLSGAKEVLFRHNNWQHLTQILGSMRRKYIDCWIVIESVYSMDGDIADLPTVRRLADQY        359
TGGT1_290980        MKLSGAKEMLFRHNNWHHLQQTLAKHRRKYKNCWIVIESVYSMDGDIADLPVVRRLADQY        359
TGME49_290980       MKLSGAKEMLFRHNNWHHLQQTLAKHRRKYKNCWIVIESVYSMDGDIADLPVVRRLADQY        359
                    ********:*******:** * *.. **** :******************.********
TGGT1_290970        KCQIIVDEAHGLGVLGKSGRGLEEHFNMPGAADIIVGTFSKSIGGVGGFITCGKDLIEFL        419
TGME49_290970       KCQIIVDEAHGLGVLGKSGRGLEEHFNMPGAADIIVGTFSKSIGGVGGFITCGKDLIEFL        419
TGGT1_290980        NCRILLDEAHGLGVLGKTGRGLEEHFNMPGAADVIVGTFSKSIGGVGGYITGDNDLVEFL        419
TGME49_290980       NCRILLDEAHGLGVLGKTGRGLEEHFNMPGAADVIVGTFSKSIGGVGGYITGDNDLVEFL        419
                    :*:*::***********:***************:**************:** .:**:***
TGGT1_290970        EYHALGSVFSAPLTAYSAGGAKKAFELMQGEHRWRIAKAQENAIYLRRALKTGNGNWPPD        479
TGME49_290970       EYHALGSVFSAPLTAYSAGGAKKAFELMQGEHRWRIAKAQENAIYLRRALKTGNGNWPPD        479
TGGT1_290980        DFHAPGSVFSAPLTAYSAGGAMMAFELMQGEQSWRIAKAQENAKYLRHALQTGLGLWPKD        479
TGME49_290980       DFHAPGSVFSAPLTAYSAGGAMMAFELMQGEQSWRIAKAQENAKYLRHALQTGLGLWPKD        479
                    ::** ***************  ********: ********** ***:**:** * ** *
TGGT1_290970        YPADKKYEVEGIECTTVIPVVFPNDPYRLCCVTRALFSKGWVVGAAMYPACPLMRPRIRI        539
```

```
TGME49_290970       YPADKKYEVEGIECTTVIPVVFPNDPYRLCCVTRALFSKGWVVGAAMYPACPLMRPRIRI        539
TGGT1_290980        YPAERKFELEGVACTTVIPVVFPHDGDRVFRVTQAMLKRGWMVAAAAYPACPLNRPRIRV        539
TGME49_290980       YPAERKFELEGVACTTVIPVVFPHDGDRVFRVTQAMLKRGWMVAAAAYPACPLNRPRIRV        539
                    ***::*:*:**: **********:*  *:  **:*::.:**:*.** ****** *****:
TGGT1_290970        TATAAYTKEIMDKFVRDLVKTTVDVPLTTEVEDGPITL        577
TGME49_290970       TATAAYTKEIMDKFVRDLVKTTVDVPLTTEVEDGPITL        577
TGGT1_290980        TATAAYNQKMMDEFVKSLVEVTVECPPTDMLR------        571
TGME49_290980       TATAAYNQKMMDEFVKSLVEVTVECPPTDMLR------        571
                    ******.:::**:**:.**:.**: * *  :.
```

3.3 Gene Expression

ToxoDB was used to the expression profiles of *Tg*SPT1 and *Tg*SPT2 in oocyst, tachyzoite and bradyzoite ME49 *T. gondii* (figure 3-4).

The expression profiles showed that *Tg*SPT1 (figure 3-4a) expression is approximately equal in oocyst and tachyzoite, however, its expression is lower in bradyzoite. In contrast, *Tg*SPT2 expression (figure 3-4B) in bradyzoite forms is higher than in oocyst and tachyzoite. This showed that *Tg*SPT1 in predominant in tachyzoite, and *Tg*SPT2 is predominant in bradyzoite. Perhaps a specific type of sphingolipid or substrate is required for each stage, and *T. gondii* regulates sphingolipid biosynthesis depending on environmental conditions or lifecycle stage. Until now no information is available for the role of sphingolipids in *T. gondii* and more study is needed. Metabolomic analyses could be of benefit, for example analysing mutant strains lacking SPT1 and SPT2.

Figure (3-4) Gene expression profiles for *Tg*SPT1 and *Tg*SPT2 in *T. gondii* life cycle stages.

A. B.

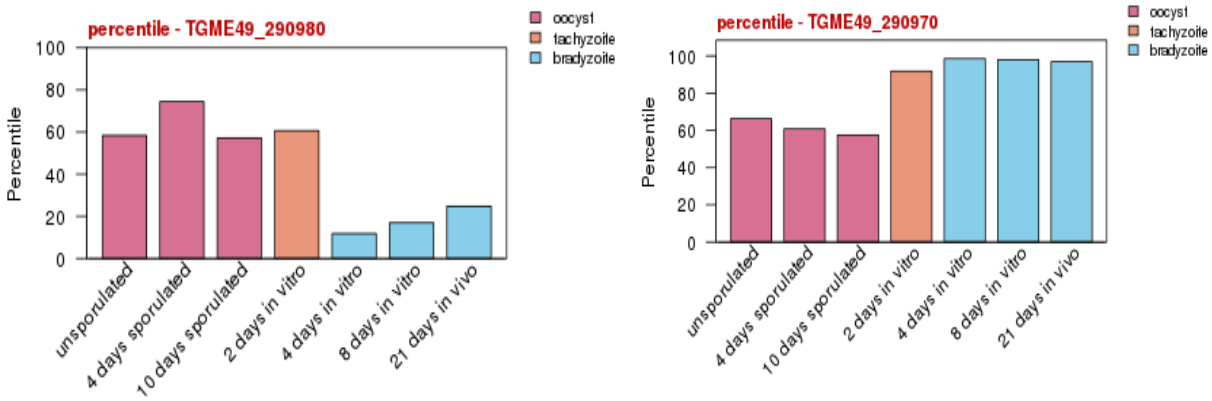

3.4 Gene origin

SPT is found in both eukaryotic and prokaryotic organisms, it is a membrane-bound heterodimeric enzyme in eukaryotes such as humans and yeast, and a cytoplasmic homodimeric enzyme in prokaryotes (Yard *et al*., 2007). In both cases the active site contains a pyridoxal phosphate (PLP) co-factor bound to a lysine residue as an internal aldimine (Shiff base) (Hanada, 2003; Yard *et al.,* 2007).

In humans, SPT consists of hSPT1 (*Hs*LCB1), and either hSPT2 (*Hs*LCB2) or hSPT3 (*Hs*LCB3) (Ikushiro and Hayashi, 2011 ; Genin *et al*., 2016). hSPT2 and hSPT3 subunits have catalytic activity due to the presence of lysine residue, whereas hSPT1 is believed to play a regulatory role due to its lack of PLP binding ability. The hSPT3 subunit has only been found in mammals, birds, and lower vertebrates (Hornemann *et al.,* 2009). Similarly, to humans, in yeast such as *Saccharomyces cerevisiae*, SPT consists of regulatory SPT1, which like hSPT1 lacks the active site lysine residue, and catalytic SPT2 which contains the active site lysine residue (Yard *et al.,* 2007).

In the Prokaryota, *Sphingomonas paucimobilis* is a Gram-negative bacteria characterised by having an outer membrane containing glycosphingolipid instead of lipopolysaccharide, and SPT catalyses the first step in glycosphingolipid biosynthesis. Overcoming difficulties analysing the bound-bound eukaryotic enzyme, Ikushiro *et al.* (2001) isolated the water-soluble SPT enzyme from *S. paucimobilis.* In this bacterium, SPT is a homodimer enzyme composed of 2 subunits of *Sp*SPT with 2 active sites - one for each subunit (Yard *et al.,* 2007). Like the eukaryotes, the active site is Lysine residue (Lys265), and a Histidine residue (His234) has been shown to be involved in PLP binding (Yard *et al.,* 2007). This well studied protein it is now used as a model to determine the origin of *Tg*SPT1 and *Tg*SPT2. Using the ClustalW Omega tool (http://www.ebi.ac.uk/Tools/msa/clustalo/) the eukaryote SPT sequences (human [*Homo sapiens*] (Hs) and yeast [*Saccharomyces cerevisiae*] (Sc)) and prokaryote SPT sequence [*Sphingomonas paucimobilis*] (Sp) were aligned with *Tg*SPT1 and *Tg*SPT2 (figure 3-5).

Figure (3-5) ClustalW for SPT alignment in eukaryotic (human and yeast) and bacterial SPT sequences. The conserved active residue site highlighted with turquoise (lysine), the conserved residue (histidine) involved in PLP binding highlighted with red. *Sp*SPT (GenBank: BAB56013.1), *Hs*LCB1 (GenBank: AAH68537.1), *Hs*LCB2 (NCBI Reference Sequence: NP_004854.1), *Hs*LCB3 (NCBI Reference Sequence: NP_001336874.1), *Sc*LCB1 (UniProtKB-P25045), *Sc*LCB2 (UniProtKB-P40970), *Tg*SPT1 (ToxoDB gene ID: TGGT1_290980) and *Tg*SPT2 (ToxoDB gene ID: 290970).

```
SpSPT       ------------------------------------------------------------    0

HsLCB1      ----------------------------------------------------MATATEQWV    9
HsLCB2      --------MRPEPGGCCCRRTV-----------------------RANGCVANGEVRNG    28
HsLCB3      --------MANPGGGAVCNGKL-----------------------HNHKKQSNGSQSRN    28
ScLCB1      --------------------------------MAHI-PEVLPKSIPIPAFIVTTSSYLWY    27
ScLCB2      ------------------------------------------------------MSTPAN    6
TgSPT1      MASGATYFTRGTGSPFL-GAGVEWASNIDLFLCAFLSASVLGILLAFFNDEVSWGSLRWS    59
TgSPT2      -MFGSVFVLDSDPMGFIGNRNVEWTTNLDFFYCAFFSASLLGVLLAFFTDDVSSGSLRWS    59

SpSPT       ------------------------------------------------------------    0
HsLCB1      LVEMVQ----------------------A--------------------LYEAPAYHLI    26
HsLCB2      YVRSSA-AAAAAAAAGQIHHV-------TQ--NGGLYK------RPFN-EAFEETPMLVA    71
HsLCB3      -----------CTKNGIVKEA-------QQNGKPHFYD------KLIV-ESFEEAPLHVM    63
ScLCB1      YFNLVL----------------------TQIPGGQFI------VSYIKKSHHDDPYRTT    58
ScLCB2      YTRVPL-----CEPEELPDDIQKENEYGTLDSPGHLYQVKSRHGKPLPEPVVDTPPYYIS    61
TgSPT1      WIATQLLPITPCSSHAVYKDVETALAKAARNKAGSK-R----ALEEFL-AALQDGTVMVL    113
TgSPT2      WIVMELLPVPRLSNHVAVKDVEGALITAAKQASGKS-Q----VFAKIV-TAAHEGTLKVL    113

SpSPT       ----------------------MTEAAA------------------QPHALPADAPDIAPE    21
HsLCB1      LEG-----ILILWIIR-----LLFSK-----TY--------KLQERSDLTVKEKEELI--    61
HsLCB2      VLTYVGYGVLTLFGYLRDFLRYWRIEK-----------------CHHATEREEQKDFVS-    113
HsLCB3      VFTYMGYGIGTLFGYLRDFLRNWGIEK-----------------CNAAVERKEQKDFVP-    105
ScLCB1      VEI-----GLILYGII-----YYLSKP-QQKKS--------LQAQKPNLSPQEIDALI--    97
ScLCB2      LLTYLNYLILIILGHVHDFLGMTFQK-------------------NKHLDLLEHDGLAP-    101
TgSPT1      LSKWS----------ARGFERLAFYWQALKIKYTAQSRRQFFYQMQKVQLKLEIKPG---    160
TgSPT2      LAQWC----------TKLHLRCWFCWHTLKLRYTAESRRQLLYQVNKVLLRLENRKG---    160
                                                              .     :
SpSPT       RDLLSKFDGLIAERQK--------LLDSGVTDPFAIVMEQVKSPTEAVI-----------    62
HsLCB1      ----EEWQPEPLVPPVPKDHPALNYNIVSGP--PSH-----------------KT-----    93
HsLCB2      --LYQDFENFYTRNLYMRIRDNWNRPICSVPGARVDIMERQSHDYNWSFKYTG-------    164
HsLCB3      --LYQDFENFYTRNLYMRIRDNWNRPICSAPGPLFDLMERVSDDYNWTFRFTG-------    156
ScLCB1      ----EDWEPEPLVDPSATDEQSWRV--AKTP--VTMEMPIQNH----------ITITRNN    139
ScLCB2      --WFSNFESFYVRRIKMRIDDCFSRPTTGVPGRFIRCIDRISHNINEYFTYSG-------    152
TgSPT1      ---ETEMQSYNDAKRYMKSRDL------------------------WPFAYEVSNVKDTQ    193
TgSPT2      ---EKEVQSYLDIKRYMQTNNL------------------------WYFAFRISDVKSQY    193
                 . :
SpSPT       ---RGKDTILLGTYNYMGMTFDPD-VIAAGKEALEKFGSGTNGSRMLNGTFHDHMEVEQA    118
HsLCB1      -VVNGKECINFASFNFLGLLDNPR-VKAAALASLKKYGVGTCGPRGFYGTFDVHLDLEDR    151
HsLCB2      --NIIKGVINMGSYNYLGFARNTGSCQEAAAKVLEEYGAGVCSTRQEIGNLDKHEELEEL    222
HsLCB3      --RVIKDVINMGSYNFLGLAAKYDESMRTIKDVLEVYGTGVASTRHEMGTLDKHKELEDL    214
ScLCB1      LQEKYTNVFNLASNNFLQLSATEP-VKEVVKTTIKNYGVGACGPAGFYGNQDVHYTLEYD    198
ScLCB2      --AVY-PCMNLSSYNYLGFAQSKGQCTDAALESVDKYSIQSGGPRAQIGTTDLHIKAEKL    209
TgSPT1      VICEGVRAYPMSSYSYLDFVREPL-VQEAALAAGRTWSTGNHGARMLGGNMRILRDLEKM    252
TgSPT2      ITCEGKRAYHMSSYSYLDFMREPL-VQEAALAAGRMWSTGNHGARMLGGNPTVIRELEQI    252
                      :.: .:: :         .       :.    .     *.       *
SpSPT       LRDFYGTTGAIVFSTGYMANLGIISTLAGKGEYVILDADSHASIYDGCQQGNAEIVRFRH    178
HsLCB1      LAKFMKTEEAIIYSYGFATIASAIPAYSKRGDIVFVDRAACFAIQKGLQASRSDIKLFKH    211
HsLCB2      VARFLGVEAAMAYGMGFATNSMNIPALVGKGCLILSDELNHASLVLGARLSGATIRIFKH    282
HsLCB3      VAKFLNVEAAMVFGMGFATNSMNIPALVGKGCLILSDELNHTSLVLGARLSGATIRIFKH    274
ScLCB1      LAQFFGTQGSVLYGQDFCAAPSVLPAFTKRGDVIVADDQVSLPVQNALQLSRSTVYYFNH    258
ScLCB2      VARFIGKEDALVFSMGYGTNANLFNAFLDKKCLVISDELNHTSIRTGVRLSGAAVRTFKH    269
TgSPT1      VGRFFGREDSLLCATGFLATMSSICAVAKEGDLIVGDNRLHASLRSGMKLSGAKEMLFRH    312
TgSPT2      IGRFFGREDALLCATGFLAAMSSICAVAKKGDLIIGDNRLHTSLRVGMKLSGAKEVLFRH    312
            :  *     ::  . .: :    : :   .   :. *      :  . : . :    *.*

SpSPT       NSVEDLDKRLGRL-----PK-----EPAKLVVLEGVYSMLGDIAPLKEMVAVAKKHGAMV    228
HsLCB1      NDMADLERLLKEQEIEDQKNPRKARVTRRFIVVEGLYMNTGTICPLPELVKLKYKYKARI    271
```

```
HsLCB2      NNMQSLEKLLKDAIVYGQPRTRR-PWKKILILVEGIYSMEGSIVRLPEVIALKKKYKAYL    341
HsLCB3      NNTQSLEKLLRDAVIYGQPRTRR-AWKKILILVEGVYSMEGSIVHLPQIIALKKKYKAYL    333
ScLCB1      NDMNSLECLLNELTE-QEKLEKLPAIPRKFIVTEGIFHNSGDLAPLPELTKLKNKYKFRL    317
ScLCB2      GDMVGLEKLIREQIVLGQPKTNR-PWKKILICAEGLFSMEGTLCNLPKLVELKKKYKCYL    328
TgSPT1      NNWHHLQQTLAK--------HRR-KYKNCWIVIESVYSMDGDIADLPVVRRLADQYNCRI    363
TgSPT2      NNWQHLTQILGS--------MRR-KYIDCWIVIESVYSMDGDIADLPTVRRLADQYKCQI    363
            ..   *   :                    :  *.::   * :  *  :  :  ::   :

SpSPT       LVDEAHSMGFFGPNGRGVYEAQGLEG--QIDFVVGTFSKSVGTVGGFVVSNHPKFEAVRL    286
HsLCB1      FLEESLSFGVLGEHGRGVTEHYGINI-DDIDLISANMENALASIGGFCCGRSFVIDHQRL    330
HsLCB2      YLDEAHSIGALGPTGRGVVEYFGLDP-EDVDVMMGTFTKSFGASGGYIGGKKELIDYLRT    400
HsLCB3      YIDEAHSIGAVGPTGRGVTEFFGLDP-HEVDVLMGTFTKSFGASGGYIAGRKDLVDYLRV    392
ScLCB1      FVDETFSIGVLGATGRGLSEHFNMDRATAIDITVGSMATALGSTGGFVLGDSVMCLHQRI    377
ScLCB2      FIDEAHSIGAMGPTGRGVCEIFGVDP-KDVDILMGTFTKSFGAAGGYIAADQWIIDRLRL    387
TgSPT1      LLDEAHGLGVLGKTGRGLEEHFNMPG--AADVIVGTFSKSIGGVGGYITGDNDLVEFLDF    421
TgSPT2      IVDEAHGLGVLGKSGRGLEEHFNMPG--AADIIVGTFSKSIGGVGGFITCGKDLIEFLEY    421
             ::*: .:* .*  ***: *  .:      *.  ..: .:..  **:
SpSPT       ACRPYIFTASLPPSVVATATTSIRKLMTA------HEKRERLWSNARALHGGLKA-----    335
HsLCB1      SGQGYCFSASLPPLLAAAAIEALNIMEEN------PGIFAVLKEKCGQIHKALQGISGL-    383
HsLCB2      HSHSAVYATSLSPPVVEQIITSMKCIMGQDGTSLGKECVQQLAENTRYFRRRLKE-----    455
HsLCB3      HSHSAVYASSMSPPIAEQIIRSLKLIMGLDGTTQGLQRVQQLAKNTRYFRQRLQE-----    447
ScLCB1      GSNAYCFSACLPAYTVTSVSKVLKLMDSN------NDAVQTLQKLSKSLHDSFASDDSL-    430
ScLCB2      DLTTVSYSESMPAPVLAQTISSLQTISGEICPGQGTERLQRIAFNSRYLRLALQR-----    442
TgSPT1      HAPGSVFSAPLTAYSAGGAMMAFELMQGE-----QSWRIAKAQENAKYLRHALQTGLGLW    476
TgSPT2      HALGSVFSAPLTAYSAGGAKKAFELMQGE-----HRWRIAKAQENAIYLRRALKTGNGNW    476
                  ::  :          :. :                    ::  :
SpSPT       -------MGFRLGTETCDSAIVAVM---LEDQEQAA-----------------------    361
HsLCB1      ----------K----VVGESLSPAFHLQLEESTGSRE-----------------------    406
HsLCB2      -------MGFIIYGN-EDSPVVPLM---LYMPAKIG-----------------------    480
HsLCB3      -------MGFIIYGN-ENASVVPLL---LYMPGKVA-----------------------    472
ScLCB1      ----------RSYVIVTSSPVSAVLHLQLTPAYRSRKFGYTCEQLFETMSALQKKSQTNK    480
ScLCB2      -------LGFIVYGV-ADSPVIPLL---LYCPSKMP-----------------------    467
TgSPT1      PKDYPAERKFELEGVACTTVIPVVF---PHDGDRVF-----------------------    509
TgSPT2      PPDYPADKKYEVEGIECTTVIPVVF---PNDPYRLC-----------------------    509
                           :   :
SpSPT       ---------MMW-----QALLDGGLYVNMARP-------PATPAGTFLLRCSICAEHTPA    400
HsLCB1      ------QDVRLLQEIVDQCMNR-SIALTRARYLEKEEKCLPPPRGRTGESCVHHQGGSPG    459
HsLCB2      ---------AFG-----REMLKRNIGVVVVGF-------PATPIIESRARFCLSAAHTKE    519
HsLCB3      ---------AFA-----RHMLEKKIGVVVVGF-------PATPLAEARARFCVSAAHTRE    511
ScLCB1      FIEPYEEEEKFLQSIVDHALINYNVLITRNTIVLKQET-LPIVP--SLKICCNAA-MSPE    536
ScLCB2      ---------AFS-----RMMLQRRIAVVVVAY-------PATPLIESRVRFCMSASLTKE    506
TgSPT1      ---------RVT-----QAMLKRGWMVAAAAY-------PACPLNRPRIRVTATAAYNQK    548
TgSPT2      ---------CVT-----RALFSKGWVVGAAMY-------PACPLMRPRIRITATAAYTKE    548
                       .      : :      :                            .

SpSPT       QIQTVLGMFQAAGRAVGVIG-----------------------------------------    420
HsLCB1      --RPALGRVPGP---WPPATQ---HAERTQDSRWPWSGLKESKNMWIFDRIVTKWCQYGP    511
HsLCB2      ILDTALKEIDEVGDLLQLKYSRHRLVPLLD-------RPFDE--------TTYEETED--    562
HsLCB3      MLDTVLEALDEMGDLLQLKYSRHKKSARP--------ELYDE--------TSFELED---    552
ScLCB1      ELKNACESVKQS---I-------------------------------------LACCQESN    557
ScLCB2      DIDYLLRHVSEVGDKLNLKSNSGKSSYDGKRQRWDIEEVIRR--------TPEDCKDDKY    558
TgSPT1      MMDEFVKSLVEVTVECPPTDMLR-------------------------------------    571
TgSPT2      IMDKFVRDLVKTTVDVPLTTEVEDG-------------------------PITL-----    577
                     .
SpSPT       ---    420
HsLCB1      IV-    513
HsLCB2      ---    562
HsLCB3      ---    552
ScLCB1      K--    558
ScLCB2      FVN    561
TgSPT1      ---    571
TgSPT2      ---    577
```

The results confirmed that both human SPT1 (*Hs*LCB1) and yeast SPT1 (*Sc*LCB1) are lacking the active site residue (lysine) (figure 3-4), and indicated that these subunits work in a regulatory role (non-catalytic role). Also, these subunits lack the histidine residue (in *Sp*SPT His234) involved in PLP binding. The other alignments have both these residues as illustrated in table (3-1).

Table (3-1) Active site and PLP binding residues within mammalian SPT2 (human and yeast) and *T. gondii* SPT1 and 2. Comparing with the bacterial model (*Sp*SPT) (Yard *et al.,* 2007).

SPT in organisms	Residue site	Suggested function
*Sp*SPT	Lys265	SPT active site
*Hs*LCB2	Lys379	SPT active site
*Hs*LCB3	Lys371	SPT active site
*Sc*LCB2	Lys367	SPT active site
*Tg*SPT1	Lys400	SPT active site
*Tg*SPT2	Lys400	SPT active site
*Sp*SPT	His234	Involved in PLP binding
*Hs*LCB2	His347	Involved in PLP binding
*Hs*LCB3	His339	Involved in PLP binding
*Sc*LCB2	His334	Involved in PLP binding
*Tg*SPT1	His369	Involved in PLP binding
*Tg*SPT2	His369	Involved in PLP binding

The results suggested that both *Tg*SPT1 and *Tg*SPT2 are catalytically active. In addition, the lack of sequence identity to the eukaryotic SPT2 and the similarity to the bacterial enzyme (28 and 30% identity, and 47 and 46% similarity, in the C-terminal region of *Tg*SPT1 and 2 respectively) indicate that the protozoan SPT has a prokaryotic origin. A recent study confirmed this by using a phylogenetic approach (Mina *et al.,* 2017) (figure 3-6).

Figure (3-6) Phylogenetic tree produced from a genetic distance matrix showing the relationship between the eukaryotic catalytic subunit of serine palmitoyltransferase (LCB2) and the prokaryotic and apicomplexan orthologues (SPT). The Opistokonta (animals and fungi) are coloured blue; the Excavata (subgroup of unicellular eukaryotes) are yellow; Amoebozoa (amoeboid protozoa) are grey; Archaeplastida (plants and algae, containing cyanobacterium-derived plastid) are green; Rodophyta (a subgroup of the Archaeplastida - red algae) are red; Chromalveolata (unicellular eukaryotes containing red algal derived plastid) are turquoise; Sphingomonadales (alphaproteobacteria with the ability tosynthesize sphingolipids) are pink (Mina *et al.,* 2017).

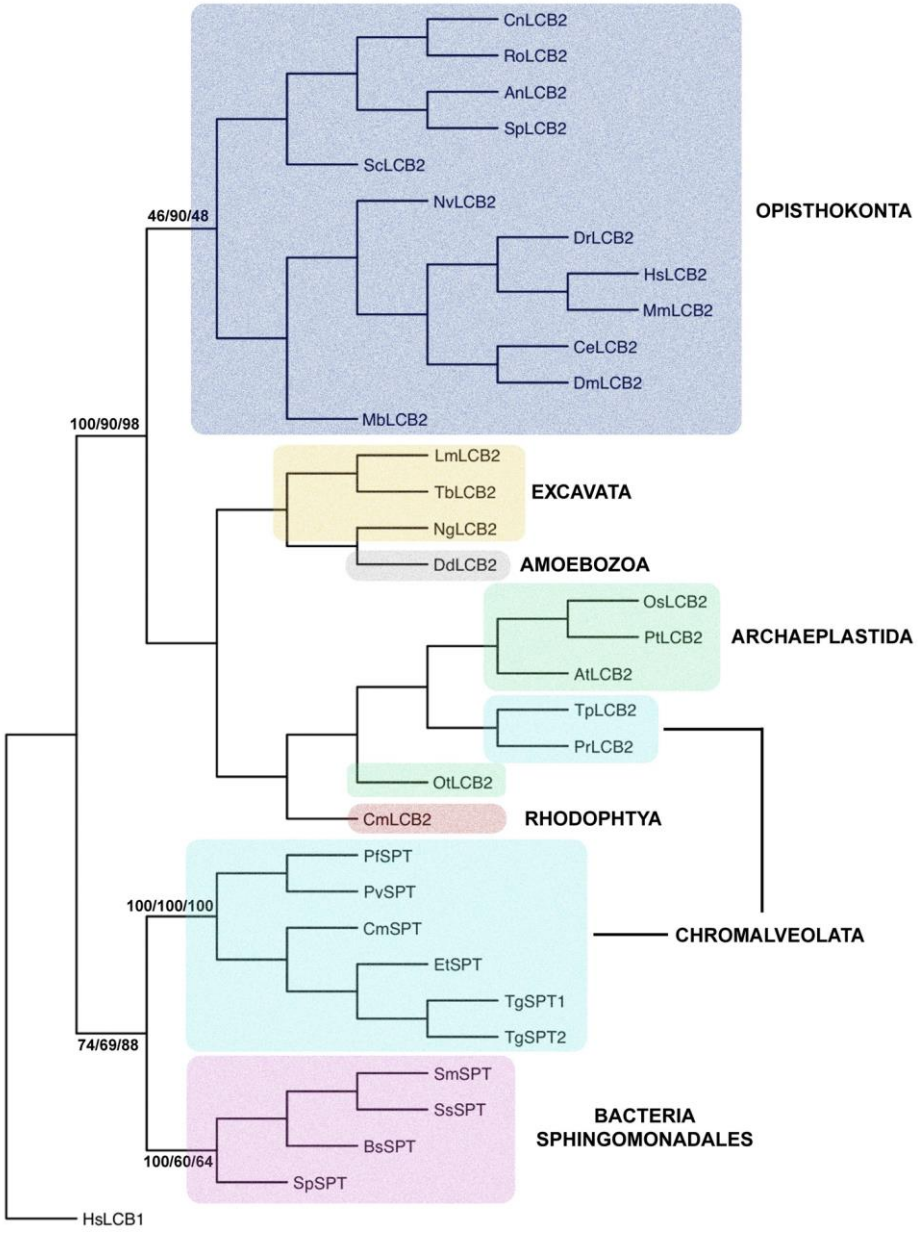

Using the *T. gondii* protein sequences in BLAST searches allowed the identification of orthologues in other apicomplexan parasites: *Eimeria tenella* – *Et*SPT; *Plasmodium falciparum*– *Pf*SPT; and *P. vivax* – *Pv*SPT (Mina *et al,* 2017). Along with the bacterial *S. paucimobilis* SPT (*Sp*Spt), as structural data is available (Yard *et al.,* 2007), the apicomplexan sequences were aligned using T-Coffee Expresso (Di Tommaso *et al.,* 2011). The results indicated the presence of an N-terminal extension in the apicomplexan SPTs (figure 3-7). Using the Phobius tool, transmembrane domains were predicted. The results indicated that the most likely transmembrane domain is within this N-terminal extension: *Tg*SPT1 a.a. 27-47 (figure 3-8A); and in *Tg*SPT2 a.a. 29-47 (figure 3-8B). Both of these lay within the (figure 3-8). Kyte and Doolittle hydrophobicity/hydrophilicity predictions supported these results, with the transmembrane domains predicted as a.a 27-48 and 29-47 for *Tg*SPT1 and *Tg*SPT2 respectively (figure 3-9).

Figure (3-7) Sequence alignment of the predicted serine palmitoyltransferases from 4 members of the Apicomplexa (*Toxoplasma gondii* – TgSPT1 and 2; *Eimeria tenella* – *Et*SPT; *Plasmodium falciparum* – *Pf*SPT; and *P. vivax* – *Pv*SPT) and the characterised enzyme from the prokaryote *Sphingomonas paucimobilis* (*Sp*SPT). Conserved residues (including those in the active site) identified by analyses of the *Sp*SPT structure and homology modelling of the human functional orthologue (LCB2), are highlighted in red, with white text denoting similarity. Blue boxes denote conserved domains. The canonical lysine demonstrated to form an internal aldimine with the co-factor PLP at *Sp*SPT position 265 is highlighted. The *N*-terminal extensions unique to the predicted apicomplexan enzymes harbour a transmembrane domain predicted by Phobius (Käll and Sonnhammer 2004), (TMD, bold underlined). The figure was produced using ESPript 3.0 (Gouet and Courcelle, 2003).

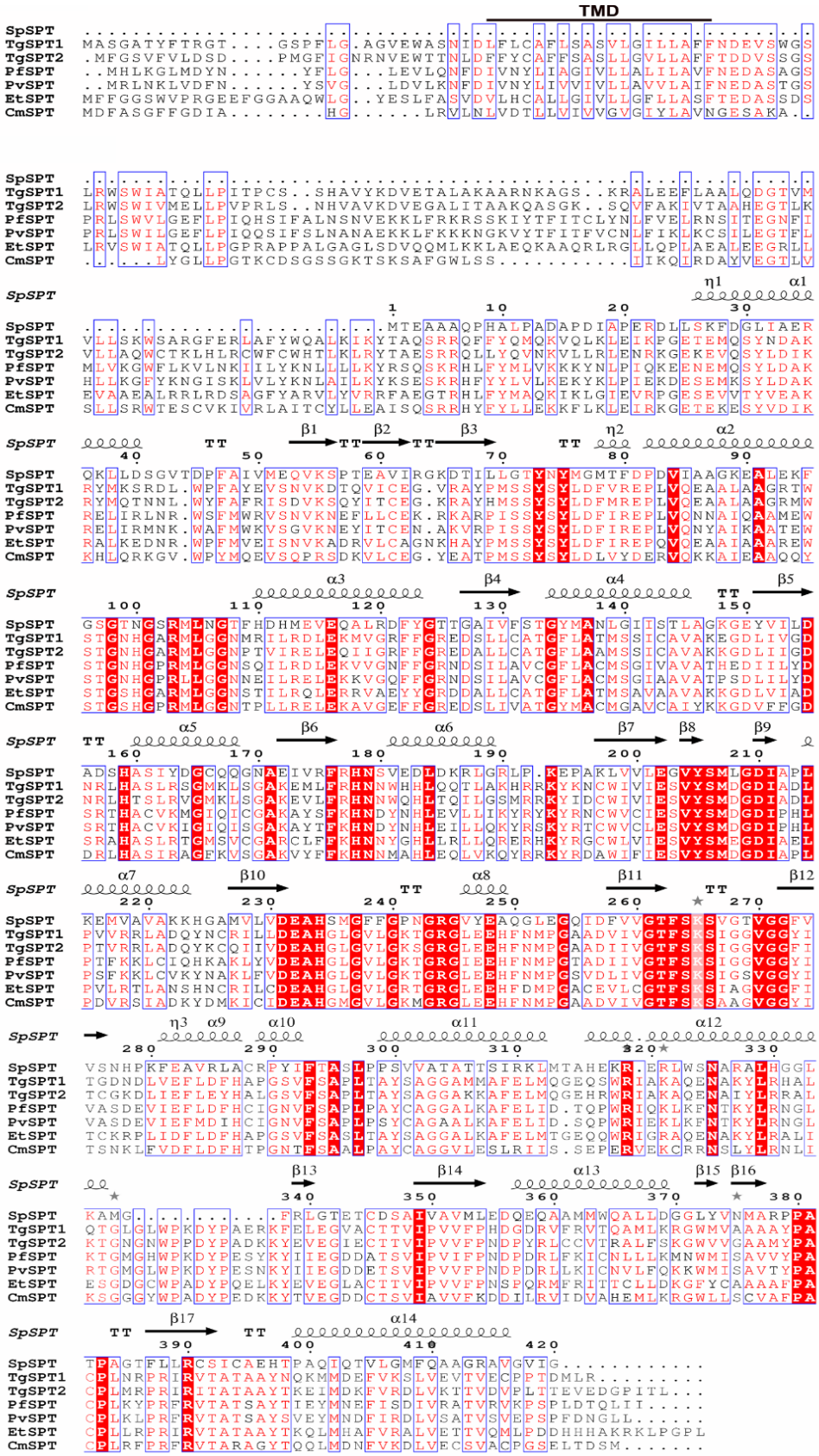
TMD
SpSPT
TgSPT1
TgSPT2
PfSPT
PvSPT
EtSPT
CmSPT

Figure (3-8) Transmembrane prediction for A. *Tg*SPT1 and B. *Tg*SPT2 by using Phobius tool (http://www.ebi.ac.uk/Tools/pfa/phobius/)

A. B.

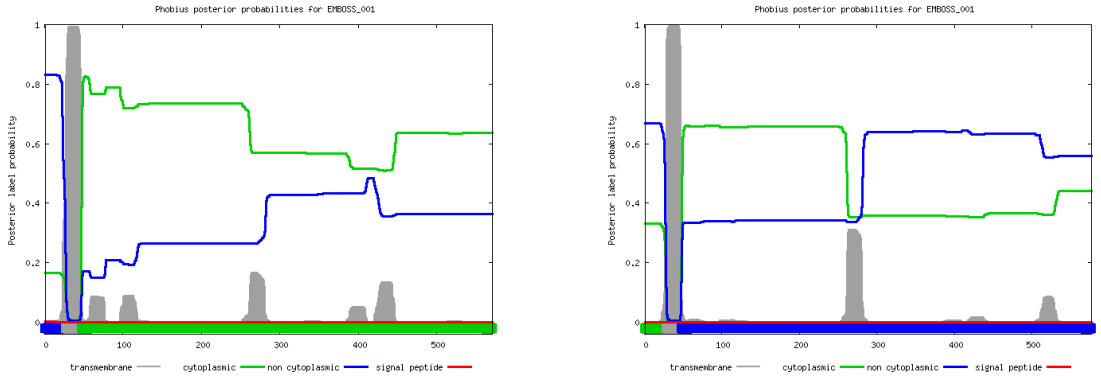

.

Figure (3-9) the hydrophobicity of Kyte and Doolittle parameter to predict the hydrophobicity/hydrophilicity of A. *Tg*SPT1 and B. *Tg*SPT2

A. B.

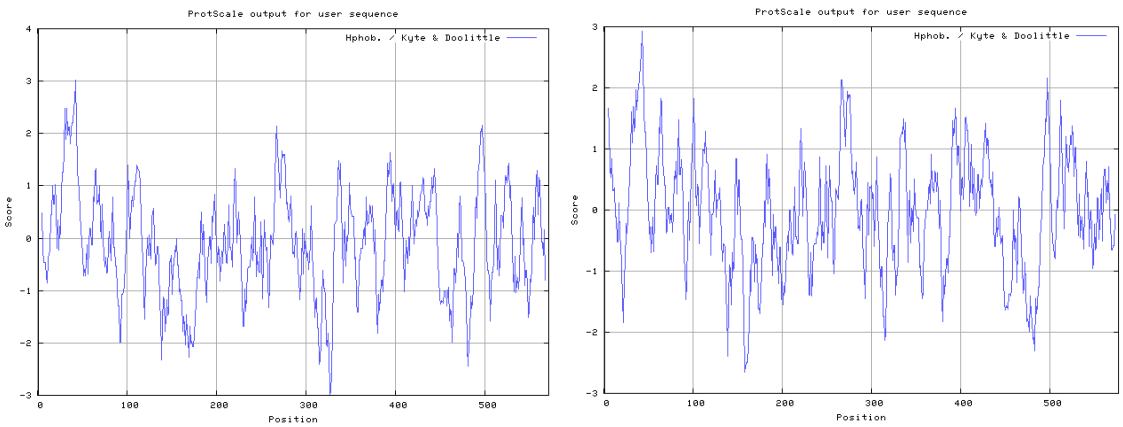

The predicted transmembrane domain in the apicomplexan SPTs indicated that, like the eukaryotic SPT, they are associated with the membranes (Han *et al.,* 2004). The prokaryote SPT lack this domain and are cytoplasmic (Yard *et al.,* 2007). It has now been confirmed that *Tg*SPT1 is ER localized (Mina *et al.,* 2017). Also, these data demonstrate that aside from *T. gondii* the Apicomplexa encode a single SPT, indicating that a gene duplication event has occurred in *T. gondii* (figure 3-7) after speciation.

Chapter four:
T. gondii sphingolipid biosynthesis

4.1 Introduction

This chapter examines the function and role of *Tg*SPT2 in the *T. gondii de novo* sphingolipid biosynthestic pathway through the analyses of biochemical activity and subcellular localization *Tg*SPT2, and the deletion of both *Tg*SPT1 and 2 by homologous recombination.

4.2 *Toxoplasma gondii* serine palmitoyltransferase 2 (*Tg*SPT2) expression and purification

Recombinant *Tg*SPT2 was expressed in *E.* coli from the plasmid pOPIN_HIS_SUMO_C3_Δ158*Tg*SPT2 (GeneScript) as described in materials and methods (Chapter 2). The fusion protein produced was *Tg*SPT2, lacking the first 158 a.a. (Δ158 *Tg*SPT2), N-terminally tagged with a histidine-tag which was used in the purification process and the Small Ubiquitin-like Modifier (SUMO) protein was used to enhance solubility and stability (Yan *et al*., 2009). A C3 containing the protease cleavage site followed the tags to allow cleavage using HRV 3C protease and purification of Δ158 *Tg*SPT2. This truncated protein was used because bioinformatic analyses indicated that the first 100 a.a. contains a transmembrane domain (Chapter 3), and removal of this domain is likely make the purified protein more soluble and easier to purify. Notably, previous studies in the Denny lab demonstrated that *Tg*SPT1 lacking 158 a.a. (Δ158 *Tg*SPT1) was soluble and catalytically activity (Thye, 2014; Mina *et al,* 2017).

Δ158 *Tg*SPT2 was purified and cleaved as described (Chapter 2), and the resultant protein analyzed using SDS-PAGE. The results showed that the HIS-SUMO-3C-*Tg*SPT2 was resistant to cleavage by the HRV 3C protease (figure 4-1) for unknown reasons, the band migrating at about 60 kDa is the fusion protein composed of Δ158 *Tg*SPT2 (46.7 kDa) and SUMO with His6x 12.2 (kDa). Further modifications in the purification or expression plasmid are needed in the future to solve this problem.

Figure (4-1) SDS-PAGE showed that the molecular weight of the purified protein was 60 kDa (the band marked with a black arrow).

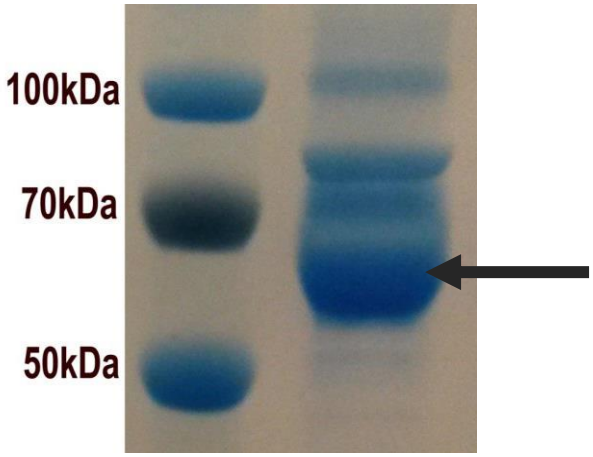

4.3 *Tg*SPT2 activity assay

To establish the activity of *Tg*SPT2, the uncleaved 60kDa fusion protein was studied as described (Chapter 2) by adding the substrates serine and palmitoyl-CoA to the protein in the presence of co-factor pyridoxal phosphate (PLP). Following incubation and separation of the lipid faction, ultra-performance liquid chromatography UPLC electron spray ionization (ESI) mass spectrometry (MS) was used to measure the formation of 3-KDS. UPLC ESI results showed that the 3-KDS, which has the molecular weight (M.W.) of 300.29 KDa, was formed with retention time (RT) 3.75 mins. The MS spectrum in figure 4-2 shows 2 peaks: 300.29, the accurate mass of 3-KDS; and 282.28, the accurate mass of 3-KDS with the loss of water (H_2O). This study demonstrated that *Tg*SPT2 is a functional, bacterially-derived, SPT even as a fusion protein. This is like *Tg*SPT1 (Mina *et al,* 2017) and indicated the important role for both SPT isoforms in the *de novo T. gondii* sphingolipid biosynthetic pathway.

Figure (4-2) Mass spectrometry of lipids extracted froman *in vitro* reaction of the *Tg*SPT2 Δ158 fusion with serine and palmitoyl CoA as substrates and PLP as co-factor. The peak 300.29 corresponds to the mass of 3-ketodihydrosphingosine $C_{18}H_{37}NO_2$, 282.28 is the same molecule with the loss of water.

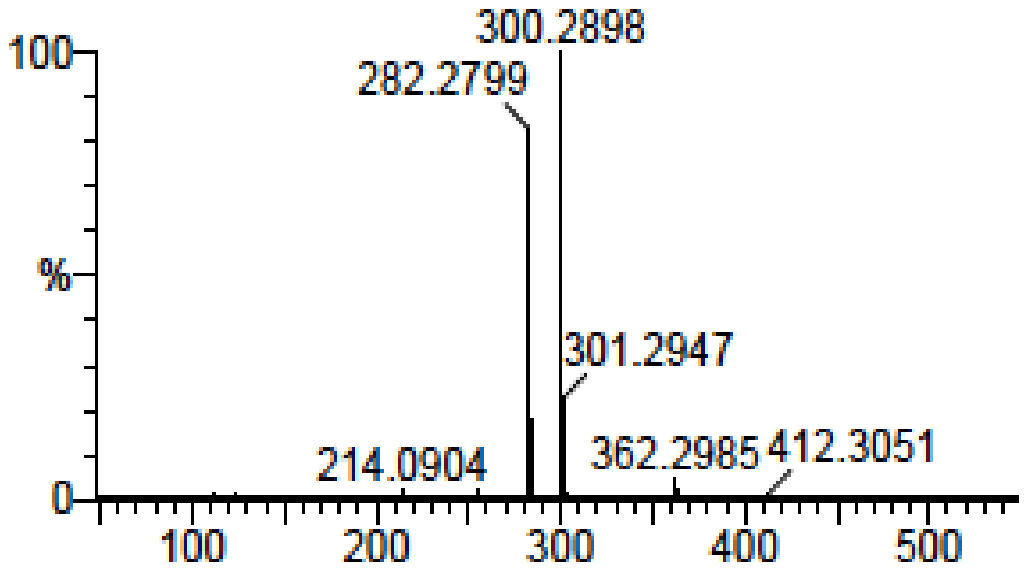

4.4 The sub-cellular localization of *Tg*SPT2

To try and understand whether *Tg*SPT2 functions as a normal ER bound eukaryotic SPT (rather than a cytoplasmic bacterial SPT) the subcellular localization of the *T. gondii* enzyme was established. To allow localization yellow fluorescent protein (YPF) was C-terminally fused to *Tg*SPT2 in the pG1-*Tg*SPT2_YFP (Chapter 2). This plasmid was transfected into isolated tachyzoite *T. gondii* and these used in infect Human Foreskin Fibroblast (HFF) cells. To allow co-localization, plasmids encoding markers for the Golgi apparatus [Golgi Reassembly and Stacking Protein (GRASP)] tagged with red fluorescent protein (RFP) (Pfluger *et al.,* 2005), and the endoplasmic reticulum [green fluorescent protein (GFP)] tagged with the ER retention signal HDEL (Boevink *et al.,* 1999) were co-transfected.

4.4.1 *Tg*SPT2 co-localization with the Golgi marker GRASP_RFP

T. gongii tachyzoites transfected with the constructed pG1*Tg*SPT2_YFP and pTub-GRASP-RFP as described (Chapter 2). HFF cells infected with these transiently transfected tachyzoites were then fixed, stained and imaged using a Zeiss Apotome microscope and, for higher resolution, a Zeiss 880 with Airyscan microscope (figure 4-3A-D). The results from the high-resolution analyses showed that the ectopically expressed *Tg*SPT2_YFP (figure 4-3B) is not localized to the Golgi apparatus (Red) (figure 4-3C, 4-3D).

Figure (4-3) Subcellular localisation of *Tg*SPT2 and GRASP imaged using the Zeiss LSM 880 microscope with Airyscan with appropriate filters. HFF and tachyzoite nuclei stained with 4',6-diamidino-2-phenylindole (DAPI) (Blue, 4-3A); *Tg*SPT2_YFP (Green, 4-3B); GRASP (Red, 4-3C); and finally (4-3D) a merge of 4-3A-C.

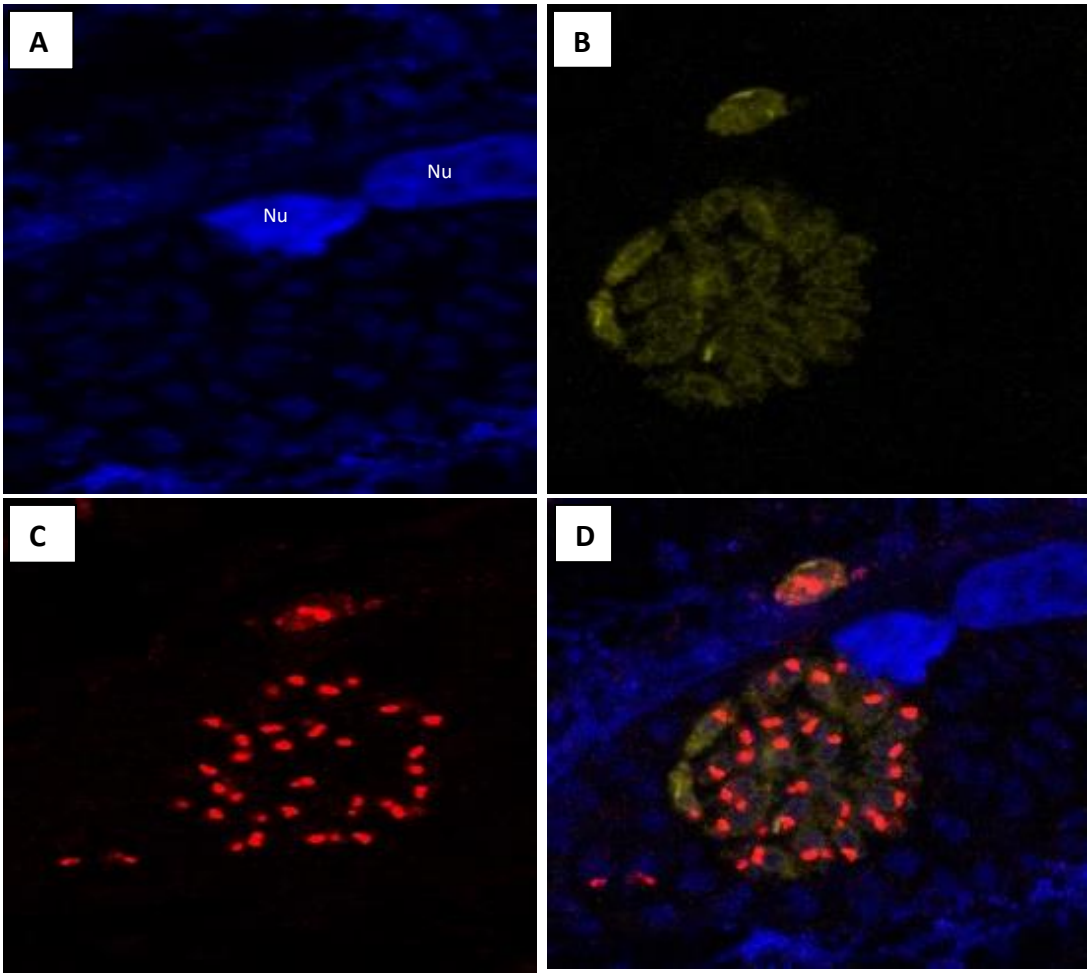

4.4.2 *Tg*SPT2 co-localization with the ER marker GFP_HDEL

The same steps as in 4.4.1 were used in this experiment except that p30-GFP_HDEL instead of pTub-GRASP-RFP was transfected with pG1*Tg*SPT2_YFP, and the fixed and stained cells subsequently imaged using DeltaVision OMX microscopy. The results showed that the *Tg*SPT2 is co-localized with GFP_HDEL (figure 4-4). Therefore, this study concluded that *Tg*SPT2 is, like the mammalian orthologue, localized to the ER. This resembles the *Tg*SPT1 isoform (Mina *et al.,* 2017), and shows that although *Tg*SPT1 and 2 are bacterial in origin, but their function in the ER like in other eukaryotes.

Figure (4-4) DeltaVision OMX imaged 125 nm optical slice of *T. gondii* within a parasitophorous vacuole (PV) of a HFF infected cell. DAPI (Figure4-4A, Blue), showing parasite nuclear (Nu) and apicoplast (Ap) DNA; Anti-GFP antibody stain (Figure4-4B, Alexa Fluor® 594, Red) of episomally expressed GFP-HDEL, showing the parasite ER) TgSPT2-YFP (Figure4-4C, Green); Merge of Figure4-4A-C showing overlap of TgSPT2-YFP with the ER marker GFP-HDEL (Figure4-4D, Yellow). Scale bar shown.

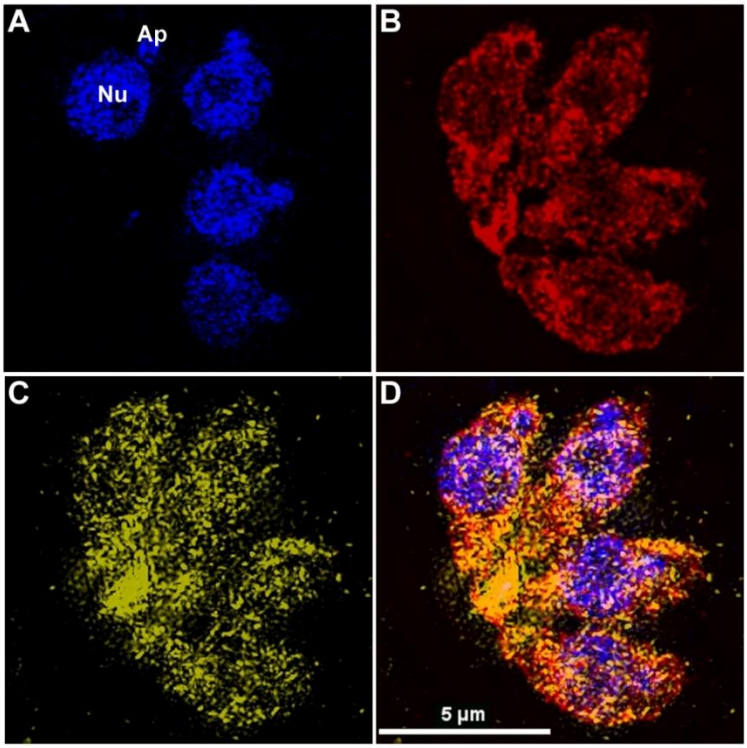

4.5 *Tg*SPT2 knockout (KO)

4.5.1 KO Plasmid (pTub5CatSagF1F2) construction and mapping

The plasmid used (pTub5CatSag1F1F2**,** made in collaboration with Dr Hosam Shams-Eldin and Philip Stahl [University of Marburg]), contained a construct designed to knockout the 2 tandem copies of *T. gondii* SPT (*Tg*SPT1 and *Tg*SPT2) by homologous recombination. This construct and the intended knockout process is shown in Figure (4-5).

Figure (4-5) *Tg*SPT1 and *Tg*SPT2 knockout by using homologous recombination

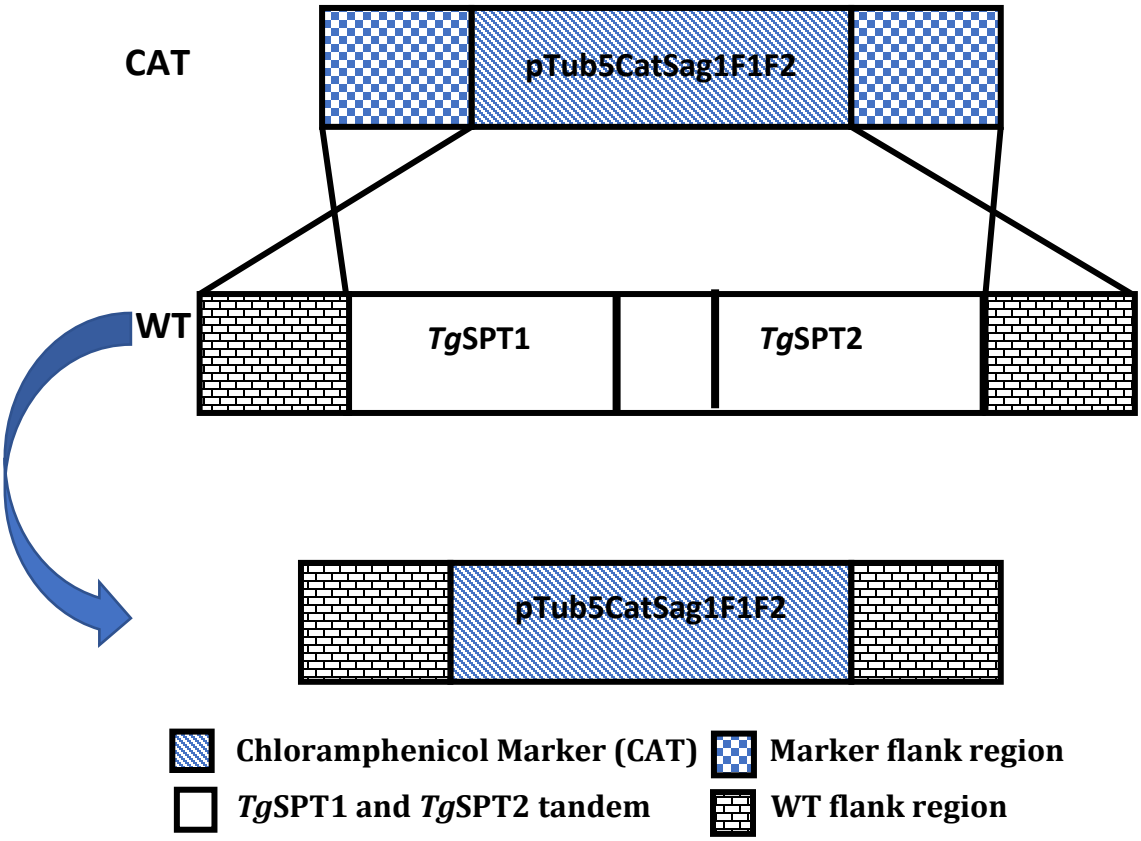

To confirm the identity of the SPT knockout construct the plasmid was mapped by digestion with the restriction enzymes NotI, NotI + XhoI, NotI + HindIII and XhoI.

Figure (4.6) Gel electrophoresis of restriction enzyme digests Figure 4.6A: kb ladder; Figure 4.6B: NotI; Figure 4.6C: NotI+XhoI; Figure 4.6D: NotI+HindIII; Figure 4.6E: XhoI

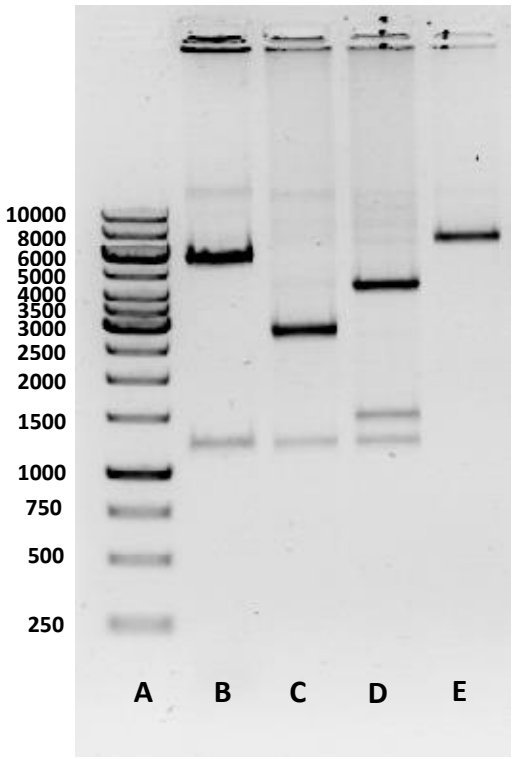

Single digestion with XhoI (Figure 4.6E) shows a single band and indicated the plasmid to be approximately 7.2 kbp in size. NotI digestion gave 2 bands of approximately 6 kbp and 1.2 kbp, indicating 2 NotI sites (Figure 4.6B). Double digestions with NotI and XhoI (Figure 4.6 C) should give three bands, with 2 NotI sites and a single XhoI site (Figure 4.6B and E), however only 2 are evident at approximately 3 kbp and 1.2 kbp. Double digestion with NotI and HindIII (Figure 4.6D) gave 3 bands as expected (approximately 4.5 kbp, 1.5 kbp and 1.2 kbp). Comparing the restriction pattern with the plasmid map (Figure 2.1) it is clear that the pattern is the expected one. The 2 rather than 3 bands seen with NotI and XhoI a result of 2 fragments being of the same size (approximately 3 kbp). This meant

that the construct could be linearized and used delete the 2 tandem SPT genes in T. gondii by homologous recombination and chloramphenicol selection.

4.5.2 *Tg*SPT1 and 2 knockouts

XhoI linearized plasmid was transfected into *T. gondii* ΔKu80-HXG (Rommereim *et al.*, 2013), The Ku80 protein is responsible for non-homologous recombination, deletion of this gene increases the rate of the homologous recombination and maximizes the changes of achieving the desired knockout. Under chloramphenicol selection, after 3 rounds of egress the parasites were collected, purified and. gDNA extracted. By using the specific primers as following:

P1: CCCCTCGAGCCCTCCACACGCTGAATTTCG
P4: CCCGAGCTCTTGATCGCAACTTTCTGTGCAGTA
P5: CCACCGTTGATATATCCC CAT
P6: GTAATTCATTAAGCATTCTGC

(P1 and P4) for construct flank regions and the chloramphenicol marker (CAT, P5 and P6) the selected parasites were analyzed for the replacement of the *Tg*SPT locus with the chloramphenicol (CAT) marker (Figure 4-7).

The wild type locus is amplified in Figure4-7B (8kb), in a successful knockout this should be lost and replaced with the CAT marker giving a smaller product (4.2kb). Therefore, there was no evidence that the knockout had been successful Figure4-7C. In further experiments various concentrations (20ng, 60 ng and 110 ng) of template *T. gondii* SPTKO-ΔKu80-HX DNA were analyzed for integration of the construct (4.2kb) and the presence of the CAT marker (0.6kb), Figure4-7D, F and H and Figure4-7E, G and I respectively. The CAT marker was detected in all samples (Figure4-7E, G and I) however only the 110ng sample (Figure4-6H) show any evidence of integration of the construct (4.2kb, arrow). Even here the band is very faint and the wild type locus (8kb) is dominant, these preliminary results suggest that *Tg*SPT1 and 2 are important for *T. gondii* fitness;

however future work is needed using for example CRISPR/Cas9 (Sidik *et al.,* 2016) to KO either *Tg*SPT1 or *Tg*SPT2 or both.

Figure (4-7) PCR screen for *Tg*SPT1 and 2 deletions. *T. gondii* ΔKu80-HX and *T. gondii* SPTKO-ΔKu80-HX. Figure 4-7A: kb Markers; Figure 4-7B: P1 and P4 from parent RHdeltaKu80; Figure 4-7C: P1 and P4 from RHdeltaKu80_SPTKO; Figure 4-7D: P1 and P4 from RHdeltaKu80_SPTKO 20ng; Figure 4-7E: P5 and P6 from RHdeltaKu80_SPTKO 20ng; Figure 4-7F: P1 and P4 from RHdeltaKu80_SPTKO 60ng; Figure 4-7G: P5 and P6 from RHdeltaKu80_SPTKO 60ng; Figure 4-7H: PCR using P1 and P4 from RHdeltaKu80_SPTKO 110ng; Figure 4-7I:P5 and P6 from RHdeltaKu80_SPTKO 110ng

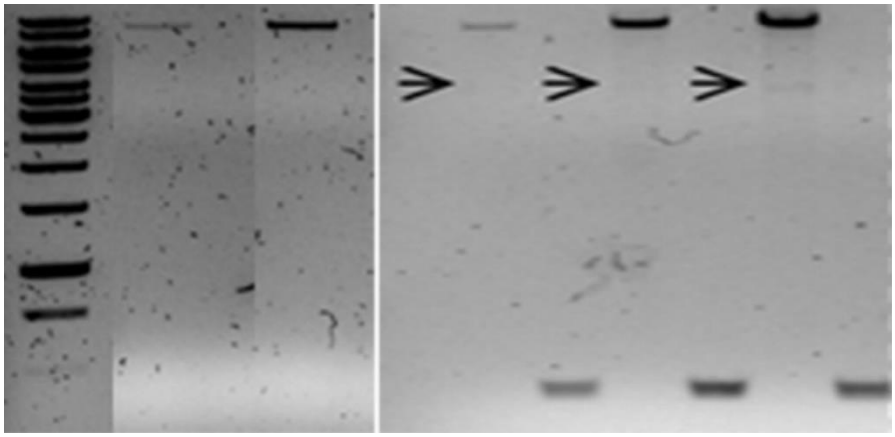

A B C D E F G H

Chapter five:

Study on the effect of AbA and its analogue Cmpd20 against T. gondii

5.1 Introduction to Aureobasidin A and its derivative compound 20 (Cmpd20)

Aureobasidin A (AbA) (figure 5.1A) is a natural cyclic depsipeptide produced by the *Auriobasidium pullulans* strain BP-1938 (Wuts *et al.,* 2015). AbA is a fungicidal and has high activity against several clinically relevant fungi, for example *Candida* spp. and *Cryptococcus neoformans.* AbA inhibits the growth of most fungi at approximately 50 nM, and is active against its target, the fungal IPCS (AUR1p, the non-mammalian sphingolipid synthase), at sub-nanomolar levels (Zhang *et al.,* 2010). However it showed only slight activity against *Aspergillus fumigatus* which has the ability to clear the compound by using an efflux pump (Takesako *et al.,* 1993; Wuts *et al.,* 2015). Attempts have been made to modify the structure of AbA to increase its effect against *A. fumigatus* (Wuts *et al.,* 2015) which found the most effective analogue generated was Compound 20 (Comp20, figure 5.1B) with a minimal inhibitory concentration (MIC) against *A. fumigatus* of 1-2 µg/ml.

Figure (5-1) Chemical structure of AbA (A) and its analogue Compound 20 (B). Adopted from Wuts *et al*., 2015, and generated by using ChemDraw software (http://www.cambridgesoft.Com/software/overview.aspx**).**

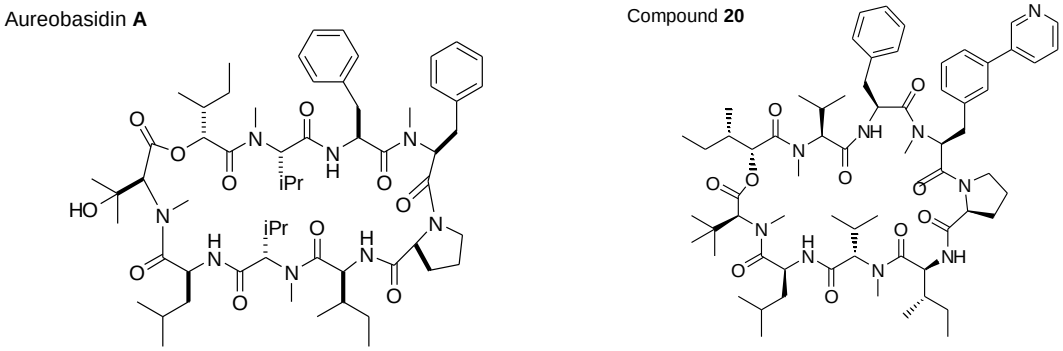

In the kinetoplastid protozoa *Leishmania major*, AbA inhibits promastigote growth with an EC_{50} of 0.6 µM, although the target is not the protozoan IPCS (Denny *et al.,* 2006). At 10 $\mu g/mL^{-1}$ AbA also inhibits the *in vitro* transformation of the related *Trypanosoma cruzi* trypomastigotes to the amastigote form (Salto *et al.,* 2003), although like *Leishmania* this is not due to IPCS inhibition (Figueiredo *et al*., 2005). It was proposed that AbA inhibits amastigote replication inside the macrophage, and trypomastigote egress, due to subversion of host cell nitric acid production and phagocytic capacity (Figueiredo *et al*., 2005). Similarly, AbA has been shown to be active against *T. gondii* tachyzoites by Sonda et al (2005), who indication that it inhibited IPC synthesis.

In this study AbA and its analogue (Cmpd20) (provided by Aureogen Biosciences Inc.) were tested to show the effect of both of them on the replication of both tachyzoite and bradyzoite *T. gondii* and parasite *de novo* sphingolipid biosynthesis.

5.2 The response of host (CHO) sphingolipid biosynthesis pathway to *T. gondii* infection

To establish the effect of *T. gondii* infection on mammalian host cell (CHO) sphingolipid biosynthesis, the modulation of host SPT (the first and rate-limiting step in sphingolipid biosynthesis), and SMS1 and SMS2 were investigated (Romano *et al.,* 2013). Initially conventional PCR was used for quality control using primers for LCB2 (subunit 2 of SPT), SMS1, SMS2 and β-tubulin (a housekeeping gene). Subsequently, real time PCR or qPCR was done to investigate the differences in gene expression for these genes of interest (LCB2, SMS1 and SMS2 with respect to β-tubulin) in infected and uninfected CHO cells. The results showed that the relative expression of host LCB2, SMS1 and SMS2 were 0.82, 1.02 and 0.93 respectively (figure 5.2), meaning that they are not significantly affected by *T. gondii* infection. This indicated that manipulation of host sphingolipid biosynthesis is not important for parasite proliferation, agreeing with the hypothesis that *T. gondii* is dependent on its *de novo* sphingolipid biosynthestic pathway (Pratt *et al.,* 2013)

Figure (5-2) RT-PCR shows expression of host sphingolipid biosynthetic enzymes are largely unaffected by *Toxoplasma* infection (GOI:HKG; n=3). β-tubulin used as housekeeping gene control (HKG).

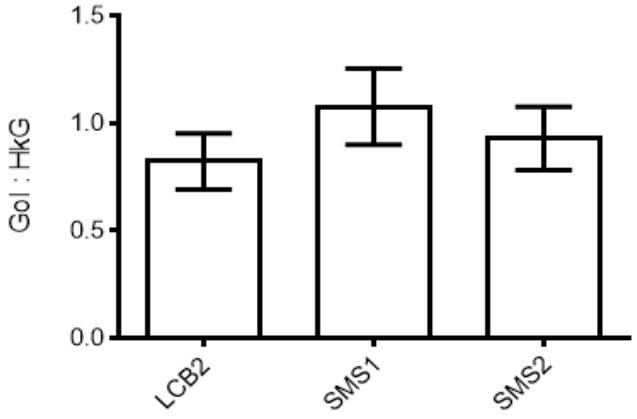

5-3 The effect of known anti-fungal sphingolipid biosynthesis inhibitors aureobasidin A (AbA) and an analogue (Cmpd 20) on *Toxoplasma* proliferation in acute and chronic infection

5.3.1 The effect of compounds on *T. gondii* proliferation in acute infection

The AbA been shown to inhibit the proliferation of tachyzoite form of *T. gondii.* The effective concentration of AbA reducing proliferation by 50% (ED_{50}) was estimated to be 0.3 μg/mL^{-1} by counting the cell number 48h post infection and 46h post AbA addition (Sonda *et al.,* 2005). To gain a more robust result, in this study we used the yellow fluorescent protein (YFP) labeled *Toxoplasma* RH-strain (RH-HX-KOYFP2-DHFR *Toxoplasma*, Gubbels *et al.,* 2003). 20h after infecting HFF host cells with these YFP expressing *T. gondii* (as described, Chapter 2), the compounds were added and the cells left without washing for 6 days and the fluorescence measured. Then the data analyzed and the ED_{50} was calculated for AbA (figure 5-3 A) and Cmpd20 (figure 5-3 B). The results demonstrated that both compounds showed activity against *Toxoplasma gondii* tachyzoites under these conditions. The ED_{50} of AbA was 0.75, 95% CI 0.60 to 0.93 μg

mL-1, and was more slightly efficacious than its analogue (Cmpd20), ED50 of 1.49, 95% CI 1.20-1.85 µg mL-1.

Figure (5-3) ED_{50} of AbA (A) and Cmpd20 (B) µg mL^{-1}; (95% CI [Confidence Interval]) against the RH-HX-KOYFP2-DHFR *T. gondii* tachyzoites in HFF cells. 6 days post addition of the compounds. In agreement with Sonda *et al.* (2005), both compounds were not toxic to HFF cells under the experimental conditions. Calculated by using GraphPad Prism 7, log (inhibitor) vs normalized response- variable slope. Representative in triplicate dataset.

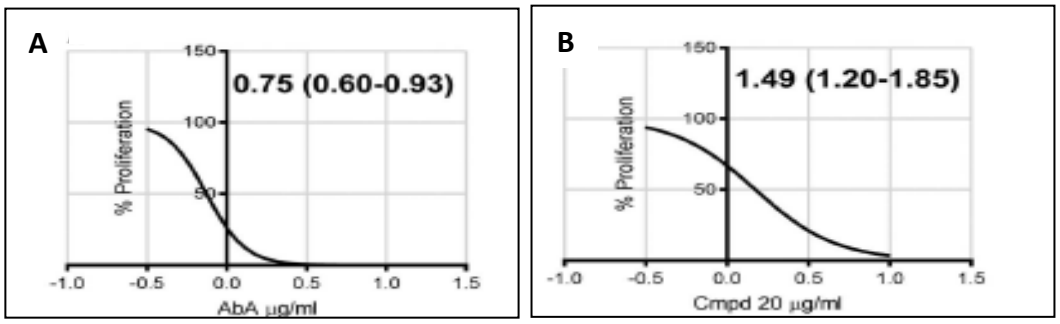

Sonda *et al.* (2005) indicated by using indirect assay (vacuole formation), that the efficacy of AbA against *T. gondii* is partially reversible after 24 h and irreversible after 48 h. For further analyses of the reversibility of the efficacy of both AbA and Cmpd20, the infected HFF cells were washed after 2 and 8 h after compound addition, then incubated for 6 days before fluorescence plates readings were taken. The results showed that AbA *T. gondii* efficacy was partially reversible after 2 h (ED_{50} of 9.58, 95% CI 6.66 to 13.76 µg mL µg mL^{-1}; figure 5-4A), and 8 h exposure (ED_{50} of 4.82, 95% CI 3.73 to 6.22 µg mL^{-1}; figure 5-4C). However, Cmpd20 activity was demonstrated to be almost completely reversible after both exposure times (2 and 8 hr; figure 5-4B and 5-4D respectively).

Figure (5-4) ED_{50} of AbA (A) and Cmpd20 (B) µg mL^{-1} wash out 2 h post compound (95% Confidence Interval), and AbA (C) and Cmpd20 (D) washout 8 h post compound (95% Confidence Interval). RH-HX-KOYFP2-DHFR *T. gondii* in HFF cells. Calculated by using GraphPad Prism 7, log (inhibitor) vs normalized response- variable slope> 10 µg mL^{-1} – ED_{50} could not be determined. Representative in triplicate dataset.

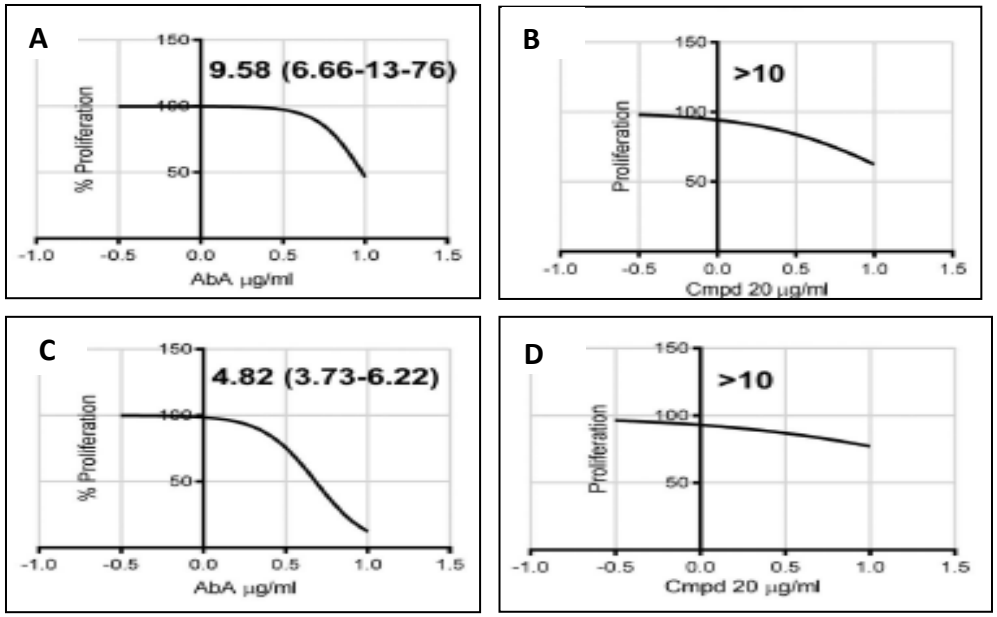

Two hypotheses may explain the efficacy of AbA and Cmpd20 against the parasites, first they may target sphingolipid biosynthesis as in the fungi; second the ability of the host cell to clear infection may be affected (Figueiredo *et al.,* 2005). In order to investigate the second hypothesis *T. gondii* tachyzoites isolated from the infected host cells as described (Chapter 2) were treated with various concentrations of AbA or Cmpd20 for 2 or 8 h and, after washing, used to infect HFF host cells for 6 days. The results showed that the efficacy of AbA after 2 h treatment (ED_{50} of 4.78, 95% CI 3.95 to 5.79 µg mL^{-1}) was greater than Cmpd 20 (figure 5-5). The longer period post-isolation (8 h) lead to untreated tachyzoites losing infectivity. These results indicated that both AbA and Cmpd20 have a direct effect on the parasite, AbA showing greater efficacy as above. This indicates that host modulation may not be a major factor in efficacy, however, in order to know are whether these compounds target parasite sphingolipid biosynthesis more analyses was needed.

Figure (5-5) Figure (5-5) ED_{50} of AbA (A) and Cmpd20 (B) µg mL^{-1} 2 h exposure to isolated RH-HX-KOYFP2-DHFR *T. gondii* tachyzoites (95% Confidence Interval). Calculated by using GraphPad Prism 7, log (inhibitor) vs normalized response- variable slope. > 10 µg mL^{-1} – ED_{50} could not be determined. Representative in triplicate dataset.

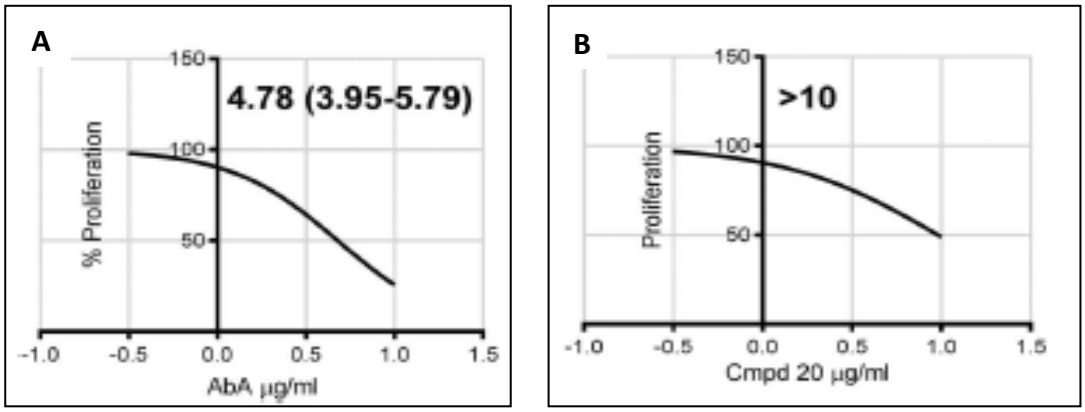

Further analyses were performed to show the effects of both compounds on the *T. gondii de novo* sphingolipid biosynthesis pathway. This study suggested in agreement with (Pratt *et al.,* 2013; Romano *et al.,* 2013) that the host sphingolipid biosynthesis is unaffected and non-essential for *T. gondii* proliferation, so *T. gondii de novo* sphingolipid biosynthesis may be regarded as an attractive drug target for antiprotozoals. Whilst some published studies reported that AbA inhibited a *Toxoplasma* IPCS (Sonda *et al.,* 2005 and Coppens *et al.,* 2013), another demonstrated that IPCS activity encoded by the *T. gondii* enzyme *Tg*SLS, was not sensitive to this compound (Pratt *et al.,* 2013). To analyze both AbA and Cmpd20 an auxotrophic *Tg*SLS complemented yeast strain (YPH499-HIS-GAL-AUR1 pRS426 *Tg*SLS with YPH499-HIS-GAL-AUR1 pRS426 AUR1 as a control) were used and their sensitivity to the compounds were tested at two concentrations (5 and 10 µg mL^{-1}). The results showed that the *Toxoplasma* enzyme (*Tg*SLS) conferred the resistance to yeast against both compounds when compared with the yeast AUR1p, which showed minimal growth (figure 5-6).

Figure (5-6) Yeast dependent on the expression of the *Toxoplasma* AUR1p orthologue *Tg*SLS (YPH499-HIS-GAL-AUR1 pRS426 *Tg*SLS) are resistant to Aureobasidin A (AbA) and Compound 20 (Cmpd 20) at 5 and 10 µg mL^{-1}. This contrasts to the sensitivity of yeast dependent on AUR1 expression (YPH499-HISGAL-AUR1 pRS426 AUR1).

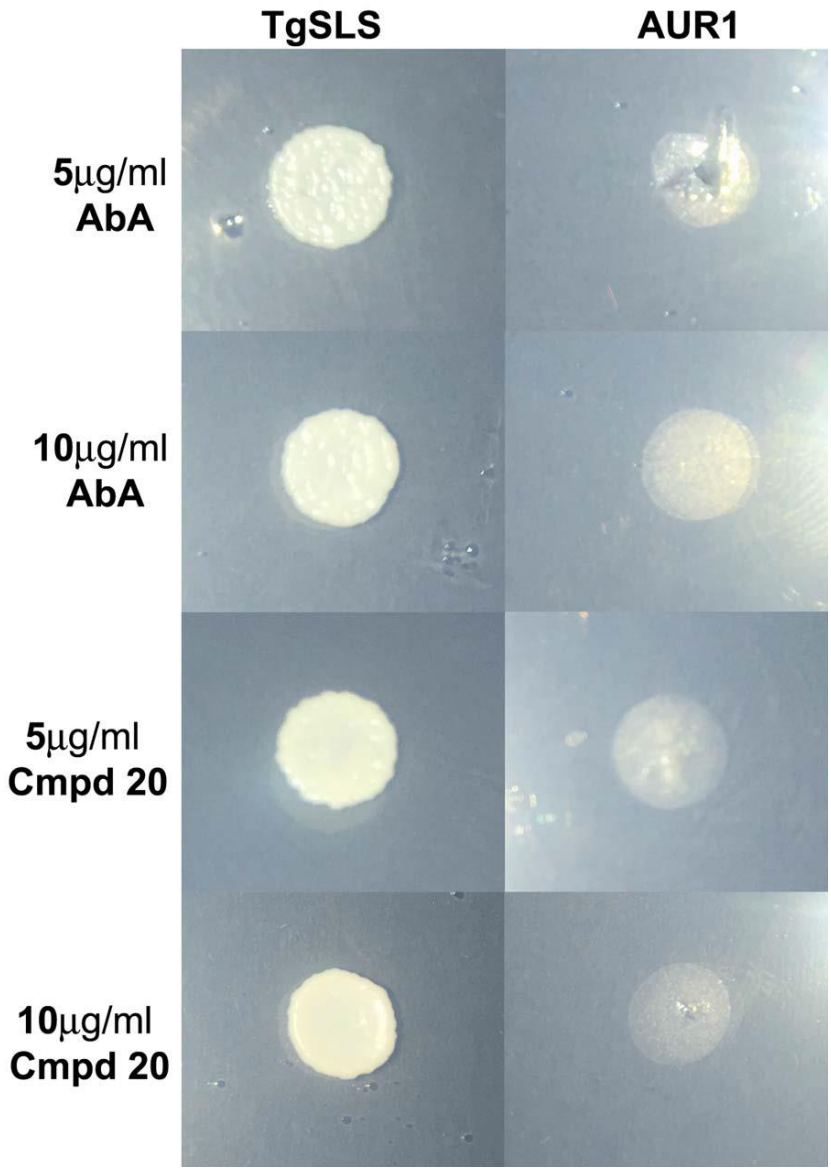

In addition to *Tg*SLS function as an IPCS in yeast and *in vitro, Toxoplasma* have also been demonstrated by using the incorporation of tritiated serine, to produce the sphingomyelin (SM) and glycosphingolipids (GSLs) like mammalian cells (Gerold and Schwarz, 2001). Many studies confirmed that the isolated *Toxoplasma* have SM, GSLs and high levels of ethanolamine phosphorylceramide (EPC) which found in low levels in mammalian cells (Welti *et al.,* 2007 ; Pratt *et al.,* 2013). To study the effects of AbA and Cmpd20 on total sphingolipid biosynthesis in *T. gondii,* parasites were metabolically labeled in the presence of the compounds as described (Chapter 2). Firstly, an experiment demonstrating total sphingolipid biosynthesis in purified *T. gondii* tachyzoites compared with that in host cells (vero cells) and *Saccharomyces cerevisiae* was performed. *T. gondii* tachyzoites were shown to synthesize a complex of sphingolipids including SM and EPC (co-migrating with mammalian equivalents (Vacaru *et al.,* 2013). IPC, clearly shown in yeast, was not detected in this experiment and 2 other species (X and Y) remain unassigned (figure 5-7).

Figure (5-7) Vero cells (Host), isolated *T. gondii* tachyzoites (Toxo) and *Saccharomyces cerevisiae* (Yeast), labeled for 1 h with NBD-C6-ceramide and complex sphingolipids then fractionated by HPTLC. Like the host cells, the parasites synthesize sphingomyelin (SM) and ethanolamine phosphorylceramide (EPC), two unique sphingolipids are also produced (X and Y). However, unlike in *S. cerevisiae,* no labelled inositol phosphorylceramide (IPC) is evident from either host or *Toxoplasma* cells. Representative dataset.

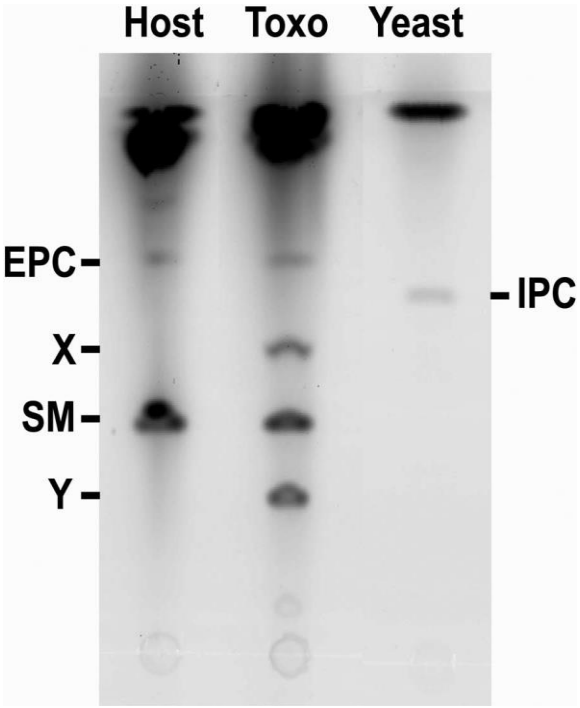

After analyzing the total sphingolipid in *T. gondii*, host and yeast, further analyses were needed to establish the effects of AbA and Cmpd20 on the *T. gondii* sphingolipid biosynthetic pathway. Isolated *T. gondii* tachyzoites were treated with AbA and Cmpd20 at 10 µg mL^{-1} for 1,4 and 7 h, before labeling with NBD-C6 ceramide for 1 h then. The results showed that the compounds had no effect on the synthesis of the sphingolipids in *T. gondii* when it compared with controls (figure 5-8). This demonstrated that neither compounds effected this pathway, and there may be another target in this parasite. However, it was clearly shown that the profile of complex sphingolipid had some changes at the times 4 and 7 h, the X and Y levels were increased at these points of times, SM

levels unchanged and EPC levels were decreased (figure 5-8). These results are indicated that the absence of host cells lead to the modification of sphingolipids or catabolism in *T. gondii.* More study, particularly metabolomic analyses of purified treated *T. gondii* with both compounds, is needed to establish the mode of action of AbA and Cmpd20 action against *T. gondii.*

Figure (5-8) Isolated Toxoplasma tachyzoites treated with Aureobasidin A (AbA) and Compound 20 (Cmpd 20) at 10 μg mL^{-1} for 1 (A), 4 (B) and 7 (C) hours before labelling with NBD-C6-ceramide for 1 h. Neither compound affected the complex sphingolipid profile synthesized at any time point when compared with the vehicle control (DMSO). SM – Sphingomyelin (SM); EPC – Ethanolamine PhosphorylCeramide; X and Y – Unclassified sphingolipids. Representative dataset.

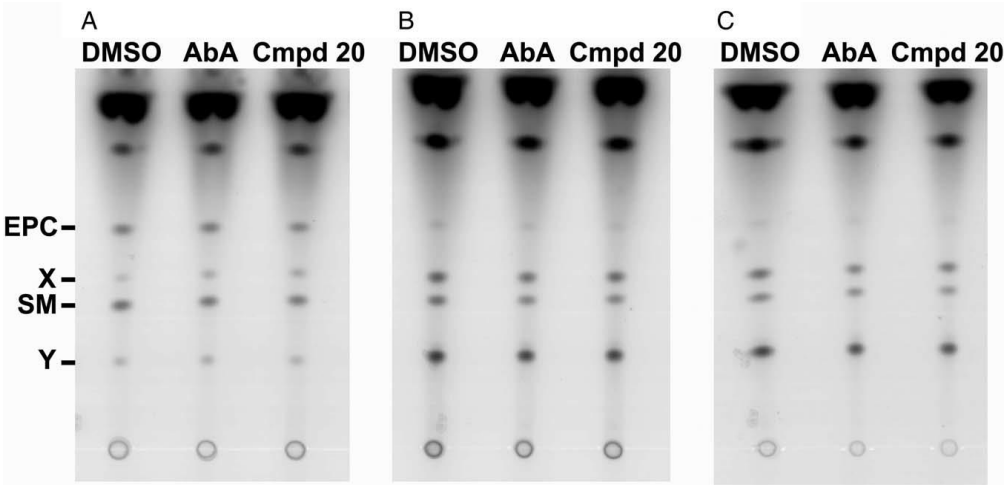

5.3.2 The compounds effects on *T. gondii* proliferation in chronic infection

The chronic infection of *T. gondii* is caused by the encysted bradyzoite stage. New therapies or drugs urgently needed against this type of infection (Antczak *et al.,* 2016). Therefore, AbA and Cmpd20 were testing against bradyzoite stage parasites.

Type II Pru strain of *T. gondii* modified to express GFP (Kim *et al.,* 2007) was used in this study. Following a pH shift to stimulate the transformation of tachyzoite into bradyzoite forms (Soete *et al.,* 1994), infected HFF cells were treated with the compounds for 3

days. The results showed promising activity against this stage (figure 5-9), again the efficacy of AbA (ED_{50} of 2.15, 95% CI 1.96 to 3.23 µg mL^{-1}) was higher than Cmpd20 (ED_{50} of 3.74, 95% CI 3.13 to 4.47 10 µg mL^{-1}). Therefore, AbA and its analogue represent promising candidates for the development of therapies to treat both acute and chronic toxoplasmosis.

Figure (5-9) ED_{50} of Aureobasidin A (A, AbA) or Compound 20 (B, Cmpd20) µg mL^{-1} (95% Confidence Interval) – against the *T. gondii* Pru bradyzoites in Human Foreskin Fibroblast (HFF) cells. Three days post addition of the compounds. Calculated using GraphPad Prism 7, log (inhibitor) vs normalized response – Variable slope. Representative in triplicate dataset.

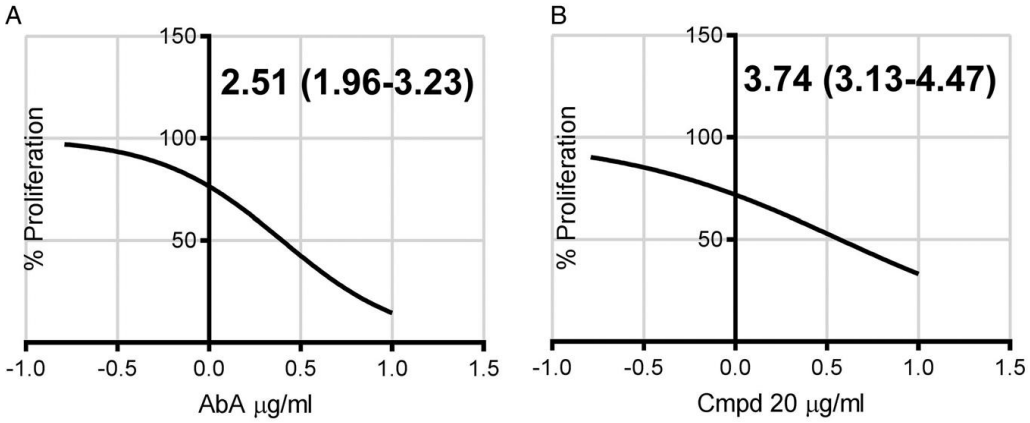

These results agreed with the others who proposed that the effect of AbA on the kinetoplastid parasites *Leishmania* spp. and *T. cruzi* is not due to the inhibition of IPCS (Figueiredo *et al.,* 2005; Denny *et al.,* 2006*;* Sevova *et al.,* 2010). These results also agree with the hypothesis that one drug may be interact with many targets (Imming *et al.,* 2006).

Chapter six:

Metabolomic and lipidomic study

6.1 Introduction

Metabolomics is an emerging technology widely used now to detect low molecular weight (<1400 Da) molecules (Vincent and Barrett, 2015) and is called the metabolome in a biological sample (Besteiro *et al.,* 2010; Paget *et al.,* 2013). These low molecular weight molecules or metabolites (for example sugars, amino acids and fatty acids; Willger *et al.,* 2009), are different in their chemical characteristics (molecular weight, solubility etc) and physical characteristics (volatility etc; Dunn and Ellis, 2005), and are essential for an organism's survival. In pathogens that have numerous life cycle stages, differences in these metabolites are important in stage differentiation. In addition, we can now investigate the response of a pathogen to drug treatment by monitoring changes in the metabolome before and after treatment (Besteiro *et al.,* 2010; Berg *et al.,* 2013). Furthermore, metabolomic analyses are fundamental in the study of the effects of genetic modification (Villas-Bôasand and Lane, 2005).

The benefits behind the metabolomic study of pathogens, including the medically important protozoan parasites, are:

i. The identification of novel parasitic metabolites which can then be used to define new drug targets. In addition, the modification of metabolic pathways resulting from treatment with a specific drug can be followed (Besteiro *et al.,* 2010).

ii. Membranes consist of fatty acids and phospholipids in a certain proportion, however under stress, such drug treatment or infection, this proportion may be changed (de Azevedo *et al*., 2014). These changes can be used as biomarkers to study the virulence of *Leishmania* spp. or its resistance to treatments for leishmaniasis (Messaoud *et al.,* 2017). Metabolomic analyses have been used to accurately detect changes in sarcosine and fatty acid biomarkers for prostate (Sreekumar *et al.,* 2009) and colorectal (Ritchie *et al.,* 2010) cancer respectively.

iii. Metabolomics can be used to analyse cellular enzymatic reactions that are controlled by many factors, for instance metabolite concentrations, signaling molecules and post-translation alterations (Saito *et al.,* 2010).

iv. Metabolite differences between the host and an infectious pathogen can be exploited to specifically target unique pathogen enzymes (Agüero *et al.,* 2008). Therefore, metabolomic analyses will help to open the door to develop more specific new drugs (Kafsack and Llinás, 2010).

In this study, we used *Leishmania major* as a model to study the role of IPC synthase in the protozoa by exploiting the availability of two specific inhibitors identified in-house, clemastine [known as anti-histamine (Riviere and Papich, 2013)] (Brown *et al,* submitted) and a benzazepine (compound 35 [CMPD35] identified in a high throughput screen of the GSK compound library, Norcliffe *et al,* submitted). The effect of these two compounds on the metabolome was analysed and, in parallel, a lipidomic study was performed to study the perturbation of IPC synthesis.

Leishmania spp. are the causative agents of leishmaniasis and are one of the protozoan parasites that cause serious human disease, alongside the related kinetoplasts *Trypansoma cruzi* (Chagas disease) and *T. brucei* (African sleeping sickness) (Kafsack and Llinás, 2010). There is an urgent need to either further develop the currently used drugs, due to their limitations resulting from toxicity, cost and route of administration; or to find new drugs that are specifically targets against the parasite, for example enzymes that modulate metabolism.

Leishmania spp. membrane lipids, and the biosynthetic enzymes that produce them, may be good drug targets due to the significant differences in the composition and function when compared with mammals (Zhang and Beverley, 2010). Phospholipids are regarded as one of the main lipid components of biological membranes, and consist of glycerophospholipid and sphingolipids. Glycerophospholipids compromise a hydrophilic head group linked to fatty alcohol chains by a phosphate group. Sphingolipids consist of a hydrophilic head group linked to a ceramide via phosphate (Ramakrishnan *et al.,* 2013). This study adds to the field by analysing metabolite perturbation with a focus on the sphingolipid biosynthetic pathway, which contains protozoan unique features (Mina and Denny, 2017).

The life cycle in *Leishmania* spp. is divided into two stages, promastigote in the sand-fly vector and amastigote within the mammalian host macrophages (Ramakrishnan *et al.,* 2013).

Leishmania amastigotes are not suitable for metabolomic studies for several reasons:

a. The difficulty of separation from the host and the inability to define if a metabolite belongs to the host or parasite (Decuypere *et al.,* 2008; Vincent *et al.,* 2014).
b. When isolated, amastigotes transform quickly to promastigote forms (Decuypere *et al.,* 2008).

These concerns can be partly overcome by the use by axenic amastigote forms, where the host cells are absent (Peña *et al.,* 2015). However, this system is not established for *L. major*, therefore the promastigote stage was used as it is easy to grow *in vitro*, this avoiding host cell metabolites (Decuypere *et al.,* 2008).

The two IPC synthase inhibitors used in this study, clemastine and the benzazepine (CMPD35), have been shown to have micromolar ED_{50} and IC_{50} against *L. major* parasites and IPC synthase. Furthermore, they are also both 10-30 fold less active against a sphingolipid-free mutant (Brown *et al,* submitted; Norcliffe *et al,* submitted). The mutant *L. major,* ΔLCB2, lacks the sphingolipid biosynthesis pathway because it lacks the first, rate limiting enzyme in sphingolipid biosynthesis (SPT) (Denny *et al,* 2004).

6.2 Effect of clemastine and benzazepine (CMPD35) on the Leishmania major FV1 metabolome

6.2.1 Results of half-time to cell death assay

This experiment was designed to select the best concentration for the metabolomic study. Two final concentrations for clemastine (10 µM and 5 µM) and for the benzazepine (80µM and 40 µM) were tested in this study.

Compound concentrations and the *L. major* promastigotes were prepared in 24-well plates, and incubated at 26°C for 20, 24 and 42 hours. The morphology and number of parasites were examined in each of these periods. Clemastine at 10µM for 20 hours lead

to approximately 50% of the promastigotes being rounded as apposed to spindle shaped. This increased to about 95% after 24 hours treatment. At the 5 µM, the effects are noticeably less. There was no significant increase in overall parasite number at all compound concentrations and time periods (Table 6.1).

Table (6-1) Clemastine treated *Leishmania major*

Compound	**Clemastine**			
Conc. (µM)	**10**		**5**	
Time (h)	**20**	**24**	**20**	**24**
% rounded morphology	~50%	~95%	~40%	~90%
No. parasites (p.ml^{-1})	4.5x10^{6}	4.3x10^{6}	4.7x10^{6}	4.2x10^{6}

The benzazepine (CMPD35) at 80 µM, 20 and 24 hours, was toxic to the parasites, approximately 30% killed at 20 hours and 40% at 24 hours. The rest were rounded but alive as determined by phase microscopy. At the 40 µM and 20 hours, 50% were rounded shape and less than 5% dead. This increased to about 10% after 24 hours treatment. With respect to the number of parasites, it was demonstrated to be dramatically decreased when compared with the clemastine treated promastigotes: for benzazepine (CMPD35) at 80 µM for 20 and 24 hours 2.9 x10^{6} p.ml^{-1} and 3.0 x10^{6} p.ml^{-1} respectively); and at 40 µM, 3.3 x10^{6} p.ml^{-1} and 3.5 x10^{6} p.ml^{-1} respectively (Table 6.2). However, no change in the shape of untreated parasites at this time of periods, also not count at this time of periods

Table (6-2) CMPD35 treated *Leishmania major*

Compound	**Benzazepine (CMPD35)**			
Conc. (µM)	**80**		**40**	
Time (h)	**20**	**24**	**20**	**24**
% rounded morphology	~50%	~50%	>50%	>50%
% dead	~30%	~40%	~5%	~10%
No. parasites (p.ml^{-1})	2.9x10^{6}	3.0x10^{6}	3.3x10^{6}	3.5x10^{6}

By increasing the treatment period to 42 hours for both compounds (clemastine and benzazepine [CMPD35]) it was demonstrated that the treated parasites were all of the rounded morphology but maintained viability. Given the toxicity at the higher concentration of benzazepine (CMPD35) seen above (Table 6.2).

Table (6-3) 42-hour clemastine and CMPD35 treatment of *Leishmania major.* Selected conditions in yellow

Compound	**Clemastine**			**CMPD35**		
Conc.	**0**	**10**	**5**	**0**	**80**	**40**
No. parasites (p.ml^{-1})	30x10^{6}	6.2x10^{6}	7.8 x10^{6}	29x10^{6}	5.8x10^{6}	6.1x10^{6}

the treatment conditions selected for metabolomic analyses were 10 µM of clemastine and 40 µM of benzazepine (CMPD35) for 42 hours (Table 6.3, yellow). This maximized compound concentration and treatment periods without compromising cell viability.

6.3 Metabolomic analyses of clemastine and benzazepine (CMPD35) treated *Leishmania major*

As mentioned above these compounds are recognized as specific IPCS inhibitors in *L. major*. Therefore, to investigate the global consequences of IPCS inhibition in this protozoan parasite metabolomic analyses were undertaken using the conditions outlined above. Analyses initially focused on *L. major* sphingolipid synthesis (Figure 6-1).

Following 42 hours compound treatment, metabolites were extracted and analyzed using LC-MS, and the data analyzed by using an Excel interface tool (IDEOM). IDEOM is a practical data analysis tool building on developed processing tools, e.g. mzMatch (a tool used for peak and annotation) and XCMS (to extract raw LC-MS data). IDEOM automatically clarifies and detects the metabolite peaks with particular consideration for the common noise and the positive and negative results obtained by LC-MS platforms (Creek *et al.,* 2012).

Figure (6-1) Sphingolipid biosynthesis pathway in *L. major* (adopted and modified from Zhang *et al.,* 2010). 3 KDS: 3 ketodihydrosphingosine; PI: phosphatidylinositol; PC: Phosphatidylcholine; PE: Phosphatidylethanolamine; IPC: Inositol phosphorylceramide; IPCS: Inositol phosphorylceramide synthase; EPC: Ethanolamine phosphorylceramide, EPCS: Ethanolamine phosphorylceramide synthase; EtN-P: ethanolamine phosphate.

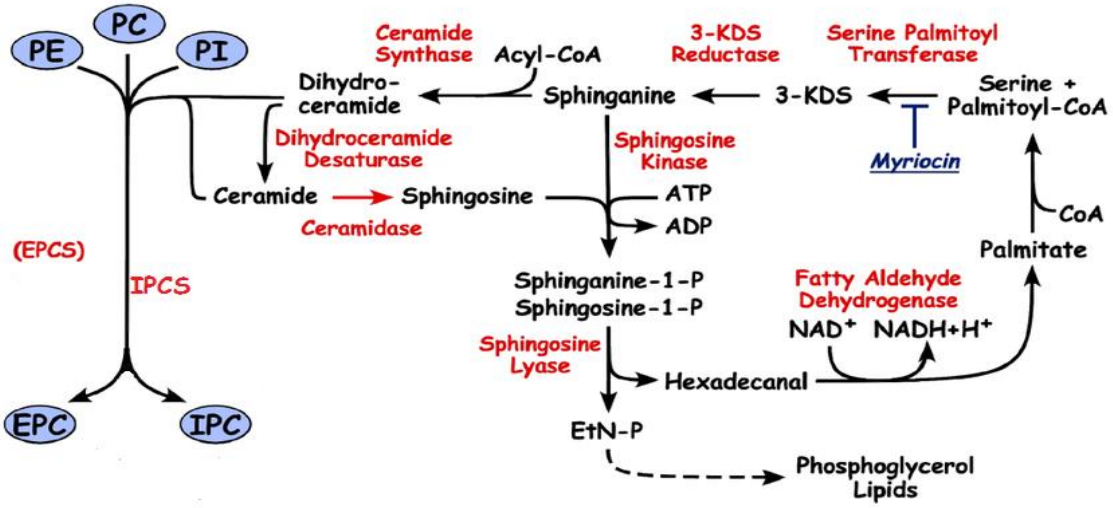

6.3.1 SL metabolite flux in *Leishmania major* promastigotes treated with clemastine

Using the IDEOM platform for analyses it was found that although there is a significant decrease in 3-ketodihydrosphingosine (3-KDS) production ([SP] 3-dehydrosphinganine; 0.47; P<0.05), there was a significant increase in most of the sphingolipid species particularly: dihydroceramide [SP (16:0)] N-(hexadecanoyl)-sphinganine; 39.65-fold; P<0.05) and ceramide [SP-hydroxy(16:0)] N-(hexadecanoyl)-4S-hydroxysphinganine; 8.37-fold; P<0.05). These increased are expected of an IPCS inhibitor, where in the absence of enzyme function there would be an increase in substrate concentration, e.g. ceramide. Other lipids connected with the pathway also change: phosphatidylinositol is increased (PI e.g O16:0/20:2 (11Z, 14Z); 13.14-fold; P<0.05). Again this was expected as it is the other substrate of IPCS synthase. Phosphatidylcholine (PC) is also increased (e.g. (18:1/P18:0) -1-(1Z - octadecenyl) -2- (9z- octadecenoyl) -Sn- glycerol-3- phosphocholine; 5.02-fold; P< 0.05), the PC (unsaturated fatty acid) significantly increase leads to increase

the membrane fluidity, and that cause the perturbation in the plasma membrane function (Alberts *et al.,* 2002;Dowhan *et al.,* 2002).In contrast levels of phosphatidylethanolamine (PE 34:0, 0.40-fold, P<0.05) decreased, given the role of serine palmitoyltransferase in PE synthesis (Table 6.1) this fitted with the observed decrease in 3-KDS. Table 6.1 shows the metabolites of interest that are changed in *L. major* when the parasites are treated with clemastine. Figure 6.2 illustrates all the perturbations that occurred within the SL biosynthesis pathway when the parasites were treated with clemastine, data which fits the hypothesis the compound is a specific IPCS inhibitor in *L. major*. Sphingomyelin (SM; from growth media) increases but not significantly.

6.3.2 SL metabolite flux in *Leishmania major* promastigotes treated with benzazepine (CMPD35)

Unlike with clemastine there were no statistically significant changes in 3-KDS (0.75-fold), dihydroceramide (0.87) or ceramide (1.79). The lack of ceramide build up with unexpected with an IPCS inhibitor. However, PI was increased (e.g PI(O-16:0/20:2(11Z,14Z)); 4.55-fold; P<0.05). Like with clemastine, PC was also increased (e.g. PC(15:0/P-18:0); 1.52-fold) and PE was significant decreased (PE 34:0, 0.54-fold P<0.05). Sphingomyelin not detected. These data provide limited support for mode of action of CMPD35 as an inhibitor of IPCS, i.e. no increase in ceramide. However, labeling experiments have clearly demonstrated a reduction in IPC synthesis on treatment (Norcliffe *et al*, submitted).

Interestingly, the metabolomics results also showed that *Leishmania* treated with clemastine has statistically significant decrease in ergosterol while *Leishmania* treated with CMPD35 has statistically significant increases in ergosterol ([ST(3:0)]ergosta-5,7,22E-trien-3beta-ol; (0.54 and 2.01-fold respectively). Ergosterol is a sterol found in cell membranes of fungi and protozoa (Thomas, and Waters, 2016), and given the relationship between sphingolipids and sterols this may be significant. Table 6.1 shows the metabolites of interest that are changed in *L. major* when the parasites are treated

with benzazepine (CMPD35). Figure 6.3 illustrates the perturbation that occurred within the SL biosynthesis pathway in *L. major* on treatment.

Table (6-4) Metabolites that are changed when *Leishmania major* are treated with clemastine (Cle) or benzazepine (CMPD35). The predicted formula, mass, pathway and confidence levels are shown

Metabolites	Formula	Mass	Pathway	Con-fidence	Cle	CMPD 35	WT
L-serine	$C_3H_7NO_3$	105.4	Glycerine, serine and threonine	10	2.59	1.25	1.0
3-KDS	$C_{18}H_{37}NO_2$	299.28	Sphingoid bases	6	0.47*	0.78	1.0
Dihydrosphinganine	**ND**	ND	ND	ND	ND	ND	ND
Dihydroceramide	$C_{34}H_{69}NO_3$	539.53	Ceramides	5	39.65*	0.78	1.0
Phytoceramide	$C_{34}H_{67}NO_4$	555.52	Ceramides	5	8.37*	1.79	1.0
Sphingosine	$C_{18}H_{39}NO_2$	301.3	SL metabolism	6	1.96	2.22	1.0
Sphingosine-1-P	$C_{18}H_{38}NO_5P$	379.25	Sphingoid bases	6	0.78	0.76	1.0
Ethanolamine-P	$C_2H_8NO_4P$	141.02	Glycerine, serine and threonine	8	0.55	2.05	1.0
CDP-ethanolamine	ND	ND	ND	ND	ND	ND	ND
Phosphatidyl-ethanolamine	$C_{39}H_{78}NO_8P$	719.55	Glycerophosphoethanoamines	7	0.40*	0.54*	1.0
Phosphatidylserine	$C_{44}H_{80}NO_{10}P$	813.55	Glycerophosphoserines	5	0.59*	0.46*	1.0
Phosphatidylcholine	$C_{44}H_{86}NO_7P$	771.61	Glycerophosphocholine	5	5.02*	1.52	1.0
Phosphatidylinositol	$C_{45}H_{85}O_{12}P$	848.58	Glycerophosphoinositol	8	13.14*	4.55*	1.0
Ergosterol	$C_{28}H_{44}O$	369.34	Sterols	5	0.54*	2.01*	1.0

Each 'metabolite' is assigned a confidence level from 0 to 10 based on an authentic standard compound (10 = most confident); Red* indicates metabolites that are significantly changed; SL: sphingolipid; ND: not detected.

Figure (6-2) Metabolites that are changed in sphingolipid biosynthesis pathway when *L. major* are treated with clemastine (Cle) (adopted and modified from Zhang *et al.*, 2010). 3 KDS: 3 ketosphinganine; PI: phosphatidylinositol; PC: Phosphatidylcholine; PE: Phosphatidylethanolamine; IPC: Inositol phosphorylceramide; IPCS: Inositol phosphorylceramide synthase; EPC: Ethanolamine phosphorylceramide, EPCS: Ethanolamine phosphorylceramide synthase; EtN-P: ethanolamine phosphate.

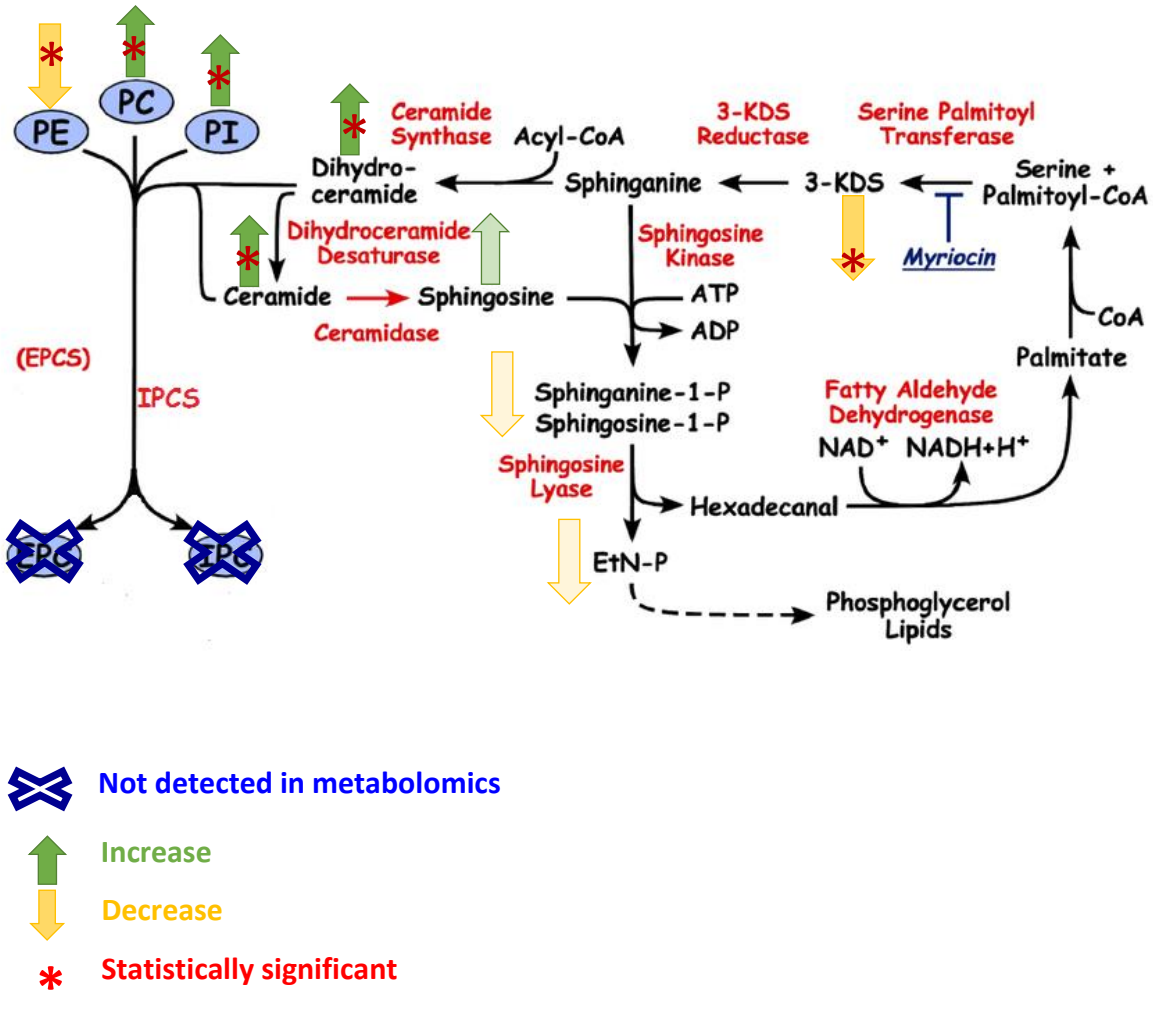

Figure (6-3) Metabolites that are changed in sphingolipid biosynthesis pathway when *L. major* are treated with benzazepine (CMPD35) (adopted and modified from Zhang *et al.*, 2010). 3 KDS: 3 ketosphinganine; PI: phosphatidylinositol; PC: Phosphatidylcholine; PE: Phosphatidylethanolamine; IPC: Inositol phosphorylceramide; IPCS: Inositol phosphorylceramide synthase; EPC: Ethanolamine phosphorylceramide, EPCS: Ethanolamine phosphorylceramide synthase; EtN-P: ethanolamine phosphate.

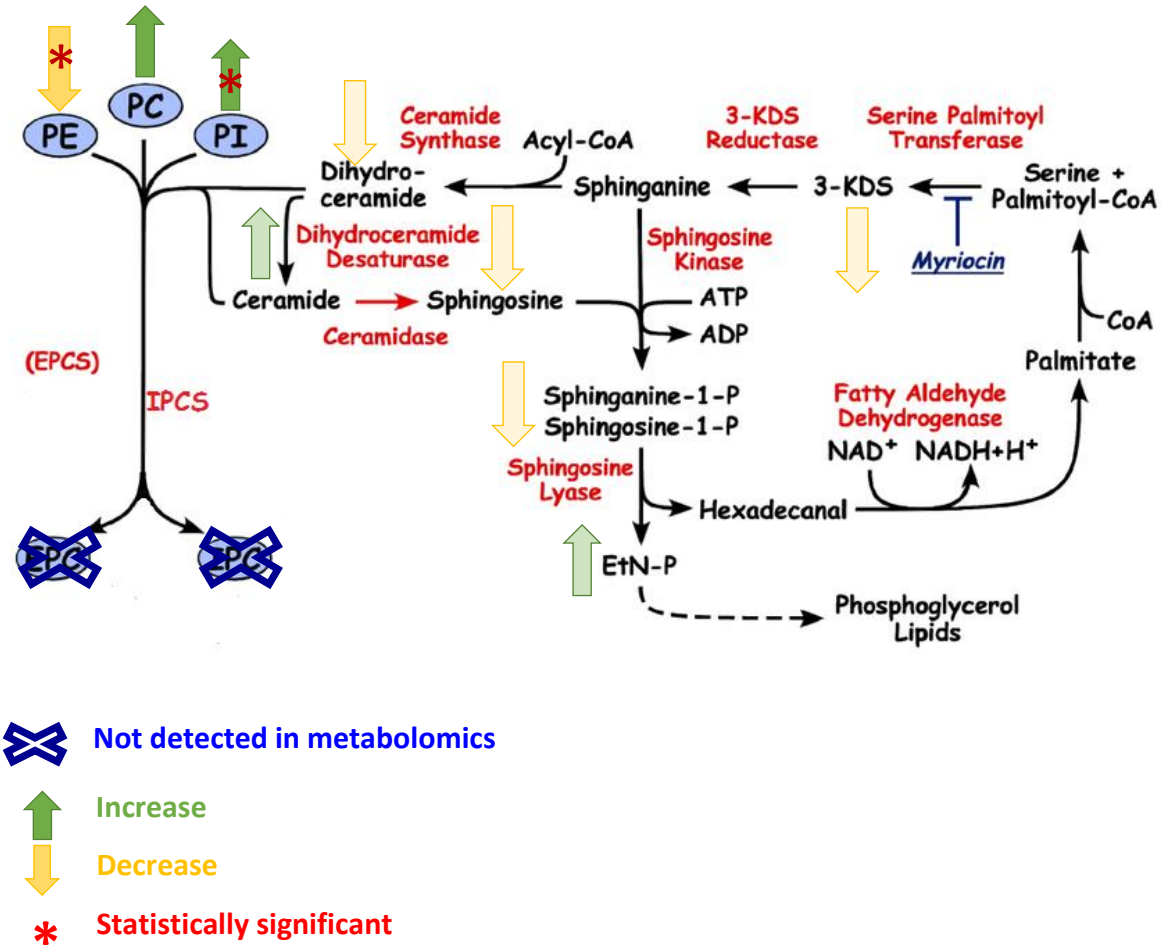

6.4 Lipidomic analyses

Lipids are the main building blocks of all cell membranes, in addition they serve as a source of energy and work as a signaling molecules within and between the cells. Furthermore, lipids anchor several proteins and glycoconjugates to the cell membrane (Tanowwitz *et al.,* 2011, Ramakrishan *et al.,* 2013). Intracellular pathogens such as the viruses, bacteria and protozoa (e.g. *Leishmania* spp.), may use host cell lipids as a source of energy or manipulate the host lipid biosynthesis for their own benefit (Ehrt, 2007). In contrast some lipids are synthesized by the pathogen itself, for example the glycosylphosphatidylinositol (GPI) lipids which anchor the lipophosphoglycans of *Leishmania* spp. to the cell surface and are essential for host specificity and parasite survival inside the sand fly (Dobson *et al.,* 2010).

To further enhance metabolomic results, lipidomic analyses have been performed to investigate mechanisms of drug resistance (Imbert *et al.,* 2012), and to confirm the action of compounds on lipid metabolism (Creek and Barrett, 2013). Metabolomic analyses demonstrated that clemastine exerted the expected (and statistically significant) influence on the *Leishmania* metabolome. To further establish the effects of this compound lipid metabolism, cells were treated with different concentrations of clemastine for 42 hours (0.1, 0.5, 1, 5 and 10 µM) before microscopic analyses. Whilst significant cell death was seen at 10 µM, 5 µM was well tolerated with cells rounded but viable. Therefore, *L. major* promastigotes were incubated with 5 µM clemastine or the vehicle for 42 hours. Lipids were extracted and analysed by ES-MS and GC-MS as described in Materials and Methods. Focusing specifically on the inositol lipids, IPC can be quantified relative to PI. The results showed that the quantity of IPC (between m/z 778.8-806.8) (Zhang *et al*., 2005) relative to PI is reduced in the treated samples (37.1%-25.6%; Figure 6-4). This demonstrated that clemastine reduces IPC synthase, presumably through inhibition of IPCS. These data agreed with the previous metabolomic results which found a large, and significant, increase in IPCS substrate (ceramide and PI) concentrations.

Figure (6-4) Lipidomics analyses of *Leishmania major* promastigotes treated with vehicle (DMSO; A), or 5 µM clemastine (B) for 42 hours. IPC's: inositol phosphoryl ceramides; PI's: phosphatidylinositol.

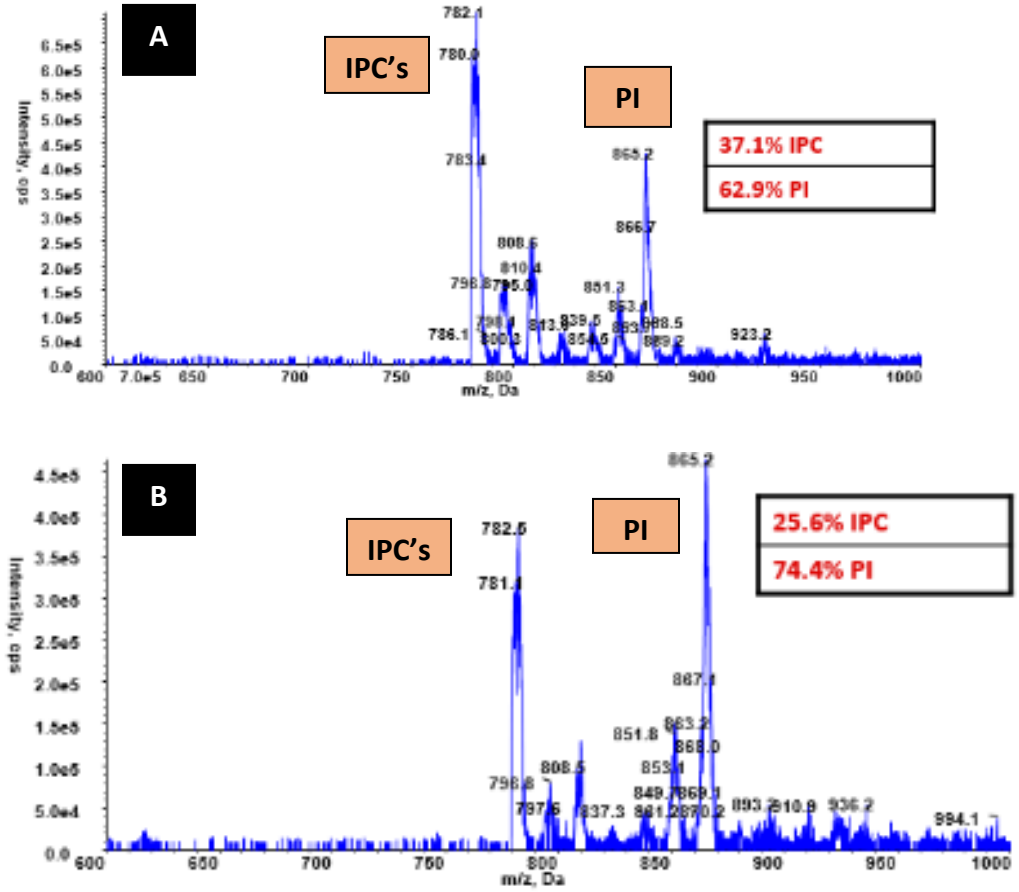

Chapter seven:
An investigation of the mode of action of the anti-leishmanial miltefosine

7.1 Introduction

Miltefosine or hexadecyl phosphate choline is an antitumor drug (Figure 7-1), which shows potent activity against *Leishmania* spp. Currently, it is the only oral drug for leishmaniasis and is now widely used in North-west India (Canuto *et al.,* 2014). It has been demonstrated that the miltefosine changes the phospholipids and sterol composition in treated tumor cells (Geilen *et al.,* 1996). Some studies suggested that the mechanism of action of the drug was related to the apoptotic process (Wright *et al.,* 2004; Sundar and Olliaro, 2007). More recently it was found that miltefosine caused a perturbation of the membrane lipids of axenic *L. donovani* amastigotes, decreasing the membrane PLs and amino acids pools, whilst SLs and sterols were increased (Armitage *et al.,* 2017).

In this study, the importance of SL synthesis in the mode of miltefosine action was investigated using *L. major* wild type promastigotes and the transgenic strain lacking SLs, *L. major* ΔLCB2 (Denny *et al,* 2004).

Figure (7-1) Chemical structure of miltefosine generated using the ChemDraw

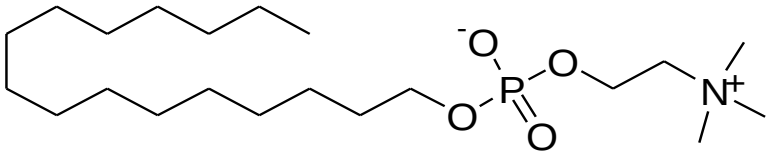

7.2 Establishing the efficacy of miltefosine against wild type and ΔLCB2 mutant *Leishmania major*

The anti-leishmanial effect of miltefosine at various concentrations was established as described in Materials and Methods and the data used to calculate the EC_{50} of the drug against wild type and ΔLCB2. The efficacy of miltefosine was approximately 3-fold lower in the mutant SL-free strain, EC_{50} 21.2 µM (95% CI 20.1-22.3) versus 6.83 µM (95% CI 6.1-7.6) in wild type promastigotes (Figure 7-2). This demonstrated that SL-free mutant parasites are more resistant to miltefosine, indicating a role for SLs in the mode of action of miltefosine.

Figure (7-2) Efficacy of miltefosine against wild type and ΔLCB2 *Leishmania major.* log (miltefosine; µM) vs % parasite proliferation. EC_{50} wild type (6.83 µM [95% CI 6.1-7.6]) and ΔLCB2 (21.2 µM [95% CI 20.1-22.3]) calculated in GraphPad Prism 7, normalised response-variable slope. Representative in triplicate datasets

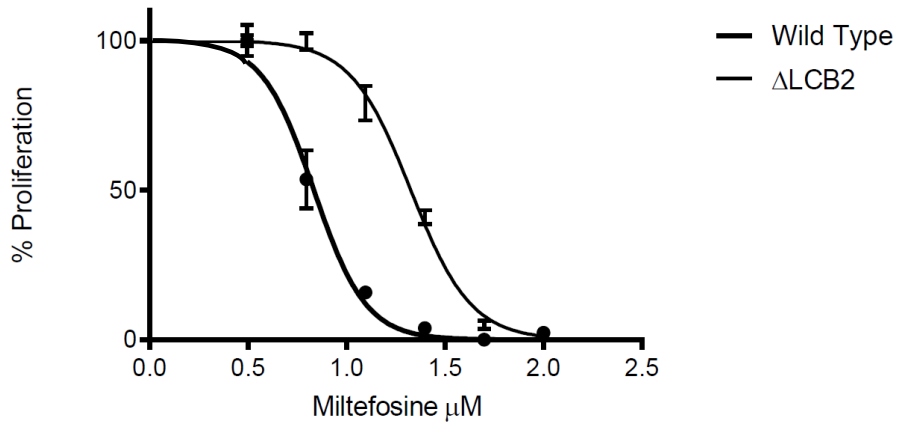

7.3 The effects of miltefosine on the *Leishmania major* wild type and ΔLCB2 metabolomes

Further analyses were performed, in collaboration with Emily Armitage and Mike Barrett (University of Glasgow), using a metabolomic approach. Two miltefosine concentrations (10 µM and 30 µM) were used to treat wild type and ΔLCB2 promastogites and the metabolites extracted using a procedure optimised such that LC-

MS and CE-MS analyses could be performed as described in Armitage *et al.* (2017). The LC-MS data allowed analyses of SLs, and the results showed a massive difference in the lipidome between the wild type and SL-free mutant promastigotes. As expected, due to the absence of a functional SPT (first enzyme in the biosynthetic pathway, most SLs were lacking in the mutant. The SLs that were detected, for instance sphinganine-1-phosphate, sphingosine ceramide (d36:1) and sphingomyelin, were almost certainly obtained from the media.

When treated with low (10 µM) and high dose (30 µM) miltefsoine, wild type *L. major* promastigote SL levels were increased dramatically, perhaps due to a stimulatory effect of the drug on the SL biosynthetic pathway or inhibition of the catabolic pathway (Figure 7-3). The latter looks more likely as the ΔLCB2 mutant accumulate SLs from the media at a higher level upon treatment (figure 7-3). Together, these data suggest that SLs have a role in the sensitivity of *Leishmania* to miltefosine, and that the drug may have a direct effect on the parasite SL biosynthetic pathway.

Figure (7-3) Fold change in abundance of all sphingolipids detected in LC-MS analyses of wild type and ΔLCB2 *Leishmania major* treated or un-treated with 10 µM or 30 µM of miltefosine. Sphingolipids that were not detected in a certain dataset are marked 'ND'.

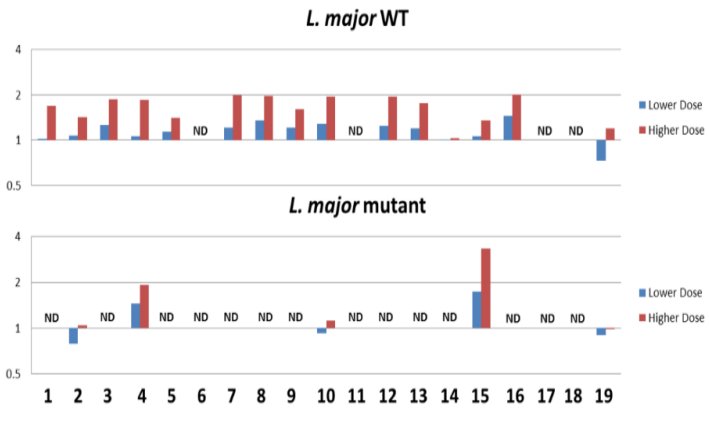

1. C16 Sphinganine
2. C16 Sphinanine-1-Phosphate
3. C16 Sphingosine
4. C18 Sphingosine / 3-Ketosphinganine
5. Dihydroceramide
6. Cer (d33:0)
7. Cer (d33:1)
8. Cer (d34:0)
9. Cer (d34:0(2OH))
10. Cer (d34:1)
11. Cer (d34:1(2OH))
12. Cer (d35:0)
13. Cer (d35:1)
14. Cer (d36:0(2OH))
15. Cer (d36:1)
16. Cer (d36:2)
17. Cer (d38:1(2OH))
18. CerP (d26:1)
19. SM (d34:2)

Chapter eight:

General discussion and Future Work

8.1 General Discussion

Toxoplasma gondii is an obligate intracellular parasite that causes toxoplasmosis and belongs to the phylum apicomplexa. Although drugs are available to treat the acute toxoplasmosis, there are still none for chronic disease (Francia *et al*. 2016). In addition, the drugs used against *T. gondii* are limited and cause many side effects (Palencia *et al.,* 2017). Therefore, there is a critical demand for new, less toxic, therapeutic agents, and by focusing on enzymes that are unique to the parasite the discovery of these may be accelerated (Palencia *et al.*, 2017). Protozoan lipid biosynthesis, particularly of sphingolipids (Denny *et al.,* 2006; Pratt *et al.,* 2013), provides such new targets. This study investigated the potential of *T. gondii* serine palmitoyltransferase (*Tg*SPT, the enzyme responsible for the first step in sphingolipid biosynthesis) as a drug target. In addition, using *Leishmania major* as a model, the effects of inhibiting inositol phosphorylceramide synthase (IPCS), an enzyme drug target found only in the parasite (Denny *et al.,* 2006), was investigated.

There are two potential SPTs encoded by *T. gondii*, *Tg*SPT1 and *Tg*SPT2 (68% identity), which were previously identified in ToxoDB (Mina *et al.,* 2017). The available expression profiles (ToxoDB.org) of these genes in oocyst, tachyzoite and bradyzoite ME49 *T. gondii* was analysed in this study. The results showed that *Tg*SPT1 is the predominantly expressed gene in tachyzoite *T. gondii*, whilst *Tg*SPT2 is up regulated bradyzoites. Both *Tg*SPT1 and SPT2 been suggested to be important for parasite fitness (Sidik *et al.*, 2016). Previous studies have shown in eukaryotic organisms is found as a heterodimer has one active site in SPT2, whilst SPT1 lacking this active site and is thought to have a regulatory role (Hornemann *et al.,* 2009). This enzyme is associated with membranes (Han *et al.,* 2004), whereas the prokaryotic SPT is cytoplasmic and forms a homodimer with two active sites (Ikushiro and Hayashi, 2001). Interestingly, bioinformatic analyses carried out in this study indicated that *Tg*SPT1 and 2 is more closely related to the well-studied bacterial SPT from Gram negative *Sphingomonas paucimobilis* (*Sp*SPT). The results showed that *Tg*SPTs have 2 active sites, like the prokaryotic enzyme (Yard *et al.,* 2007) and possess a potential transmembrane domain. Biochemical assay carried out here confirmed *Tg*SPT2 as a genuine serine palmitoyltransferase, like *Tg*SPT1 (Mina *et al.,*

2017). In addition, like *Tg*SPT1 and mammalian orthologues (Mina *et al.,* 2017) it is located in the ER. An attempt at knocking out both TgSPT1 and 2 in this work was unsuccessful, indicating that the enzyme is essential. Together, these findings demonstrate that whilst *Tg*SPTs have a prokaryotic origin they have a eukaryotic function, and gene deletion attempts indicated that the enzyme is a potential drug target.

In parallel, gene expression profiles of host SPT, and sphingomyelin synthase (SMS) 1 and 2, were investigated to determine the role of host biosynthesis in *T. gondii* proliferation. Gene expression were unaffected by *T. gondii* infection, indicating that the parasite depends upon *de novo* sphingolipid biosynthesis. Therefore, two antifungal IPCS inhibitors AbA and Cmpd20 (Wuts *et al.,* 2015) were analysed against *T. gondii* tachyzoites and bradyzoites. As previously shown for AbA (Sonda *et al.,* 2005), both compounds have an effect on parasite proliferation but not on host cells, with AbA showing higher efficacy. However, in contrast to previous reports (Sonda *et al.,* 2005), neither compound inhibited sphingolipid biosynthesis. Therefore, this work did not chemically validate sphingolipid biosynthesis as a drug target, although the efficacy observed for both compounds against the chronic, bradyzoite stage may prove important (Antczak *et al.,* 2016).

To further investigate the role of IPCS in protozoan parasites, *L. major* promastigotes were used as a model to study metabolomic and lipidomic changes on inhibition of the enzyme. In-house developed inhibitors of *L. major* IPCS, for instance clemastine and benzazepine (Cmpd35) were utilised (Brown *et al.,* submitted; Norcliffe *et al,* submitted). In addition, the oral antileishmanial drug miltefosine was investigated using similar approaches to determine its effects in sphingolipid biosynthesis (collaborative work with Emily Armitage and Mike Barrett [University of Glasgow]).

Metabolomics is the quantitative measurement of the effect of a specific event (drug treatment, infection, etc; (Holmes *et al.,* 2008). The effects of the two specific IPCS inhibitors against *L. major* were analysed using with the data showing that ceramide, a substrate for IPCS and a pro-apoptotic substance, accumulated in large amounts. More focused, lipidomic analyses, showed that IPC (the enzyme product) was dramatically

decreased in clemastine treated parasites. These data confirmed that the sphingolipid biosynthetic pathway is targeted by these anti-leishmanial compounds.

Finally, the anti-leishmanial drug miltefosine showed reduced activity against a transgenic strain of *L. major* lacking sphingolipid biosynthesis (ΔLCB2; Denny *et al.,* 2004) compared to wild type. This suggested the sphingolipid synthesis has a role in sensitivity to the drug, metabolomic analyses supported this, agreeing with previous studies (Rybczynska *et al.,* 2001; Wright *et al.,* 2004).

Taken together, the present findings further characterised the *T. gondii* sphingolipid biosynthetic pathway and indicated the potential to target this in drug discovery efforts. In addition, metabolomic and lipidomic approaches confirmed that clemastine targets *L. major* IPCS and also suggested a role for sphingolipids in miltefosine resistance.

8.2 Future work

As the importance of sphingolipid biosynthesis pathway in this parasite, more study is required to detect the possible drug target in this pathway focusing on the enzymes that responsible to produce an important sphingolipids for instance ceramide synthase which responsible to form the ceramide.

Since one of the outcomes of this study showed that both *Tg*SPT1 and *Tg*SPT2 are important for parasite proliferation, the efforts to make a mutant parasite lacking either *Tg*SPT1 or *Tg*SPt2 or both are required to show the importance of both enzymes in acute and chronic toxoplasmosis by using CRISPR-Cas9.Furthermore, the metabolomics analysis will be crucial to study the global effects of these knockouts on *T. gondii,* taking into account modifying the metabolomic procedure to avoid the host contaminants.

This study showed that both AbA and its analogue CMPD20 were active against the parasite, however the sphingolipid biosynthesis is not the drug target, so more analysis needs to show the mode of action of AbA and its analogues against *T. gondii* tachyzoites and bradyzoites by using metabolomic analysis.

Further studies should investigate the mode of clemastine action in axenic amastigote stage of *Leishmania* spp. to avoid the host contaminants.

References

References

- Agüero, F., Al-Lazikani, B., Aslett, M., Berriman, M., Buckner, F.S., Campbell, R.K., Carmona, S., Carruthers, I.M., Chan, A.E., Chen, F. and Crowther, G.J., 2008. Genomic-scale prioritization of drug targets: the TDR Targets database. *Nature reviews. Drug discovery, 7(11)*, p.900.
- Akhoundi, M., Kuhls, K., Cannet, A., Votýpka, J., Marty, P., Delaunay, P. and Sereno, D., 2016. A historical overview of the classification, evolution, and dispersion of *Leishmania* parasites and sandflies. *PLoS Negl Trop Dis*, 10(3), p.e0004349.
- Alberts, B., Johnson, A., Lewis, J., Walter, P., Raff, M. and Roberts, K., 2002. Molecular Biology of the Cell 4th Edition: International Student Edition.
- Alonso, P. and Noor, A.M., 2017. The global fight against malaria is at crossroads. *The Lancet*.
- Alqaisi, A.Q.I., Mbekeani, A.J., Llorens, M.B., Elhammer, A.P. and Denny, P.W., 2017. The antifungal Aureobasidin A and an analogue are active against the protozoan parasite *Toxoplasma gondii* but do not inhibit sphingolipid biosynthesis. *Parasitology*, pp.1-8.
- Alvar, J., Vélez, I.D., Bern, C., Herrero, M., Desjeux, P., Cano, J., Jannin, J., den Boer, M. and WHO Leishmaniasis Control Team, 2012. Leishmaniasis worldwide and global estimates of its incidence. *PloS one*, 7(5), p.e35671.
- Annaloro, C., Olivares, C., Usardi, P., Onida, F., Della Volpe, A., Tagliaferri, E. and Deliliers, G.L., 2009. Retrospective evaluation of amphotericin B deoxycholate toxicity in a single centre series of haematopoietic stem cell transplantation recipients. *Journal of antimicrobial chemotherapy* 63, pp.625-626..
- Ansari, S., Miri-Aliabad, G. and Yousefian, S., 2013. Leishman-Donovan bodies at bone marrow examination. *European journal of pediatrics*, 172(11), pp.*1561*-1562.
- Antczak, M., Dzitko, K. and Długońska, H., 2016. Human toxoplasmosis–Searching for novel chemotherapeutics. *Biomedicine & Pharmacotherapy*, 82, pp.677-684.
- Armitage, E. G., Alqaisi, A. Q. I.,Godzien, J., Peña, I., Mbekeani, A. J. ,Alsonso-Herranz, V., López-Gonzálvez, A., Martín, J., Fiandor-Román, J. M.,Gabarro, R., Denny, P. W.,

Barrett, M. P. and Barbas, C. 2017. A complex interplay between sphingolipid and sterol metabolism revealed by perturbations to the Leishmania metabolome caused by miltefosine [submitted to *Antimicrobial Agents and Chemotherapy*].

- Ashcroft, F.M. and Gribble, F.M., 2000. New windows on the mechanism of action of K ATP channel openers. *Trends in pharmacological sciences*, 21(11), pp.439-445.
- Ashford, R.W., 2000. The leishmaniases as emerging and reemerging zoonoses. *International journal for parasitology*, 30(12), pp.1269-1281.
- Azzouz, N., Rauscher, B., Gerold, P., Cesbron-Delauw, M.F., Dubremetz, J.F. and Schwarz, R.T., 2002. Evidence for de novo sphingolipid biosynthesis in Toxoplasma gondii. *International journal for parasitology*, *32*(6), pp.677-684.
- Bai, Y., He, S., Zhao, G., Chen, L., Shi, N., Zhou, H., Cong, H. and Zhu, X.Q., 2012. *Toxoplasma gondii*: bioinformatics analysis, cloning and expression of a novel protein *Tg*IMP1*. Experimental parasitology*, 132(4), pp.458-464.
- Barbosa, B. F.; Gomes, A. O. ; Ferro, E. A. V.; Napolitano, D. R.; Mineo, J. R. and Silva, N. M. 2012. Enrofloxacin is able to control *Toxoplasma gondii* infection in both in vitro and in vivo experimental models. *J. Veterinary Parasitology* 187, pp. 44– 52
- Barratt, G. and Legrand, P., 2005. Comparison of the efficacy and pharmacology of formulations of amphotericin B used in treatment of leishmaniasis. *Current opinion in infectious diseases*, 18(6), pp.527-530.
- Bartke, N. and. Hannun, Y. A. 2009. Bioactive sphingolipids: metabolism and function. *J. of Lipid Res.* S91-S96.
- Baum, J., Papenfuss, A.T., Baum, B., Speed, T.P. and Cowman, A.F., 2006. Regulation of apicomplexan actin-based motility. *Nature Reviews Microbiology*, *4*(8), pp.621-628.
- Beattie, A.E., Gupta, S.D., Frankova, L., Kazlauskaite, A., Harmon, J.M., Dunn, T.M. and Campopiano, D.J., 2013. The pyridoxal 5'-phosphate (PLP)-dependent enzyme serine palmitoyltransferase (SPT): effects of the small subunits and insights from bacterial mimics of human hLCB2a HSAN1 mutations. *BioMed research international*, 2013, pp. 1-13.

- Ben Salah, A., Ben Messaoud, N., Guedri, E., Zaatour, A., Ben Alaya, N., Bettaieb, J., Gharbi, A., Belhadj Hamida, N., Boukthir, A., Chlif, S. and Abdelhamid, K., 2013. Topical paromomycin with or without gentamicin for cutaneous leishmaniasis. New England *Journal of Medicine*, 368(6), pp.524-532.
- Benaim, G., García-Marchán, Y., Reyes, C., Uzcanga, G. and Figarella, K., 2013. Identification of a sphingosine-sensitive Ca^{2+} channel in the plasma membrane of *Leishmania mexicana*. *Biochemical and biophysical research communications*, 430(3), pp.1091-1096.
- Berg, M., Vanaerschot, M., Jankevics, A., Cuypers, B., Maes, I., Mukherjee, S., Khanal, B., Rijal, S., Roy, S., Opperdoes, F. and Breitling, R., 2013. Metabolic adaptations of *Leishmania donovani* in relation to differentiation, drug resistance, and drug pressure. *Molecular microbiology*, *90*(2), pp.428-442.
- Berrow, N. S., Alderton, D., Sainsbury, S., Nettleship, J., Assenberg, R., Rahman, N., Stuart, D. I., and Owens, R. J. (2007) A versatile ligation-independent cloning method suitable for high-throughput expression screening applications. *Nucleic Acids Res*. 35, e45
- Besteiro, S., Dubremetz, J.F. and Lebrun, M., 2011. The moving junction of apicomplexan parasites: a key structure for invasion. *Cellular microbiology*, 13(6), pp.797-805.
- Besteiro, S., Duy, S.V., Perigaud, C., Lefebvre-Tournier, I. and Vial, H.J., 2010. Exploring metabolomic approaches to analyse phospholipid biosynthetic pathways in *Plasmodium*. *Parasitology*, 137(9), pp.1343-1356.
- Beyrer, C., Villar, J.C., Suwanvanichkij, V., Singh, S., Baral, S.D. and Mills, E.J., 2007. Neglected diseases, civil conflicts, and the right to health. *The Lancet*, 370(9587), pp.619-627.
- Bihari, M. 2008. Side Effects – What You Need to Know. Former about.com.
- Bisanz C, Bastien O, Grando D, Jouhet J, Maréchal E, Cesbron-Delauw M.F. 2006. *Toxoplasma gondii* acyl-lipid metabolism: de novo synthesis from apicoplast-

generated fatty acids versus scavenging of host cell precursors. *Biochem J*. 394, pp. 197–205.

- Black, M. W. and Boothroyd, J.C. 2000. Lytic Cycle of *Toxoplasma gondii. Microbiology and Molecular Biology Reviews*. 64 (3), pp.607–623.
- Blackman, M.J. and Carruthers, V.B., 2013. Recent insights into apicomplexan parasite egress provide new views to a kill. *Current opinion in microbiology*, 16(4), pp.459-464.
- Blader IJ, Manger ID, Boothroyd JC. Micro-array analysis reveals previously unknown changes in *Toxoplasma gondii*-infected human cells. *J Biol Chem* 2001;276:24223–31
- Blader, I.J. and Saeij, J.P., 2010. Communication between *Toxoplasma gondii* and its host: impact on parasite growth, development, immune evasion, and virulence. *Apmis,* 117(5-6), pp.458-476.
- Bleicher, K.H., Böhm, H.J., Müller, K. and Alanine, A.I., 2003. Hit and lead generation: beyond high-throughput screening. *Nature reviews Drug discovery*, 2(5), pp.369-378.
- Boevink, P., Martin, B., Oparka, K., Santa Cruz, S. and Hawes, C., 1999. Transport of virally expressed green fluorescent protein through the secretory pathway in tobacco leaves is inhibited by cold shock and brefeldin A. *Planta*, 208(3), pp.392-400.
- Bolt, H.L., Eggimann, G.A., Denny, P.W. and Cobb, S.L., 2016. Enlarging the chemical space of anti-leishmanials: a structure–activity relationship study of peptoids against *Leishmania mexicana*, a causative agent of cutaneous leishmaniasis. *MedChemComm*, 7(5), pp.799-805.
- Bougdour, A., Tardieux, I. and Hakimi, M.A., 2014. *Toxoplasma* exports dense granule proteins beyond the vacuole to the host cell nucleus and rewires the host genome expression. *Cellular microbiology*, 16(3), pp.334-343.
- Brossier, F. and Sibley, L.D., 2005. *Toxoplasma gondii*: microneme protein MIC2. *The international journal of biochemistry & cell biology*, 37(11), pp.2266-2272.
- Buede, R., Rinker-Schaffer, C., Pinto, W.J., Lester, R.L. and Dickson, R.C., 1991. Cloning and characterization of LCB1, a Saccharomyces gene required for

biosynthesis of the long-chain base component of sphingolipids. *Journal of bacteriology*, 173(14), pp.4325-4332.

- Bumb, R.A., Prasad, N., Khandelwal, K., Aara, N., Mehta, R.D., Ghiya, B.C., Salotra, P., Wei, L., Peters, S. and Satoskar, A.R., 2013. Long-term efficacy of single-dose radiofrequency-induced heat therapy vs. intralesional antimonials for cutaneous leishmaniasis in India. *British Journal of Dermatology*, 168(5), pp.1114-1119.
- Burri, C., and Brun, R. 2003. Human African trypanosomiasis. In Manson's tropical diseases. G.C. Cook and A.I. Zumla, editors. 21st edition. W.B. Saunders/Elsevier. Edinburgh, United Kingdom. pp.1303–1323.
- Calderaro A.; Peruzzi, S.; Piccolo, G.; Gorrini, C.; Montecchini, S.; Rossi, S. ; Chezzi, C.; Dettori G. 2009. Laboratory diagnosis of *Toxoplasma gondii* infection. *Int. J. Med. Sci.* 6, pp. 135-136.
- Canadian AIDS International Exchange (CATI). 1997. Toxoplasmosis. 1-3.
- Canuto, G.A., Castilho-Martins, E.A., Tavares, M.F., Rivas, L., Barbas, C. and López-Gonzálvez, Á., 2014. Multi-analytical platform metabolomic approach to study miltefosine mechanism of action and resistance in *Leishmania*. *Analytical and bioanalytical chemistry*, *406*(14), pp.3459-3476.
- Carey, K.L., Westwood, N.J., Mitchison, T.J. and Ward, G.E., 2004. A small-molecule approach to studying invasive mechanisms of *Toxoplasma gondii. Proceedings of the National Academy of Sciences of the United States of America*, 101(19), pp.7433-7438.
- Carneiro, P.P., Conceição, J., Macedo, M., Magalhães, V., Carvalho, E.M. and Bacellar, O., 2016. The role of nitric oxide and reactive oxygen species in the killing of *Leishmania braziliensis* by monocytes from patients with cutaneous leishmaniasis. *PloS one*, 11(2), p.e0148084.
- Carruthers, V.B. and Sibley, L.D., 1997. Sequential protein secretion from three distinct organelles of *Toxoplasma gondii* accompanies invasion of human fibroblasts. *European journal of cell biology*, 73(2), pp.114-123.

- Casadevall, A. and Pirofski, l. A. 2003. The damage-response framework of microbial pathogenesis. *Nat. Rev. Micrbiol.* 1, pp. 17-24.
- Castillo, E., A Dea-Ayuela, M., Bolás-Fernández, F., Rangel, M. and E Gonzalez-Rosende, M., 2010. The kinetoplastid chemotherapy revisited: current drugs, recent advances and future perspectives. *Current medicinal chemistry*, 17(33), pp.4027-4051.
- Cavalier-Smith, T., 1991. Archamoebae: the ancestral eukaryotes?. *Biosystems*, 25(1-2), pp.25-38.
- Chadbourne, F.L., Raleigh, C., Ali, H.Z., Denny, P.W. and Cobb, S.L., 2011. Studies on the antileishmanial properties of the antimicrobial peptides temporin A, B and 1Sa. *Journal of Peptide Science*, 17(11), pp.751-755.
- Chambouvet, A., Valigurová, A., Pinheiro, L.M., Richards, T.A. and Jirků, M., 2016. *Nematopsis temporariae* (Gregarinasina, Apicomplexa, Alveolata) is an intracellular infectious agent of tadpole livers. *Environmental microbiology reports*, 8(5), pp.675-679.
- Chappuis, F., Sundar, S., Hailu, A., Ghalib, H., Rijal, S., Peeling, R.W., Alvar, J. and Boelaert, M., 2007. Visceral leishmaniasis: what are the needs for diagnosis, treatment and control?. *Nature reviews microbiology*, 5(11), pp.873-882.
- Charron, A.J. and Sibley, L.D., 2002. Host cells: mobilizable lipid resources for the intracellular parasite *Toxoplasma gondii. Journal of cell science*, 115(15), pp.3049-3059.
- Chaussabel, D., Semnani, R.T., McDowell, M.A., Sacks, D., Sher, A. and Nutman, T.B., 2003. Unique gene expression profiles of human macrophages and dendritic cells to phylogenetically distinct parasites. *Blood*, 102(2), pp.672-681.
- Chavez, J.A., Knotts, T.A., Wang, L.P., Li, G., Dobrowsky, R.T., Florant, G.L. and Summers, S.A., 2003. A role for ceramide, but not diacylglycerol, in the antagonism of insulin signal transduction by saturated fatty acids. *Journal of Biological Chemistry*, *278*(12), pp.10297-10303.

- Chávez-Fumagalli, M.A., Ribeiro, T.G., Castilho, R.O., Fernandes, S.O.A., Cardoso, V.N., Coelho, C.S.P., Mendonça, D.V.C., Soto, M., Tavares, C.A.P., Faraco, A.A.G. and Coelho, E.A.F., 2015. New delivery systems for amphotericin B applied to the improvement of leishmaniasis treatment. *Revista da Sociedade Brasileira de Medicina Tropical*, 48(3), pp.235-242.
- Checkley, W., White, A.C., Jaganath, D., Arrowood, M.J., Chalmers, R.M., Chen, X.M., Fayer, R., Griffiths, J.K., Guerrant, R.L., Hedstrom, L. and Huston, C.D., 2015. A review of the global burden, novel diagnostics, therapeutic, and vaccine targets for cryptosporidium. *The Lancet Infectious Diseases*, 15(1), pp.85-94.
- Cintra, W.M. and De Souza, W., 1985. Immunocytochemical localization of cytoskeletal proteins and electron microscopy of detergent extracted tachyzoites of *Toxoplasma gondii*. *Journal of submicroscopic cytology*, 17(4), pp.503-508.
- Clark, E.L. and Blake, D.P., 2012. Genetic mapping and coccidial parasites: Past achievements and future prospects. *Journal of biosciences*, 37(5), pp.879-886.
- Coffey, M.J., Jennison, C., Tonkin, C.J. and Boddey, J.A., 2016. Role of the ER and Golgi in protein export by Apicomplexa. *Current opinion in cell biology*, 41, pp.18-24.
- Coppens, I., 2013. Targeting lipid biosynthesis and salvage in apicomplexan parasites for improved chemotherapies. *Nature Reviews Microbiology*, 11(12), pp.823-835.
- Coppens, I., Sinai, A.P. and Joiner, K.A., 2000. *Toxoplasma gondii* exploits host low-density lipoprotein receptor-mediated endocytosis for cholesterol acquisition. *The Journal of cell biology,* 149(1), pp.167-180.
- Cotton, J.A., 2017. The Expanding World of Human Leishmaniasis. *Trends in parasitology*, 33(5), pp.341-344.
- Creek, D.J. and Barrett, M.P., 2014. Determination of antiprotozoal drug mechanisms by metabolomics approaches. *Parasitology*, 141(1), pp.83-92.
- Creek, D.J., Anderson, J., McConville, M.J. and Barrett, M.P., 2012. Metabolomic analysis of trypanosomatid protozoa. *Molecular and biochemical parasitology*, 181(2), pp.73-84.

- Croft, S.L. and Coombs, G.H., 2003. Leishmaniasis–current chemotherapy and recent advances in the search for novel drugs. *Trends in parasitology*, 19(11), pp.502-508.
- Croft, S.L. and Engel, J., 2006. Miltefosine—discovery of the antileishmanial activity of phospholipid derivatives. *Transactions of the Royal Society of Tropical Medicine and Hygiene*, 100(Supplement_1), pp.S4-S8.
- Daher, W. and Soldati-Favre, D., 2009. Mechanisms controlling glideosome function in apicomplexans. *Current opinion in microbiology*, 12(4), pp.408-414.
- Dalloul, R.A. and Lillehoj, H.S., 2006. Poultry coccidiosis: recent advancements in control measures and vaccine development. Expert review of vaccines, 5(1), pp.143-163.
- Dantas-Torres, F., Lorusso, V., Testini, G., de Paiva-Cavalcanti, M., Figueredo, L.A., Stanneck, D., Mencke, N., Brandão-Filho, S.P., Alves, L.C. and Otranto, D., 2010. Detection of *Leishmania infantum* in Rhipicephalus sanguineus ticks from Brazil and Italy. *Parasitology research*, 106(4), pp.857-860.
- de Azevedo, A.F., de Lisboa Dutra, J.L., Santos, M.L.B., de Alexandria Santos, D., Alves, P.B., de Moura, T.R., de Almeida, R.P., Fernandes, M.F., Scher, R. and Fernandes, R.P.M., 2014. Fatty acid profiles in *Leishmania* spp. isolates with natural resistance to nitric oxide and trivalent antimony. *Parasitology research*, 113(1), pp.19-27.
- Decuypere, S., Vanaerschot, M., Rijal, S., Yardley, V., Maes, L., De Doncker, S., Chappuis, F. and Dujardin, J.C., 2008. Gene expression profiling of *Leishmania* (*Leishmania*) *donovani*: overcoming technical variation and exploiting biological variation. *Parasitology*, 135(2), pp.183-194.
- Del Carmen, M.G., Mondragon, M., Gonzalez, S. and Mondragon, R., 2009. Induction and regulation of conoid extrusion in *Toxoplasma gondii*. *Cellular microbiology*, 11(6), pp.967-982.
- Del Grande, C., Galli, L., Schiavi, E., Dell'Osso, L. and Bruschi, F., 2017. Is *Toxoplasma gondii* a Trigger of Bipolar Disorder? *Pathogens*, 6(1), p.3.

- Delgado, A., Casas, J., Llebaria, A., Abad, J.L. and Fabrias, G., 2006. Inhibitors of sphingolipid metabolism enzymes. *Biochimica et Biophysica Acta (BBA)-Biomembranes*, 1758(12), pp.1957-1977.
- Demicheli, C., Ochoa, R., da Silva, J.B., Falcão, C.A., Rossi-Bergmann, B., de Melo, A.L., Sinisterra, R.D. and Frézard, F., 2004. Oral delivery of meglumine antimoniate-β-cyclodextrin complex for treatment of leishmaniasis. *Antimicrobial agents and chemotherapy*, 48(1), pp.100-103.
- Denny, P.W., Goulding, D., Ferguson, M.A. and Smith, D.F., 2004. Sphingolipid-free *Leishmania* are defective in membrane trafficking, differentiation and infectivity. *Molecular microbiology*, 52(2), pp.313-327.
- Denny, P.W., Shams-Eldin, H., Price, H.P., Smith, D.F. and Schwarz, R.T., 2006. The protozoan inositol phosphorylceramide synthase a novel drug target that defines a new class of sphingolipid synthase. *Journal of Biological Chemistry*, 281(38), pp.28200-28209.
- Desjeux, P., 2001. The increase in risk factors for leishmaniasis worldwide. *Transactions of the Royal Society of Tropical Medicine and Hygiene*, 95(3), pp.239-243.
- Desjeux, P., 2004. Leishmaniasis: current situation and new perspectives. *Comparative immunology, microbiology and infectious diseases,* 27(5), pp.305-318.
- Di Tommaso, P., Moretti, S., Xenarios, I., Orobitg, M., Montanyola, A., Chang, J.M., Taly, J.F. and Notredame, C., 2011. T-Coffee: a web server for the multiple sequence alignment of protein and RNA sequences using structural information and homology extension. *Nucleic acids research*, 39(suppl_2), pp.W13-W17.
- Dobson, D.E., Kamhawi, S., Lawyer, P., Turco, S.J., Beverley, S.M. and Sacks, D.L., 2010. *Leishmania major* survival in selective *Phlebotomus papatasi* sand fly vector requires a specific SCG-encoded lipophosphoglycan galactosylation pattern. *PLoS pathogens*, 6(11), p.e1001185.
- Dowhan, W. and Bogdanov, M., 2002. Functional roles of lipids in membranes. *New Comprehensive Biochemistry*, 36, pp.1-35.

- Dorlo, T.P., Balasegaram, M., Beijnen, J.H. and de Vries, P.J., 2012. Miltefosine: a review of its pharmacology and therapeutic efficacy in the treatment of leishmaniasis. *Journal of Antimicrobial Chemotherapy*, 67(11), pp.2576-2597.
- Dubey J. P. 2009. History of the discovery of the life cycle of *Toxoplasmosis gondii*, *International Journal of Parasitology*, 39, pp. 877-882.
- Dunn, W.B. and Ellis, D.I., 2005. Metabolomics: current analytical platforms and methodologies*. TrAC Trends in Analytical Chemistry,* 24*(4),* pp.285-294.
- Ehrt, S. and Schnappinger, D., 2007. Mycobacterium tuberculosis virulence: lipids inside and out. *Nature medicine*, 13(3), pp.284-285.
- Eliot, A.C. and Kirsch, J.F., 2004. Pyridoxal phosphate enzymes: mechanistic, structural, and evolutionary considerations. *Annual review of biochemistry*, 73(1), pp.383-415.
- Fairlamb, A.H., 2003. Target discovery and validation with special reference to trypanothione. Drugs against parasitic diseases: *R&D methodologies and issues*, pp.107-118.
- Fekadu, A., Shibre, T. and Cleare, A.J., 2010. Toxoplasmosis as a cause for behaviour disorders-overview of evidence and mechanisms. *Folia parasitologica*, 57(2), p.105.
- Fichera, M.E. and Roos, D.S., 1997. A plastid organelle as a drug target in apicomplexan parasites. *Nature*, 390(6658), pp.407-409.
- Field, V., Gautret, P., Schlagenhauf, P., Burchard, G.D., Caumes, E., Jensenius, M., Castelli, F., Gkrania-Klotsas, E., Weld, L., Lopez-Velez, R. and de Vries, P., 2010. Travel and migration associated infectious diseases morbidity in Europe, 2008. *BMC Infectious Diseases*, 10(1), p.330.
- Figueiredo, J.M., Mendonça-Previato, L., Previato, J.O. and Heise, N., 2005. Characterization of the inositol phosphorylceramide synthase activity from *Trypanosoma cruzi*. Biochemical Journal, 387(2), pp.519-529.
- Filisetti, D. and Candolfi, E., 2004. Immune response to Toxoplasma gondii. *Ann Ist Super Sanita*, 40(1), pp.71-80.

- Flegr, J. 2013. Influence of latent *Toxoplasma* infection on human personality, physiology and morphology: pros and cons of the *Toxoplasma*–human model in studying the manipulation hypothesis. *The Journal of Experimental Biology* 216, pp.127-133.
- Fletcher, K., Issa, R. and Lockwood, D.N.J., 2015. Visceral leishmaniasis and immunocompromise as a risk factor for the development of visceral leishmaniasis: a changing pattern at the hospital for tropical diseases, London. PloS one, 10(4), p.e0121418.
- Foulet, F., Botterel, F., Buffet, P., Morizot, G., Rivollet, D., Deniau, M., Pratlong, F., Costa, J.M. and Bretagne, S., 2007. Detection and identification of *Leishmania* species from clinical specimens by using a real-time PCR assay and sequencing of the cytochrome B gene. *Journal of clinical microbiology*, 45(7), pp.2110-2115.
- Fox, B.A., Gigley, J.P. and Bzik, D.J., 2004. *Toxoplasma gondii* lacks the enzymes required for de novo arginine biosynthesis and arginine starvation triggers cyst formation. *International journal for parasitology*, 34(3), pp.323-331.
- Francia, M.E., Dubremetz, J.F. and Morrissette, N.S., 2016. Basal body structure and composition in the apicomplexans *Toxoplasma* and *Plasmodium*. *Cilia*, *5*(1), p.3.
- Frearson, J.A., Wyatt, P.G., Gilbert, I.H. and Fairlamb, A.H., 2007. Target assessment for antiparasitic drug discovery. *Trends in parasitology*, 23(12), pp.589-595.
- Frénal, K. and Soldati-Favre, D., 2009. Role of the parasite and host cytoskeleton in apicomplexa parasitism. *Cell host & microbe*, 5(6), pp.602-611.
- Gajria, B., Bahl, A., Brestelli, J., Dommer, J., Fischer, S., Gao, X., Heiges, M., Iodice, J., Kissinger, J.C., Mackey, A.J. and Pinney, D.F., 2007. ToxoDB: an integrated *Toxoplasma gondii* database resource. *Nucleic acids research*, 36(suppl_1), pp.D553-D556.
- Gashaw, I., Ellinghaus, P., Sommer, A. and Asadullah, K., 2012. What makes a good drug target?. *Drug discovery today,* 17, pp.S24-S30.
- Geilen, C.C., Wieder, T. and Orfanos, C.E. 1996. Phosphatidylcholine biosynthesis as a target for phospholipid analogues. *Adv. Exp. Med. Biol.* 416, pp.333–336.

- Genin, M. J., Gonzalez Valcarcel, I. C., Holloway, W. G., Lamar, J., Mosior, M., Hawkins, E., Estridge, T., Weidner, J., Seng, T. & Yurek, D. 2016. Imidazopyridine and Pyrazolopiperidine Derivatives as Novel Inhibitors of Serine Palmitoyl Transferase. *Journal of medicinal chemistry*, 59, pp.5904-5910.
- George, S.S., Bishop, J.V., Titus, R.G. and Selitrennikoff, C.P., 2006. Novel compounds active against *Leishmania major*. *Antimicrobial agents and chemotherapy*, 50(2), pp.474-479.
- Gerold, P. and Schwarz, R.T., 2001. Biosynthesis of glycosphingolipids de-novo by the human malaria parasite *Plasmodium falciparum*. *Molecular and biochemical parasitology*, 112(1), pp.29-37.
- Giovannini, D., Späth, S., Lacroix, C., Perazzi, A., Bargieri, D., Lagal, V., Lebugle, C., Combe, A., Thiberge, S., Baldacci, P. and Tardieux, I., 2011. Independent roles of apical membrane antigen 1 and rhoptry neck proteins during host cell invasion by apicomplexa. *Cell host & microbe*, 10(6), pp.591-602.
- Goldston, A.M., Powell, R.R. and Temesvari, L.A., 2012. Sink or swim: lipid rafts in parasite pathogenesis. *Trends in parasitology*, 28(10), pp.417-426.
- Gossage, S.M., Rogers, M.E. and Bates, P.A., 2003. Two separate growth phases during the development of *Leishmania* in sand flies: implications for understanding the life cycle. *International journal for parasitology*, 33(10), pp.1027-1034.
- Goto, H. and Lindoso, J.A.L., 2010. Current diagnosis and treatment of cutaneous and mucocutaneous leishmaniasis. *Expert review of anti-infective therapy*, 8(4), pp.419-433.
- Gottesman, M.M., 2002. Mechanisms of cancer drug resistance. *Annual review of medicine*, 53(1), pp.615-627.
- Gouet, P., Robert, X. and Courcelle, E., 2003. ESPript/ENDscript: extracting and rendering sequence and 3D information from atomic structures of proteins. *Nucleic acids research*, 31(13), pp.3320-3323.

- Graindorge, A., Frénal, K., Jacot, D., Salamun, J., Marq, J.B. and Soldati-Favre, D., 2016. The conoid associated motor MyoH is indispensable for *Toxoplasma gondii* entry and exit from host cells. *PLoS Pathog*, 12(1), p.e1005388.
- Gramiccia, M. and Gradoni, L., 2005. The current status of zoonotic leishmaniases and approaches to disease control. *International journal for parasitology*, 35(11), pp.1169-1180.
- Grigg, M.E., Ganatra, J., Boothroyd, J.C. and Margolis, T.P., 2001. Unusual abundance of atypical strains associated with human ocular toxoplasmosis. *The Journal of infectious diseases*, 184(5), pp.633-639.
- Gubbels, M.J. and Striepen, B., 2004. Studying the cell biology of apicomplexan parasites using fluorescent proteins. *Microscopy and Microanalysis*, 10(05), pp.568-579.
- Gubbels, M.J., Lehmann, M., Muthalagi, M., Jerome, M.E., Brooks, C.F., Szatanek, T., Flynn, J., Parrot, B., Radke, J., Striepen, B. and White, M.W., 2008. Forward genetic analysis of the apicomplexan cell division cycle in *Toxoplasma gondii. PLoS Pathog*, 4(2), p.e36.
- Gubbels, M.J., Li, C. and Striepen, B., 2003. High-throughput growth assay for Toxoplasma gondii using yellow fluorescent protein. *Antimicrobial Agents and Chemotherapy*, 47(1), pp.309-316.
- Gupta, G., Oghumu, S. and Satoskar, A.R., 2013. Mechanisms of immune evasion in leishmaniasis. *Advances in applied microbiology*, 82, p.155.
- Gutiérrez-Kobeh, L., De Oyarzabal, E., Argueta, J., Wilkins, A., Salaiza, N., Fernández, E., López, O., Aguirre, M. and Becker, I., 2013. Inhibition of dendritic cell apoptosis by *Leishmania mexicana* amastigotes. *Parasitology research*, 112(4), pp.1755-1762.
- Haldar, K., Mohandas, N., Samuel, B.U., Harrison, T., Hiller, N.L., Akompong, T. and Cheresh, P., 2002. Protein and lipid trafficking induced in erythrocytes infected by malaria parasites. *Cellular microbiology*, *4*(7), pp.383-395.
- Hammoudi, P.M., Jacot, D., Mueller, C., Di Cristina, M., Dogga, S.K., Marq, J.B., Romano, J., Tosetti, N., Dubrot, J., Emre, Y. and Lunghi, M., 2015. Fundamental roles

of the Golgi-associated *Toxoplasma* aspartyl protease, ASP5, at the host-parasite interface. *PLoS Pathog*, 11(10), p.e1005211.

- Han, G., Gable, K., Yan, L., Natarajan, M., Krishnamurthy, J., Gupta, S.D., Borovitskaya, A., Harmon, J.M. and Dunn, T.M., 2004. The topology of the Lcb1p subunit of yeast serine palmitoyltransferase. *Journal of Biological Chemistry*, 279(51), pp.53707-53716.
- Han, G., Gupta, S.D., Gable, K., Niranjanakumari, S., Moitra, P., Eichler, F., Brown, R.H., Harmon, J.M. and Dunn, T.M., 2009. Identification of small subunits of mammalian serine palmitoyltransferase that confer distinct acyl-CoA substrate specificities. *Proceedings of the National Academy of Sciences*, 106(20), pp.8186-8191.
- Hanada K. 2003. Corrigendum to ‘‘Serine palmitoyltransferase, a keyenzyme of sphingolipid metabolism’’ *Biochim. Biophys. Acta*. 1632, pp. 16-30.
- Hanada, K., 2005. Sphingolipids in infectious diseases. *Japanese journal of infectious diseases*, 58(3), p.131.
- Handman, E. and Bullen, D.V., 2002. Interaction of *Leishmania* with the host macrophage. *Trends in parasitology*, 18(8), pp.332-334.
- Heaslip AT, Nishi M, Stein B, Hu K 2011. The motility of a human parasite, *Toxoplasma gondii*, is regulated by a novel lysine methyltransferase. *PLoS pathogens*. 7(9), p.e.1002201
- Heaslip, A.T., Ems-McClung, S.C. and Hu, K., 2009. *Tg*ICMAP1 is a novel microtubule binding protein in *Toxoplasma gondii*. *PLoS One*, 4(10), p.e7406.
- Hellier, I., Dereure, O., Tournillac, I., Pratlong, F., Guillot, B., Dedet, J.P. and Guilhou, J.J., 2000. Treatment of Old World cutaneous leishmaniasis by pentamidine isethionate. *Dermatology*, 200(2), pp.120-123.
- Heung L. J., Chiara L. and Maurizio D. P. 2006. Role of Sphingolipids in Microbial Pathogenesis. *Infect. Immun.*, 74(1), p.28.
- Holland, G.N. 2003. Ocular toxoplasmosis: a global reassessment. Part I: epidemiology and course of disease. *Am J Ophthalmol.* 136(6), p.973-88.

- Holland, W. L., Brozinick, J. T., Wang, L.-P., Hawkins, E. D., Sargent, K. M., Liu, Y., Narra, K., Hoehn, K. L., Knotts, T. A. & Siesky, A. 2007. Inhibition of ceramide synthesis ameliorates glucocorticoid-, saturated-fat-, and obesity-induced insulin resistance. *Cell metabolism*, 5 (3), pp.167-179.
- Holmes, E., Wilson, I.D. and Nicholson, J.K., 2008. Metabolic phenotyping in health and disease. *Cell*, 134(5), pp.714-717.
- Hornemann, T., Penno, A., Rütti, M.F., Ernst, D., Kivrak-Pfiffner, F., Rohrer, L. and von Eckardstein, A., 2009. The SPTLC3 subunit of serine palmitoyltransferase generates short chain sphingoid bases. *Journal of Biological Chemistry*, 284(39), pp.26322-26330.
- Hornemann, T., Richard, S., Rütti, M.F., Wei, Y. and von Eckardstein, A., 2006. Cloning and initial characterization of a new subunit for mammalian serine-palmitoyltransferase. *Journal of Biological Chemistry*, 281(49), pp.37275-37281.
- Hotez, P.J., 2008. Neglected infections of poverty in the United States of America. *PLoS Negl Trop Dis*, 2(6), p.e256.
- Hsu, F.F., Turk, J., Zhang, K. and Beverley, S.M., 2007. Characterization of inositol phosphorylceramides from *Leishmania major* by tandem mass spectrometry with electrospray ionization. *Journal of the American Society for Mass Spectrometry*, 18(9), pp.1591-1604.
- Hu, K., Johnson, J., Florens, L., Fraunholz, M., Suravajjala, S., DiLullo, C., Yates, J., Roos, D.S. and Murray, J.M., 2006. Cytoskeletal components of an invasion machine—the apical complex of *Toxoplasma gondii*. *PLoS Pathog*, 2(2), p.e13.
- Hu, K., Mann, T., Striepen, B., Beckers, C.J., Roos, D.S. and Murray, J.M., 2002. Daughter cell assembly in the protozoan parasite *Toxoplasma gondii*. *Molecular biology of the cell*, 13(2), pp.593-606.
- Hughes, J.P., Rees, S., Kalindjian, S.B. and Philpott, K.L., 2011. Principles of early drug discovery. *British journal of pharmacology*, 162(6), pp.1239-1249.

- Huitema, K., van den Dikkenberg, J., Brouwers, J.F. and Holthuis, J.C., 2004. Identification of a family of animal sphingomyelin synthases. *The EMBO journal*, 23(1), pp.33-44.
- Huitema, K., van den Dikkenberg, J., Brouwers, J.F. and Holthuis, J.C., 2004. Identification of a family of animal sphingomyelin synthases. *The EMBO journal*, *23*(1), pp.33-44.
- Humen, M.A., Pérez, P.F. and Moal, L.L., 2011. Lipid raft-dependent adhesion of Giardia intestinalis trophozoites to a cultured human enterocyte-like Caco-2/TC7 cell monolayer leads to cytoskeleton-dependent functional injuries. *Cellular microbiology*, *13*(11), pp.1683-1702.
- Hunter, P.R. and Nichols, G., 2002. Epidemiology and clinical features of *Cryptosporidium* infection in immunocompromised patients. *Clinical microbiology reviews*, 15(1), pp.145-154.
- Hurrell, B.P., Regli, I.B. and Tacchini-Cottier, F., 2016. Different *Leishmania* species drive distinct neutrophil functions. *Trends in parasitology*, 32(5), pp.392-401.
- Huynh, M.H. and Carruthers, V.B., 2009. Tagging of endogenous genes in a *Toxoplasma gondii* strain lacking Ku80. *Eukaryotic cell*, 8(4), pp.530-539.
- Ikai, K., Takesako, K., Shiomi, K., Moriguchi, M., Umeda, Y., Yamamoto, J., Kato, I. and Naganawa, H., 1991. Structure of aureobasidin A. *The Journal of antibiotics*, 44(9), pp.925-933.
- Ikushiro, H. and Hayashi, H., 2011. Mechanistic enzymology of serine palmitoyltransferase. *Biochimica et Biophysica Acta (BBA)-Proteins and Proteomics*, 1814(11), pp.1474-1480.
- Ikushiro, H., Hayashi, H. and Kagamiyama, H., 2001. A Water-soluble Homodimeric Serine Palmitoyltransferase from *Sphingomonas paucimobilis* EY2395T Strain purification, characterization, cloning, and overproduction. *Journal of Biological Chemistry*, 276(21), pp.18249-18256.
- Imbert, L., Ramos, R.G., Libong, D., Abreu, S., Loiseau, P.M. and Chaminade, P., 2012. Identification of phospholipid species affected by miltefosine action in *Leishmania*

donovani cultures using LC-ELSD, LC-ESI/MS, and multivariate data analysis. *Analytical and bioanalytical chemistry*, 402(3), pp.1169-1182.

- Imming, P., Sinning, C. and Meyer, A., 2006. Drugs, their targets and the nature and number of drug targets. *Nature reviews Drug discovery*, 5(10), pp.821-834.
- Isaza, J.P. and Alzate, J.F., 2016. Genome microsatellite diversity within the Apicomplexa phylum. *Molecular Genetics and Genomics*, 291(6), pp.2117-2129.
- Joiner, K.A. and Roos, D.S., 2002. Secretory traffic in the eukaryotic parasite Toxoplasma gondii. *J Cell Biol*, 157(4), pp.557-563.
- Joshi, A., Narain, J.P., Prasittisuk, C., Bhatia, R., Hashim, G., Jorge, A., Banjara, M. and Kroeger, A., 2008. Can visceral leishmaniasis be eliminated from Asia?. *Journal of vector borne diseases,* 45(2), p.105.
- Kafsack, B.F. and Llinás, M., 2010. Eating at the table of another: metabolomics of host-parasite interactions. *Cell host & microbe,* 7(2), pp.90-99.
- Käll, L., Krogh, A. and Sonnhammer, E.L., 2004. A combined transmembrane topology and signal peptide prediction method. *Journal of molecular biology*, 338(5), pp.1027-1036.
- Kamerkar, S. and Davis, P.H., 2012. *Toxoplasma* on the brain: understanding host-pathogen interactions in chronic CNS infection. *Journal of parasitology research*, 2012.
- Karimi, S., Kim, S. and Cavedon, L., 2011. Drug side-effects: What do patient forums reveal. In *The second international workshop on Web science and information exchange in the medical Web* (pp. 10-11). ACM.
- Katris, N.J., van Dooren, G.G., McMillan, P.J., Hanssen, E., Tilley, L. and Waller, R.F., 2014. The apical complex provides a regulated gateway for secretion of invasion factors in *Toxoplasma. PLoS pathog,* 10(4), p.e1004074.
- Kaye, P. and Scott, P., 2011. Leishmaniasis: complexity at the host–pathogen interface. *Nature Reviews Microbiology*, 9(8), pp.604-615.

- Kedzierski, L., Anuratha S., Joan M. C., Philip C. A., Peter C. J., and Katherine K. 2009. "Leishmaniasis: current treatment and prospects for new drugs and vaccines." *Current medicinal chemistry* 16(5), pp. 599-614.
- Kemp, L.E., Yamamoto, M. and Soldati-Favre, D., 2013. Subversion of host cellular functions by the apicomplexan parasites. *FEMS microbiology reviews*, 37(4), pp.607-631.
- Kerridge, B.T., Khan, M.R. and Sapkota, A., 2012. Terrorism, civil war, one-sided violence and global burden of disease*. Medicine, Conflict and Survival,* 28(3), pp.199-218.
- Khan, A., Taylor, S., Su, C., Mackey, A.J., Boyle, J., Cole, R., Glover, D., Tang, K., Paulsen, I.T., Berriman, M. and Boothroyd, J.C., 2005. Composite genome map and recombination parameters derived from three archetypal lineages of *Toxoplasma gondii. Nucleic acids research*, 33(9), pp.2980-2992.
- Kim, K. and Weiss, L.M., 2004. *Toxoplasma gondii*: the model apicomplexan. *International journal for parasitology*, 34(3), pp.423-432.
- Kim, S.K., Fouts, A.E. and Boothroyd, J.C., 2007. *Toxoplasma gondii* dysregulates IFN-γ-inducible gene expression in human fibroblasts: insights from a genome-wide transcriptional profiling. *The Journal of Immunology*, 178(8), pp.5154-5165.
- Krishnamurthy, S., Deng, B., del Rio, R., Buchholz, K.R., Treeck, M., Urban, S., Boothroyd, J., Lam, Y.W. and Ward, G.E., 2016. Not a Simple Tether: Binding of *Toxoplasma gondii* AMA1 to RON2 during Invasion Protects AMA1 from Rhomboid-Mediated Cleavage and Leads to Dephosphorylation of Its Cytosolic Tail. *mBio*, 7(5), pp.e00754-16.
- Kyte, J. and Doolittle, R.F., 1982. A simple method for displaying the hydropathic character of a protein. *Journal of molecular biology*, 157(1), pp.105-132.
- Lack, J.B., Reichard, M.V. and Van Den Bussche, R.A., 2012. Phylogeny and evolution of the Piroplasmida as inferred from 18S rRNA sequences. *International journal for parasitology*, 42(4), pp.353-363.

- Landfear, S.M., Tran, K.D. and Sanchez, M.A., 2015. Flagellar membrane proteins in kinetoplastid parasites. *IUBMB life*, 67(9), pp.668-676.
- Lang, C., Groß, U. and Lüder, C.G., 2007. Subversion of innate and adaptive immune responses by Toxoplasma gondii. *Parasitology research*, 100(2), pp.191-203.
- Leifso, K., Cohen-Freue, G., Dogra, N., Murray, A. and McMaster, W.R., 2007. Genomic and proteomic expression analysis of *Leishmania* promastigote and amastigote life stages: the *Leishmania* genome is constitutively expressed. *Molecular and biochemical parasitology*, 152(1), pp.35-46.
- Lester, R.L. and Dickson, R.C., 1992. Sphingolipids with inositolphosphate-containing head groups. *Advances in lipid research*, 26, pp.253-274.
- Li, Z.H., Ramakrishnan, S., Striepen, B. and Moreno, S.N., 2013. *Toxoplasma gondii* relies on both host and parasite isoprenoids and can be rendered sensitive to atorvastatin. *PLoS Pathog*, 9(10), p.e1003665.
- Lige B, Romano JD, Bandaru VVR, Ehrenman K, Levitskaya J, Sampels V, Haughey NJ, Coppens, I. 2011. Deficiency of a Niemann-Pick, type C1-related protein in *Toxoplasma* is associated with multiple lipidoses and increased pathogenicity. *PLoS. Pathog.* 7, e1002410.
- Lindholm, D., Wootz, H. and Korhonen, L., 2006. ER stress and neurodegenerative diseases. *Cell Death & Differentiation*, 13(3), pp.385-392.
- Liu, J., Wetzel, L., Zhang, Y., Nagayasu, E., Ems-McClung, S., Florens, L. and Hu, K., 2013. Novel thioredoxin-like proteins are components of a protein complex coating the cortical microtubules of Toxoplasma gondii. *Eukaryotic cell*, 12(12), pp.1588-1599.
- Lowther, J., Naismith, J. H., Dunn, T. M., and Campopiano, D. J. (2012) Structural, mechanistic and regulatory studies of serine palmitoyltransferase. *Biochem Soc Trans* 40, 547-554.
- Luscombe, N.M., Greenbaum, D. and Gerstein, M., 2001. What is bioinformatics? A proposed definition and overview of the field. *Methods of information in medicine*, 40(4), pp.346-358.

- Madrid-Aliste, C.J., Dybas, J.M., Angeletti, R.H., Weiss, L.M., Kim, K., Simon, I. and Fiser, A., 2009. EPIC-DB: a proteomics database for studying Apicomplexan organisms. *BMC genomics*, 10(1), p.38.
- Mandala, S.M., Thornton, R.A., Milligan, J., Rosenbach, M., Garcia-Calvo, M., Bull, H.G., Harris, G., Abruzzo, G.K., Flattery, A.M., Gill, C.J. and Bartizal, K., 1998. Rustmicin, a potent antifungal agent, inhibits sphingolipid synthesis at inositol phosphoceramide synthase. *Journal of Biological Chemistry*, 273(24), pp.14942-14949.
- Mandlik, V., Shinde, S., Chaudhary, A. and Singh, S., 2012. Biological network modeling identifies IPCS in *Leishmania* as a therapeutic target*. Integrative Biology*, 4(9), pp.1130-1142.
- Manger, I.D., Hehl, A.B. and Boothroyd, J.C., 1998. The surface of *Toxoplasma* tachyzoites is dominated by a family of glycosylphosphatidylinositol-anchored antigens related to SAG1. *Infection and immunity*, 66(5), pp.2237-2244.
- Mansueto, P., Seidita, A., Vitale, G. and Cascio, A., 2014. Leishmaniasis in travelers: a literature review. *Travel medicine and infectious disease*, 12(6), pp.563-581.
- Many, A. and Koren, G. 2006. Toxoplasmosis during pregnancy, *Canadian Family Physician*, 52: 29-32.
- Marcondes, M., Biondo, A.W., Gomes, A.A.D., Silva, A.R.S., Vieira, R.F.C., Camacho, A.A., Quinn, J. and Chandrashekar, R., 2011. Validation of a *Leishmania infantum* ELISA rapid test for serological diagnosis of Leishmania chagasi in dogs. *Veterinary parasitology*, 175(1), pp.15-19.
- McGregor, A. "WHO warns of epidemic leishmania." 1998. 575.
- McGwire, B.S. and Satoskar, A.R., 2013. Leishmaniasis: clinical syndromes and treatment. *Qjm*, p.hct116.
- Meissner, M., 2013. The asexual cycle of apicomplexan parasites: new findings that raise new questions. *Current opinion in microbiology*, 16(4), p.421.
- Meissner, M., Ferguson, D.J. and Frischknecht, F., 2013. Invasion factors of apicomplexan parasites: essential or redundant?. *Current opinion in microbiology*, 16(4), pp.438-444.

- Merrill, A.H., 2002. De novo sphingolipid biosynthesis: a necessary, but dangerous, pathway. *Journal of Biological Chemistry*, 277(29), pp.25843-25846.
- Messaoud, H.B.B., Guichard, M., Lawton, P., Delton, I. and Azzouz-Maache, S., 2017. Changes in Lipid and Fatty Acid Composition during Intramacrophagic Transformation of *Leishmania donovani* Complex Promastigotes into Amastigotes. *Lipids*, 52(5), pp.433-441.
- Meyerhoff, A., 1999. US Food and Drug Administration approval of AmBisome (liposomal amphotericin B) for treatment of visceral leishmaniasis. *Clinical Infectious Diseases*, pp.42-48.
- Mina, J.G., Pan, S.Y., Wansadhipathi, N.K., Bruce, C.R., Shams-Eldin, H., Schwarz, R.T., Steel, P.G. and Denny, P.W., 2009. The *Trypanosoma brucei* sphingolipid synthase, an essential enzyme and drug target. *Molecular and biochemical parasitology*, 168(1), pp.16-23.
- Mina, J.G. and Denny, P.W., 2017. Everybody needs sphingolipids, right! Mining for new drug targets in protozoan sphingolipid biosynthesis. *Parasitology*, special issue review, pp.1-14.
- Mina, J.G., Thye, J.K., Alqaisi, A.Q., Bird, L.E., Dods, R.H., Groftehauge, M.K., Mosely, J.A., Pratt, S., Shams-Eldin, H., Schwarz, R.T., Pohl, E. and Denny, P. W. 2017. Functional and phylogenetic evidence of a bacterial origin for the first enzyme in sphingolipid biosynthesis in a phylum of eukaryotic protozoan parasites. *Journal of Biological Chemistry*, 292(92): pp. 1208-12219.
- Mineo, J.R., McLeod, R., Mack, D., Smith, J., Khan, I.A., Ely, K.H. and Kasper, L.H., 1993. Antibodies to *Toxoplasma gondii* major surface protein (SAG-1, P30) inhibit infection of host cells and are produced in murine intestine after peroral infection. *The Journal of Immunology,* 150(9), pp.3951-3964.
- Mital, J., Meissner, M., Soldati, D. and Ward, G.E., 2005. Conditional expression of *Toxoplasma gondii* apical membrane antigen-1 (TgAMA1) demonstrates that TgAMA1 plays a critical role in host cell invasion. *Molecular biology of the cell,* 16(9), pp.4341-4349.

- Mondragon, R. and Frixione, E., 1996. Ca2+-Dependence of Conoid Extrusion in *Toxoplasma gondii Tachyzoites. Journal of Eukaryotic Microbiology*, 43(2), pp.120-127.
- Monge-Maillo, B. and López-Vélez, R., 2013. Therapeutic options for visceral leishmaniasis. *Drugs*, 73(17), pp.1863-1888.
- Monge-Maillo, B., Norman, F.F., Cruz, I., Alvar, J. and Lopez-Velez, R., 2014. Visceral leishmaniasis and HIV coinfection in the Mediterranean region. *PLoS Negl Trop Dis*, 8(8), p.e3021.
- Montoya, J.G. and Liesenfield, O. 2004. *Toxoplasmosis*. Lancet. 363: 1965-1976.
- Moreno, S.N. and Docampo, R., 2003. Calcium regulation in protozoan parasites. *Current opinion in microbiology*, 6(4), pp.359-364.
- Morrissette, N.S. and Sibley, L.D., 2002. Cytoskeleton of apicomplexan parasites. *Microbiology and Molecular Biology Reviews*, 66(1), pp.21-38.
- Mougneau, E., Bihl, F. and Glaichenhaus, N., 2011. Cell biology and immunology of *Leishmania. Immunological reviews*, 240(1), pp.286-296.
- Mount, D.W., 2007. Using the basic local alignment search tool (BLAST). *Cold Spring Harbor Protocols*, 2007(7), pp.pdb-top17.
- Mùller, J. and Hemphill, A. 2011. Drug target identification in intracellular and extracellular protozoan parasites. *Curr. Trop. Med. Chem.* 11: 2029-2038.
- Nagano, S., Lin, T.Y., Edula, J.R. and Heddle, J.G., 2014. Unique features of apicoplast DNA gyrases from *Toxoplasma gondii* and Plasmodium falciparum. *BMC bioinformatics*, 15(1), p.416.
- Nagiec, M.M., Baltisberger, J.A., Wells, G.B., Lester, R.L. and Dickson, R.C., 1994. The LCB2 gene of Saccharomyces and the related LCB1 gene encode subunits of serine palmitoyltransferase, the initial enzyme in sphingolipid synthesis. *Proceedings of the National Academy of Sciences*, 91(17), pp.7899-7902.
- Nagiec, M.M., Nagiec, E.E., Baltisberger, J.A., Wells, G.B., Lester, R.L. and Dickson, R.C., 1997. Sphingolipid synthesis as a target for antifungal drugs complementation of the inositol phosphorylceramide synthase defect in a mutant strain of

Saccharomyces cerevisiae by the AUR1 gene. *Journal of Biological Chemistry*, 272(15), pp.9809-9817.

- Naula, C., Parsons, M. and Mottram, J.C., 2005. Protein kinases as drug targets in trypanosomes and *Leishmania*. *Biochimica et Biophysica Acta (BBA)-Proteins and Proteomics*, 1754(1), pp.151-159.
- Negera, E., Gadisa, E., Hussein, J., Engers, H., Kuru, T., Gedamu, L. and Aseffa, A., 2012. Treatment response of cutaneous leishmaniasis due to *Leishmania aethiopica* to cryotherapy and generic sodium stibogluconate from patients in Silti, Ethiopia. *Transactions of the Royal Society of Tropical Medicine and Hygiene*, 106(8), pp.496-503.
- Ngô, H.M., Hoppe, H.C. and Joiner, K.A., 2000. Differential sorting and post-secretory targeting of proteins in parasitic invasion. *Trends in cell biology*, 10(2), pp.67-72.
- Nichols, B.A. and Chiappino, M.L., 1987. Cytoskeleton of *Toxoplasma gondii*. The *Journal of protozoology*, 34(2), pp.217-226.
- Nishi, M., Hu, K., Murray, J.M. and Roos, D.S., 2008. Organellar dynamics during the cell cycle of *Toxoplasma gondii*. *Journal of cell science*, 121(9), pp.1559-1568.
- Nozzi, M., Del Torto, M., Chiarelli, F. and Breda, L., 2014. Leishmaniasis and autoimmune diseases in pediatric age. *Cellular immunology*, 292(1), pp.9-13.
- Ogretmen, B. and Hannun, Y. A. 2004. Biologically active sphingolipids in cancer pathogenesis and treatment. *Nature Reviews Cancer,* 4**,** pp.604-616.
- Ohanian, J. and Ohanian, V. 2001. Sphingolipids in mammalian cell signalling. *Cellular and Molecular Life Sciences CMLS*, 58 (14), pp.2053-2068.
- Okamoto, N. and Keeling, P.J., 2014. The 3D structure of the apical complex and association with the flagellar apparatus revealed by serial TEM tomography in *Psammosa pacifica*, a distant relative of the Apicomplexa. *PloS one*, 9(1), p.e84653.
- Pace, D. 2014. Leishmaniasis. *Journal of Infection,* 69, supplement 1, S10-S18.
- Paget, T., Haroune, N., Bagchi, S. and Jarroll, E., 2013. Metabolomics and protozoan parasites. *Acta parasitologica*, 58(2), pp.127-131.

- Palencia, A., Bougdour, A., Brenier-Pinchart, M.P., Touquet, B., Bertini, R.L., Sensi, C., Gay, G., Vollaire, J., Josserand, V., Easom, E. and Freund, Y.R., 2017. Targeting *Toxoplasma gondii* CPSF3 as a new approach to control toxoplasmosis. *EMBO Molecular Medicine*, 9(3), pp.385-394.
- Pedersen, M.G., Mortensen, P.B., Norgaard-Pedersen, B. and Postolache, T.T., 2012. *Toxoplasma gondii* infection and self-directed violence in mothers. *Archives of general psychiatry*, 69(11), pp.1123-1130.
- Peña, I., Manzano, M.P., Cantizani, J., Kessler, A., Alonso-Padilla, J., Bardera, A.I., Alvarez, E., Colmenarejo, G., Cotillo, I., Roquero, I. and de Dios-Anton, F., 2015. New compound sets identified from high throughput phenotypic screening against three kinetoplastid parasites: an open resource. *Scientific reports*, *5*.
- Peters, P., Miller, R.K. and Schaefer, C., 2015. General commentary on drug therapy and drug risks in pregnancy. In *Drugs during Pregnancy and Lactation (Third Edition)* (pp. 1-23).
- Pfluger, S.L., Goodson, H.V., Moran, J.M., Ruggiero, C.J., Ye, X., Emmons, K.M. and Hager, K.M., 2005. Receptor for retrograde transport in the apicomplexan parasite *Toxoplasma gondii*. *Eukaryotic cell*, 4(2), pp.432-442.
- Porchet-Hennere, E. and Nicolas, G., 1983. Are rhoptries of Coccidia really extrusomes?. *Journal of ultrastructure research*, 84(2), pp.194-203.
- Postigo, J.A.R., 2010. Leishmaniasis in the world health organization eastern mediterranean region. *International journal of antimicrobial agents*, *36*, pp.S62-S65.
- Pralhada Rao, R., Vaidyanathan, N., Rengasamy, M., Mammen Oommen, A., Somaiya, N. and Jagannath, M.R., 2013. Sphingolipid metabolic pathway: an overview of major roles played in human diseases. *Journal of lipids*, 2013, pp.1-13.
- Pratt, S. *et al.* 2013. Sphingolipid synthesis and scavenging in the intracellular apicomlexan parasite, *Toxoplasma gondii. Mol. Biochem. Parasitol.,* 12,265-277
- Ramakrishnan, S., Docampo, M.D., MacRae, J.I., Ralton, J.E., Rupasinghe, T., McConville, M.J. and Striepen, B., 2015. The intracellular parasite *Toxoplasma gondii*

depends on the synthesis of long-chain and very long-chain unsaturated fatty acids not supplied by the host cell. *Molecular microbiology*, *97*(1), pp.64-76.

- Ramakrishnan, S., Serricchio, M., Striepen, B. and Bütikofer, P., 2013. Lipid synthesis in protozoan parasites: a comparison between kinetoplastids and apicomplexans. *Progress in lipid research*, *52*(4), pp.488-512.
- Rampersad, S.N., 2012. Multiple applications of Alamar Blue as an indicator of metabolic function and cellular health in cell viability bioassays. *Sensors*, *12*(9), pp.12347-12360.
- Ready, P.D., 2000. Sand fly evolution and its relationship to *Leishmania* transmission. *Memorias do Instituto Oswaldo Cruz*, 95(4), pp.589-590.
- Reed, S.G., 1996. Diagnosis of leishmaniasis. *Clinics in dermatology*, 14(5), pp.471-478.
- Reger, J.F., 1967. The fine structure of the gregarine Pyxinoides balani parasitic in the barnacle *Balanus tintinnabulum*. *Journal of Eukaryotic Microbiology*, 14(3), pp.488-497.
- Reithinger, R., Dujardin, J.C., Louzir, H., Pirmez, C., Alexander, B. and Brooker, S., 2007. Cutaneous leishmaniasis. *The Lancet infectious diseases*, 7(9), pp.581-596.
- Reithinger, R., Mohsen, M., Wahid, M., Bismullah, M., Quinnell, R.J., Davies, C.R., Kolaczinski, J. and David, J.R., 2005. Efficacy of thermotherapy to treat cutaneous leishmaniasis caused by *Leishmania tropica* in Kabul, Afghanistan: a randomized, controlled trial. *Clinical infectious diseases*, 40(8), pp.1148-1155.
- Ribeiro-Gomes, F.L., Peters, N.C., Debrabant, A. and Sacks, D.L., 2012. Efficient capture of infected neutrophils by dendritic cells in the skin inhibits the early anti-leishmania response. *PLoS Pathog*, 8(2), p.e1002536.
- Rice, D.R., Vacchina, P., Norris-Mullins, B., Morales, M.A. and Smith, B.D., 2016. Zinc (II)-Dipicolylamine Coordination Complexes as Targeting and Chemotherapeutic Agents for *Leishmania major. Antimicrobial agents and chemotherapy*, 60(5), pp.2932-2940.

- Ritchie, S.A., Ahiahonu, P.W., Jayasinghe, D., Heath, D., Liu, J., Lu, Y., Jin, W., Kavianpour, A., Yamazaki, Y., Khan, A.M. and Hossain, M., 2010. Reduced levels of hydroxylated, polyunsaturated ultra long-chain fatty acids in the serum of colorectal cancer patients: implications for early screening and detection. *BMC medicine*, 8(1), p.13.
- Riviere, J.E. and Papich, M.G. eds., 2013. *Veterinary pharmacology and therapeutics*. John Wiley & Sons.
- Romano J.D., Sonda S, Bergbower E, Smith ME, Coppens I. 2013. *Toxoplasma gondii* salvages sphingolipids from the host Golgi through the rerouting of selected Rab vesicles to the parasitophorous vacuole. *Mol Biol Cell.,* 24, pp.1974-1995.
- Roy, C.R. and Mocarski, E.S., 2007. Pathogen subversion of cell-intrinsic innate immunity. *Nature immunology*, 8(11), pp.1179-1187.
- Rybczynska, M., Spitaler, M., Knebel, N.G., Boeck, G., Grunicke, H. and Hofmann, J., 2001. Effects of miltefosine on various biochemical parameters in a panel of tumor cell lines with different sensitivities. *Biochemical pharmacology*, 62(6), pp.765-772.
- Saito, N., Ohashi, Y., Soga, T. and Tomita, M., 2010. Unveiling cellular biochemical reactions via metabolomics-driven approaches. *Current opinion in microbiology*, 13(3), pp.358-362.
- Salto, M.L., Bertello, L.E., Vieira, M., Docampo, R., Moreno, S.N. and de Lederkremer, R.M., 2003. Formation and remodeling of inositolphosphoceramide during differentiation of *Trypanosoma cruzi* from trypomastigote to amastigote. *Eukaryotic Cell,* 2*(4)*, pp.756-768.
- Saravolatz, L.D., Bern, C., Adler-Moore, J., Berenguer, J., Boelaert, M., den Boer, M., Davidson, R.N., Figueras, C., Gradoni, L., Kafetzis, D.A. and Ritmeijer, K., 2006. Liposomal amphotericin B for the treatment of visceral leishmaniasis. *Clinical Infectious Diseases*, 43(7), pp.917-924.
- Savoia, D., 2015. Recent updates and perspectives on leishmaniasis. *The Journal of Infection in Developing Countries*, 9(06), pp.588-596.

- Seifert, K., 2011. Structures, targets and recent approaches in anti-leishmanial drug discovery and development. *The open medicinal chemistry journal*, 5. pp.31-39.
- Sereno, D., Da Silva, A.C., Mathieu-Daude, F. and Ouaissi, A., 2007. Advances and perspectives in *Leishmania* cell based drug-screening procedures. *Parasitology internationa*l, 56(1), pp.3-7.
- Serreno-Martín, X., Payares, G., De Lucca, M., Martinez, J.C., Mendoza-León, A. and Benaim, G., 2009. Amiodarone and miltefosine act synergistically against *Leishmania mexicana* and can induce parasitological cure in a murine model of cutaneous leishmaniasis. *Antimicrobial agents and chemotherapy*, 53(12), pp.5108-5113.
- Sevova, E.S., Goren, M.A., Schwartz, K.J., Hsu, F.F., Turk, J., Fox, B.G. and Bangs, J.D., 2010. Cell-free synthesis and functional characterization of sphingolipid synthases from parasitic trypanosomatid protozoa. *Journal of Biological Chemistry*, 285(27), pp.20580-20587.
- Shanmugasundram, A., Gonzalez-Galarza, F.F., Wastling, J.M., Vasieva, O. and Jones, A.R., 2012. Library of Apicomplexan Metabolic Pathways: a manually curated database for metabolic pathways of apicomplexan parasites. *Nucleic acids research*, 41(D1), pp.D706-D713.
- Sheiner, L., Vaidya, A.B. and McFadden, G.I., 2013. The metabolic roles of the endosymbiotic organelles of *Toxoplasma* and *Plasmodium* spp. *Current opinion in microbiology*, 16(4), pp.452-458.
- Shen, B. and Sibley, L.D., 2012. The moving junction, a key portal to host cell invasion by apicomplexan parasites. *Current opinion in microbiology*, 15(4), pp.449-455.
- Sher, A., Tosh, K. and Jankovic, D., 2016. Innate recognition of *Toxoplasma gondii* in humans involves a mechanism distinct from that utilized by rodents. *Cellular & molecular immunology,* 14: 36-42.
- Sibley LD, Weidner E, Krahenbuhl JL. Phagosome acidification blocked by intracellular *Toxoplasma gondii*. *Nature* 1985; 315: 416–419.
- Sidik, S.M., Huet, D., Ganesan, S.M., Huynh, M.H., Wang, T., Nasamu, A.S., Thiru, P., Saeij, J.P., Carruthers, V.B., Niles, J.C. and Lourido, S., 2016. A genome-wide CRISPR

screen in *toxoplasma* identifies essential apicomplexan genes. *Cell*, *166*(6), pp.1423-1435.

- Sievers, F. and Higgins, D.G., 2014. Clustal Omega, accurate alignment of very large numbers of sequences. *Multiple sequence alignment methods*, pp.105-116.
- Simarro, PP, Jannin, J and Cattand, P. 2009 Eliminating human African trypanosomiasis: where do we stand and what comes next? *PLoS. Med.*, 5(2), p.e55.
- Simons, K. and Ikonen, E., 1997. Functional rafts in cell membranes. *Nature*, 387(6633), pp.569-572.
- Singh, N., Kumar, M. and Singh, R.K., 2012. Leishmaniasis: current status of available drugs and new potential drug targets. *Asian Pacific Journal of Tropical Medicine*, 5(6), pp.485-497.
- Soete, M., Camus, D. and Dubrametz, J.F., 1994. Experimental induction of bradyzoite-specific antigen expression and cyst formation by the RH strain of *Toxoplasma gondii* in vitro. *Experimental parasitology*, 78(4), pp.361-370.
- Solano-Gallego, L., Rossi, L., Scroccaro, A.M., Montarsi, F., Caldin, M., Furlanello, T. and Trotta, M., 2012. Detection of *Leishmania infantum* DNA mainly in *Rhipicephalus sanguineus* male ticks removed from dogs living in endemic areas of canine leishmaniosis. *Parasites & vectors*, 5(1), p.98.
- Soldati-Favre, D., 2008. Molecular dissection of host cell invasion by the apicomplexans: the glideosome. *Parasite*, 15(3), pp.197-205.
- Sonda, S. and Hehl, A. B. 2006. Lipid Biology of Apicomplexa: perspectives for new drug targets particularly for *Toxoplasma gondii*. *TRENDS in Paeasitology*. 22 (1): 41-47.
- Sonda, S. *et al.* 2005. Inhibitory effect of aureobasidin A on *Toxoplasma gondii*. *Antimicrob. Agent. Chemothera.,* 49 (5), pp. 1794 – 1801.
- Sotirakou, S.. and Wozniak, G., 2011. Clinical expression of autoimmune hepatitis in a nine-year-old girl with visceral leishmaniasis. *Polish Journal of Pathology*, 62(2), pp.118-119.

- Soto, J., Rea, J., Valderrama, M., Toledo, J., Valda, L., Ardiles, J. and Berman, J., 2009. Efficacy of extended (six weeks) treatment with miltefosine for mucosal leishmaniasis in Bolivia. *The American journal of tropical medicine and hygiene*, 81(3), pp.387-389.
- Spiegel, S. and Milstien, S., 2003. Sphingosine-1-phosphate: an enigmatic signalling lipid. *Nature reviews. Molecular cell biology*, 4(5), p.397.
- Sreekumar, A., Poisson, L.M., Rajendiran, T.M., Khan, A.P., Cao, Q., Yu, J., Laxman, B., Mehra, R., Lonigro, R.J., Li, Y. and Nyati, M.K., 2009. Metabolomic profiles delineate potential role for sarcosine in prostate cancer progression. *Nature*, 457(7231), p.910.
- Stuart, K., Brun, R., Croft, S., Fairlamb, A., Gürtler, R.E., McKerrow, J., Reed, S. and Tarleton, R., 2008. Kinetoplastids: related protozoan pathogens, different diseases. *The Journal of clinical investigation*, 118(4), pp.1301-1310.
- Sumpf, K., Nast, R., Downie, B., Salinas, G. and Lüder, C.G., 2017. Histone deacetylase inhibitor MS-275 augments expression of a subset of IFN-γ-regulated genes in *Toxoplasma gondii*-infected macrophages but does not improve parasite control. *Experimental Parasitology*, 180, pp.45-54.
- Sundar, S. and Olliaro, P.L., 2007. Miltefosine in the treatment of leishmaniasis: clinical evidence for informed clinical risk management. *Therapeutics and clinical risk management*, 3(5), p.733.
- Sundar, S., Jha, T.K., Thakur, C.P., Bhattacharya, S.K. and Rai, M., 2006. Oral miltefosine for the treatment of Indian visceral leishmaniasis. *Transactions of the Royal Society of Tropical Medicine and Hygiene*, 100, pp.S26-S33.
- Sundar, S., Lockwood, D.N., Agrawal, G., Rai, M., Makharia, M.K. and Murray, H.W., 2001. Treatment of Indian visceral leishmaniasis with single or daily infusions of low dose liposomal amphotericin B: randomised trialCommentary: cost and resistance remain issues. *Bmj*, 323(7310), pp.419-422.
- Suss-Toby, E., Zimmerberg, J. and Ward, G.E., 1996. *Toxoplasma* invasion: the parasitophorous vacuole is formed from host cell plasma membrane and pinches off via a fission pore. *Proceedings of the National Academy of Sciences*, 93(16), pp.8413-8418.

- Suzuki, E., Tanaka, A.K., Toledo, M.S., Levery, S.B., Straus, A.H. and Takahashi, H.K., 2008. Trypanosomatid and fungal glycolipids and sphingolipids as infectivity factors and potential targets for development of new therapeutic strategies. *Biochimica et Biophysica Acta (BBA)*, 1780(3), pp.362-369.
- Tafesse, F.G., Huitema, K., Hermansson, M., van der Poel, S., van den Dikkenberg, J., Uphoff, A., Somerharju, P. and Holthuis, J.C., 2007. Both sphingomyelin synthases SMS1 and SMS2 are required for sphingomyelin homeostasis and growth in human HeLa cells. *Journal of Biological Chemistry*, 282(24), pp.17537-17547.
- Takesako, K., Kuroda, H., Inoue, T., Haruna, F., Yoshikawa, Y., Kato, I., Uchida, K., Hiratani, T. and Yamaguchi, H., 1993. Biological properties of aureobasidin A, a cyclic depsipeptide antifungal antibiotic. *The Journal of antibiotics*, 46(9), pp.1414-1420.
- Tanowitz, H.B., Jelicks, L.A., Machado, F.S., Esper, L., Qi, X., Desruisseaux, M.S., Chua, S.C., Scherer, P.E. and Nagajyothi, F., 2011. Adipose tissue, diabetes and Chagas disease. *Advances in parasitology*, *76*, p.235.
- Tatonetti, N. P. ; Liu, T. and Altman, R. B. 2009. Predicting drug side-effects by chemical systems biology. *Genome Biology*, 10:238.
- Thomas, R.S. and Waters, M.D. eds., 2016. *Toxicogenomics in Predictive Carcinogenicity*. Royal Society of Chemistry.
- Thye, J.K., 2014. *The diverse roles of the Pseudomonas aeruginosa phospholipase PlcH and the Toxoplasma gondii serine palmitoyltransferase in sphingolipid biochemistry* (Doctoral dissertation, Durham University
- Tuon, F.F., Gomes-Silva, A., Da-Cruz, A.M., Duarte, M.I.S., Neto, V.A. and Amato, V.S., 2008. Local immunological factors associated with recurrence of mucosal leishmaniasis. *Clinical Immunology*, 128(3), pp.442-446.
- Vacaru, A.M., van den Dikkenberg, J., Ternes, P. and Holthuis, J.C., 2013. Ceramide phosphoethanolamine biosynthesis in Drosophila is mediated by a unique ethanolamine phosphotransferase in the Golgi lumen. *Journal of Biological Chemistry*, *288*(16), pp.11520-11530.

- van Dooren, G.G. and Striepen, B., 2013. The algal past and parasite present of the apicoplast. *Annual review of microbiology,* 67, pp.271-289.
- Van Meer, G., Voelker, D.R. and Feigenson, G.W., 2008. Membrane lipids: where they are and how they behave. *Nature reviews. Molecular cell biology*, 9(2), p.112.
- Vermelho, A.B., Capaci, G.R., Rodrigues, I.A., Cardoso, V.S., Mazotto, A.M. and Supuran, C.T., 2017. Carbonic anhydrases from *Trypanosoma* and *Leishmania* as anti-protozoan drug targets. *Bioorganic & Medicinal Chemistry*. 25 (5): 1543-1555.
- Villas-Bôas, S.G., Rasmussen, S. and Lane, G.A., 2005. Metabolomics or metabolite profiles?. *TRENDS in Biotechnology*, 23(8), p.385.
- Vinayak, S., Pawlowic, M.C., Sateriale, A., Brooks, C.F., Studstill, C.J., Bar-Peled, Y., Cipriano, M.J. and Striepen, B., 2015. Genetic modification of the diarrhoeal pathogen *Cryptosporidium parvum*. *Nature*, 523(7561), pp.477-480.
- Vincent, I.M. and Barrett, M.P., 2015. Metabolomic-based strategies for anti-parasite drug discovery. *Journal of biomolecular screening,* 20*(1),* pp.44-55.
- Vincent, I.M., Weidt, S., Rivas, L., Burgess, K., Smith, T.K. and Ouellette, M., 2014. Untargeted metabolomic analysis of miltefosine action in Leishmania infantum reveals changes to the internal lipid metabolism. *International Journal for Parasitology: Drugs and Drug Resistance*, 4(1), pp.20-27.
- Vyas, S.P. and Gupta, S., 2006. Optimizing efficacy of amphotericin B through nanomodification. *International journal of nanomedicine*, 1(4), p.417.
- Wakeman, K.C., Heintzelman, M.B. and Leander, B.S., 2014. Comparative ultrastructure and molecular phylogeny of Selenidium melongena n. sp. and S. terebellae Ray 1930 demonstrate niche partitioning in marine gregarine parasites (apicomplexa). *Protist*, 165(4), pp.493-511.
- Wang, J.L., Huang, S.Y., Behnke, M.S., Chen, K., Shen, B. and Zhu, X.Q., 2016. The past, present, and future of genetic manipulation in *Toxoplasma gondii. Trends in parasitology*, 32(7), pp.542-553.

- Wasmuth, J., Daub, J., Peregrín-Alvarez, J.M., Finney, C.A. and Parkinson, J., 2009. The origins of apicomplexan sequence innovation. *Genome research*, 19(7), pp.1202-1213.
- Wedsworth, J. M.; Clarke, D. J.; McMahon, S. A.; Lowther, J. P.; Beattie, A. E.; Langridge-Smith, P. R. R.; Broughton, H. B.; Dunn, T. M.; Naismith, J. H.; and Campopiano, D. J. 2013. The Chemical Basis of Serine Palmitoyltransferase Inhibition by Myriocin. *J. Am. Chem. Soc.* 135, pp.14276−14285.
- Weiss, L.M. and Kim, K., 2000. The development and biology of bradyzoites of *Toxoplasma gondii.* Frontiers in bioscience: a journal and virtual library, 5, p.D391.
- Weiss, L.M. and Kim, K., 2007. Bradyzoite development. In *Toxoplasma gondii*. Elsevier Ltd.
- Weiss, L.M., Fiser, A., Angeletti, R.H. and Kim, K., 2009. *Toxoplasma gondii* proteomics. *Expert review of proteomics*, 6(3), pp.303-313.
- Welter, B.H., Goldston, A.M. and Temesvari, L.A., 2011. Localisation to lipid rafts correlates with increased function of the Gal/GalNAc lectin in the human protozoan parasite, *Entamoeba histolytica*. *International journal for parasitology*, 41(13), pp.1409-1419.
- Welti, R., Mui, E., Sparks, A., Wernimont, S., Isaac, G., Kirisits, M., Roth, M., Roberts, C., Bott'e, C., Mar\'echal, E. and others, 2007. Lipidomic analysis of *Toxoplasma gondii* reveals unusual polar lipids. *Biochemistry*, 46(48):13882--13890.
- WHO (2012) World Malaria Report 2012. Geneva, Switzerland: World Health Organisation.
- Willger, S.D., Grahl, N., Willger, S.D., Grahl, N. and Cramer Jr, R.A., 2009. *Aspergillus fumigatus* metabolism: clues to mechanisms of in vivo fungal growth and virulence. *Medical mycology*, *47*, pp.S72-S79.
- William, J., Sullivan J. and Jeffers, V. 2012. Mechanisms of *Toxoplasma gondii* persistence and latency. *FEMS Microbiol Rev 36:* 717–733.

- Woodhall, D., Jones, J.L., Cantey, P.T., Wilkins, P.P. and Montgomery, S.P., 2014. Neglected parasitic infections: what every family physician needs to know. *American family physician*, 89(10), pp. 803-811.
- Wright, M.M., Howe, A.G. and Zaremberg, V., 2004. Cell membranes and apoptosis: role of cardiolipin, phosphatidylcholine, and anticancer lipid analogues. *Biochemistry and cell biology*, 82(1), pp.18-26.
- Wuts, P.G., Simons, L.J., Metzger, B.P., Sterling, R.C., Slightom, J.L. and Elhammer, A.P., 2015. Generation of broad-spectrum antifungal drug candidates from the natural product compound aureobasidin A. *ACS medicinal chemistry letters*, 6(6), pp.645-649.
- Xynos, I.D., Tektonidou, M.G., Pikazis, D. and Sipsas, N.V., 2009. Leishmaniasis, autoimmune rheumatic disease, and anti–tumor necrosis factor therapy, Europe. *Emerging infectious diseases*, 15(6), p.956.
- Yan, Y., Orcutt, S.J. and Strickler, J.E., 2009. The use of SUMO as a fusion system for protein expression and purification. *Chemistry Today*, 27(6), pp.42-47.
- Yard, B.A., Carter, L.G., Johnson, K.A., Overton, I.M., Dorward, M., Liu, H., McMahon, S.A., Oke, M., Puech, D., Barton, G.J. and Naismith, J.H., 2007. The structure of serine palmitoyltransferase; gateway to sphingolipid biosynthesis. *Journal of molecular biology*, 370(5), pp.870-886.
- Yolken, R.H., Dickerson, F.B. and Fuller Torrey, E., 2009. *Toxoplasma* and schizophrenia. *Parasite immunology*, 31(11), pp.706-715.
- Young, S.A., Mina, J.G., Denny, P.W. and Smith, T.K., 2012. Sphingolipid and ceramide homeostasis: potential therapeutic targets. *Biochemistry research international*, 2012, pp.1-12.
- Zhang, K., Bangs, J.D. and Beverley, S.M., 2010. Sphingolipids in parasitic protozoa. *Sphingolipids as Signaling and Regulatory Molecules*, pp.238-248.
- Zhang, K., Hsu, F.F., Scott, D.A., Docampo, R., Turk, J. and Beverley, S.M., 2005. *Leishmania* salvage and remodelling of host sphingolipids in amastigote survival and acidocalcisome biogenesis. *Molecular microbiology*, 55(5), pp.1566-1578.

- Zhang, K., Showalter, M., Revollo, J., Hsu, F.F., Turk, J. and Beverley, S.M., 2003. Sphingolipids are essential for differentiation but not growth in *Leishmania*. *The EMBO journal*, 22(22), pp.6016-6026.
- Zhang, O., Wilson, M.C., Xu, W., Hsu, F.F., Turk, J., Kuhlmann, F.M., Wang, Y., Soong, L., Key, P., Beverley, S.M. and Zhang, K., 2009. Degradation of host sphingomyelin is essential for *Leishmania* virulence. *PLoS Pathog*, 5(12), p.e1000692.
- Zhong, W., Jeffries, M.W. and Georgopapadakou, N.H., 2000. Inhibition of Inositol Phosphorylceramide Synthase by Aureobasidin A in Candida and *Aspergillus* Species. *Antimicrobial agents and chemotherapy*, 44(3), pp.651-653.

Appendices

Research publication

SPECIAL ISSUE ARTICLE

The antifungal Aureobasidin A and an analogue are active against the protozoan parasite *Toxoplasma gondii* but do not inhibit sphingolipid biosynthesis

A. Q. I. ALQAISI[1,2], A. J. MBEKEANI[1], M. BASSAS LLORENS[1], A. P. ELHAMMER[3] *and* P. W. DENNY[1]*

[1] *Department of Biosciences, Lower Mountjoy, Stockton Road, Durham DH1 3LE, UK*
[2] *Biology Department, College of Science, University of Baghdad, Baghdad, Iraq*
[3] *Aureogen Biosciences Inc, 4717 Campus Drive Suite 2300,Kalamazoo, MI 49008, USA*

(*Received 7 February 2017; revised 17 March 2017; accepted 23 March 2017*)

SUMMARY

Toxoplasma gondii is an obligate intracellular protozoan parasite of the phylum Apicomplexa, and toxoplasmosis is an important disease of both humans and economically important animals. With a limited array of drugs available there is a need to identify new therapeutic compounds. Aureobasidin A (AbA) is an antifungal that targets the essential inositol phosphorylceramide (IPC, sphingolipid) synthase in pathogenic fungi. This natural cyclic depsipeptide also inhibits *Toxoplasma* proliforation, with the protozoan IPC synthase orthologue proposed as the target. The data presented here show that neither AbA nor an analogue (Compound 20), target the protozoan IPC synthase orthologue or total parasite sphingolipid synthesis. However, further analyses confirm that AbA exhibits significant activity against the proliferative tachyzoite form of *Toxoplasma*, and Compound 20, whilst effective, has reduced efficacy. This difference was more evident on analyses of the direct effect of these compounds against isolated *Toxoplasma*, indicating that AbA is rapidly microbicidal. Importantly, the possibility of targeting the encysted, bradyzoite, form of the parasite with AbA and Compound 20 was demonstrated, indicating that this class of compounds may provide the basis for the first effective treatment for chronic toxoplasmosis.

Key words: *Toxoplasma*, sphingolipid biosynthesis, Aureobasidin A, bradyzoite.

INTRODUCTION

Aureobasidin A (AbA; Fig. 1) is a cyclic depsipeptide antifungal antibiotic isolated from the fungus *Aureobasidium pullulans* R106 (Ikai *et al.* 1991; Takesako *et al.* 1991). Resistance in *Saccharomycin cerevisiae* was found to be conferred by dominant negative mutations in the Aureobasidin resistance (AUR1) gene (Heidler and Radding, 1995). Subsequently, AUR1 was identified as encoding the essential inositol phosphorylceramide (IPC) synthase activity in fungi (Nagiec *et al.* 1997). AbA has been shown to be an irreversible inhibitor of the *S. cerevisiae* IPC synthase, acting in a time dependant manner (Aeed *et al.* 2009), with the toxic effects associated with both a build up of the bioactive substrate ceramide and the deprivation of IPC (Cerantola *et al.* 2009). Recent efforts have utilized a semi-synthetic approach to generate analogues of AbA which demonstrate improved activity against some pathogenic fungal species, for example *Aspirgillus fumigatus* (Wuts *et al.* 2015).

IPC is an essential sphingolipid found in fungi, plants and some protozoa (Young *et al.* 2012). In contrast, mammals lack IPC and instead synthesize sphingomyelin (SM) as their major sphingolipid species using SM synthase (Huitema *et al.* 2004). Complex sphingolipids, such as IPC and SM, are major components of the outer leaflet of eukaryotic plasma membranes that are thought to be involved, together with sterols, in the formation of microdomains known as lipid rafts. These rafts have been proposed to function in a diverse array of processes from the polarised trafficking of lipid-modified proteins, to the assembly and activation of signal transduction complexes (Simons and Ikonen, 1997). The non-mammalian nature of IPC synthase makes it an attractive drug target, and it has been validated as such in both the pathogenic fungi and the kinetoplastid protozoa (Georgopapadakou, 2000; Hanada, 2005; Mina *et al.* 2009, 2010).

Toxoplasma gondii is an obligate, intracellular protozoan parasite, able to invade and colonize a wide variety of nucleated vertebrate cells. It is a member of the Apicomplexa, a diverse phylum

* Corresponding author. Department of Biosciences, Biophysical Sciences Institute, Lower Mountjoy, Stockton Road, Durham DH1 3LE, UK. E-mail: p.w.denny@durham.ac.uk

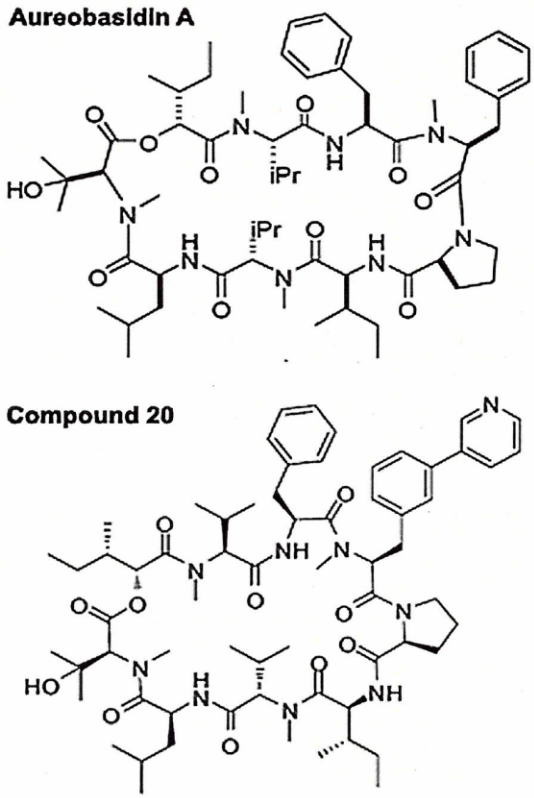

Fig. 1. The structures of the cyclic depsipeptide compounds Aureobasidin A and its analogue Compound 20 (Wuts *et al.* 2015).

including important pathogens of domestic animals and humans such as *Eimeria* (the etiological agent of coccidiosis in poultry), *Theileria* (East Coast Fever in Cattle), *Cryptosporidium* (diarrhoea) and *Plasmodium* (malaria). In common with other apicomplexans *Toxoplasma* has a complex lifecycle, involving a definitive, feline, host; and both rapidly proliferative, tachyzoite forms (all tissues in acute disease) and slowly dividing, bradyzoite forms (muscle and brain tissue cysts in chronic disease) (Dubey, 1977). *Toxoplasma* is an opportunistic pathogen and is a significant cause of disease (toxoplasmosis) in the immunocompromised: particularly organ transplant recipients, those receiving anticancer chemotherapy and AIDS patients (Chowdhury, 1986). *In utero* toxoplasmosis is also a significant cause of congenital defects in humans (Chowdhury, 1986) and spontaneous abortion in economically important domestic animals (Dubey, 1977). The diseases listed above are associated with rapidly dividing, tachyzoite *Toxoplasma,* either directly acquired or the result of the reactivation of a chronic infection. However, in addition, bradyzoite, chronic, toxoplasmosis has been associated with psychiatric disorders, including schizophrenia (Webster *et al.* 2013). The drugs available for acute toxoplasmosis (tachyzoite stage) have various problems with efficacy and safety, furthermore no treatments are available for chronic disease (encysted bradyzoite stage) therefore new therapies are urgently required (Antczak *et al.* 2016).

The synthesis of IPC by *Toxoplasma* was first reported on the basis of metabolic labelling experiments (Sonda *et al.* 2005) and subsequently confirmed using directed mass spectrometry (Pratt *et al.* 2013). In addition, inhibition of parasite IPC synthesis by AbA was indicated and the tractability of this natural compound as a new lead proposed (Sonda *et al.* 2005; Coppens, 2013). Utilising AbA and the availability of a well characterized orthologue with improved pharmacokinetic properties, Compound 20 (Fig. 1, modified with a pyridyl group at AbA position 4; Wuts *et al.* 2015), here we examine the effect of these compounds on the *Toxoplasma* AUR1 orthologue (*Tg*SLS; (Pratt *et al.* 2013) and total sphingolipid biosynthesis; and on the proliferation of both tachyzoite and bradyzoite form parasites. The results demonstrate that whilst both compounds inhibit the proliferation of *Toxoplasma*, neither inhibits *Tg*SLS nor total sphingolipid biosynthesis as previously proposed (Sonda *et al.* 2005; Coppens, 2013). However, despite uncertainty regarding the mode of action, the ability of this class of cyclic depsipeptides to clear encysted bradyzoite-like form *Toxoplasma* from infected tissue culture cells marks them as a possibly unique therapy for chronic toxoplasmosis.

MATERIALS AND METHODS

Cell culture

Toxoplasma gondii (strains RH-TATi-1 (Meissner *et al.* 2002), RH-HX-KO-YFP2-DHFR (Gubbels *et al.* 2003) and Pru-GRA2-GFP-DHFR (Kim *et al.* 2007) were maintained in Vero, Human Foreskin Fibroblast (HFF) or Chinese Hamster Ovary (CHO) cells grown in DMEM (Invitrogen) supplemented with 10% fetal bovine serum (FBS) at 37 °C and 5% CO_2. Type II *Toxoplasma* (Pru strain) tachyzoites were differentiated to the bradyzoite-like form in HFF cells via an alkaline shift to pH8 as previously described (Soete *et al.* 1994).

Metabolic labelling

Saccharomoyces cerevisiae and Vero cells were labelled with 5 μM of NBD C_6-ceramide complexed with Bovine Serum Albumin (BSA) (Invitrogen) for use as controls as previously (Denny *et al.* 2006). *Toxoplasma* tachyzoites were separated from host cell material by filtration through 3 and 5 mm polycarbonate filters (Millipore) after disruption by passage through a narrow gauge needle. Released parasites were then isolated by centrifugation at

1430 ***g*** for 15 min at room temperature, washed and resuspended in serum-free DMEM (Invitrogen) at 10^7 mL^{-1} and incubated for 1 h at 37 °C before the addition of NBD C_6-ceramide complexed with BSA to 5 μM, and a further 1 h at 37 °C. For the inhibitor studies, AbA or Compound 20 were added to isolated *Toxoplasma* at 10 μg mL^{-1} and incubated at 37 °C for 1, 4 or 7 h, before the addition of NBD C_6-ceramide complexed with BSA to 5 μM and a further incubation at 37 °C for 1 h. Lipids were extracted and analysed by HPTLC as previously described (Mina *et al.* 2009).

Toxoplasma susceptibility assay

HFF cells were seeded at 10^4 cells per well in 96 well microtitre plates (Nunc). After 18 h at 37 °C isolated *Toxoplasma* RH-HX-KO-YFP2-DHFR (Gubbels *et al.* 2003) were inoculated into the host cells at 6250 parasites per well. Following a further 20 h incubation compounds were added at the appropriate concentrations. In an additional experiment, isolated tachyzoite parasites were pre-treated with compounds for 2 and 8 h, then washed, prior to infection of HFF cells. For bradyzoite assays, the *Toxoplasma* Pru-GRA2-GFP-DHFR (Kim *et al.* 2007) tachyzoites were added at the same concentration but then transformed as described (Soete *et al.* 1994) before the addition of the compounds. Plates were washed after 2 or 8 h, or not, as described in text. The plates were read using a Biotek Synergy H4 plate reader (Ex 510 nm; Em 540 nm) after 6 or 3 days, respectively.

Yeast susceptibility assay

YPH499-HIS-GAL-AUR1 (a yeast strain in which expression of the essential IPC synthase, AUR1p, is under the control of a galactose promoter) complemented with *Tg*SLS or AUR1 (Denny *et al.* 2006; Pratt *et al.* 2013) were assayed for susceptibility to AbA and Compound 20. The transgenic yeast strains were maintained on SD -HIS -URA agar (0·17% Bacto yeast nitrogen base, 0·5% ammonium sulphate, 2% glucose, containing the appropriate nutritional supplements) at 30 °C. To analyse susceptibility to AbA and Compound 20 plates containing 5 or 10 μg mL^{-1} of the compound were prepared and 10 μL of an aqueous suspension of yeast spotted onto the surface before incubation at 30 °C.

Transcript analyses

For the mRNA analyses, total RNA from equivalent numbers of CHO cells infected for 72 h with *Toxoplasma* RH-TATi parasites, or non-infected, was extracted using the RNeasy kit (Qiagen) according to the manufacturer's protocol. Following DNase treatment (RQ1, Promega) cDNA was synthesized using the ImProm-II Reverse Transcription System (Promega) according to manufacturer's protocol. Quantitative PCR (qPCR) was performed in a RotorGene® RG3000 (Corbett Research) using SYBR Green Jump-Start Taq Ready Mix (Sigma Aldrich) according to the manufacturer's instructions. The hamster, *Cricetulus griseus*, *CgLcb2* (encoding subunit 2 of SPT) was amplified using the primer pair – 5′CAGACAACTTTGTTTTCGG3′ and 5′GGGTGGCATTGTAGGGC3′. The reference gene, *CgβTub*, was amplified using the primer pair – 5′TAAAACGACGGCCAG*TG*AGC3′ and 5′TCT CC*TG*GCGAG*TG*C*TG*C3′. The qPCR was carried out in triplicate on 3 replicates with an annealing temperature 55°C for *CgLcb2* and *CgβTub*.

RESULTS

Comparing the effect of AbA and its analogue Compound 20 on the proliferation of the Toxoplasma tachyzoite form

AbA has previously been shown to inhibit the proliferation of the rapidly dividing, tachyzoite form of *Toxoplasma*. The effective concentration of compound reducing proliferation by 50% (ED_{50}) was calculated as 0·3 μg mL^{-1} by cell counting 48 h post infection and 46 h post addition of AbA (Sonda *et al.* 2005). In order to gain a more rapid and robust dataset to facilitate comparative analyses of the efficacy of AbA and Compound 20 we utilised the availability of the yellow fluorescent protein labelled *Toxoplasma*, RH-strain (Gubbels *et al.* 2003). Gubbels *et al.* demonstrated the tractability of this system by comparison with β-galactosidase producing parasites. Following validation and parameter setting (data not shown), HFF cells were plated onto 96-well plates and infected with 6250 *Toxoplasma* per well as described in the section Materials and Methods. After 20 h the compounds were added and, without washing, the plate incubated for 144 h (6 days) before fluorescent readings were taken. Following data analyses the ED_{50} was calculated as described (Fig. 2). As can been seen both AbA and Compound 20 showed activity against *Toxoplasma* RH tachyzoites. However, the parent compound (ED_{50} of 0·75, 95% CI 0·60 to 0·93 μg mL^{-1}) was slightly more efficacious than its derivative (ED_{50} of 1·49, 95% CI 1·20 to 1·85 μg mL^{-1}). This differential activity was even more evident on further analyses. Previously, using an indirect assay (vacuole formation), it has been indicated that the efficacy of AbA against *Toxoplasma* is partially reversible after 24, but not 48 h, exposure (Sonda *et al.* 2005). To further analyse the reversibility of the efficacy of cyclic depsipeptides, the infected HFF cells were washed following 2 and 8 h of compound treatment and proliferation then followed for 6 days as previously (Fig. 2). In

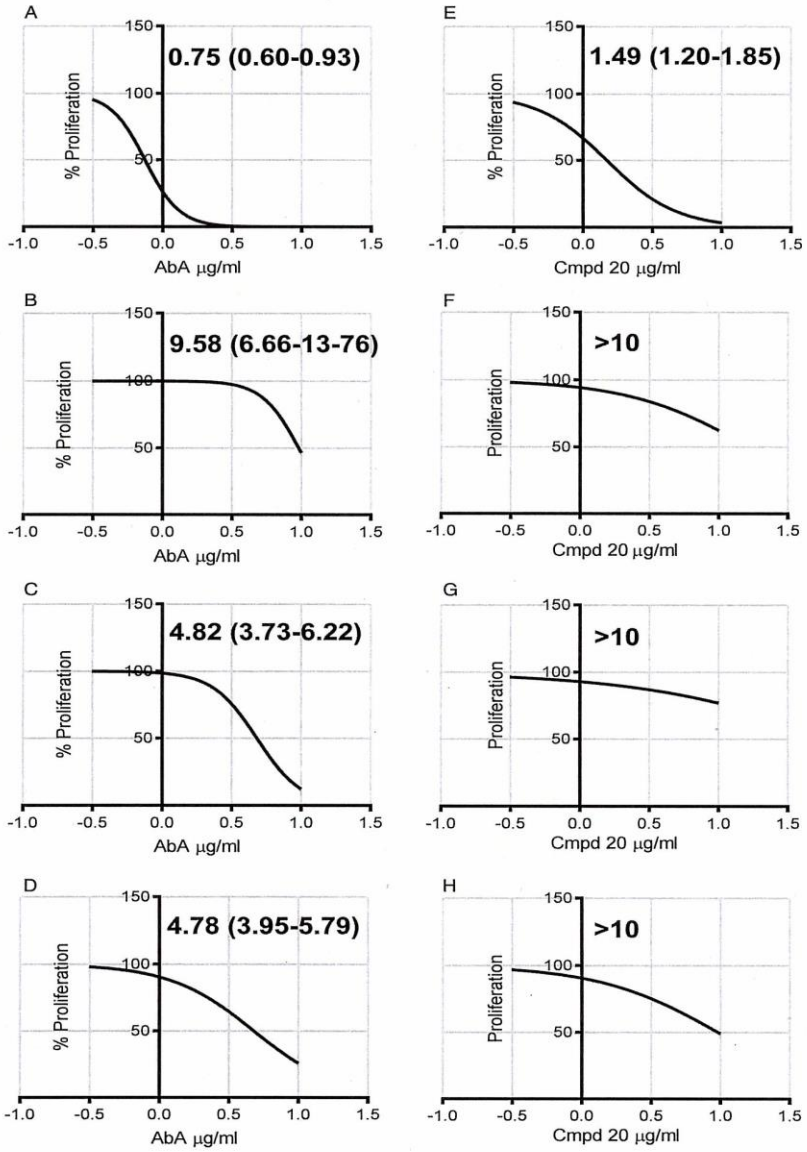

Fig. 2. ED_{50} of Aureobasidin A (AbA, A-D) or Compound 20 (Cpmd 20, E-H) – $\mu g\ mL^{-1}$; (95% Confidence Interval) – against the Toxoplasma RH tachyzoite form in HFF cells. 6 days post addition of the compounds. In agreement with Sonda *et al.* (2005), both compounds were non-toxic to HHF cells under the conditions employed. A and B: no wash out post-compound addition; C and D: wash out 2 h post-compound addition; E and F: wash out 8 h post-compound addition; G and H: 2 h pre-treatment of isolated parasites pre-infection. Calculated using GraphPad Prism 7, log (inhibitor) *vs* normalized response – Variable slope. $>10\ \mu g\ mL^{-1}$ – ED_{50} could not be determined. Representative in triplicate dataset.

keeping with Sonda *et al.* (2005) efficacy was partially reversible, but *Toxoplasma* were clearly susceptible to AbA in an 8 h treatment (ED_{50} of 4·82, 95% CI 3·73 to 6·22 $\mu g\ mL^{-1}$), and even 2 h exposure demonstrated some activity (ED_{50} of 9·58, 95% CI 6·66 to 13·76 $\mu g\ mL^{-1}$). However, in contrast, the activity of Compound 20 was demonstrated to be almost completely reversible under the conditions employed.

Interestingly, the unrelated kinetoplastid protozoa, *Trypanosoma cruzi* (the causative agent of American Trypanosomiasis or Chagas disease) has

also been shown to be sensitive to AbA, with the IPC synthase again proposed as the target (Salto *et al.* 2003). However, enzyme analyses did not confirm this and it was suggested that the compound acts on the host to promote clearance of the parasite (Figueiredo *et al.* 2005). In order to test this hypothesis in *Toxoplasma* infection, tachyzoite parasites were isolated from infected cells as described in the section Materials and Methods and then treated with various concentrations of AbA and Compound 20 prior to washing and infecting host HFF cells. A 2 h treatment again demonstrated that AbA was effective (ED_{50} of 4·78, 95% CI 3·95 to 5·79 $\mu g\ mL^{-1}$), whilst the analogue was inactive (Fig. 2). Longer periods post-isolation (8 h) lead to untreated parasites losing infectivity.

The sensitivity of the Toxoplasma gondii sphingolipid synthase and sphingolipid synthesis per se to AbA and its analogue Compound 20

Host sphingolipid biosynthesis is unaffected by (Fig. S1) and non-essential for (Pratt *et al.* 2013; Romano *et al.* 2013), *Toxoplasma* proliferation. Therefore, *de novo* synthesis of sphingolipids is an attractive target for new antiprotozoal drug leads. The antifungal sphingolipid (IPC) synthase inhibitor AbA has been proposed to inhibit the *Toxoplasma* orthologue (Sonda *et al.* 2005; Coppens, 2013). However, analyses of an enzyme isolated from *Toxoplasma* demonstrating IPC synthase activity (*Tg*SLS) did not support this conclusion (Pratt *et al.* 2013). Utilizing the previously constructed, auxotropic, *Tg*SLS complemented yeast strains (YPH499-HIS-GAL-AUR1 pRS426 *Tg*SLS, with YPH499-HIS-GAL-AUR1 pRS426 AUR1 as a control), the sensitivity of the protozoan enzyme to AbA and Compound 20 was analysed (Fig. 3). The results clearly demonstrated that the *Toxoplasma* enzyme conferred resistance to yeast against both cyclic depsipeptides at concentrations lethal to yeast reliant on AUR1 activity (5 and 10 $\mu g\ mL^{-1}$). However, whilst *Tg*SLS clearly functions as an IPC synthase in yeast and *in vitro*, *Toxoplasma* have also been demonstrated, by the incorporation of tritiated serine, to synthesize sphingomyelin (SM) and glycosphingolipids (GSLs) (Gerold and Schwarz, 2001). The presence of SM and GSLs in isolated *Toxoplasma* was subsequently confirmed using mass spectrometry (Welti *et al.* 2007; Pratt *et al.* 2013). In addition, relatively high levels of ethanolamine phosphorylceramide (EPC), a non-abundant species in mammalian cells, were also reported (Welti *et al.* 2007; Pratt *et al.* 2013). In light of this synthetic complexity, and the potential of enzymatic diversity, the effect of AbA and Compound 20 on total sphingolipid biosynthesis in *Toxoplasma* was investigated. Labelling isolated *Toxoplasma* with NBD-C_6-ceramide as described in the section Materials and Methods demonstrated that the parasite synthesized a complex of sphingolipid species, including SM and EPC (co-migrating with mammalian equivalents; Vacaru *et al.* 2013). However, IPC was not evident and 2 other species (X and Y) remain unassigned (Fig. 4). The addition of AbA and Compound 20 at 10 $\mu g\ mL^{-1}$ for 1, 4 and 7 h, before 1 h NBD-C_6-ceramide labelling, had no effect on the synthesis of the sphingolipids compared with controls (Fig. 5). This demonstrated that this class of cyclic depsipeptides do not exert their activity through inhibition or dysregulation of sphingolipid biosynthesis. However, it is notable that the complex sphingolipid profile produced does change as the time post parasite isolation increases, with the levels of labelled lipids X and Y increased at 4 and 7 h, EPC levels decreased and SM levels unchanged (Fig. 5). This indicated that the stress of isolation from the host cell leads to the modification sphingolipid biosynthesis or to catabolism.

Comparing the efficacy of AbA and its analogue Compound 20 against the encysted Toxoplasma bradyzoite form

With a complete lack of treatments available for chronic disease, in which *Toxoplasma* has reached the encysted bradyzoite stage, new therapies are urgently needed (Antczak *et al.* 2016). Therefore, although the mode of action of the cyclic depsipeptides remains unclear, the efficacy of these compounds against the encysted form of the parasite was analysed. Utilizing the Type II Pru strain of *Toxoplasma* modified to express GFP (Kim *et al.* 2007) we analysed the efficacy of AbA and Compound 20 against HFF cells infected with parasites transformed into a bradyzoite-like stage using an established protocol (Soete *et al.* 1994). Following 3 days of exposure, both compounds demonstrated promising activity against the encysted *Toxoplasma* (Fig. 6), again AbA demonstrated slightly higher efficacy (ED_{50} of 2·51, 95% CI 1·96 to 3·23 $\mu g\ mL^{-1}$) than Compound 20 (ED_{50} of 3·74, 95% CI 3·13 to 4·47 $\mu g\ mL^{-1}$). This showed that the cyclic depsipeptides may represent promising candidates for therapies to treat both acute and chronic toxoplasmosis.

DISCUSSION

Toxoplasma is an important cause of disease in humans and domestic animals. Whilst there are several drugs available to treat acute (tachyzoite stage) toxoplasmosis, there is a complete absence of effective therapies for chronic disease (encysted bradyzoite stage; Antczak *et al.* 2016). It has been demonstrated that *Toxoplasma* remain able to replicate in CHO cells where the activity of the first and rate limiting step in sphingolipid biosythesis, serine

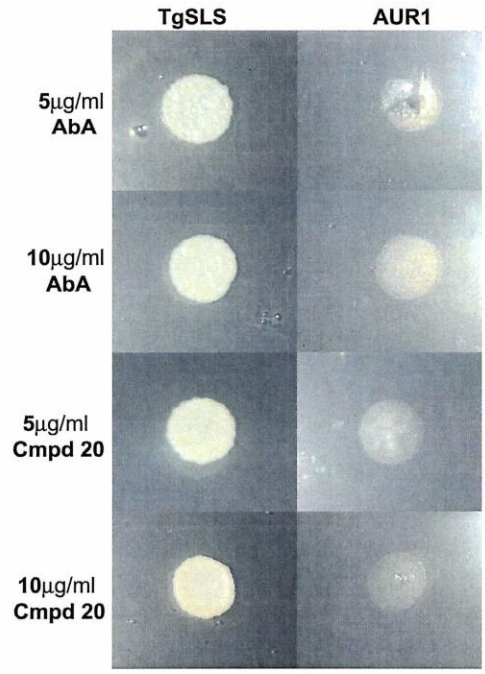

Fig. 3. Yeast dependent on the expression of the Toxoplasma AUR1p orthologue *Tg*SLS (YPH499-HIS-GAL-AUR1 pRS426 *Tg*SLS) are resistant to Aureobasidin A (AbA) and Compound 20 (Cmpd 20) at 5 and 10 μg mL^{-1}. This contrasts to the sensitivity of yeast dependent on AUR1 expression (YPH499-HIS-GAL-AUR1 pRS426 AUR1).

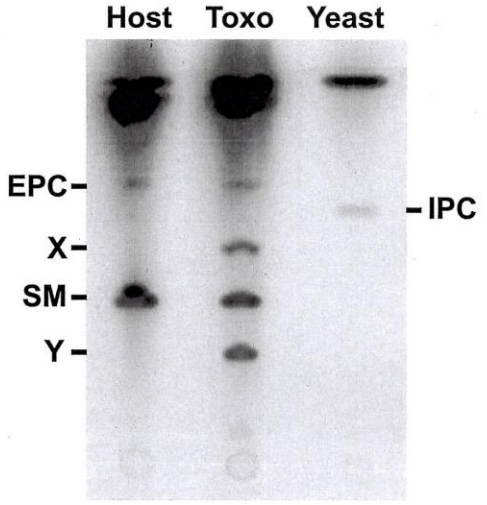

Fig. 4. Vero cells (Host), isolated *Toxoplasma* tachyzoites (Toxo) and *Saccharomyces cerevisiae* (Yeast), labelled for 1 h with NBD-C6-ceramide and complex sphingolipids then fractionated by HPTLC. Like the host cells, Toxoplasma parasites synthesize sphingomyelin (SM) and ethanolamine phosphorylceramide (EPC), two unique sphingolipids are also produced (X and Y). However, unlike in *S. cerevisiae*, no labelled inositol phosphorylceramide (IPC) is evident from either host or *Toxoplasma* cells. Representative dataset.

palmitoyltransferase (SPT), was greatly reduced and complex sphinglipid levels consequently lowered (Hanada *et al.* 1992; Pratt *et al.* 2013). In addition, in this study we showed that key enzymes in host (CHO) sphingolipid biosynthesis are unaffected by *Toxoplasma* infection (Fig. S1). Together, these data indicated that targeting the *de novo Toxoplasma* sphingolipid biosynthetic pathway could represent a viable strategy towards the identification of new antiprotozoals. A strategy that could also be applicable to other apicomplexan parasites such as *Plasmodium* spp. (Lauer *et al.* 1995), and one that has is already being investigated for kinetoplastid protozoan pathogens (Denny *et al.* 2006; Mina *et al.* 2009, 2010, 2011).

To these ends it has been suggested that the antifungal cyclic depsipeptide, AbA exerts its effect on *Toxoplasma* by inhibiting a sphinglipid (IPC) synthase, an orthologue of its validated target in yeast (Nagiec *et al.* 1997; Sonda *et al.* 2005). Given the status of the fungal and kinetoplastid IPC synthases as promising drug targets (Young *et al.* 2012), the identification of the *Toxoplasma* orthologue (Pratt *et al.* 2013) led to its consideration as a target for anti-apicomplexan drugs. *Tg*SLS functions as an IPC synthase and the product was identified in parasite extracts using directed mass spectrometry. However, AbA was demonstrated to be non-active against the enzyme activity *in vitro* (Pratt *et al.* 2013).

To investigate this compound class further, here we utilized the availability of AbA and a synthetically modified analogue, Compound 20 (Wuts *et al.* 2015), to test the efficacy and mode of action of these cyclic depsipeptides against *Toxoplasma*. As expected, neither compound inhibited the growth of transgenic yeast dependent on the expression of *Tg*SLS (Fig. 3). Furthermore, the compounds also exhibited no effect on the synthesis of complex sphingolipids in *Toxoplasma* (Fig. 5). Interestingly, no IPC synthesis was apparent indicating that this activity may be low, in tachyzoites at least. However, both SM and EPC (Azzouz *et al.* 2002; Welti *et al.* 2007) were clearly produced, as well as 2 uncharacterised complex sphingolipids (Fig. 4). However, despite this lack of dysregulation of sphingolipid biosythesis, both AbA and Compound 20 are active against the tachyzoite form of the parasite in infected HHF cells. AbA exhibited greater efficacy and, unlike Compound 20, demonstrated a rapid and direct 'cidal activity against the *Toxoplasma* parasite (Fig. 2). Furthermore, and importantly, both AbA and Compound 20 clear encysted bradyzoite-like

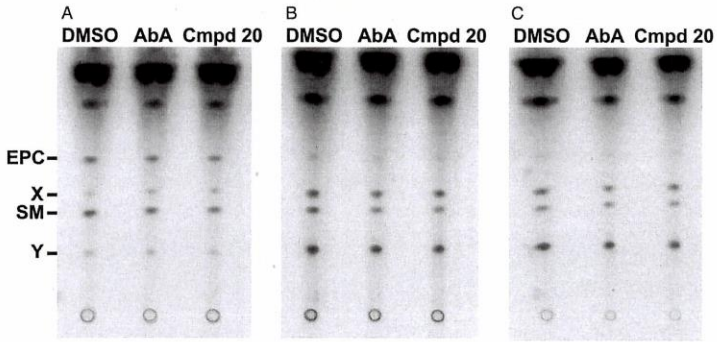

Fig. 5. Isolated *Toxoplasma* tachyzoites treated with Aureobasidin A (AbA) and Compound 20 (Cmpd 20) at 10 μg mL^{-1} for 1 (A), 4 (B) and 7 (C) hours before labelling with NBD-C6-ceramide for 1 h. Neither compound affected the complex sphingolipid profile synthesized at any time point when compared with the vehicle control (DMSO). SM – Sphingomyelin (SM); EPC – Ethanolamine PhosphorylCeramide; X and Y – Unclassified sphingolipids. Representative dataset.

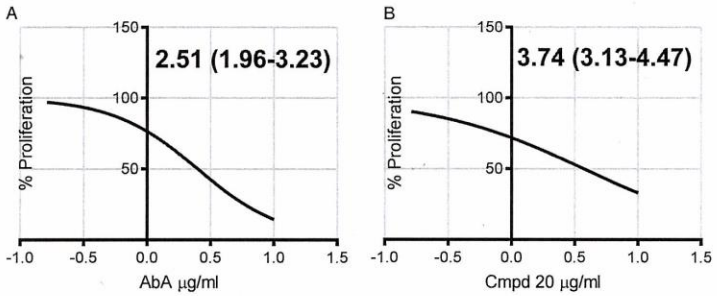

Fig. 6. ED_{50} of Aureobasidin A (A, AbA) or Compound 20 (B, Cpmd 20) – μg mL^{-1} (95% Confidence Interval) – against the Toxoplasma Pru bradyzoite form in Human Foreskin Fibroblast (HFF) cells. Three days post addition of the compounds. In agreement with Sonda *et al.* (2005), both compounds were non-toxic to HHF cells under the conditions employed. Calculated using GraphPad Prism 7, log(inhibitor) *vs* normalized response – Variable slope. Representative in triplicate dataset.

form *Toxoplasma* from infected tissue culture at low concentrations (Fig. 6). Given the well established lack of toxicity of these compounds to mammalian cells, coupled with the promising pharmacokinetic properties of Compound 20 (Wuts *et al.* 2015), this class of cyclic depsipeptides may form the basis of a unique therapy for chronic toxoplasmosis and perhaps, some psychiatric disorders.

SUPPLEMENTARY MATERIAL

To view supplementary material for this article, please visit https://doi.org/10.1017/S0031182017000506.

ACKNOWLEDGMENTS

We thank Ian Edwards (Durham University) for technical support and John Mina for helpful discussions. We are also indebted to Dominique Soldati-Favre (University of Geneva), Markus Meissner (University of Glasgow) and Boris Striepen (University of Georgia) for provision of the cell lines utilized and Aureogen Inc for providing the compounds.

FINANCIAL SUPPORT

This work was supported by the Biotechnology and Biological Research Council (BB/M024156/1 to PWD). AQIA was funded by the Government of Iraq. AJM and MBL were funded by BBSRC Impact and NPRONET awards to PWD.

REFERENCES

Aeed, P. A., Young, C. L., Nagiec, M. M. and Elhammer, A. P. (2009). Inhibition of inositol phosphorylceramide synthase by the cyclic peptide Aureobasidin A. *Antimicrobial Agents and Chemotherapy* **53**, 496–504.

Antczak, M., Dzitko, K. and Dlugonska, H. (2016). Human toxoplasmosis-Searching for novel chemotherapeutics. *Biomedicine and Pharmacotherapy* **82**, 677–684.

Azzouz, N., Rauscher, B., Gerold, P., Cesbron-Delauw, M. F., Dubremetz, J. F. and Schwarz, R. T. (2002). Evidence for *de novo* sphingolipid biosynthesis in *Toxoplasma gondii*. *International Journal for Parasitology* **32**, 677–684.

Cerantola, V., Guillas, I., Roubaty, C., Vionnet, C., Uldry, D., Knudsen, J. and Conzelmann, A. (2009). Aureobasidin A arrests growth of yeast cells through both ceramide intoxication and deprivation of essential inositolphosphorylceramides. *Molecular Microbiology* **71**, 1523–1537.

Chowdhury, M. N. (1986). Toxoplasmosis: a review. *Journal of Medicine* **17**, 373–396.

Coppens, I. (2013). Targeting lipid biosynthesis and salvage in apicomplexan parasites for improved chemotherapies. *Nature Reviews Microbiology* **11**, 823–835.

Denny, P. W., Shams-Eldin, H., Price, H. P., Smith, D. F. and Schwarz, R. T. (2006). The protozoan inositol phosphorylceramide synthase: a novel drug target which defines a new class of sphingolipid synthase. *Journal of Biological Chemistry* **281**, 28200–28209.

Dubey, J. P. (1977). *Toxoplasma, Hammondia, Besnotia, Sarcocystis*, and other cyst-forming coccidia of man and animals. In *Parasitic Protozoa* (ed. Kreier, J. P.), pp. 101–237. Academic Press, New York.

Figueiredo, J. M., Dias, W. B., Mendonca-Previato, L., Previato, J. O. and Heise, N. (2005). Characterization of the inositol phosphorylceramide synthase activity from *Trypanosoma cruzi*. *Biochemical Journal* **387**, 519–529.

Georgopapadakou, N. H. (2000). Antifungals targeted to sphingolipid synthesis: focus on inositol phosphorylceramide synthase. *Expert Opinions on Investigative Drugs* **9**, 1787–1796.

Gerold, P. and Schwarz, R. T. (2001). Biosynthesis of glycosphingolipids de-novo by the human malaria parasite *Plasmodium falciparum*. *Molecular and Biochemical Parasitology* **112**, 29–37.

Gubbels, M. J., Li, C. and Striepen, B. (2003). High-throughput growth assay for *Toxoplasma gondii* using yellow fluorescent protein. *Antimicrobial Agents and Chemotherapy* **47**, 309–316.

Hanada, K. (2005). Sphingolipids in infectious diseases. *Japanese Journal of Infectious Diseases* **58**, 131–148.

Hanada, K., Nishijima, M., Kiso, M., Hasegawa, A., Fujita, S., Ogawa, T. and Akamatsu, Y. (1992). Sphingolipids are essential for the growth of Chinese hamster ovary cells. Restoration of the growth of a mutant defective in sphingoid base biosynthesis by exogenous sphingolipids. *Journal of Biological Chemistry* **267**, 23527–23533.

Heidler, S. A. and Radding, J. A. (1995). The AUR1 gene in *Saccharomyces cerevisiae* encodes dominant resistance to the antifungal agent Aureobasidin A (LY295337). *Antimicrobial Agents and Chemotherapy* **39**, 2765–2769.

Huitema, K., Van Den Dikkenberg, J., Brouwers, J. F. and Holthuis, J. C. (2004). Identification of a family of animal sphingomyelin synthases. *EMBO Journal* **23**, 33–44.

Ikai, K., Takesako, K., Shiomi, K., Moriguchi, M., Umeda, Y., Yamamoto, J., Kato, I. and Naganawa, H. (1991). Structure of Aureobasidin A. *Journal of Antibiotics* (*Tokyo*) **44**, 925–933.

Kim, S. K., Fouts, A. E. and Boothroyd, J. C. (2007). *Toxoplasma gondii* dysregulates IFN-gamma-inducible gene expression in human fibroblasts: insights from a genome-wide transcriptional profiling. *Journal of Immunology* **178**, 5154–5165.

Lauer, S. A., Ghori, N. and Haldar, K. (1995). Sphingolipid synthesis as a target for chemotherapy against malaria parasites. *Proceeds of the National Academy of Sciences USA* **92**, 9181–9185.

Meissner, M., Schluter, D. and Soldati, D. (2002). Role of *Toxoplasma gondii* myosin A in powering parasite gliding and host cell invasion. *Science* **298**, 837–840.

Mina, J. G., Pan, S. Y., Wansadhipathi, N. K., Bruce, C. R., Shams-Eldin, H., Schwarz, R. T., Steel, P. G. and Denny, P. W. (2009). The *Trypanosoma brucei* sphingolipid synthase, an essential enzyme and drug target. *Molecular and Biochemical Parasitology* **168**, 16–23.

Mina, J. G., Mosely, J. A., Ali, H. Z., Shams-Eldin, H., Schwarz, R. T., Steel, P. G. and Denny, P. W. (2010). A plate-based assay system for analyses and screening of the *Leishmania major* inositol phosphorylceramide synthase. *International Journal of Biochemistry and Cell Biology* **42**, 1553–1561.

Mina, J. G., Mosely, J. A., Ali, H. Z., Denny, P. W. and Steel, P. G. (2011). Exploring Leishmania major inositol phosphorylceramide synthase (*Lmj*IPCS): insights into the ceramide binding domain. *Organic and Biomolecular Chemistry* **9**, 1823–1830.

Nagiec, M. M., Nagiec, E. E., Baltisberger, J. A., Wells, G. B., Lester, R. L. and Dickson, R. C. (1997). Sphingolipid synthesis as a target for antifungal drugs. Complementation of the inositol phosphorylceramide synthase defect in a mutant strain of *Saccharomyces cerevisiae* by the AUR1 gene. *Journal of Biological Chemistry* **272**, 9809–9817.

Pratt, S., Wansadhipathi-Kannangara, N. K., Bruce, C. R., Mina, J. G., Shams-Eldin, H., Casas, J., Hanada, K., Schwarz, R. T., Sonda, S. and Denny, P. W. (2013). Sphingolipid synthesis and scavenging in the intracellular apicomplexan parasite, *Toxoplasma gondii*. *Molecular and Biochemical Parasitology* **187**, 43–51.

Romano, J. D., Sonda, S., Bergbower, E., Smith, M. E. and Coppens, I. (2013). *Toxoplasma gondii* salvages sphingolipids from the host Golgi through the rerouting of selected Rab vesicles to the parasitophorous vacuole. *Molecular Biology of the Cell* **24**, 1974–1995.

Salto, M. L., Bertello, L. E., Vieira, M., Docampo, R., Moreno, S. N. and de Lederkremer, R. M. (2003). Formation and remodeling of inositolphosphoceramide during differentiation of *Trypanosoma cruzi* from trypomastigote to amastigote. *Eukaryotic Cell* **2**, 756–768.

Simons, K. and Ikonen, E. (1997). Functional rafts in cell membranes. *Nature* **387**, 569–572.

Soete, M., Camus, D. and Dubremetz, J. F. (1994). Experimental induction of bradyzoite-specific antigen expression and cyst formation by the RH strain of *Toxoplasma gondii in vitro*. *Experimental Parasitology* **78**, 361–370.

Sonda, S., Sala, G., Ghidoni, R., Hemphill, A. and Pieters, J. (2005). Inhibitory effect of Aureobasidin A on *Toxoplasma gondii*. *Antimicrobial Agents and Chemotherapy* **49**, 1794–1801.

Takesako, K., Ikai, K., Haruna, F., Endo, M., Shimanaka, K., Sono, E., Nakamura, T., Kato, I. and Yamaguchi, H. (1991). Aureobasidins, new antifungal antibiotics. Taxonomy, fermentation, isolation, and properties. *Journal of Antibiotics* (*Tokyo*) **44**, 919–924.

Vacaru, A. M., van den Dikkenberg, J., Ternes, P. and Holthuis, J. C. (2013). Ceramide phosphoethanolamine biosynthesis in *Drosophila* is mediated by a unique ethanolamine phosphotransferase in the Golgi lumen. *Journal of Biological Chemistry* **288**, 11520–11530.

Webster, J. P., Kaushik, M., Bristow, G. C. and McConkey, G. A. (2013). *Toxoplasma gondii* infection, from predation to schizophrenia: can animal behaviour help us understand human behaviour? *Journal of Experimental Biology* **216**, 99–112.

Welti, R., Mui, E., Sparks, A., Wernimont, S., Isaac, G., Kirisits, M., Roth, M., Roberts, C. W., Botte, C., Marechal, E. and McLeod, R. (2007). Lipidomic analysis of *Toxoplasma gondii* reveals unusual polar lipids. *Biochemistry* **46**, 13882–13890.

Wuts, P. G., Simons, L. J., Metzger, B. P., Sterling, R. C., Slightom, J. L. and Elhammer, A. P. (2015). Generation of broad-spectrum antifungal drug candidates from the natural product compound Aureobasidin A. *ACS Medical Chemistry Letters* **6**, 645–649.

Young, S. A., Mina, J. G., Denny, P. W. and Smith, T. K. (2012). Sphingolipid and ceramide homeostasis: potential therapeutic targets. *Biochemistry Research International* **2012**, 248135.

JBC ARTICLE

⌘ Author's Choice

Functional and phylogenetic evidence of a bacterial origin for the first enzyme in sphingolipid biosynthesis in a phylum of eukaryotic protozoan parasites

Received for publication, April 20, 2017, and in revised form, June 1, 2017 Published, Papers in Press, June 2, 2017, DOI 10.1074/jbc.M117.792374

John G. Mina[‡], Julie K. Thye[§], Amjed Q. I. Alqaisi[‡¶], Louise E. Bird[‖], Robert H. Dods[§], Morten K. Grøftehauge[§], Jackie A. Mosely[§], Steven Pratt[‡], Hosam Shams-Eldin[**], Ralph T. Schwarz[**], Ehmke Pohl[‡§], and Paul W. Denny[‡1]

From the Departments of [‡]Biosciences and [§]Chemistry, Durham University, Durham DH1 3LE, United Kingdom, the [¶]Biology Department, College of Science, University of Baghdad, Baghdad 10071, Iraq, the [‖]Oxford Protein Production Facility UK, Research Complex at Harwell, Rutherford Appleton Laboratory, Didcot OX11 0FA, United Kingdom, and the [**]Institut für Virologie, Zentrum für Hygiene und Infektionsbiologie, Philipps-Universität Marburg, 35043 Marburg, Germany

Edited by George M. Carman

***Toxoplasma gondii* is an obligate, intracellular eukaryotic apicomplexan protozoan parasite that can cause fetal damage and abortion in both animals and humans. Sphingolipids are essential and ubiquitous components of eukaryotic membranes that are both synthesized and scavenged by the Apicomplexa. Here we report the identification, isolation, and analyses of the *Toxoplasma* serine palmitoyltransferase, an enzyme catalyzing the first and rate-limiting step in sphingolipid biosynthesis: the condensation of serine and palmitoyl-CoA. In all eukaryotes analyzed to date, serine palmitoyltransferase is a highly conserved heterodimeric enzyme complex. However, biochemical and structural analyses demonstrated the apicomplexan orthologue to be a functional, homodimeric serine palmitoyltransferase localized to the endoplasmic reticulum. Furthermore, phylogenetic studies indicated that it was evolutionarily related to the prokaryotic serine palmitoyltransferase, identified in the Sphingomonadaceae as a soluble homodimeric enzyme. Therefore this enzyme, conserved throughout the Apicomplexa, is likely to have been obtained via lateral gene transfer from a prokaryote.**

Toxoplasma gondii is an obligate, intracellular protozoan parasite that is able to invade and colonize a wide variety of nucleated vertebrate cells. It is a member of the Apicomplexa, a diverse phylum including important pathogens of humans and domestic animals such as *Plasmodium* (the causative agent of malaria), *Cryptosporidium* (diarrhea), *Eimeria* (coccidiosis in poultry), and *Theileria* (East Coast fever in cattle). *Toxoplasma* has emerged as an important opportunistic pathogen, and toxoplasmosis is one of the primary opportunistic diseases in the immunocompromised, particularly AIDS patients, those receiving anti-cancer chemotherapy, and organ transplant recipients (1). *Toxoplasma* infection *in utero* is also a significant cause of spontaneous abortion in economically important domestic animals (2) and congenital defects in humans (1).

As an intracellular parasite, *Toxoplasma* has a dynamic relationship with its host cell, including both the synthesis and scavenging of key lipid species (3, 4), such as sphingolipids (5–7). Sphingolipids are amphipathic lipids consisting of a sphingoid backbone acylated with a long-chain fatty acid and having a polar head group. Although the basic sphingolipid, ceramide, is a secondary signaling molecule involved in, for example, apoptosis (8–10), modified or complex sphingolipids are major components of the outer leaflet of eukaryotic plasma membranes involved, together with sterols, in the formation of microdomains commonly known as lipid rafts. These domains have been proposed to function in a diverse array of processes from the polarized trafficking of lipid-modified proteins to the assembly and activation of signal transduction complexes (11). The first, rate-limiting enzyme in sphingolipid biosynthesis is serine palmitoyltransferase (SPT),[2] a pyridoxal phosphate (PLP)-dependent class II aminotransferase that catalyzes the Claisen-like condensation of L-serine and, typically, palmitoyl-CoA to form 3-ketodihydrosphingosine (KDS) (12) (Fig. 1). Subsequently, *N*-acylation of the sphingoid base in the endoplasmic reticulum (ER) leads to the formation of ceramide. Following transport to the Golgi apparatus, ceramide is used to form modified or complex sphingolipids, sphingomyelin (SM), or glycosphingolipid (GSL), for example (10, 13). In all eukaryotes studied to date, SPT is composed of a core heterodimer of two evolutionary related proteins that spans the membrane of the ER (14). One subunit, LCB2, contains the canonical PLP-binding and catalysis domain, whereas the other, LCB1, is not thought to bind this co-factor but to be important for complex stability (12). Both subunits are essential for enzyme activity in *Saccharomyces cerevisiae* (15), and analyses of temperature-sensitive SPT mutants have demonstrated

This work was supported by Biotechnology and Biological Research Council Grants BB/D52396X/1 and BB/M024156/1 (to P. W. D. and E. P.) and a British Council/Deutscher Akademischer Austauschdienst Academic Research Collaboration Award (to P. W. D. and R. T. S.). The authors declare that they have no conflicts of interest with the contents of this article.

This article contains supplemental Figs. S1–S3.

[1] To whom correspondence should be addressed: Dept. of Biosciences, Durham University, Lower Mountjoy, Stockton Rd., Durham DH1 3LE, United Kingdom. Tel.: 44-191-3343983; E-mail: p.w.denny@durham.ac.uk.

[2] The abbreviations used are: SPT, serine palmitoyltransferase; KDS, 3-ketodihydrosphingosine; PLP, pyridoxal phosphate; ER, endoplasmic reticulum; LCB, long-chain base; SM, sphingomyelin; GSL, glycosphingolipid; SAXS, small-angle X-ray scattering; F-MDist, Fitch Margoliash distance; RAxML, randomized accelerated maximum likelihood; PhyML, phylogeny maximum likelihood; HFF, human foreskin fibroblast.

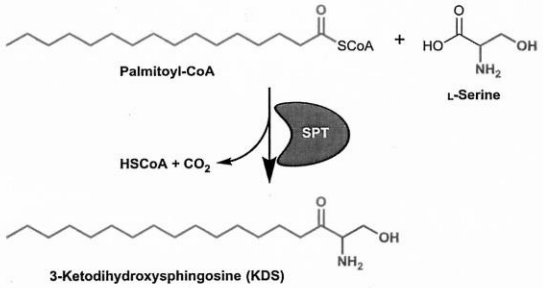

Figure 1. Schematic showing the chemical reaction catalyzed by the SPT in which the enzyme catalyzes the condensation of serine and palmitoyl-CoA to form KDS with the release of coenzyme A (*HSCoA*) and CO_2.

that *de novo* synthesis of sphingolipids and their precursors is pivotal in a wide spectrum of cellular processes including endocytosis, stress responses, and protein trafficking (16–18). Members of the Prokaryota also encode a functional SPT, which was first characterized in *Sphingomonas paucimobilis* (12, 19). However, in contrast to the eukaryotic paralogue, the bacterial enzyme is a soluble, homodimeric PLP-dependent class II aminotransferase and has been proposed to represent an evolutionary precursor of the heterodimeric eukaryotic SPT (20). Despite the divergence in primary sequence, the crystal structure of the *S. paucimobilis* enzyme revealed a symmetrical dimer with the co-factor PLP bound to each subunit in a manner predicted to be conserved in the eukaryotic SPT subunit, LCB2 (21).

Like other eukaryotes, apicomplexan *Toxoplasma* and *Plasmodium* spp. synthesize sphingolipids *de novo*, including both SM and GSLs (5, 22, 23). Sphingolipid-enriched lipid microdomains have been implicated in the interaction of *Plasmodium falciparum* with the host erythrocyte (24). However, host sphingolipid biosynthesis is non-essential for the proliferation of *Toxoplasma* (6, 7), indicating that *de novo* synthesis is important for parasitism (3). *Toxoplasma* were known to produce both SM and GSLs (5), but until recently the mechanics of sphingolipid metabolism in *Toxoplasma* and other apicomplexans remained enigmatic. However, the first functionally characterized enzyme in the apicomplexan sphingolipid biosynthetic pathway has now been described as an ortholog of the yeast inositol phosphorylceramide synthase (an enzyme with no mammalian equivalent) (6). To enable further understanding and analyses, the identification and characterization of the key enzyme components in the apicomplexan *de novo* pathway is essential. Although our characterization of the *Toxoplasma* inositol phosphorylceramide synthase has initiated this process (6) significant gaps remain, not least the formal identification of the apicomplexan SPT, the first and rate-limiting step in sphingolipid biosynthesis (12). Importantly, in the absence of a defined SPT, the incorporation of tritiated serine into sphingolipid species during metabolic labeling of isolated *Toxoplasma* and *P. falciparum* indicated the presence of an active apicomplexan SPT (22, 25).

Here we describe the identification and characterization of the *Toxoplasma* SPT, which represents a new class of eukaryotic enzyme with a very surprising, prokaryotic, origin. These studies shed new light on the evolution of these protozoan parasites and present a paradigm shift in the way the origin of sphingolipid biosynthesis is considered.

Results

A putative apicomplexan serine palmitoyltransferase

In all eukaryotes studied to date, including members of the protozoa, the first enzyme in the sphingolipid biosynthetic pathway, SPT (13), is composed of two related subunits (LCB1 and LCB2) (26). However, initial BLAST searches of the complete, annotated genome databases of both *T. gondii* (http://toxodb.org (60)) and *P. falciparum* (http://plasmodb.org (61)),[3] using a range of LCB1 and LCB2 protein sequences, failed to locate genes encoding either SPT subunit. Given that both of these parasites have been shown to possess SPT activity (22, 25), this represented a major paradox.

Further interrogation of the *Toxoplasma* genome database using BLAST and the conserved 10 residue PLP-binding domain (PROSITE consensus PS00599) common to all eukaryotic SPT LCB2 proteins (27), identified two closely related (68% identical), tandemly encoded, predicted type II PLP-dependent aminotransferases with no known function. Surprisingly, the putative PLP-binding sites from both proteins were both completely conserved with respect to the 12 residue PLP-binding motif (GTFSKS*XXXX*GG) identified in the Sphingomonadaceae bacterial SPT (28). Further analyses demonstrated that the best characterized bacterial SPT, from *S. paucimobilis*, showed limited homology with the identified *Toxoplasma* proteins: 28 and 30% identity and 47 and 46% similarity in the C-terminal region (64% of total predicted protein) of TgSPT1 and TgSPT2, respectively (20). In addition, using the BLAST tool and the predicted *Toxoplasma* protein sequences, singly encoded orthologues of the putative apicomplexan SPT were also found in the genome databases of *Plasmodium* spp. and the chicken pathogen *Eimeria tenella.* Comparison of the primary amino acid sequences of the putative apicomplexan proteins with the bacterial SPT indicated the presence of an *N*-terminal extension, which harbors a transmembrane region absent in the prokaryotic polypeptide (Fig. 2).

Taken together, these observations clearly indicated that the putative apicomplexan SPT is radically different to those of all other eukaryotes studied thus far. To prove this, it was vital to demonstrate the functionality of the apicomplexan SPT.

TgSPT1 is a functional serine palmitoyltransferase

The complete open reading frame of the predominant, tachyzoite expressed, *Toxoplasma* SPT, TgSPT1 (see http://toxodb.org for transcriptomic data),[3] was cloned into the yeast expression vector, pRS426-MET, to create pRS426-TgSPT1. In the auxotrophic yeast strain YPH499-HIS-GAL-LCB2, the essential PLP-binding, catalytic SPT subunit LCB2 (15) is under the control of a GAL1 promoter. In non-permissive glucose-containing SD medium, which inhibits expression from the GAL1 promoter, the yeast are non-viable. Transformation with pRS426-TgSPT1 allowed the growth of YPH499-HIS-GAL-

[3] Please note that the JBC is not responsible for the long-term archiving and maintenance of this site or any other third party hosted site.

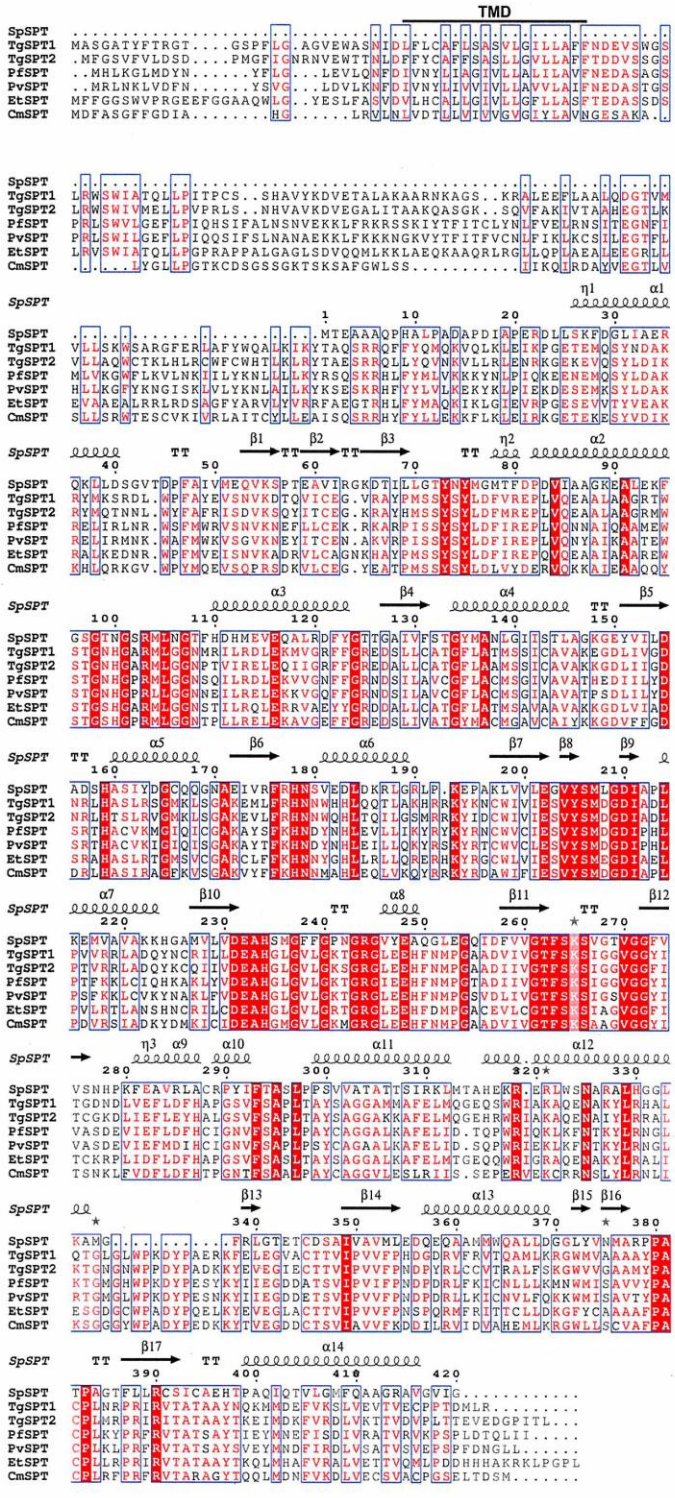
TMD
SpSPT
TgSPT1
TgSPT2
PfSPT
PvSPT
EtSPT
CmSPT

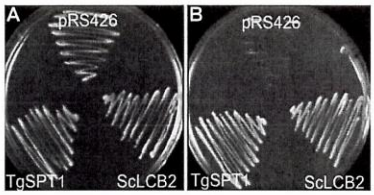

Figure 3. Transformed auxotrophic yeast grown on selective medium with either galactose (*A*) or glucose (*B*). Both ScLcb2 and TgSPT1 rescue the mutant *S. cerevisiae* that are deficient in endogenous ScLcb2 when grown in the presence of glucose (*B*). pRS246 is the empty vector control.

LCB2 in this media, as did the ectopic expression of *S. cerevisiae* LCB2. In contrast, the empty vector, pRS426-MET, did not rescue the growth of the auxotrophic yeast strain (Fig. 3). These data strongly indicate that TgSPT1 is a functional orthologue of the *S. cerevisiae* LCB2 and, therefore, at least part of the *T. gondii* serine palmitoyltransferase.

To analyze the functionality of TgSPT1 *in vitro*, a series of constructs were made in collaboration with the Oxford Protein Purification Facility in the vector pOPINS3C, where the insert is N-terminally fused to a cleavable N-HIS SUMO tag (29, 30). Following triage based on expression levels and product solubility, a series of these fusion proteins (with N-terminal deletions of 143, 158, 176, and 180 amino acids) were expressed, purified, and subjected to preliminary functional analyses using palmitoyl-CoA and ^{14}C-labeled serine as substrates (supplemental Fig. S1). The truncated construct TgSPT1 Δ158 was selected for further analyses. Mass spectrometry demonstrated the reaction product of the enzyme to be KDS (Fig. 4), and therefore TgSPT1 is a *bona fide* SPT.

To further understand enzyme function, small-angle X-ray scattering (SAXS) was utilized to determine the shape of the protein in solution and investigate whether TgSPT1 forms a homodimer similar to the bacterial orthologue. The results are summarized in Fig. 5*A*, which shows the experimentally derived shape of the molecule in gray as a bead model and superimposed a ribbon diagram of the homodimeric homology model of *Tg*SPT1 based on the known crystal structure of the *Sphingobacterium multivorum* SPT (52). The *ab initio* envelope shows very good agreement with the homodimeric model, where the core of the enzyme adopts a similar conformation to the bacterial orthologue. The elongated shape of the envelope indicated increased conformational flexibility of the termini of the protein. Using the homology model of the TgSPT1 dimer, the theoretical X-ray scattering data calculated with CRYSOL (31) revealed some discrepancies with the experimental data (Fig. 5*B*). Although the shape of the curve was similar, the low intensity values are higher in the experimental data consistent with a more elongated/or larger shape as shown in the *ab initio* envelope. Furthermore, the homology model indicated that the co-factor PLP can bind precisely to the predicted binding motifs in each monomer at the dimer interface of the structural model (Fig. 5*C*). Therefore, the *Toxoplasma* and by extension the apicomplexan SPTs are functional as homodimers. This resembles the bacterial situation (19) rather than the so far universal eukaryotic model of core heterodimeric modality (14). However, in contrast to the Prokaryota, where SPT is a soluble enzyme (20), the eukaryotic enzyme complex is associated with the membrane of the endoplasmic reticulum (14). As discussed above, the *N*-terminal extension contains a predicted transmembrane domain, and the data indicate that this does not influence functionality *in vitro*. It is noteworthy that Uniprot (www.uniprot.org) has predicted the *P. falciparum* SPT N-terminal region to target the protein to the apicoplast (32), a vestigial plastid that harbors the machinery for several lipid biosynthetic pathways (33). However, the ability of TgSPT1 to complement for a deficiency of LCB2 in auxotrophic mutant yeast (Fig. 3) indicated that the protozoal enzyme is targeted to the ER, which is the locale for SPT activity in this and other eukaryotes (14). Episomal expression of tagged TgSPT1-TY and the ER marker GFP-HDEL (34, 35) allowed co-localization by immunofluorescence microscopy and indicated that TgSPT1 is an ER rather than apicoplast-localized enzyme in *Toxoplasma* (Fig. 6, *A–D*). Furthermore, using a rat polyclonal antibody raised against TgSPT1 Δ158, the native protein was shown to have a similar ER localization pattern (Fig. 6, *E–H*). Looking at a larger vacuole showed the same localization pattern of native TgSPT1 (Fig. 7, *A–D*). In addition, the larger quantity of data available here facilitated quantitative co-localization analyses illustrated by scatterplots (Fig. 7, *E–G*). These show two-dimensional histograms of differentially labeled cell compartments (see axes labels for the channel/wavelength) at the same spatial region. A linear correlation demonstrates a strong spatial correlation between the channels, and the slope indicates the relative intensities (36, 37). The plot in Fig. 7*E* demonstrated a strong correlation of TgSPT1 (antiSPT-AF594) with GFP-HDEL (antiGFP-AF488) and ER localization. In contrast, neither TgSPT1 (antiSPT-AF594) nor GFP-HDEL (anti-GFP-AF488) showed any significant correlation with DAPI-stained nuclei (Fig. 7, *F* and *G*). In an additional control experiment, TgSPT1 (antiSPT-AF594) showed no significant correlation with episomally expressed, cytosolic GFP (supplemental Fig. S2). Together, these data demonstrated that TgSPT1 has a canonical eukaryotic subcellular localization, the ER.

In summary, TgSPT1 represents a new class of eukaryotic SPTs found in the Apicomplexa. Although it functionally and structurally resembles the prokaryotic enzymes, its membrane localization and place in an apparently conventional eukaryotic synthetic pathway (6) demonstrate that it serves a conventional eukaryotic role.

Figure 2. Sequence alignment of the predicted SPT from four members of the Apicomplexa (*T. gondii, TgSPT1* and *TgSPT2; E. tenella, EtSPT; P. falciparum, PfSPT;* and *Plasmodium vivax, PvSPT*) and the characterized enzyme from the prokaryote *S. paucimobilis* (*SpSPT*). Conserved residues (including those in the active site) identified by analyses of the SpSPT structure and homology modeling of the human functional orthologue (LCB2), are highlighted in *red*, with *red text* denoting similarity. *Blue boxes* denote conserved domains. The canonical lysine demonstrated to form an internal aldimine with the co-factor PLP at SpSPT position 265 is highlighted (21). The N-terminal extensions unique to the predicted apicomplexan enzymes harbor a transmembrane domain predicted by TMPRED (TMD, *bold* and *underlined*). The figure was produced using ESPript 3.0 (59).

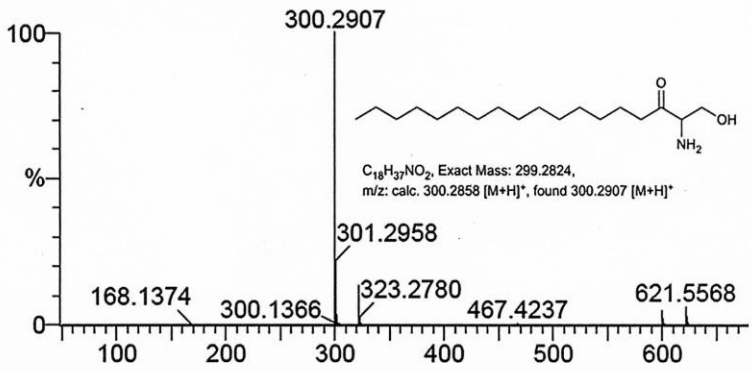

Figure 4. Mass spectrometry positive ion spectrum of lipids extracted from *in vitro* reaction of TgSPT1 Δ158 with serine and palmitoyl CoA as substrates. The peak 300.29 corresponds to the mass of 3-ketodihydrosphinganine.

A surprising evolutionary origin for the apicomplexan serine palmitoyltransferase

The data presented above detail the identification and functional characterization of TgSPT1, a eukaryotic enzyme, which in terms of its primary sequence and homodimeric structure resembles the prokaryotic "sister" enzymes. Our comprehensive sequence searches of the protozoan genome databases identified closely related orthologues of TgSPT1/2 in *Plasmodium* spp., *E. tenella*, and *Cryptosporidium muris*. Unlike *Toxoplasma*, these members of the Apicomplexa maintain a single SPT copy, indicating that TgSPT1 and TgSPT2 resulted from a gene duplication event that occurred post-speciation of the phylum. Interestingly, *Cryptosporidium hominis* and *Cryptosporidium parvum*, unlike *C. muris*, completely lack any gene encoding for SPT, despite the genomic region being syntenic between all three species (Fig. 8*A*). This suggests that *C. hominis* and *C. parvum* have selectively lost the first and rate-limiting step in sphingolipid biosynthesis, probably reflecting a specific adaptation of the parasite-host relationship.

To further analyze the evolutionary origin of the divergent apicomplexan SPT, phylogenetic analyses of a conserved region, including the PLP-binding site, were carried out. Using ClustalW (38) to align the predominant conserved region (Fig. 2 and supplemental Fig. S3), followed by Fitch Margoliash distance (F-MDist) (39), randomized accelerated maximum likelihood (RAxML) (40), and phylogeny maximum likelihood (PhyML) (41), the relationship of the apicomplexan SPT with both the eukaryotic catalytic subunit, LCB2, and the prokaryotic homodimeric SPT were determined (Fig. 8*B*). It was clear that the apicomplexan sequences do not represent conventional eukaryotic LCB2, with the kingdom to which they belong, the Chromalveolatea, split across the two major clades. The predicted catalytic subunits of the SPT from the Chromalveolate *Thalassiosira pseudonana* and *Phytophthora ramorum* group with high certainty with the conventional LCB2 subunits; however, the apicomplexan SPTs form a clade, supported by bootstrap values, with the prokaryotic sequences. This bioinformatic approach strongly indicated that the homodimeric apicomplexan enzyme is a divergent eukaryotic SPT of prokaryotic origin.

Discussion

The *Toxoplasma* serine palmitoyltransferase, TgSPT, was identified as being encoded by two closely related genes and was found to be conserved as a single copy throughout the Apicomplexa. TgSPT1 demonstrated the ability to complement an auxotrophic yeast LCB2 mutant, and functionality was confirmed by analyses of expressed and purified TgSPT1. However, the predicted protozoan enzyme is highly divergent compared with the heterodimeric enzyme characterized throughout the Eukaryota. SAXS, coupled with homology modeling, demonstrated that the protein forms a homodimer, thereby resembling the prokaryotic rather that the eukaryotic paralogue. This relationship was further confirmed by phylogenetic analyses, which demonstrated the apicomplexan sequences as being most closely related to the prokaryotic SPT, with the protozoan SPT showing divergence from the catalytic SPT subunit (LCB2) in all other eukaryotes, including fellow members of the Chromalveolata. These data strongly indicated that the apicomplexan SPT was derived from horizontal transfer from a prokaryotic species (probably a member of Alphaproteobacteria) and demonstrated that the evolution of eukaryotic sphingolipid biosynthesis is more complex than previously recognized. These data also add to the evolutionary complexity of the Apicomplexa, protozoan parasites known to harbor a vestigial plastid (the apicoplast) as a remnant of an ancient algal endosymbiotic event (42).

Experimental procedures

Bioinformatics analyses

The 10 residue canonical, degenerate, PLP-binding domain common to all eukaryotic SPT subunit 2 proteins (43) was used to search the complete genome database of *T. gondii* (http://toxodb.org)[3] with WU-BLAST (Gish, W. (1996–2003)). Two hits were identified: TGME49_090980 (TgSPT1) and TGME49_090970 (TgSPT2). The protein sequence of TgSPT1 and WU-BLAST were subsequently used to search the *Plasmodium*, *Eimeria*, and *Cryptosporidium* genome databases (http://plasmodb.org and http://genedb.org).[3] NCBI-BLAST was used to compare the hits against the NCBI protein

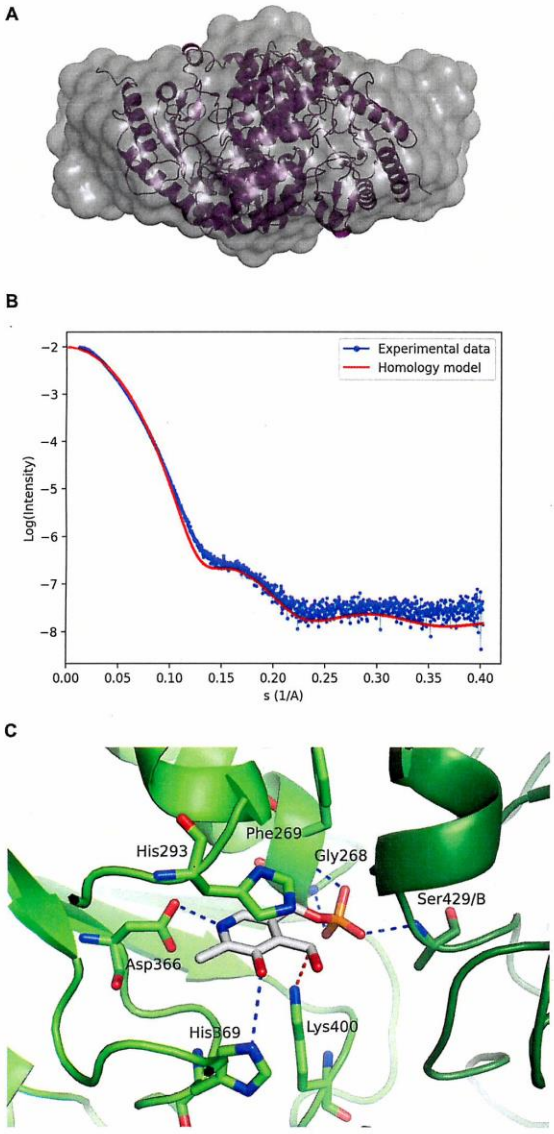

Figure 5. *A*, SAXS generated envelope overlaying a homology model of the TgSPT1 dimer. *B*, SAXS data (binned mode as *blue dots*), superimposed with the calculated scattering curve using the homology mode (in *red*). *C*, close-up of the PLP binding site of the homology model of TgSPT1 based on the crystal structure of SPT from *S. multivorum*. The key PLP binding residues depicted with *cyan* bonds in a ball-and-stick representation are conserved in the family (see Fig. 2). The numbering corresponds to the TgSPT1 sequence. Note that Ser-429/B belongs to the second subunit of the homodimer.

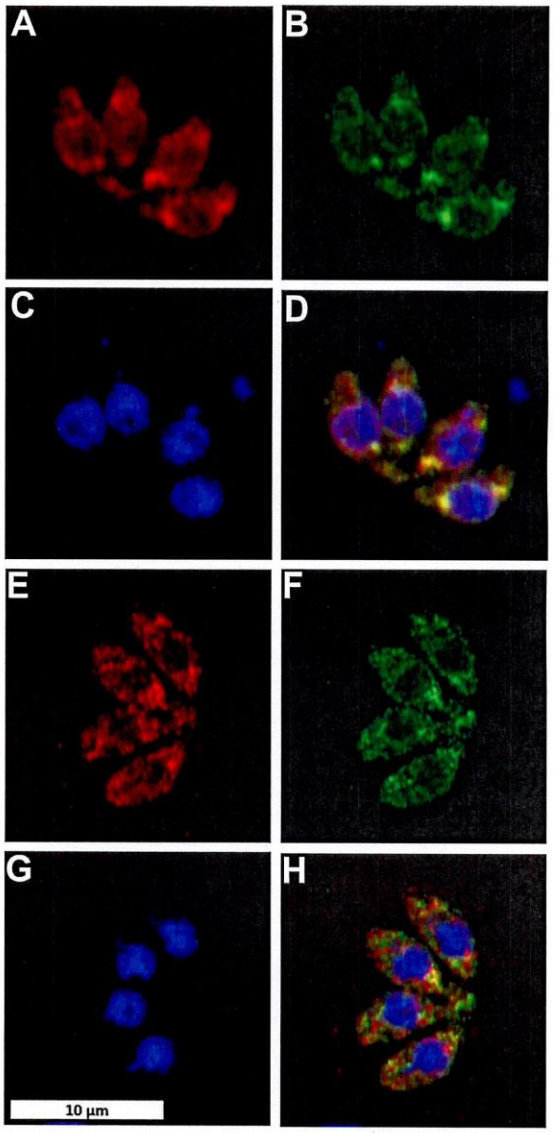

Figure 6. Toxoplasma stained for ectopically expressed TgSPT1-TY (*A*, AlexaFluor594, *red*) and endogenous TgSPT1 (*E*, AlexaFluor594, *red*); ectopically expressed ER marker GFP-HDEL (*B* and *F*, AlexaFluor488, *green*); and DNA (*C* and *G*, DAPI, *blue*). Co-localization of TgSPT1, ectopically expressed and endogenous, with GFP-HDEL is shown in merge of *A* and *B* (*D*, *yellow*) and *E* and *F* (*H*, *yellow*), respectively. The *scale bar* is equivalent to 10 μm.

sequence database. Exploiting the structural data available for the bacterial *S. paucimobilis* enzyme (21), representatives of the apicomplexan and bacterial SPTs were aligned using T-Coffee Expresso (44). The resulting multiple sequence alignment was reformatted in T-Coffee with the command "t_coffee -other_pg seq_reformat -in <msa> -output sim" to yield the identity values.

TgSPT1 isolation and cloning

T.gondii RH hxgprt- were propagated in vero cells (both kind gifts from Dominique Soldati-Favre, University of Geneva, Geneva, Switzerland) and isolated as described previously (45). RNA was then extracted using the RNeasy® kit (Qiagen) according to the yeast protocol. Following quantitation using Nanodrop® 2000 (ThermoFisher), cDNA was synthesized using random primers and the SuperScript® III kit (Thermo-

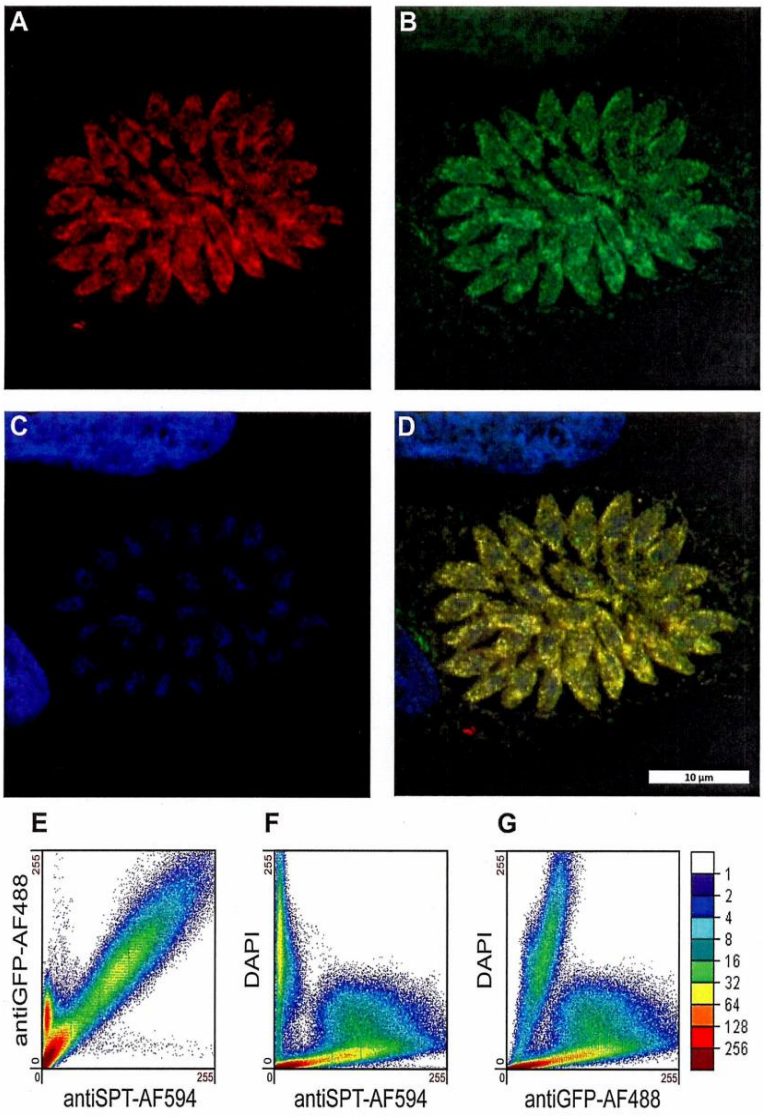

Figure 7. Endogenous TgSPT1 (*A*, AlexaFluor594, *red*) and ectopically expressed ER marker GFP-HDEL (*B*, AlexaFluor488, *green*) co-localize as shown in the merged image (*D*, *yellow*). The *scale bar* is equivalent to 10 μm. In support of this, the scatterplot (*E*) demonstrates the strong correlation of TgSPT1 (antiSPT-AF594) with GFP-HDEL (antiGFP-AF488). In contrast, neither TgSPT1 (antiSPT-AF594) nor GFP-HDEL (antiGFP-AF488) show any significant correlation with DAPI-stained (*C*) nuclei (*F* and *G*). The *color scale* represents the number of pixels as indicated.

Fisher) as directed by the manufacturer. Full-length TgSPT1 was then amplified by PCR using the proofreading DNA polymerase *Pfu* (Promega) and primers TgSPT5′HindIII CCC-**AAGCTT**GCATGGCTTCGGGTGCAACGTACTTC and TgSPT3′NotI ATAAGAAT**GCGGCCGC**TCATCGGAG-CATGTCAGTGGGTGGG (restriction sites in bold). The coding sequence was then cloned into the pET24a vector (Novagen). Subsequently, a series of deletion constructs were cloned into a series of pOPIN bacterial expression and, following transformation in a variety of *Escherichia coli* strains, screened for expression of soluble protein at the Oxford Protein Production Facility using their standardized protocols for high throughput analyses (30).

Yeast complementation

The YPH499-HIS-GAL-LCB2 *S. cerevisiae* strain was constructed in YPH499 (Mat a; ura3-52; lys2-801amber; ade2-101ochre; trp1-63; his3-200; leu2-1) (Stratagene) by bringing the expression of the yeast LCB2 gene under the control of the stringently regulated GAL1 promoter that is repressed in the presence of glucose as described before (25, 46). The following primer sequences were used for amplification of the HIS/GAL

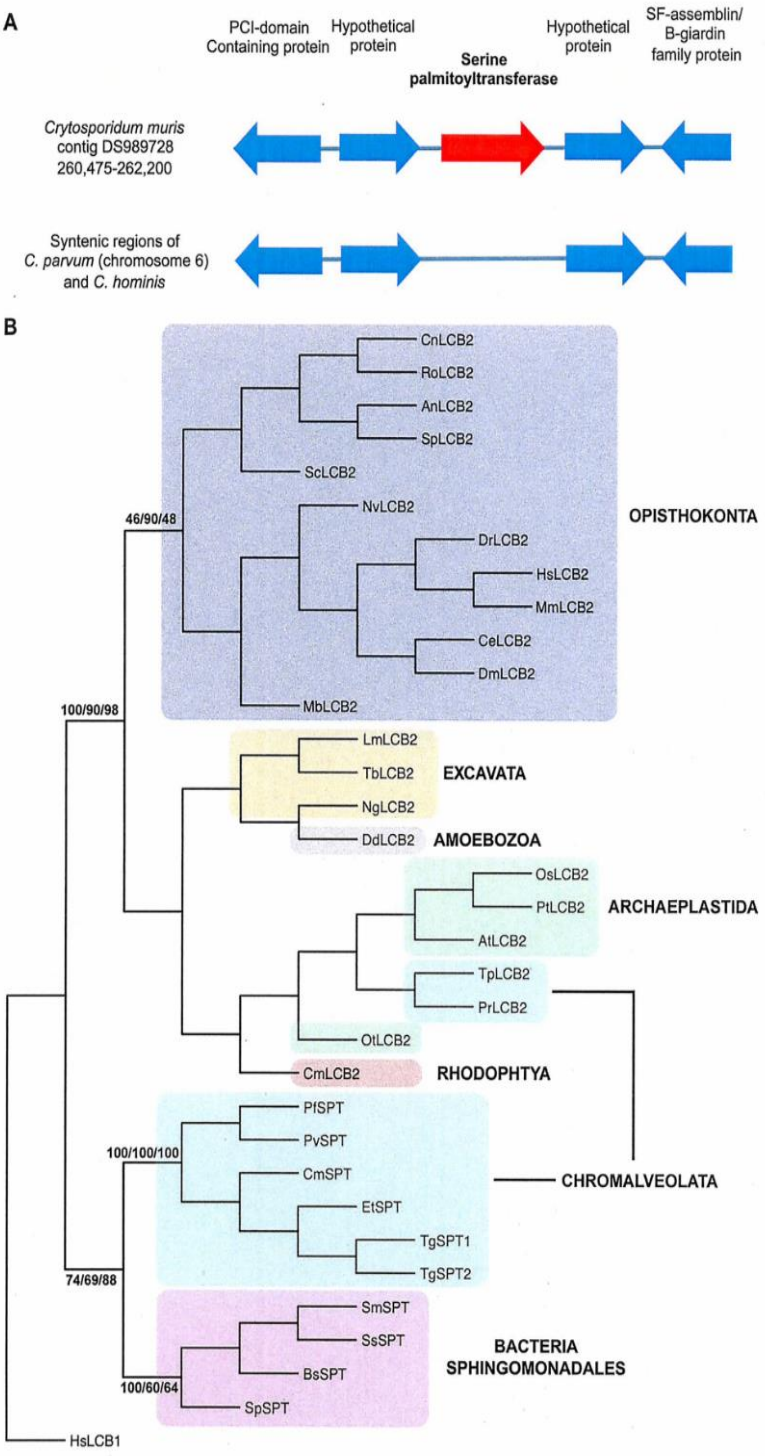
A
PCI-domain Containing protein
Hypothetical protein
Serine palmitoyltransferase
Hypothetical protein
SF-assemblin/ B-giardin family protein
Crytosporidum muris contig DS989728 260,475-262,200
Syntenic regions of C. parvum (chromosome 6) and C. hominis
B
CnLCB2
RoLCB2
AnLCB2
SpLCB2
ScLCB2
NvLCB2
DrLCB2
HsLCB2
MmLCB2
CeLCB2
DmLCB2
MbLCB2
OPISTHOKONTA
46/90/48
100/90/98
LmLCB2
TbLCB2
NgLCB2
EXCAVATA
DdLCB2
AMOEBOZOA
OsLCB2
PtLCB2
AtLCB2
ARCHAEPLASTIDA
TpLCB2
PrLCB2
OtLCB2
CmLCB2
RHODOPHYTA
PfSPT
PvSPT
CmSPT
EtSPT
TgSPT1
TgSPT2
CHROMALVEOLATA
100/100/100
74/69/88
SmSPT
SsSPT
BsSPT
SpSPT
BACTERIA SPHINGOMONADALES
100/60/64
HsLCB1

cassette: (*a*) sequence for integration upstream of the coding region (nucleotides −200 to −150) Lcb2HisGalS, TAAGTTTCATTACTATTTTCTATTATTATCTGCAACTTTTTATTAGTTAGgggcgaattggagctccac and (*b*) sequence for integration at the initiation codon (nucleotides +1 to +50 Lcb2HisGalAS, TAAGTTTCATTACTATTTTCTATTATTATCTGCAACTTTTTATTAGTTAGgggcgaattggagctccac. The numbers indicate the nucleotide positions in the *S. cerevisiae* DNA sequence, with the adenosine of the ATG initiation codon being defined as position +1. The 19-bp sequences at the 3′ ends of these oligonucleotides that are homologous to the sequences of the vector pGAL/HIS3 and serve as a template for amplification of the GAL1/HIS3-cassette are shown with lowercase letters. Transformation into the haploid YPH499 strain, selection on minimal medium lacking histidine but containing galactose, and confirmation of the insertion of the HIS-GAL fragment were performed as previously (46). YPH499-HIS-GAL-LCB2 was maintained in SGR medium (4% galactose, 2% raffinose, 0.17% Bacto yeast nitrogen base, 0.5% ammonium sulfate) with galactose/raffinose rather than non-permissive dextrose as the carbohydrate source. For rapid cultivation of the mutant, YPGR medium (4% galactose, 2% raffinose, 1% yeast extract, 2% peptone) was routinely used.

The *S. cerevisiae* lcb2 coding region was amplified from genomic DNA (Invitrogen) using primers (Sclcb2SEcoRI GGG**GAATTC**ATGAGTACTCCTGCAAACTATACCCG and Sclcb2ASXhoI GGG**CTCGAG**AACAAAATACTTGTCGTCCTTACAATC, with restriction sites shown in bold type), and the product was cloned into pRS426MET25 to create pRS426 ScLCB2. Similarly, the TgSPT1 coding sequence was amplified (TgSPT5′SpeI **ACTAGT**ATGGCTTCGGGTGCAACGTACTTC and TgSPT3′HindIII CGC**AAGCTT**TCATCGGAGCATGTCAGTGGGTGG, with restriction sites in bold type) and cloned into the yeast expression vector to create pRS246 TgSPT1. The YPH499-HIS-GAL-LCB2 *S. cerevisiae* strain was transformed with pRS426 ScLCB2 or pRS426 TgSPT1 and functionally complemented transformants selected on non-permissive SD medium (0.17% Bacto yeast nitrogen base, 0.5% ammonium sulfate, and 2% dextrose) containing the nutritional supplements necessary to allow selection of transformants.

TgSPT1 protein production and purification

At the Oxford Protein Purification Facility four N-terminal deletion constructs (TgSPT1 Δ143, Δ158, Δ177, and Δ180) in the pOPINS3C vector (containing a HIS-SUMO tag and a 3C protease cleavage site) showed good expression levels of soluble protein in Rosetta II (DE3) pLysS *E. coli* grown in Overnight Express™ Instant TB autoinduction medium (Novagen) with 50 μg/ml ampicillin and 35 μg/ml chloramphenicol (Sigma-Aldrich). Protein production was scaled up to 2-liter baffled flasks using the same medium and conditions, incubated at 37 °C until A_{600} reached 0.5 then the temperature was reduced to 25 °C (TgSPT1 Δ158, Δ177, and Δ180) and incubation continued for a further 24 h or 15 °C (TgSPT1 Δ143) and 48 h. Following harvesting of the cells by centrifugation and freeze-thawing at −80 °C, the pellets were suspended in lysis buffer (50 mM Tris, pH 7.5, 500 mM NaCl, 20 mM imidazole, 0.2% Tween 20® (v/v), 10 μg/ml DNase, 10 μg/ml RNase (all Sigma-Aldrich), and EDTA-free protease inhibitors (Roche)) before lysis by sonication and isolation of the soluble fraction following centrifugation. HIS-SUMO-tagged TgSPT1 fusions were then isolated using a His trap FF 5-ml column (GE Healthcare Life Sciences) equilibrated with 50 mM Tris, pH 7.6, 500 mM NaCl, 20 mM imidazole, 25 μM PLP ,and 5% glycerol (v/v) (all Sigma-Aldrich), and FPLC (Akta). Bound protein was then eluted in 50 mM Tris, pH 7.6, 500 mM NaCl, 1 M imidazole, 25 μM PLP, and 5% glycerol (v/v) before dialysis into 10 mM Tris, pH 7.6, 150 mM NaCl, 25 μM PLP, and 5% glycerol (v/v) using a Slide-A-Lyzer cassette (Thermo Scientific). To cleave the purification tag, the dialysis step was performed in the presence of the Human RhinoVirus 3C Protease (HRV 3C; Qiagen). Following concentration using a spin concentrator (Agilent Technologies), samples were injected onto on a 1-ml MonoQ 5/50 GL anion exchange column (GE Healthcare) pre-equilibrated with wash buffer (10 mM Tris, pH 8, 100 mM NaCl) using FPLC. The flow-through, containing cleaved and purified protein, was collected, concentrated, and dialyzed in appropriate buffers, and quantified using a Nanodrop® 2000.

TgSPT enzymatic assay

Initially, TgSPT1 activity was assessed using a methodology based on a published radiochemical assay (21). In a 500-μl reac-

Figure 8. *A*, schematic illustrating the gene arrangement in the region surrounding the encoded *C. muris* serine palmitoyltransferase, compared with the syntenic regions of *C. parvum* and *C. hominis* chromosome 6. *B*, phylogenetic tree produced from a genetic distance matrix showing the relationship between the eukaryotic catalytic subunit of serine palmitoyltransferase (LCB2) and the prokaryotic and apicomplexan orthologues (SPT). The Opistokonta (animals and fungi) are colored *blue*; the Excavata (subgroup of unicellular eukaryotes) are *yellow*; Amoebozoa (amoeboid protozoa) are *gray*; Archaeplastida (plants and algae, containing cyanobacterium-derived plastid) are *green*; Rodophyta (a subgroup of the Archaeplastida, red algae) are *red*; Chromalveolata (unicellular eukaryotes containing red algal derived plastid) are *turquoise*; and Sphingomonadales (alphaproteobacteria with the ability to synthesize sphingolipids) are *pink*. The bootstrap values of the major clades are shown where they are greater than 60 at common nodes for the three methodologies employed: F-MDist, RAxML, and PhyML. The non-catalytic subunit of the human serine palmitoyltransferase (HsLCB1) was utilized as the outgroup. Sequences used in the analyses were equivalent to those aligned to TgSPT1 amino acids 228–411. Sequence information: LCB1, serine palmitoyltransferase subunit 1; LCB2, palmitoyltransferase subunit 2; SPT, serine palmitoyltransferase. NBCI accession numbers: HsLCB1: *Homo sapiens*, EAW62806; HsLCB2: *H. sapiens*, NP_004854; MmLCB2: *Mus muscalis*, NP_035609; DmLCB2: *Drosophila melanogaster*, BAA83721; CeLCB2: *Caenorhabditis elegans*, Q20375; DrLCB2, *Danio rerio*, NP_001108213; OsLCB2: *Oryza sativa*, BAD88168.1; AtLCB2: *Arabidopsis thaliana*, NP_001031932.1; DdLCB2: *Dictyostelium discodium*, XP_635115. Joint Genome Institute accession numbers: NvLCB2: *Nematostella vectensis*, 241814; MbLCB2: *Monosiga brevicollis*, 34401; PtLCB2: *Populus trichocarpa*, 834365; OtLCB2: *Ostreococcus tauri*, 16411; TpLCB2: *T. pseudonana*, 255691; PrLCB2: *P. ramorum*, 71166; NgLCB2: *Naegleria gruberi*, 82916; SpSPT: *S. paucimobilis*, Q93UV0_PSEPA; SmSPT: *S. multivorum*, A7BFV6_9SPHI; SsSPT: *Sphingobacterium spiritivorum*, A7BFV7_9SPHI; BsSPT: *Bacteriovorax stolpii*, A7BFV8_9DELT. Universal Protein Resource accession numbers: ScLCB2: *S. cerevisiae*, P40970; CnLCB2: *Cryptococcus neoformans*, J9VYF7; SpLCB2: *Schizosaccharomyces pombe*, Q09925; AnLCB2: *Aspergillus nidulans*, Q5BEC8; RoLCB2: *Rhizopus oryzae*, I1BXF5. *Cyanidioschyzon merolae* Genome Project accession number: CmLCB2: *Cyanidioschyzon merolae*, CMJ240C. ToxoDB accession numbers: TgSPT1: *T. gondii*, TGME49_090980; TgSPT2, TGME49_090970. GeneDB accession numbers: PfSPT: *P. falciparum*, PF14_0155; PvSPT, *P. vivax*; CmSPT: *C. muris*, B6ACS8_CRYMR; TbLCB2: *Trypanosoma brucei*, Tb927.10.4050; LmLCB2: *Leishmania major*, LmjF35.0320. Sanger Institute accession number: EtSPT: *E. tenella*, dev_EIMER_contig_00020813.

tion volume (50 μM HEPES, pH 7.6, 150 mM KCl, 0.2 mM EDTA, 5% glycerol, 25 μM PLP), 20 μM of the purified protein was reacted with 20 mM L-[^{14}C]serine (GE Healthcare) and 1.6 mM palmitoyl CoA (Sigma-Aldrich) for 75 min at 37 °C. The organic phase was isolated following the addition of 1 ml of $CHCl_3$:CH_3OH (2:1 v/v) and analyzed by high-performance thin layer chromatography (Merck) in a $CHCl_3$:CH_3OH:NH_4OH, 40:10:1, solvent system. Images were captured using a AR-2000 Radio-TLC and Imaging Scanner (Bioscan). Subsequently, mass spectrometry was utilized to definitively identify the reaction products under the same conditions as above, but using cold serine and 5-fold greater volumes. Following purification as above, reaction products were analyzed, and accurate masses were obtained, using a Thermo-Finnigan LTQ FT mass spectrometer.

Subcellular localization of TgSPT1

Primers were designed to amplify the TgSPT1 coding sequence: TgSPT5′EcoRV CGC**GATATC**ATGGCTTCGGGTGCAACGTACTTC and TgSPT3′NsiI CGC**ATGCA**TTCGGAGCATGTCAGTGGGTGG (with restriction sites in bold type). The resultant PCR product was cloned into pTUB8MycGFPPfMyoAtailTy-HX (kind gift from Dominique Soldati-Favre) (47) to create pG1-TgSPT1-TY. Transfections were carried out using a 4D Nucleofector (Lonza), protocol FI 158 and 20-μl reaction volumes in 16 reaction strips. Briefly, *Toxoplasma* were maintained in human foreskin fibroblasts (HFFs, ATCC). Parasites freshly lysed from one T75 flask of HFF cells were homogenized by passage through a 25-gauge needle and isolated by centrifugation at 1500 × *g* for 10 min at 4 °C. The pellet was resuspended in the P3 buffer with added supplement (Lonza), and *Toxoplasma* concentration was adjusted to 10^7 ml^{-1}. 20 μl of this parasite suspension was added to a dried pellet of ethanol-precipitated ~10 μg of P30-GFP-HDEL (kind gift from Kristin Hager, University of Notre Dame) (48), and/or pG1-TgSPT1-TY plasmid was transferred to the transfection strips and electroporated. Subsequently, 100 μl of medium was added, and 10 μl or 20 μl were added to 24-well plates containing confluent HFF cells grown on glass coverslips. The plates were incubated at 37 °C, 5.0% CO_2 for the appropriate time period.

The cells were fixed in 4% paraformaldehyde in PBS (pH 7.4) for 15 min and then permeablized with 0.4% (v/v) Triton X-100 in PBS for 10 min, before incubation in blocking buffer (PBS supplemented with 1% (w/v) BSA; Sigma-Aldrich), 0.1% fish skin gelatin (Sigma-Aldrich), and 0.1% (v/v) Triton X-100) for 15 min at room temperature. Samples were incubated with a mouse monoclonal anti-TY antibody (1:200; kind gift from Keith Gull, University of Oxford, Oxford, UK) or the primary anti-TgSPT1 Δ158 rat polyclonal (Cambridge Research Biochemicals, 1:200), and an anti-GFP rabbit polyclonal antibody (Clontech, 1:200) in blocking buffer overnight at 4 °C. After PBS washing, samples were incubated with Alexa Fluor® 594 anti-mouse or anti-rat and Alexa Fluor® 488 anti-rabbit secondary antibodies (ThermoFisher) at 1:500 in blocking buffer for 1 h at room temperature. The samples were incubated with DAPI (Sigma-Aldrich) in PBS for 10 min, mounted using Vectashield H-1000 (Vector labs), and sealed with nail polish before imaging.

All images were obtained using laser scanning confocal microscope Zeiss LSM 880 with AiryScan equipped with excitation laser 405, Argon 458, 488, 514, He-Ne 543, 594, and 633 and AiryScan filter set combinations BP 420–480 + BP 495–550, BP 420–480 + BP 495–620, BP 420–480 + LP 605, BP 465–505 + LP 525, BP 495–550 + LP 570, and BP 570–620 + LP 645. For each image, the dynamic range was checked to avoid saturation, except with the DAPI stain where host cells masked the detection of parasite nuclei at low gain/laser power values. AiryScan images were automatically processed using default values. Zeiss CZI images were exported to TIFF file format using Zen (Blue Edition version 2.3, Carl Zeiss Microscopy GmbH, 2011) and analyzed using ImageJ Fiji package (49). Co-localization was assessed using the ScatterJn plugin and scatter plots (36, 37). The scatterplots show two-dimensional histograms of two channels at the same spatial region. Data points are generated as $n(x,y)$, where n is the number of pixels in each channel, and x,y are discrete values 0–255, and these data points are displayed as a scatterplot of 256 × 256 matrix in which the element (x,y) contains the number of data points with coordinates (x,y). The number of pixels is represented by a color scale. A linear correlation demonstrates a strong spatial correlation between the channels, and the slope indicates the relative intensities. Negative controls were checked between DAPI and the Golgi marker, pTub-GRASP-RFP (50), and no positive correlation was found.

Homology modeling

The TgSPT1 homology model was constructed using the Δ158 SPT sequence with the HHPred server (http://toolkit.tuebingen.mg.de/hhpred (62))[3] (51), which identified the crystal structure of SPT from *S. multivorum* (52) as the closest orthologue (Protein Data Bank code 3A2B) and aligned the sequences based on sequence identity and the predicted secondary structure of TgSPT1 and the actual secondary structure of 3A2B. The biologically relevant homodimer was used as a template to produce five preliminary models with MODELLER (53). The model with the lowest *molpdf* score was taken forward to the next step, in which PLP was added based on the known bacterial SPT structure. After another minimizing step, the two loops of residues 472–494 that are absent in the bacterial structure, were modeled using MODELLER (54). The optimal conformation was based on the lowest *molpdf* and *DOPE* scores, as well as manual inspection using interactive computer graphics.

Small angle X-ray scattering

SAXS data were collected using the Δ158 SPT construct on Beamline B21 at the Diamond Light Source in size exclusion chromatography HPLC mode (55). Prior to data collection, the sample was concentrated to ~5 mg/ml. The elution peak was exposed for 5 min. The images collected after the 4-min mark showed signs of radiation damage by analysis of radius of gyration and were discarded. The raw images were processed, and the background as subtracted in DAWN (56) at the beamline. Low q values outside the linear part of the Guinier plot were

removed in ScÅtter along with $q > 0.2519$ and D_{max} calculated to 133 Å. Further data processing was performed using ATSAS (57). PRIMUS calculated D_{max} to 138 Å and the Porod volume to 150387 Å^3, equivalent to 94 kDa using the rule of thumb of dividing the Porod volume by 1.6 Å^3/Da, a good fit of a dimer of the TgSPT1 D158 construct at 46 kDa per monomer. Fifteen 2-fold dimer envelope models were created in DAMMIF using the ATSAS server, a consensus envelope was created by DAMAVER, and that envelope was used as a starting point for DAMMIN (58). The DAMMIN envelope was superposed with the homology model in SUPCOMB, and the result was rendered in PyMol 1.7. CRYSOL (31) was used to calculate the theoretical X-ray scattering data from the homology model.

Phylogenetic analyses

The selected predicted protein sequences were aligned using ClustalW, edited to remove non-aligned regions, and then realigned in ClustalW with the output selected as a PHYLIP file (supplemental Fig. S3). This alignment was then subjected to three different phylogenetic analyses: F-MDist (39), RAxML (40), and PhyML (41). Bootstrap values were calculated for each analysis and used to establish the strength of the common clades in a consensus tree generated from the F-MDist data using DRAWGRAM in PHYLIP (39).

Author contributions—J. G. M., J. K. T., and A. Q. I. A. conducted most of the experiments and analyzed the results. L. E. B. managed the construct assembly and analyses at Oxford Protein Purification Facility. R. H. D. optimized the protein expression. M. K. G. performed the SAXS experimental and analyses. J. A. M. conducted the mass spectrometry. S. P. cloned the cDNA. H. S.-E. constructed the conditional yeast mutant. R. T. S., E. P., and P. W. D. designed and managed the experimental. P. W. D. conceived the idea for the project and wrote the paper with E. P. and J. G. M.

Acknowledgments—We thank the Department of Chemistry Mass Spectrometry Service for analytical support. Also, thanks to Martin Walsh from the Diamond Light Source; Christopher Barnes, Ian Edwards, Tim Hawkins, Joanne Robson, Catherine Bruce, and Emily Cardew from the Department of Biosciences; and Robek Pal from the Department of Chemistry for technical input, support, and many helpful discussions. We gratefully acknowledge the provision of beam time and excellent support by the BL21 staff at the Diamond Light Source. Materials were kindly provided by Prof. Dominique Soldati-Favre (Geneva), Dr. Kristin Hagar (Notre Dame), and Prof. Keith Gull (Oxford). This work was also supported by Grant-in-Aid from Oxford Protein Purification Facility.

References

1. Chowdhury, M. N. (1986) Toxoplasmosis: a review. *J. Med.* **17,** 373–396
2. Dubey, J. P. (1977) Toxoplasma, Hammondia, Besnotia, Sarcocystis, and other cyst-forming coccidia of man and animals. In: *Parasitic Protozoa* (Kreier, J. P., ed) pp. 101–237, Academic Press, New York
3. Coppens, I. (2013) Targeting lipid biosynthesis and salvage in apicomplexan parasites for improved chemotherapies. *Nat. Rev. Microbiol.* **11,** 823–835
4. Coppens, I. (2014) Exploitation of auxotrophies and metabolic defects in Toxoplasma as therapeutic approaches. *Int. J. Parasitol.* **44,** 109–120
5. Azzouz, N., Rauscher, B., Gerold, P., Cesbron-Delauw, M. F., Dubremetz, J. F., and Schwarz, R. T. (2002) Evidence for *de novo* sphingolipid biosynthesis in *Toxoplasma gondii*. *Int. J. Parasitol.* **32,** 677–684
6. Pratt, S., Wansadhipathi-Kannangara, N. K., Bruce, C. R., Mina, J. G., Shams-Eldin, H., Casas, J., Hanada, K., Schwarz, R. T., Sonda, S., and Denny, P. W. (2013) Sphingolipid synthesis and scavenging in the intracellular apicomplexan parasite, *Toxoplasma gondii*. *Mol. Biochem. Parasitol.* **187,** 43–51
7. Romano, J. D., Sonda, S., Bergbower, E., Smith, M. E., and Coppens, I. (2013) *Toxoplasma gondii* salvages sphingolipids from the host Golgi through the rerouting of selected Rab vesicles to the parasitophorous vacuole. *Mol. Biol. Cell* **24,** 1974–1995
8. Prieschl, E. E., and Baumruker, T. (2000) Sphingolipids: second messengers, mediators and raft constituents in signaling. *Immunol. Today* **21,** 555–560
9. Pszenny, V., Ehrenman, K., Romano, J. D., Kennard, A., Schultz, A., Roos, D. S., Grigg, M. E., Carruthers, V. B., and Coppens, I. (2016) A lipolytic lecithin:cholesterol acyltransferase secreted by *Toxoplasma* facilitates parasite replication and egress. *J. Biol. Chem.* **291,** 3725–3746
10. Young, S. A., Mina, J. G., Denny, P. W., and Smith, T. K. (2012) Sphingolipid and ceramide homeostasis: potential therapeutic targets. *Biochem. Res. Int.* **2012,** 248135
11. Simons, K., and Ikonen, E. (1997) Functional rafts in cell membranes. *Nature* **387,** 569–572
12. Lowther, J., Naismith, J. H., Dunn, T. M., and Campopiano, D. J. (2012) Structural, mechanistic and regulatory studies of serine palmitoyltransferase. *Biochem. Soc. Trans.* **40,** 547–554
13. Hanada, K. (2003) Serine palmitoyltransferase, a key enzyme of sphingolipid metabolism. *Biochim. Biophys. Acta* **1632,** 16–30
14. Han, G., Gable, K., Yan, L., Natarajan, M., Krishnamurthy, J., Gupta, S. D., Borovitskaya, A., Harmon, J. M., and Dunn, T. M. (2004) The topology of the Lcb1p subunit of yeast serine palmitoyltransferase. *J. Biol. Chem.* **279,** 53707–53716
15. Nagiec, M. M., Baltisberger, J. A., Wells, G. B., Lester, R. L., and Dickson, R. C. (1994) The LCB2 gene of *Saccharomyces* and the related LCB1 gene encode subunits of serine palmitoyltransferase, the initial enzyme in sphingolipid synthesis. *Proc. Natl. Acad. Sci. U.S.A.* **91,** 7899–7902
16. Zanolari, B., Friant, S., Funato, K., Sütterlin, C., Stevenson, B. J., and Riezman, H. (2000) Sphingoid base synthesis requirement for endocytosis in *Saccharomyces cerevisiae*. *EMBO J.* **19,** 2824–2833
17. Perry, D. K. (2002) Serine palmitoyltransferase: role in apoptotic de novo ceramide synthesis and other stress responses. *Biochim. Biophys. Acta* **1585,** 146–152
18. Funato, K., Vallée, B., and Riezman, H. (2002) Biosynthesis and trafficking of sphingolipids in the yeast *Saccharomyces cerevisiae*. *Biochemistry* **41,** 15105–15114
19. Ikushiro, H., Hayashi, H., and Kagamiyama, H. (2003) Bacterial serine palmitoyltransferase: a water-soluble homodimeric prototype of the eukaryotic enzyme. *Biochim. Biophys. Acta* **1647,** 116–120
20. Ikushiro, H., Hayashi, H., and Kagamiyama, H. (2001) A water-soluble homodimeric serine palmitoyltransferase from *Sphingomonas paucimobilis* EY2395T strain: purification, characterization, cloning, and overproduction. *J. Biol. Chem.* **276,** 18249–18256
21. Yard, B. A., Carter, L. G., Johnson, K. A., Overton, I. M., Dorward, M., Liu, H., McMahon, S. A., Oke, M., Puech, D., Barton, G. J., Naismith, J. H., and Campopiano, D. J. (2007) The structure of serine palmitoyltransferase; gateway to sphingolipid biosynthesis. *J. Mol. Biol.* **370,** 870–886
22. Gerold, P., and Schwarz, R. T. (2001) Biosynthesis of glycosphingolipids de-novo by the human malaria parasite *Plasmodium falciparum*. *Mol. Biochem. Parasitol.* **112,** 29–37
23. Lauer, S. A., Ghori, N., and Haldar, K. (1995) Sphingolipid synthesis as a target for chemotherapy against malaria parasites. *Proc. Natl. Acad. Sci. U.S.A.* **92,** 9181–9185
24. Haldar, K., Mohandas, N., Samuel, B. U., Harrison, T., Hiller, N. L., Akompong, T., and Cheresh, P. (2002) Protein and lipid trafficking induced in erythrocytes infected by malaria parasites. *Cell Microbiol.* **4,** 383–395
25. Shams-Eldin, H., Azzouz, N., Kedees, M. H., Orlean, P., Kinoshita, T., and Schwarz, R. T. (2002) The GPI1 homologue from *Plasmodium falciparum* complements a *Saccharomyces cerevisiae* GPI1 anchoring mutant. *Mol. Biochem. Parasitol.* **120,** 73–81

26. Denny, P. W., and Smith, D. F. (2004) Rafts and sphingolipid biosynthesis in the kinetoplastid parasitic protozoa. *Mol. Microbiol.* **53,** 725–733
27. Denny, P. W., Goulding, D., Ferguson, M. A., and Smith, D. F. (2004) Sphingolipid-free *Leishmania* are defective in membrane trafficking, differentiation and infectivity. *Mol. Microbiol.* **52,** 313–327
28. Ikushiro, H., Islam, M. M., Tojo, H., and Hayashi, H. (2007) Molecular characterization of membrane-associated soluble serine palmitoyltransferases from *Sphingobacterium multivorum* and *Bdellovibrio stolpii*. *J. Bacteriol.* **189,** 5749–5761
29. Berrow, N. S., Alderton, D., Sainsbury, S., Nettleship, J., Assenberg, R., Rahman, N., Stuart, D. I., and Owens, R. J. (2007) A versatile ligation-independent cloning method suitable for high-throughput expression screening applications. *Nucleic Acids Res.* **35,** e45
30. Bird, L. E. (2011) High throughput construction and small scale expression screening of multi-tag vectors in *Escherichia coli*. *Methods* **55,** 29–37
31. Svergun, D., Barberato, C., and Koch, M. H. (1995) CRYSOL: a program to evaluate X-ray solution scattering of biological macromolecules from atomic coordinates. *J. Appl. Crystallogr.* **28,** 768–773
32. Zuegge, J., Ralph, S., Schmuker, M., McFadden, G. I., and Schneider, G. (2001) Deciphering apicoplast targeting signals: feature extraction from nuclear-encoded precursors of *Plasmodium falciparum* apicoplast proteins. *Gene* **280,** 19–26
33. van Dooren, G. G., and Striepen, B. (2013) The algal past and parasite present of the apicoplast. *Annu. Rev. Microbiol.* **67,** 271–289
34. Agrawal, S., van Dooren, G. G., Beatty, W. L., and Striepen, B. (2009) Genetic evidence that an endosymbiont-derived endoplasmic reticulum-associated protein degradation (ERAD) system functions in import of apicoplast proteins. *J. Biol. Chem.* **284,** 33683–33691
35. Ramakrishnan, S., Docampo, M. D., Macrae, J. I., Pujol, F. M., Brooks, C. F., van Dooren, G. G., Hiltunen, J. K., Kastaniotis, A. J., McConville, M. J., and Striepen, B. (2012) Apicoplast and endoplasmic reticulum cooperate in fatty acid biosynthesis in apicomplexan parasite *Toxoplasma gondii*. *J. Biol. Chem.* **287,** 4957–4971
36. Zeitvogel, F., and Obst, M. (2016) ScatterJn: An ImageJ plugin for scatterplot-matrix analysis and classification of spatially resolved analytical microscopy data. *J. Open Res. Software* **4,** e5
37. Zeitvogel, F., Schmid, G., Hao, L., Ingino, P., and Obst, M. (2016) ScatterJ: an ImageJ plugin for the evaluation of analytical microscopy datasets. *J. Microsc.* **261,** 148–156
38. Larkin, M. A., Blackshields, G., Brown, N. P., Chenna, R., McGettigan, P. A., McWilliam, H., Valentin, F., Wallace, I. M., Wilm, A., Lopez, R., Thompson, J. D., Gibson, T. J., and Higgins, D. G. (2007) Clustal W and Clustal X version 2.0. *Bioinformatics* **23,** 2947–2948
39. Felsenstein, J. (1989) Mathematics *vs.* evolution: mathematical evolutionary theory. *Science* **246,** 941–942
40. Stamatakis, A. (2014) RAxML version 8: a tool for phylogenetic analysis and post-analysis of large phylogenies. *Bioinformatics* **30,** 1312–1313
41. Guindon, S., and Gascuel, O. (2003) A simple, fast, and accurate algorithm to estimate large phylogenies by maximum likelihood. *Syst. Biol.* **52,** 696–704
42. Arisue, N., and Hashimoto, T. (2015) Phylogeny and evolution of apicoplasts and apicomplexan parasites. *Parasitol. Int.* **64,** 254–259
43. Huitema, K., van den Dikkenberg, J., Brouwers, J. F., and Holthuis, J. C. (2004) Identification of a family of animal sphingomyelin synthases. *EMBO J.* **23,** 33–44
44. Di Tommaso, P., Moretti, S., Xenarios, I., Orobitg, M., Montanyola, A., Chang, J. M., Taly, J. F., and Notredame, C. (2011) T-Coffee: a web server for the multiple sequence alignment of protein and RNA sequences using structural information and homology extension. *Nucleic Acids Res.* **39,** W13–W17
45. Denny, P., Preiser, P., Williamson, D., and Wilson, I. (1998) Evidence for a single origin of the 35 kb plastid DNA in apicomplexans. *Protist* **149,** 51–59
46. Denny, P. W., Shams-Eldin, H., Price, H. P., Smith, D. F., and Schwarz, R. T. (2006) The protozoan inositol phosphorylceramide synthase: a novel drug target that defines a new class of sphingolipid synthase. *J. Biol. Chem.* **281,** 28200–28209
47. Herm-Götz, A., Weiss, S., Stratmann, R., Fujita-Becker, S., Ruff, C., Meyhfer, E., Soldati, T., Manstein, D. J., Geeves, M. A., and Soldati, D. (2002) *Toxoplasma gondii* myosin A and its light chain: a fast, single-headed, plus-end-directed motor. *EMBO J.* **21,** 2149–2158
48. Hager, K. M., Striepen, B., Tilney, L. G., and Roos, D. S. (1999) The nuclear envelope serves as an intermediary between the ER and Golgi complex in the intracellular parasite *Toxoplasma gondii*. *J. Cell Sci.* **112,** 2631–2638
49. Schneider, C. A., Rasband, W. S., and Eliceiri, K. W. (2012) NIH Image to ImageJ: 25 years of image analysis. *Nat. Methods* **9,** 671–675
50. Pfluger, S. L., Goodson, H. V., Moran, J. M., Ruggiero, C. J., Ye, X., Emmons, K. M., and Hager, K. M. (2005) Receptor for retrograde transport in the apicomplexan parasite *Toxoplasma gondii*. *Eukaryot. Cell* **4,** 432–442
51. Söding, J., Biegert, A., and Lupas, A. N. (2005) The HHpred interactive server for protein homology detection and structure prediction. *Nucleic Acids Res.* **33,** W244–W248
52. Ikushiro, H., Islam, M. M., Okamoto, A., Hoseki, J., Murakawa, T., Fujii, S., Miyahara, I., and Hayashi, H. (2009) Structural insights into the enzymatic mechanism of serine palmitoyltransferase from *Sphingobacterium multivorum*. *J. Biochem.* **146,** 549–562
53. Eswar, N., Webb, B., Marti-Renom, M. A., Madhusudhan, M. S., Eramian, D., Shen, M. Y., Pieper, U., and Sali, A. (2006) Comparative protein structure modeling using Modeller. *Curr. Protoc. Bioinformatics*, Chapter 5, Unit 5.6
54. Fiser, A., and Sali, A. (2003) ModLoop: automated modeling of loops in protein structures. *Bioinformatics* **19,** 2500–2501
55. De Maria Antolinos, A., Pernot, P., Brennich, M. E., Kieffer, J., Bowler, M. W., Delageniere, S., Ohlsson, S., Malbet Monaco, S., Ashton, A., Franke, D., Svergun, D., McSweeney, S., Gordon, E., and Round, A. (2015) ISPyB for BioSAXS, the gateway to user autonomy in solution scattering experiments. *Acta Crystallogr. D Biol. Crystallogr.* **71,** 76–85
56. Basham, M., Filik, J., Wharmby, M. T., Chang, P. C., El Kassaby, B., Gerring, M., Aishima, J., Levik, K., Pulford, B. C., Sikharulidze, I., Sneddon, D., Webber, M., Dhesi, S. S., Maccherozzi, F., Svensson, O., *et al.* (2015) Data analysis WorkbeNch (DAWN). *J. Synchrotron Radiat.* **22,** 853–858
57. Petoukhov, M. V., Franke, D., Shkumatov, A. V., Tria, G., Kikhney, A. G., Gajda, M., Gorba, C., Mertens, H. D., Konarev, P. V., and Svergun, D. I. (2012) New developments in the program package for small-angle scattering data analysis. *J. Appl. Crystallogr.* **45,** 342–350
58. Tuukkanen, A. T., Kleywegt, G. J., and Svergun, D. I. (2016) Resolution of ab initio shapes determined from small-angle scattering. *IUCrJ* **3,** 440–447
59. Gouet, P., Robert, X., and Courcelle, E. (2003) ESPript/ENDscript: extracting and rendering sequence and 3D information from atomic structures of proteins. *Nucleic Acids Res.* **31,** 3320–3323
60. Gajria, B., Bahl, A., Brestelli, J., Dommer, J., Fischer, S., Gao, X., Heiges, M., Iodice, J., Kissinger, J. C., Mackey, A. J., Pinney, D. F., Roos, D. S., Stoeckert, C. J., Jr., Wang, H., and Brunk, B. P. (2008) ToxoDB: an integrated toxoplasma gondii database resource. *Nucleic Acids Res.* **36,** D553–D556
61. Aurrecoechea, C., Brestelli, J., Brunk, B. P., Dommer, J., Fischer, S., Gajria, B., Gao, X., Gingle, A., Grant, G., Harb, O. S., Heiges, M., Innamorato, F., Iodice, J., Kissinger, J. C., Kraemer E., et al. (2009) PlasmoDB: a functional genomic database for malaria parasites. *Nucleic Acids Res.* **37,** D539–D543
62. Alva, V., Nam, S. Z., Söding, J., and Lupas, A. N. (2016) The MPI bioinformatics Toolkit as an integrative platform for advanced protein sequence and structure analysis. *Nucleic Acids Res.* **44,** W410–W415

Functional and phylogenetic evidence of a bacterial origin for the first enzyme in sphingolipid biosynthesis in a phylum of eukaryotic protozoan parasites

John G. Mina, Julie K. Thye, Amjed Q. I. Alqaisi, Louise E. Bird, Robert H. Dods, Morten K. Grøftehauge, Jackie A. Mosely, Steven Pratt, Hosam Shams-Eldin, Ralph T. Schwarz, Ehmke Pohl and Paul W. Denny

J. Biol. Chem. 2017, 292:12208-12219.
doi: 10.1074/jbc.M117.792374 originally published online June 2, 2017
